

MICROSCOPIC REORGANIZATION RESULTING FROM VARYING
PERIODS OF NEURONAL ISOLATION IN CATS' CEREBRAL CORTEX

A Dissertation
Presented to
the Faculty of the Graduate School
University of Manitoba

In Partial Fulfillment
of the Requirements for the Degree
Doctor of Philosophy

by
Harvey Weisman
December 1969

Dedicated
to the memory of my father
JACK WEISMAN

who taught me, during his lifetime, that he who
does not increase his knowledge decreases it.

ACKNOWLEDGEMENTS

I cannot express too strongly my appreciation and thanks to those who helped me in this study.

- | | |
|-------------------------------------|--|
| Dr. Carl Pinsky | My supervisor, who always gave generously of his skill and patience. |
| My wife Sandra | For her encouragement, advice, and typing of this manuscript. |
| Prof. E.W. Mazerall | For providing the formula and program for the trigonometric correction factor. |
| Mr. W.J. Davidson | For his diligent supervision during the preparation of the figures. |
| Dr. Z. Gorchynski | For the preparation of chronic slabs. |
| Mr. Rome Innes
Mr. Harold Strom | For their help in preparing acute slabs. |
| Mr. Roy Simpson | For his help in preparing photographic plates. |
| To my daughters,
Nancy and Karen | For their quiescent cooperation. |

TABLE OF CONTENTS

	Page
ACKNOWLEDGEMENTS	iii
LIST OF TABLES	viii
LIST OF FIGURES	ix
LIST OF PLATES	xii
STATEMENT OF THE PROBLEM	xiv
 HISTORICAL REVIEW	 1
1. INTRODUCTION TO GROSS ANATOMY	
Gross Anatomical and Developmental Features of the Cat's Brain	
Gross anatomy of the cat's brain	
Phylogeny	3
Surface Topography	4
General topography of cerebrum	
Ventral surface	5
Dorsal surface	6
2. MICROSCOPIC ANATOMY OF THE CAT'S CEREBRAL CORTEX	8
Intact cerebral cortex	
Cytology of Intact Cerebral Cortex	11
Perikaryon inclusions	15
Nissl substance	
Neurofibrils	18
Mitochondria	20
Golgi apparatus	22
Pigment granules	25
Centrosome	28
The nucleus	29
Nucleolus	31
Axon	34
Myelin	37
Dendrites	42
The Synapse	60

HISTORICAL REVIEW, cont.

Page

Cytoarchitectonics	67
Total volume of the cerebral cortex	68
Variable thickness of the cortex	69
Total number of neurons in the cerebral cortex	70
Neuron population density in the cerebral cortex	72
Dendritic Spines	75
Histology of the Isolated Cerebral Cortex	77
Cytological preservation	83
Cytological degeneration	
Regeneration in the cerebral cortex	
3. EFFECTS of ENVIRONMENTAL MANIPULATION on MORPHOLOGY of NEURONS	89
METHODS AND MATERIALS	92
1. SURGICAL PROCEDURES	
Intact cerebral cortex	
Preparation of neuronally isolated slabs of cerebral cortex	97
Acute isolation	102
Chronic isolation	
2. HISTOLOGICAL TECHNIQUE	105
Fixative	107
Staining (Metallic impregnation)	108
Dehydration	
Infiltration and embedding	109
Sectioning and mounting	111
3. ANALYTICAL METHODS	114
Measurement of histological parameters	115
Intact cortex	
Dimensions of gyri and cortical depth	
Gyrus width and cortical depth	
Neuron population density	120
Acutely isolated cortex	124
Dimensions of gyri, isolated slabs and cortical depth	
Neuron population density	127
Chronically isolated cortex	128
Slab and gyrus dimensions, cortical depth	
Neuron population density	131

METHODS AND MATERIALS, cont.	Page
Measurement of cytological parameters	131
Intact cortex	137
Isolated cortex	143
4. DISCUSSION of METHODS	144
Non-neuronal cerebral cortical cells	
RESULTS	
1. GROSS APPEARANCE	151
Intact gyrus	
Acute gyrus	152
Chronic gyrus	153
2. HISTOLOGY of CORTICAL PREPARATIONS	155
Intact cortex	
Acute cortex	164
Chronic cortex	170
3. HISTOLOGICAL DIMENSIONS	175
Intact gyrus	
Acutely isolated gyrus	177
Chronically isolated gyrus	182
4. NEURON POPULATION DENSITY	192
Intact cortex	
Acutely isolated cortex	197
Chronically isolated cortex	205
5. ANALYSIS OF DENDRITES	219
Distribution of dendrite density	220
Angulation at branch points	226
Dendritic spine density	231
Dendrite wedges	234
Basilar dendrodendritic pathways	238
Trifurcated branch point	245
Structural variations and electrical stimulation	249
DISCUSSION	
1. HISTOMORPHOLOGICAL CHANGES FOLLOWING NEURONAL ISOLATION	252
2. NEURON POPULATION DENSITY	266

DISCUSSION, cont.	Page
3. DISTRIBUTION of DENDRITE DENSITY	275
4. ANGULATION at BRANCH POINTS	279
5. DENDRITIC SPINE DENSITY	280
6. DENDRITE WEDGES	282
7. BASILAR DENDRODENDRITIC PATHWAYS	283
8. TRIFURCATED BRANCH POINT	286
9. STRUCTURAL REGRESSION OF CHRONIC SLABS	287
SUMMARY	289
New observations	293
BIBLIOGRAPHY	296
APPENDIX	325

LIST OF TABLES

Table	Page
1. Mean Dimensions of Five Intact Left Gyri and Five Homotopes	176
2. Mean Dimensions of Five Acute Isolated Gyri and Four Homotopes (Microns)	180
3. Mean Dimensions of Six Chronic Isolated Gyri and Three Homotopes (Microns)	183
4. Mean Neuron Population Density of Observed Neurons per mm ³	193
5. Distribution of Dendrite Density	221
6. Mean Angle at Branch Points per Quadrant	227
7. Dendrite Spine Density	232
8. Distribution of Dendritic Wedge Density	239a

LIST OF FIGURES

Fig.		Page
1.	Dorsal View of Cat Cerebral Hemispheres	96
2.	Dorsal View of Cat Cerebral Hemispheres	99
3.	Diagram of Coronal Section in the Left Intact Gyrus	117
4.	Diagram to show Subdivision of Intact Cerebral Cortex into Segments	121
5.	Coronal View of Gyrus with Acutely Isolated Slab	125
6.	Coronal View of Acutely Isolated Slab showing Cortical Subdivision into Segments for Neuron Population Density Studies	129
7.	Coronal Section of Gyrus with Chronically Isolated Slab	132
8.	Coronal Section of Chronically Isolated Slab showing Subdivisions for Neuron Population Density	134
9.	Coronal View of Intact Cortex with Subdivision of Cortex into 4 Quadrants for Measurements of Cytological Parameters	138
10.	Diagrammatic Presentation of Apical Dendritic Tree showing Zone Distribution and Designation of Branch Order	142
11.	Mean Gyrus Width Plotted Against Mean Cortex Depth from 5 Intact Left Gyri	178
12.	Mean Widths in 5 Acute Left Gyri and their Slabs	181
13.	Mean Cortex Depths in 5 Left Acutely Isolated Gyri and their Slabs	184
14.	Mean Widths of 6 Chronic Left Gyri and 5 Intact Left Gyri	185
15.	Mean Slab Width Plotted Against Mean Gyrus Width from 6 Chronic Gyri	188

	x
Fig.	Page
16. Mean Cortex Depth of 6 Chronic Slabs	189
17. Mean Depths of Non-Isolated Cortex in each of the 3 Types of Gyri and their Homotopes	190
18. Neuron Population Density in 1 Intact Left Gyrus	195
19. Neuron Population Density in 1 Intact Homotopic Gyrus	196
20. Coronal Section of Intact Left Cortex, Mean of 1 Slab (3 sections only)	198
21. Coronal Section of Intact Homotopic Cortex, Mean of 1 Slab (5 sections)	199
22. Mean Neuron Population in 1 Intact Left Gyrus	200
23. Mean Neuron Population Density in 1 Intact Right Gyrus	201
24. Neuron Population Density in 5 Acute Left Slabs	203
25. Neuron Population Density in 4 Acute Homotopic Slabs	204
26. Coronal Section of Acute Left Slab Cortex, Mean of 5 Acute Slabs	206
27. Coronal Section of Acute Homotopic Cortex, Mean of 4 Slabs	207
28. Mean Neuron Population Density in 5 Acute Left Slabs	208
29. Mean Neuron Population Density in 4 Acute Right Slabs	209
30. Neuron Population Density in 5 Chronic Left Slabs	211
31. Neuron Population Density in 1 Chronic Homotopic Gyrus	212
32. Coronal Section of Chronic Left Cortex, Mean of 5 Chronic Slabs	213
33. Coronal Section of Chronic Homotopic Cortex, Mean of 1 Gyrus (2 Sections only)	215
34. Mean Neuron Population Density in 5 Chronic Left Slabs	216

Fig.		Page
35.	Mean Neuron Population Density in 1 Chronic Homotopic Gyrus	217
36.	Mean Neuron Population Density for each Category of Cortical Preparation	218b
37.	Comparison of Branch Points per Zone in Intact Left Gyrus, Acute Left Slab and Chronic Left Slab	222
38.	Mean Dendritic Density, Averaged from all 4 Quadrants in the 3 Different Kinds of Cortical Preparation	223
39.	Mean Angle at Branch Points for each Quadrant in the 3 Types of Cortical Preparation	230

LIST OF PLATES

Plate	Page
I Coronal Section, Intact Gyrus, 12.5X	118
II High Magnification of Glial Line, 500X	119
III Coronal Section of Intact Gyrus, 12.5X	156
IV Coronal Section of Intact Gyrus, 12.5X	157
V Coronal Section of Intact Gyrus, 12.5X	158
VI Coronal Section of Intact Gyrus, 12.5X	159
VII Coronal Section of Intact Gyrus, 12.5X	160
VIII Intact Cortex, 200X	162
IX Intact Upper Cortical Region, 125X	163
X Coronal Section, Gyrus with Acute Slab, 12.5X	165
XI Coronal Section, White Matter of Acute Slab, 25X	166
XII Coronal Section, White Matter of Acute Slab, 25X	168
XIII Coronal Section of Gyrus with Acute Slab, 12.5X	169
XIV Coronal Section, Gyrus with Chronic Slab, 12.5X	171
XVI Chronic Slab, Upper Cortical Region, 35.5X	173
XVII Chronic Slab, Subpial Region, 500X	174
XVIII Camera Lucida Drawings, dendritic trees	225
XIX Intact Cortex, Upper Cortical Half, 200X	235
XX Acute Slab, Lower Cortical Half, 200X	236
XXI High Magnification of Wedge Area Shown in Plate XX	237
XXII Acute Slab, Dendrite Wedge, 600X	239b

Plate		Page
XXIII	Intact Gyrus, Upper Cortical Half, 200X	241
XXIV	Chronic Slab, Upper Cortical Half, 200X	242
XXV	Acute Slab, Composite Photograph, 1250X	243
XXVI	Intact Gyrus, Composite Photograph, 1250X	244
XXVII	Coronal Section, Intact Left Gyrus, 25X	246
XXVIII	Upper Cortical Half, Right Side from Plate XXVII, 200X	247
XXIX	High Magnification of Trifurcated Branch Point, 1250X	248
XXX	Acute Left Slab, Dendrite Section, 1500X	251

STATEMENT OF THE PROBLEM

A major aim of this study was to determine whether there are histomorphological changes in chronically isolated neuronal slabs in cat cerebral cortex which could account for any of the known alterations in the electrical activity of such a preparation. Studies by others have found that the electrical responses obtained from the intact suprasylvian gyrus, from an acutely isolated slab cut on this gyrus and from a chronically isolated slab prepared in this gyrus differ from each other in various degrees. Electrical activity in the chronically isolated slab is more primitive than that in the intact gyrus or in the acutely isolated slab. Evidence for a structural correlate of such a regression to a more primal state was sought among the histological features examined in this study.

The general character of the research of this structure-function study was determined by a simple but fundamentally important postulate. This postulate is that the CNS consists of neurons which interact with each other. The anatomical parameters that were quantified and examined were chosen, with this central hypothesis in mind, by making two assumptions concerning

the cytology and histology of the cat's cerebral cortex. These assumptions were: 1) that there may be a dependence of cytological density upon histological volume, i.e., that the packing density of neurons and of dendritic processes is interrelated with the total volume of available cerebral cortex; 2) that the nature of the interaction and anatomical relationships between neurons would be altered as a result of neuronal isolation.

The interdisciplinary nature of this structure-function study became evident in the early planning stages of this investigation. Not only anatomical relationships, but other factors as well, could be expected to influence interactions between neurons. These factors are so diverse that consideration of them must involve concepts encompassed by the major disciplines of biochemistry and physiology. Moreover, the fundamental concepts of comparative vertebrate anatomy, comparative histology and neurohistology, cytology, histopathology and neurophysiology were considered essential adjuncts for the academic requirements of this study. Therefore, the author of this thesis has attempted to integrate the salient and relative interdisciplinary concepts in a comprehensive Historical Review.

the cytology and histology of the cat's cerebral cortex. These assumptions were: 1) that there may be a dependence of cytological density upon histological volume, i.e., that the packing density of neurons and of dendritic processes is interrelated with the total volume of available cerebral cortex; 2) that the nature of the interaction and anatomical relationships between neurons would be altered as a result of neuronal isolation.

HISTORICAL REVIEW

1. INTRODUCTION TO GROSS ANATOMY

Gross Anatomical and Developmental Features of the Cat's Brain.

The cat, in particular Felis domesticus (Linnaeus, 1758), is generally accepted as a species which provides a model for understanding various features of the central nervous system throughout most of the mammals (Straus-Durckheim, 1845; Mivart, 1874; Williams, 1875; Wilder, 1881). Those features of the mammalian central nervous system which are of greatest importance to the observations resulting from this work will be seen to include the following: the gross anatomy of the brain; the relationships between the principal structures in the brain; embryonic development of the cerebral cortex; factors governing connections between neuronal units; the histomorphology and the cytomorphology of the cerebral cortex. A general review of these features is presented in the body of this section and some illustrations of the material in this review are provided in the Appendix to this thesis.

Gross anatomy of the cat's brain. The brain, or encephalon, is the anterior enlargement of that part of the central nervous system which is encased within

the cranial cavity (Reighard and Jennings, 1951; Elliott, 1963; Truex and Carpenter, 1964). It is a direct continuation of the spinal cord and may be regarded as a tubular structure with enlarged cavities and with walls which are thickened and folded.

In the early stages of embryonic development the dorsal neural tube at its anterior end forms three major hollow expanded areas (Truex and Carpenter, 1964; c.f. Appendix, Fig. 1). Rapid and unequal growth of the developing brain within the limited confines of the cranial cavity results in several flexures which correspond partly to the external bendings of the head and neck regions of young embryos (Bartelmaz and Evans, 1926; Arey, 1965). The three embryonic vesicles, which are a basic feature in all developing vertebrates, give rise to the principal structures in the adult mammalian brain. These, along with their major subdivisions, are noted in the following summary:

A. PROSENCEPHALON

1. TELENCEPHALON

Rhinencephalon
Corpora striata
Cerebral cortex

2. DIENCEPHALON

Epithalamus
Thalamus
Hypothalamus

B. MESENCEPHALON

1. MESENCEPHALON

Corpora quadrigemina
Tegmentum
Crura cerebri

C. RHOMBENCEPHALON

1. METENCEPHALON

Cerebellum
Pons

2. MYELENCEPHALON

Medulla oblongata.

A detailed account of the anatomical relationship of these structures to each other may be found in several authoritative reference texts (Arey, 1965; Elliott, 1963; Truex and Carpenter, 1964). Their general relationships, arising from the primitive divisions in the embryonic neural tube, are illustrated in Appendix, Fig. 1.

Phylogeny. Ascendancy in the phylogeny of the brain throughout the vertebrate classes is characterized by a correlative increase in the complex interconnections between neuronal elements in that part of the cerebrum which had come to be known by Broca in 1878 (cited in Truex and Carpenter, 1964) as the cortex of the limbic system (Kluver and Burg, 1939; Nauta, 1958; Kaada, 1960). The limbic cortex is part of an integrative system which is considered to be essential to those activities associated with the preservation of the organism, for example, determination and desire for flight, fight, feeding,

mating and care of the young (Papez, 1929 and 1937; Hess, 1948, 1954, 1956; Kogan, 1949; Kluver, 1950; Kaada, 1951; Gellhorn, 1953; Kaada, Jansen and Andersen, 1953; Beritoff, 1965). The presence of additional integrative systems in mammals is accompanied by a correlative increase in the number of projection fibres which either originate or terminate in the roof of the cerebral hemispheres (Bonin, 1950; Sholl, 1956; Young, 1957). The view is widely held that the increase of signals from ascending fibres is associated with the development of new intracerebral association fibres which increase the ability of the cerebral cortex to store and process the information contained in the higher order of internal and external environmental events (Kappers, Huber and Crosby, 1936; Prosser, 1959; Glees, 1961; Young, 1964). In the higher mammalian orders an expansive development of the cerebral hemispheres is observed; this takes the form of a mantle-like neocortex.

Surface Topography

General topography of cerebrum. The cerebrum in the cat consists of right and left hemispheres which are separated from each other by a longitudinal fissure. The surface topography of the neopallium is highly convoluted and the gross anatomy of the dorsal and lateral surfaces of the cerebrum is generally delineated in terms of their prominent convolutions. These have been

described as gyri (Owen, 1868) and, also, as furrows or sulci (Smith, 1902); the convoluted topography of the cerebrum is often referred to as being gyrencephalic. The term fissure was used originally to designate the demarcation between paleopallium (olfactory areas of the cerebral cortex) and neopallial (extensive new cortex) regions (Kappers, Huber and Crosby, 1936) but has more recently been applied to the larger furrows, for example, longitudinal fissure, lateral fissure. Early convention among neuroanatomists (Kappers, Huber and Crosby, 1936) divided the gyrencephalic cerebral hemispheres into several lobes according to the disposition of the surface convolutions. These lobes have been well described in several authoritative reference texts (Papez, 1929; Kappers, Huber and Crosby, 1936; Elliott, 1963; Truex and Carpenter, 1964).

Ventral Surface. The ventral aspect of the cat's brain has been extensively described by several authors (Wilder, 1873, 1879, 1880, 1881, 1901; Winkler, 1914; Papez, 1929; Kappers, Huber and Crosby, 1936; Reighard and Jennings, 1951). Some features of this aspect are illustrated in Appendix Fig. 2. The olfactory bulbs and the associated olfactory stalk of the cat and other carnivores are large (Golgi, 1875; Edinger, 1908; Cajal, 1911; Winkler and Potter, 1914); they are relatively smaller in the higher primates (Golgi, 1875; van Gehuchten and Martin, 1891; Barker, 1899).

Dorsal Surface. The nonconvoluted neopallium found in the lower order of the mammalia was termed lissencephalic by Owen (1868); this form contrasts with the convoluted gyrencephalic form in the higher orders. It is the extensive morphological development of the neopallium which conceals most of the dorsal surface of the phylogenetically older limbic system and, as well, the cranial end of the medulla oblongata (Wilder, 1881; Winkler and Potter, 1914; Papez, 1929). In the cat brain, where an extensively convoluted neopallium is present, the dorsal surface exhibits four readily discernible areas (Appendix, Fig. 3); these are: the anterior end of the olfactory lobes, the convoluted cerebral hemispheres, the flocculi of the cerebellum and the posterior two-thirds of the medulla oblongata. It is clear from the foregoing observations that the development of the lateral and dorsal surfaces of the cerebral hemispheres in the cat is relatively more expansive than that of the ventral aspect; this may also be observed in Appendix, Figs. 2, 3.

Each cerebral hemisphere is subdivided into three broadly defined lobes. The subdivisions according to Papez (1929) were as follows: the frontal lobe - comprising all of the cerebral cortex mediad and cranial to the coronal sulcus or in the morphological variation the coronansate sulcus; the parietal lobe - comprising all of the cerebral cortex situated between the coronal

and anterior ectosylvian sulci to include the lateral, suprasylvian, coronal and anterior ectosylvian gyri; the occipital lobe - comprising the remainder of the caudal area of the cerebral hemisphere.

The Reighard and Jennings (1951) subdivision of the cerebral hemispheres delineated the frontal from the temporal lobes by the anterior ectosylvian sulcus. The temporal and the occipital lobes were not distinctly marked off from one another.

Two illustrations that summarize these classification differences are found in Appendix, Figs. 4 and 5.

2. MICROSCOPIC ANATOMY of the CAT'S CEREBRAL CORTEX

Intact cerebral cortex. The earliest recorded suggestion that the cerebral cortex is organized at a microscopic level was made by Gennari in 1776. He observed a white line in that region of the human brain which is now known to be the primary visual receiving area of the cerebral cortex. This anatomical landmark came to be known as the "Line of Gennari".

The use of light microscopy by Baillarger (1840) subsequently revealed that Gennari's Line is made up of two light bands separated by a thin dark band. However, the first recorded observation which described relatively detailed aspects of the histological pattern in the cerebral cortex was attributed to Meynert in 1867. He noted that the cerebral cortex in the mammal often has the appearance of being laminated by five horizontal layers of brain cells.

The development of fibrillar stains for myelin (Weigert, 1885; Pal, 1887), aniline dye stains for nerve cell bodies (Nissl, unpublished, circa 1885) and the metallic silver impregnation technique (Golgi, 1878), gave rise to the development of cytoarchitectonic - cellular - and myeloarchitectonic - fibrillar - descriptions of cortical layers in the brain. Architectonics, as defined by Lorente de No (1949), "is concerned, not so much with the structure of the cortex as with subdivision of the brain into regions of specific

structure".

The discovery that there were regional differences in the cortical laminations (Lewis, 1878; Cajal, 1891; Hammarberg, 1895; Brodmann, 1905; Campbell, 1905) reinforced the notion that the brain could be finely subdivided into different regions on the basis of its local microstructure.

The cytoarchitectonic schemes of Brodmann (1903) and of Campbell (1903) for a six-layered, rather than a five-layered, cerebral cortex were quickly accepted, and are still referred to by many authorities (Elliott, 1963; Truex and Carpenter, 1964; Ruch and Patton, 1965) as a rough basis for considering cortical structure. The innate difficulty in drawing any hard and fast conclusions from cortical cytoarchitectonics is illustrated by considering the erroneous conclusions which some leading early investigators drew concerning the cell layering in the human embryonic cortex. A cytological stain, after Nissl's method, failed to show any layering in the human cerebral cortex until the sixth month of embryonic life; it was therefore concluded that the neocortex is not layered until the sixth month of gestation (Brodmann, 1909). It was then argued from this view that all the six-layered regions of the cerebral cortex were homogenic in origin. These regions were later termed isocortex by Vogt (1919), to indicate their presumed uniform developmental relationship to the

other structurally similar regions of the cerebrum. Brodmann (1909) concluded also that the rhinencephalic cortex was heterogenic in origin, since laminations were either deficient or poorly developed in the adult. Vogt (1919) described this region as allocortex, thus separating it off as the "other cortex". Thus a body of presumed embryonic and structural principles was accepted as the basis for understanding the development and structure-function relations of the brain. The fundamental evidence for these concepts was badly shaken, however, when Lorente de No (1934a) applied the Golgi method to the early embryonic neocortex; his techniques permitted the identification of different cell types as early as the third month in embryonic life. de No concluded, on the basis of regional cellular relationships, that layering was present in the embryo at a very early stage. Thus, the main argument for assuming a homogenic basis for the isocortex was undoubtedly badly shaken. Nevertheless, the nomenclature and, indeed, the concepts developed over the period just cited have persisted and remain in the literature as though they had a more genuine basis in reality. Most workers in the field appear to have agreed, at least tacitly, to retain the original terminology, possibly for want of general agreement on any better. The erroneous concepts remain as an implicit snare for anyone who leans too heavily on acceptance of views held

in conformity in the literature.

Cytology of Intact Cerebral Cortex

As early as 1838 Schleiden and Schwann introduced the Cell Theory to explain how tissues were made up of structurally independent units. They termed these units cells. This term had first been employed by Hooke in 1665 to describe the empty spaces he saw in thin slices of dead cork with the aid of a simple microscope. The work of Schleiden and Schwann was followed by improvements in stain technology and microscopy; this eventually led to the formulation of the Neuron Theory or Neuron Doctrine by Waldeyer in 1891. The salient points of this doctrine, which was later summarized by Polyak (1955) and by Ranson and Clarke (1959), were as follows:

- a) The neuron is a genetic unit which is derived from the embryonic neuroblast.
- b) The neuron is the structural unit of the nervous system and remains structurally independent throughout the lifetime of the organism.
- c) The neuron is a functional unit which is physiologically specific as the sole conduction unit of the nervous system.
- d) The trophic unit of the neuron is the cell body, or perikaryon, from which all nerve processes - dendrites and axons - develop as outgrowths of its cytoplasm.

Of the three categories of neurons recognized by the current authoritative texts on neuroanatomy - unipolar, bipolar and multipolar cells - only the latter type are found in the cerebral cortex. A large number of early cytological studies on the morphology of the cerebral cortex have been cited by Kappers et al (1936); these are: Golgi, 1886; Mondino, 1887; Martinotti, 1889; Ramon y Cajal, 1890, '91, '96, '99, 1900-'06, '11; Retzius, 1891; '93, '94; Veratti, 1897; Schaffer, 1897, 1905; Simarro, 1900; Held, 1902; Donaggio, 1903; Soukhanoff, 1903; Rossi, 1905; Joris, 1904; van Gehuchten, 1904; Marinesco, 1905; Bayon, 1905; Michotte, 1905; Bielschowsky and Brodinann, 1905 and Sugita, 1918.

The findings of these studies resulted in five recognized types of cortical neurons - pyramidal, stellate, fusiform, horizontal cells of Cajal and cells of Martinotti (Appendix, Fig. 6). A brief description of these cortical neurons, after the classical descriptive works of Cajal and others, is presented in the immediately following section of this review. A representative drawing of each type of cortical neuron, following the Golgi preparation technique, is given in the Appendix, Fig. 6.

Pyramidal cell. This neuron type is by far the most prevalent among cortical neurons (Sholl, 1953, 1956; Mitra, 1955). The basic structural pattern of a

pyramidal cell is that of a conically shaped perikaryon whose apical end forms a main dendritic shaft. The narrow conical end of the perikaryon is directed towards the pial surface. The main apical dendritic shaft branches dichotomously to form an arborization pattern while the basilar end of the perikaryon bears many dendrites and one main axon. Morphological variations in the height of the perikaryon were classified as small (12u), Medium (20u to 25u), large (30u to 35u) and as giant pyramidal cells or Betz cells (45u to 50u) according to the scheme proposed by Kappers et al (1936). These heights vary irregularly with each of the following: the position of the perikaryon in terms of the different levels in the cortex; the volume of the cell body; the cellular surface area of the cell body and the nature of the apical dendritic arborization (Bok, 1934, 1936, 1939, 1959; Bok and Kip, 1939a, 1939b).

Intermingled with the upright pyramidal cells in the deeper layers of the cortex are the sparsely distributed "reverse pyramids" or Martinotti cells. In these neurons the cone of the perikaryon from which the main apical dendrite emerges is directed away from the pial surface and an axon emerges from the upper surface of the perikaryon to ramify in the subpial area of the cortex (Martinotti, 1889). Cajal (1899),

using a methylene blue stain preparation, and Barker (1901), using a Nissl stain, showed that the Martinotti cell has a relatively large and rounded vesicular nucleus, which contains a readily identifiable hyperchromatic nucleolus.

Stellate cells. This type of neuron is distributed throughout the layers of the cerebral cortex and is found in larger numbers in layer IV. The perikaryon is small and is usually either stellate or polygonal in shape. Several dendrites, usually four to eight in number, emerge directly from the perikaryon and pass in all directions. Stellate cell types have been categorized according to the parameters of their dendrites (Ramon-Moliner, 1962). A short axon terminates close to the cell body.

Fusiform cells. These cells are found usually in the deepest layers of the cerebral cortex. The perikaryon has a spindle shape with two dendrites which emerge from opposite poles of the cell body. One dendrite usually ascends to the subpial layer while the opposite dendrite arborizes in the immediate area. A single axon emerges from the middle of the perikaryon and forms an association tract in the white matter.

Horizontal cells of Cajal. These neurons are subpial in position and resemble small fusiform cells. Their dendrites and long axons run horizontally and arborize in layer I.

Perikaryon inclusions.

Nissl substance. Treatment of mammalian cerebral cortex with Nissl stain shows the presence of basophilic bodies in the cytoplasmic perikarya of cortical neurons. These basophilic inclusions were first called Nissl bodies or Nissl substance (Nissl, 1884) and were renamed tigroid bodies by von Lenhossek (1895). Descriptive accounts of the tigroid bodies by Nissl, von Lenhossek, Cajal (1899) and others were summarized by Barker (1901) as follows: The substance occurs in a variety of forms and sizes. Tigroid bodies may be arranged in rows, groups or networks which are usually in physical association with either small or coarse granules and an occasional vacuole-like vesicle. The coarse granules may appear in three forms, as follows:

- a) Nuclear caps - hollowed cones with a terminal cap distributed over the nucleus and cytoplasm.
- b) Wedges of division - short networks found at the base of dendrite branch points.
- c) Tigroid spindles - elongated spindles, becoming thin at their extremities.

Tigroid bodies are not found in the axon or in the area of the perikaryon from which the axon emerges (axon hillock).

Palay and Palade (1955), using the electron-microscope, identified the tigroid bodies as consisting of a fine tubular network of endoplasmic reticulum covered by fine granules 100 Å to 300 Å in diameter. These narrow tubules vary structurally to form flattened cisternae which sometimes anastomose with each other, or otherwise become arranged as parallel layers of membranes (de Robertis, Porter, Claude and Fullam, 1945; Porter, 1953). Occasionally the granules were found to have been arranged along the outer linear length of the endoplasmic reticulum as single rows while at other times they were aggregated as rosettes. They may also occur as single granules. Nongranular endoplasmic reticulum was found in the axon hillock as well as within the axon. In this regard Schade and Ford (1965) have stated that "whether or not these base endoplasmic reticulum do truly represent the skeleton of Nissl substance is not yet known".

That tigroid bodies contain a nucleoprotein was inferred by van Herwerden (1913) who studied the effects of nuclease treatment of the neuron. Heidenhain (1911) stated that the tigroid bodies are "a vitally organized substance related to the nuclear material". Edstrom

and Hyden (1954) provided the critical evidence for the presence of ribonucleic acid along with associated protein (RNA-P) in these bodies; they hydrolyzed RNA-P that had been extracted from dissected anterior horn cells. The amount of perikaryon RNA-P has been estimated to vary from 70 to 1550 pg/cell in a range of neuron types (Edstrom, 1956; Edstrom and Pigon, 1958; Hyden, 1959). It is well established (Hultin, 1950; Littlefield et al, 1955; Siekevitz and Palade, 1958) that RNA-P is influenced by the nucleus and is concerned with protein synthesis.

A correlation between neuron metabolic activity and the degree of chromophilia and chromophobia in neurons was proposed by Einarson and Krogh (1955). Moderate neuron metabolic activity was associated with large tigroid clumps and termed chromoneutral. Slightly increased neuron metabolic activity was associated with moderate chromophobia and was shown to correspond to a decrease in RNA-P concentration. This would indicate that the rate of RNA-P replenishment was slower than the rate of intracellular metabolism. Einarson and Krogh proposed that extreme chromophobia (chromatolysis) would correspond to neuron metabolic exhaustion, axon laceration and neuron pathology while extreme chromophilia would be related to functional inactivity.

There is a larger concentration of tigroid bodies

in the large ventral horn motor neurons than in the sensory neurons of the dorsal root ganglion (Nissl, 1884, 1903). Wide ranges in their distribution, shape and size in the various neuron types was the basis of yet another classification scheme by Nissl. Filamentous and granular tigroid bodies were categorized as being either peripheral or central in cytoplasmic distribution.

Neurofibrils. Optical microscopic examination has revealed that a reticular network of small fibrils is distributed inside the perikaryon, axon and dendritic processes of presumably every cerebral cortical neuron. These small fibrils were first described by Schultze (1871) and later by Golgi (1878) after the development of his reduced silver technique for staining nerve tissue. Subsequent improvements of this method by Bielschowsky (1904), Cajal (1904) and by Bodian (1936, 1937) has added very little to the earlier descriptions by Held (1896), Barker (1899, 1901), Bethe (1903), Cajal (1904, 1909) and others (c.f. Hyden, 1960; Truex and Carpenter, 1964).

Neurofibrils appear as homogeneous threads that interlace, or sometimes anastomose, with each other in the perikaryon. Peripheral fibrils appeared more fibrillar than the "endoplasmic" or centrally located counterpart. Inside the dendrites and axons the fibril

arrangement appears to be more parallel to the long axis of the processes and more closely grouped in the axon. The theory that they were artifacts of fixation (Matsumoto, 1920; Lewis and Lewis, 1924) was criticized by Weiss and Wong (1936), who observed the fibrils in tissue culture, and also by Hoerr (1936), who made similar observations in studies which utilized the freeze-dry method.

Electronmicroscopic observations suggested to some investigators that the neurofibrils might correspond to neurofilaments or protofibrils 60\AA to 100\AA in diameter (Palay and Palade, 1955; Tennyson, 1962; Rhodin, 1963). Another opinion expressed the view that the fibrils were artifacts resulting from the application of fixation on agranular endoplasmic reticulum (David, Brown and Mallion, 1961). Palay and Palade (1955) have expressed the view that fixation could aggregate neurofilaments to form the neurofibrils of light microscopy. Hyden (1960) stated that linear aggregation of previously dissociated globular proteins would form such filamentous structures. Goldby (1961) advanced the theory that neurofilaments within the perikaryon and processes form part of the cell's intracellular supportive system.

The function of neurofibrils and/or neurofilaments is unknown.

Mitochondria. These cytoplasmic organelles were described by Altmann in 1890 as consisting of cytoplasmic granules which are just barely visible with the light microscope. Michaelis (1900) demonstrated that Janus Green B, a vital dye, selectively stained mitochondria in isolated living cells. Structural polymorphism is displayed by mitochondria in the form of granules, rods, filaments, loops and vesicles (Benda, 1898; Held, 1897; Alzheimer, 1910; Cowdry, 1912). This structural diversity is influenced by heat, hypertonic and hypotonic solutions, carbon dioxide and fat solvents. As their age advances mitochondria show a tendency to become rounded out and swollen (Ernster and Lindberg, 1958).

Several quantitative studies have shown that differing numbers of mitochondria are found in different types of nervous and non-nervous cells (Cowdry, 1914). They are comparatively more frequent in epithelial cells of the intestine than in nerve cells (Thomas, 1947, 1948; Zeiger, 1955); in the latter their highest numbers have been found in anterior horn cells of the spinal cord, in Purkinje cells of the cerebellum and in vagal ganglionic cells (Choja, 1936; Hartmann, 1948, 1949). Cowdry (1914) observed that mitochondria in nerve cells are distributed around the nucleus, between tigroid bodies and in dendrites and axons; they are,

however, apparently absent at the axon hillock. These organelles are particularly abundant in metabolically active areas such as the perikaryon, synaptic end bulbs and in sensory and motor nerve endings (Palay and Palade, 1955; Hartmann, 1956; Dempsey, 1956).

A mitochondrion, seen with the electron microscope, consists of an outer limiting double membrane that structurally resembles a cell membrane. There are extensions of the inner membrane internally arranged as membranous folds or cristae mitochondriales. These extensions of the inner membrane are arranged either transversely or longitudinally in the filamentous form and radially in the granular form (Palade, 1952; Sjostrand, 1956). The mitochondrial chamber is filled either with a granular or with a filamentous matrix (deRobertis and Raffo, 1957). The membrane of the cristae is covered on its outer face by small "elementary particles" of polygonal shape (Fernandez-Moran, 1962). These particles appear to be attached by a thin stalk to the membrane of the cristae.

Altmann (1890) was an outstanding contributor to the knowledge concerning mitochondria. From the work he did at the end of the nineteenth century he made the remarkably farsighted prediction that the organelle would be related to cellular oxidation. Somewhat later Batelli and Stern (1912) demonstrated

the presence of respiratory enzymes within the insoluble part of the cell. The isolation and identification of mitochondria from living cells was accomplished by Bensley and Hoerr (1934). Investigations on the isolate, done subsequent to this work, showed that positive reactions existed for several enzymatic functions.

The localization of mitochondrial enzymes has been described in a review by Lehninger (1962). The respiratory enzymes of succinic and diphosphopyridine nucleotide (DPN) dehydrogenases, cytochrome oxidases and phosphorylating enzymes are found on the mitochondrial membrane while the matrix contains the enzymes involved in the Krebs and Fatty acid cycles and, as well, nucleotides and inorganic electrolytes. A structure-function relationship can thus be postulated since a filamentous and branched form of mitochondrion will have more internal cristae with respiratory enzymes than will the spherical form. Similarly, a reduction and compaction in size of the mitochondrial chamber might be expected to result in a corresponding reduction in the amount of enzymes available for the Krebs and Fatty acid cycles.

Golgi apparatus. The presence of a relatively coarse reticular network within the perikaryon of nerve cells was demonstrated by Golgi in 1898. The technique he used involved a chromic or an osmium-silver impreg-

nation treatment of ganglionic neurons. The reticular network was most often observed as perinuclear in position and came to be described as the Golgi apparatus or complex. This reticulum often displays morphological variations which some investigators confused with forms of mitochondria; these forms appear as filamentous threads, granules, loops and vesicles (Hibbard, 1945; Bensley, 1951). On occasion, the reticulum may be observed to lie within the larger dendritic processes of a nerve cell (Sanchez, 1916). Further studies by Golgi and by others demonstrated that the complex is present also in cells of non-nervous tissue or other nervous-type cells (Hibbard, 1945). The Golgi apparatus was reported by Gatenby (1953) to have been observed in living cells of the sympathetic nervous system. This observation argues, in some measure, against a possible artifactual origin of the Golgi complex.

The effect of axon transection on the Golgi complex was studied by Penfield (1920, 1921). He noted that the initial effect, termed retispersion, is the dispersion of the complex to the periphery of the perikaryon. This is soon followed by the disappearance of the Golgi complex; this was termed retisolution. Cyclic changes in the distribution of the Golgi complex have been studied more recently by Tewari and Bourne (1962a, 1962b). They suggested that cyclic changes in

the distribution of the Golgi complex in the perikaryon of spinal ganglionic cells are correlated to a cyclic functional activity. An earlier study (van Breemen, Anderson and Reger, 1958) intimated that the Golgi complex may serve as the source for membrane-bound synaptic vesicles.

An electronmicroscope study of nervous tissue by Fernandez-Moran (1957) identified the lamellated agranular endoplasmic reticulum as being the Golgi complex observed by means of light microscopy. Recent advances in the study of the fine structure of the Golgi complex in pancreatic exocrine cells have demonstrated that the Golgi complex is associated with secretory end products (Farquhar and Wellings, 1957; Mollenhauer and Whaley, 1963; Warshawsky et al, 1963; Caro and Palade, 1964; Novikoff et al, 1964; Jamieson and Palade, 1967a, 1967b). The site of protein synthesis appears to take place at the granular endoplasmic reticulum while the aggregation and condensation of the secretory granules lies with the cisternae of the Golgi complex.

Most of the current information on the fine structure of the Golgi complex has been summarized by Ham (1965); he has interpreted various morphological features and categorized them into three main components, as follows:

a) Flattened vesicles. These are relatively wide and thin, and are stacked upon each other; the possibility that they are longitudinal tubules of narrow caliber is ruled out from studies of the Golgi complex in plant cells. The terminal portions of the flattened channel or vesicle are usually dilated.

b) Secretory vesicles. These are presumably dilated terminal ends that have budded off from the flattened vesicle. The contents of the secretory vesicle are more condensed than those of the flattened vesicle; the form of secretory vesicle is usually rounded.

c) Microvesicles. These are small smooth-walled vesicles of unknown origin. They act as carriers of protein material from granular endoplasmic reticulum to the larger Golgi complex.

Ham's scheme, although comprehensive, must not be regarded as definitive regarding the structures he has described. The functional role of the Golgi complex in the neuron is still speculative. It may be related to the flow of products synthesized in the organelles of the perikaryon to the entire length of the dendrites.

Pigment granules. The early identification of pigment granules of melanin within the perikaryon of certain nerve cells is credited to Muhlmann (1900, 1901) and to Oberstein (1903). The pigment, dark brown or black, was usually found aggregated in a semi-dense

mass and, on fewer occasions, dispersed throughout the cytoplasmic perikaryon. It was found to be confined to nuclear cell masses such as the substantia nigra.

Their chemical constituents were determined by Stein (1955) as consisting of 30% protein, 1-5% lipids, <0.3% ribonucleic acid, 5-10% carbohydrates and traces of copper, iron and zinc. No particular function, as yet, has been attributed to the presence of neuron melanin pigments.

A second type of pigment, lipofuscin, is usually found in the perikaryon of the most of the larger neurons. This pigment was thoroughly discussed by Hyden (1960) in a recently published review on the morphology, chemistry and physical properties of the neuron. That review, in part, summarizes the key studies on the pigment; these have been done by Pilcz (1895); Muhlmann (1900, 1901); Obersteiner (1903); Oberndorfer (1921); Volkmann (1932); Zeglio (1935); Bethe and Fluck (1937) and by Altschul (1938). Several characteristics of the pigments have been noted to occur during the aging processes of the neuron. Small traces of the pigment appear as light yellow granules in human cerebral cortical neurons during the first ten years of age. These become progressively darker and in some cases so numerous during the next ten years that the perikaryon becomes filled and deformed. Altschul (1938) proposed the idea that the pigment is

a "wear and tear substance" which supports nerve cells "with decreasing capacity as age advances". The yellow pigment increases to a maximum amount at the age of 40 to 50 years and does not decrease thereafter with increasing age (Hyden, 1960).

The results from an earlier study by Hyden and Lindstrom (1950) suggested a possible physico-chemical link between the concentration of RNA and the amount of lipofuscin pigment. This possible interdependence was later doubted when it was shown that amounts of cytoplasmic RNA increases from 3 to 40 years of age, remains constant from 40 to 55 and is significantly decreased at greater age. There is no corresponding decrease in the amount of lipofuscin in neurons at these greater ages.

The increased lipofuscin granules in older age has been reported to form an intrapigmentary fibrillar network that displaced neurofibrils towards the periphery of the perikaryon (Sosa, 1935, 1952). This condition was followed by a neurofibrillolysis which Sosa termed Lipofuscin Neurofibrillar Degeneration (LND). The chemical composition of lipofuscin granules is still unsolved. A purified suspension of lipofuscin granules was prepared and analyzed by Siebert et al (1958); they concluded that the granules contained insoluble inactive proteins. Lipofuscin accumulation was shown to increase

in young and old rats with Vitamin E deficiency when compared to healthy young rats (Wunscher and Kustner, 1967). Reichel et al (1968) have demonstrated that there was more lipofuscin pigment per section volume in the hippocampus region than in the cerebral cortex of young and old rats.

It may be stated that the function of lipofuscin granules in nerve cells remains another unsolved problem. The granules increase in amount with age but no measurable impairment of neural function has been reported as correlated with an increase in the granules.

Centrosome. Boveri, Heidenhain and van Beneden (circa 1890) found that this cytoplasmic organelle was intimately linked with the mechanism of mitotic and meiotic cell division. The classical investigations in neurocytology and neurohistology (see list of standard reference texts in Bibliography) had established that adult neurons were characterized by, among many things, their apparent lack of a centrosome and general inability to replicate themselves. However, the presence of a centrosome in adult frog neurons was reported by van Lenhossek (1895) and by Dehler (1895). Cajal (1909) found centrosomes in reptile and in mammalian neurons; also, of particular interest, he reported their presence in the large pyramidal cells of the postcentral gyrus of a thirty-year old man.

The centrosome, when present, occupies a variable position in the perikaryon during the maturation of the neuron. Held (1909) observed that as the axon develops during the embryonic stage of the animal the centrosome is situated at the axon hillock; it later shifts to the area from where the principal dendrite will eventually emerge. Electronmicroscope observations of the centrosome were made by Amano (1957); Hamada (1958) and by Rhodin (1963). In these studies the centrosome was observed to consist of two distinct granules, each termed a centriole. The granules were usually composed of nine groups of filaments, arranged in a circle with three filaments in each group.

The nucleus. There have been numerous descriptive accounts on the morphology of the neuron nucleus by Cajal, Nissl, Barker and other early investigators who have been previously referred to in this thesis. Their findings on nuclear morphology will be presented here in an abbreviated form. The nucleus, 3 to 18 microns in diameter, was observed to be spherical and usually centrally situated in the perikaryon; in cells of the nucleus dorsalis of Clarke in the spinal cord the nucleus was found peripherally situated. The neuron, in most observations, was seen to be mononucleated but bi- and trinucleated neurons were observed in the pelvic autonomic ganglia. A prominent hyperchromatic nucleolus

was observed in the hypochromatic nucleoplasm.

The expression of a constant relation between the volume of the nucleus and that of the cytoplasm in various tissue cells was made by Hertwig (1903). This relation was termed the Karyo-plasmic ratio. The extent to which this ratio could be applied to the nerve cell was studied extensively by Bok, who began his investigations in 1934. A review of Bok's measured determinations on the nucleus was recently presented (Bok, 1959) and is here paraphrased in the following summary:

- a) The volume of the nucleus varies far less than does that of the perikaryon.
- b) In a large perikaryon the nucleus is large but occupies a relatively small fraction of the total area of the perikaryon; in the small perikaryon the nucleus occupies a relatively large fraction of the total perikaryon area.
- c) The total surface area of the perikaryon is directly proportional to the volume of the nucleus.
- d) The volume of the cytoplasm of the perikaryon is directly proportional to the square of the nuclear volume.
- e) The nuclear volume is proportional to the radius of the dendrite tree; this radius is taken to be the vertical extension from the perikaryon to the distal end of the apical dendrites.

The ultrafine structure of the nuclear membrane has been studied by de Robertis (1954a), Hartmann (1953), Palay and Palade (1955), Brachet (1961), and by Brachet and Mirsky (1961). Their observations indicated that the membrane is composed of two layers, an inner and an outer. These inner and outer layers appear to be a structural modification of convoluted agranular and granular endoplasmic reticulum which extends from the nucleus to an indefinite position in the perikaryon. Thus some areas of the outer component of the nuclear membrane appear to be covered by ribosome granules while other areas are nude. Furthermore, electronmicrographs indicate that pores, or fenestrations, in the nuclear membrane are located between adjacent endoplasmic reticular channels. The investigators cited have concluded that these pores form the escape route for nuclear products such as ribonucleic acid (RNA) passing from the nucleoplasm to the cytoplasm.

Nucleolus. The nucleolus is a small dense mass, rich in RNA, which is situated within the nucleus of both animal and plant cells (Caspersson, 1950; Vincent, 1955). It usually lies adjacent to the nuclear membrane (Gonzales Ramirez, 1963). An electron-microscope study has indicated that a nucleolar membrane is lacking in all cells (Rhodin, 1963).

Variations in the volume of the nucleolus, from 2 to $60\mu^3$, have been related to the physiologic state of the cell (Grimm, 1949; Wischnitzer, 1960). There appears to be no correlation between the size of the nucleus and that of the nucleolus. Olszewski (1947) and Beheim-Schwarzback (1955) have reported that more than one nucleolus may be observed in some nerve cells. There have been no reports of a structure-metabolic function for those cells with an extra nucleolus.

Hyden and Larsson (1956) have reported that the nucleolus has a very high density. This investigation, however, was carried out on fixed material which would normally react to the fixative by undergoing some degree of shrinkage and tissue condensation. The nucleolar RNA content of nerve cells in dry-frozen tissue was measured by Nurnberger (1952) and by Edstrom and Eichner (1958b). The RNA amount by weight varied from 0.5% to 2.0%; the amount also varied with the type of nerve cell examined.

A threadlike structure, a nucleolenema, has been observed to lie within the amorphous ground substance of the nucleolus (Estable and Sotelo, 1951). The thread gave a Feulgen negative reaction.

A small nucleolar satellite in nerve cells containing deoxyribonucleic acid (DNA) was reported by Barr and Bertram (1949, 1951) and by Moore and Barr (1953).

The satellite consists of the heterochromatin regions of the X chromosome. The sex chromatin, stained and resolved by light microscopy, in the XX of the female, has been used with success for sex determination of the species.

Axon

Waldeyer's first use of the term neuron in 1891 referred to a polarized cell with processes having distinct terminations. Those nerve processes which were presumed to carry impulses toward the nerve cell body were termed dendrites and the specificity of their functional direction was termed cellulopetal. Nerve impulses were considered to be carried away from the cell body by a single process termed the neuraxes or axone (more modern-axon); its functional specificity was referred to as cellulofugal.

Barker (1901) provided an early historical review on the histology of the brain and presented a non-documented statement that cortical axons may sometimes arise from the initial distal part of a dendrite or from the axon-hillock. Recent documented evidence presented in authoritative texts have shown that cortical axon emergence is confined entirely to the axon-hillock of the nerve cell body. The diameter of the axon varies from 0.2u for some cells to as much as 8-9u for the axon of the Betz Cell (Bishop and Smith, 1964). Each axon fibre within the cerebral cortex appears to be of essentially uniform diameter.

Structural variations of the neurons have been the basis of several classification schemes. Golgi (1894) observed several variations in the axonal lengths of

cortical neurons and devised the following scheme:

Golgi's Cell Type I has an axon of considerable length usually arising from a large perikaryon which contains large masses of Nissl substance. This type of axon, termed inaxone by Golgi, becomes surrounded by a thin myelin sheath roughly beginning a few microns distance from the soma and ending a few microns before the synaptic termination. The axonal termination lies outside the neuron territory which is roughly demarcated as the outer limit of the cell's dendritic plexus.

Golgi's Cell Type II, called dendraxone by Golgi, has a very short unmyelinated axon which terminates within the neuron territory. The cell body of the latter type is usually small and contains fine granules of Nissl substance. Intermediate forms between Cell Types I and II are known to occur but with far less frequency than do those types of the classification scheme.

Long myelinated axons within the cerebral cortex give rise to myelinated collaterals whose branches are generally at right angles to the main axonal fibre. On the other hand unmyelinated lateral axonal branches, which arise from the unmyelinated distal part of the main axon in Cell Type I, remain unmyelinated. The latter were termed Side Fibrils of Golgi.

Cajal (1889) proposed another classification scheme for cortical neurons which was based on the number

of axonal branches per neuron. A neuron which was noted to have two distinct axons emerge from the same perikaryon was called a diaxon neuron. According to Cajal the cerebral cortex of a one-day old dog appeared to have some neurons with several axons. This type of neuron was called a polyaxon neuron. A neuron whose axon was divided into nearly equal parts was called a schizaxon neuron. A fourth type of cerebral cortical neuron was found to be void of axons and it was called anaxon neuron.

The terminal branches of collateral and principal axonal fibres, termed by Barker (1901) as ultimate branches, enter into intimate regional and structural relations with cell bodies and dendrite branches of other neurons. These terminal arborizations are the so-called telodendrons. Cajal (1889) observed that a telodendron from one neuron was able to establish several relationships with cell bodies and axons of other neurons. This formed the basis of his theory for the "avalanche conduction pathway".

The axon, as described earlier in this thesis, contains an axoplasm that is structurally distinct from other nerve processes. The neurofibrils, which are abundant, are tightly packed and generally lie parallel to each other. Mitochondria are also numerous and are dispersed throughout the length of the axon. Nissl

substance, prominently present in dendrites and the perikaryon, is absent in the axon hillock and axoplasm. The axolemma, as observed with the light microscope, appears structurally similar to the plasmalemma of the perikaryon and dendrites. The axoplasm contains relatively less ribosomes than does the cytoplasm of the perikaryon and is devoid of granular endoplasmic reticulum (Rhodin, 1963).

Myelin. Axons may be differentiated by the presence or absence of a proteolipid encasement, the so-called myelin sheath. Myelinated fibres of the Peripheral Nervous System (PNS) were observed to be birefringent (Erenberg, 1849) and were later noted to have their optic axis radially arranged (Klebs, 1865). Further studies by Schmitt and Bear (1937) laid the foundation for the theory that myelin was composed of a bimolecular lipid leaflet which alternated with thin layers of protein. Later, Schmitt (1941) was able to conclude that myelin sheets were concentrically arranged. Both myelinated and unmyelinated types of fibres were found in the PNS, the latter type in the postganglionic fibres of the Autonomic Nervous System (Fulton, 1949).

A simple nucleated epithelial-like membrane, the Sheath of Schwann or Neurolemma, completely encloses the myelin. The myelin sheath in the PNS is formed around the axon just distal to the cell body and terminates

approximately 2 microns from the distal end of the fibre. The sheath in the PNS is regularly interrupted by an encircling constriction, the Node of Ranvier (Ranvier, 1878). In several authoritative reference texts it is reported that in the vertebrates axonal branches off myelinated axons originate only at a Node of Ranvier. The bare axon segment at the node, which is slightly constricted, is covered by a few cilia-like extensions from the two adjacent Schwann cells.

There is a marked difference, between neurons in the PNS and in the Central Nervous System(CNS), in the origin and degree of myelinization of their axonal fibres (Geren, 1954; Robertson, 1955, 1958; Uzman and Nogueira-Graf, 1957). The origin of myelin in the PNS has at different times been erroneously attributed to a secretion product from the neurolemma (Ranvier, 1878), from the axon (Bardeen, 1903; von Kolliker, 1904) and to a structural differentiation in the peripheral part of the axon (Apathy, 1897; Gothlin, 1917; Speidel, 1933). Several investigators (Geren, 1954; Fernandez-Moran, 1950 and Sjostrand, 1953) were able to prove that myelin in the PNS originates from Schwann cells. The process of myelination in mouse sciatic nerve was studied by Uzman and Nogueira-Graf (1957) who used electron-microscopy. They were of the opinion that the Schwann cell wraps around the axon and elaborates, as an intra-

cellular lipid secretion product, several spirally arranged laminations. Robertson (1959) and Peters (1960) have since been able to prove that myelin is made up of a series of plasma membranes which are elaborated from Schwann cells and are not an intracellular secretion product of those cells.

The PNS myelin sheath is obliquely interrupted by Clefts or Incisures of Schmidt-Lantermann. It was the opinion of several classical neurohistologists, and reported in 1931 by Bruno, that the clefts indicated areas of poor preservation and were therefore artifactual. It has since been shown that the clefts are local shearing defects in the lamellae of the myelin (Robertson, 1958; Rhodin, 1963). These extend from the axolemma to the neurolemma. The infolding of the inner myelin lamination which forms the axon-myelin junction with the axolemma is termed the internal mesaxon and the outer myelin lamination which joints the plasmolemma of the Schwann cell is termed the external mesaxon.

Axons in the CNS may be either myelinated or unmyelinated. The axonal fibres of the subpial layer of the cerebral cortex are mainly unmyelinated (Rhodin, 1963); the axonal fibres in the remainder of the cortical layers are myelinated (Cajal, 1909). It was the considered opinion of Cajal (1928) and of Bielschowsky (1928) that the myelin sheath in the CNS is interrupted

by Nodes of Ranvier. However, the limitations of the optical systems used at that time could not adequately have resolved such fine structures since CNS myelin appears to be much narrower and thinner than its counterpart in the PNS. Nodes of Ranvier were observed with the aid of the electronmicroscope in the myelin of the optical cranial nerve (Peters, 1960) and in the CNS myelin (Rhodin, 1963).

The process of myelination in the CNS takes its origin from the oligodendroglial cells (Luse, 1956). It was at one time claimed that Schwann cells were present in the CNS (Plenk, 1934), but this has since been disproved by Luse (1956) and by Bunge (1961). This latter investigator theorized that the process from one glial cell wraps around two adjacent axonal fibres to form the myelin sheath. Schade and Forde (1965) have since presented the view that processes from several glial cells are required to form the myelin laminations of a neuron in the CNS. This latter theory, if true, could account for the unequal number of myelin laminations observed around the same axon within a relatively short distance.

Cytochemical analysis of PNS myelin was reported to demonstrate the presence of cholesterol, phospholipids, certain cerebroside and some fatty acids (Finean, 1957). It was also reported that there is very

little free water between the lipid and protein layers of the sheath. A proteinaceous material within the sheath sometimes forms a reticulum, the neurokeratin network. Structural variations in the pattern of this net has been correlated with the type of fixative used to prepare the tissue for light microscopy (Huber, 1957).

The thickness of the myelin sheath in the PNS was measured and found to be directly correlated with the diameter of the axon (Schmitt and Bear, 1937); Taylor, 1940, 1941a,b; Werndle and Taylor, 1943; Sanders, 1948). A direct structure-function relationship has been shown to exist between also the propagation velocity of the impulse and the diameter of the nerve fibre (Gasser and Grundfest, 1939).

Dendrites

In 1838 Schleiden and Schwann introduced their Cell Theory. Their presentation was soon followed by the recognition and development of some of the important principles and techniques for tissue fixation and staining. These techniques were applied to a wide variety of tissues, including those of the nervous system. The cytoplasmic stains that were used in those early studies gave a somewhat uniform chromophilia of neuroglial and neuronal cell bodies and a chromophobia of their respective processes. Such results made it difficult for the investigators of that period to correlate the relationships between the various cytological structures they observed. Nevertheless several histologists of the classical descriptive period (1840-1900) contributed to the discovery that nerve processes were of two kinds, axons and dendrites, and that they were structurally and functionally related to nerve cell bodies. Polyak (1957), in his monumental publication, The Vertebrate Visual System, cites several early investigators who made significant contributions to our knowledge concerning such structure-function relationships in nerve tissue; the references cited are as follows: Remak (1839, 1853, 1854), Helmholtz (1843), Corti (1850, 1854), Koelliker (1854), J. von Gerlach

(1858), Stilling (1859), Deiters (1865) and Schultze (1866, 1869, 1872, 1873).

The early recognition that a nerve impulse could be conducted away from the cell body for long distances by an elongate axis cylinder (Bell and Magendie, circa 1835) probably led to the general acceptance of the term axon for that nerve process. The resemblance of dendritic arborizations within the CNS to dichotomous branching patterns in trees resulted in their being named after dendron, the Greek noun for tree.

The cytological differences between axons and dendrites was summarized by Barker (1901) in his review of brain histology. He described dendrites as neuron processes originating directly from the perikaryon or as branches of other dendrites. They were seen to emerge from the perikaryon as a wide oval cone with a gradual diminution in their diameter "owing to manifold subdivision" (Barker, 1901). He reported that the structural similarities between dendrite and perikaryon cytoplasm formed the basis for the theory that dendrites were protoplasmic extensions of the cell body. He stated also that the dendritic branching would result in an enormous increase in the neuron's protoplasmic surface area. Barker's review did not report on or indicate whether any quantitative determinations had been made on dendritic diameter and surface area variations.

Dendrites were further differentiated from axons by their "prickle-like projections" (Barker, 1901); Cajal (1899) was able clearly to observe these with both Golgi and with methylene-blue preparations. These lateral buds originally were termed gemmules; in the current literature they have become known as dendritic spines (Valverde, 1967; Snider, 1967; Globus and Scheibel, 1967). Dendritic varicosities sometimes were observed to be present after various techniques for tissue preparation; their presence was also noted to accompany certain types of brain pathology (Mungai, 1967).

No special significance had been attached to these varicosities since it was difficult to determine if they were artifacts of fixation, dehydration or staining procedures.

Specific areas of the mammalian CNS may be identified by their general dendritic architecture which, within certain limits of structural variation, is retained as species constant. An authoritative neuroanatomy text by Truex and Carpenter (1964) summarized in illustrative form Fox's studies (personal communication) of Golgi preparations in monkey CNS. Neurons that were cited as characteristic examples are as follows: Purkinje cell of cerebellar cortex, pyramidal cell of cerebral cortex, neuron of inferior olivary nucleus, granule cell of cerebellar cortex, small gelatinosa cell

of spinal trigeminal nucleus, ovoid cell of nucleus of tractus solitarius, large stellate cell of reticular formation, spindle cell of substantia gelatinosa of spinal cord, large neuron of spinal trigeminal nucleus, neuron of putamen of lenticular nucleus, double pyramidal cell from Ammon's horn of hippocampal cortex, neuron of thalamic nucleus and a neuron from globus pallidus of lenticular nucleus. The dendrites in all of the foregoing examples are never sheathed by myelin and usually show acute angles at points of branching.

Several important subclassification schemes have been proposed for both pyramidal and for stellate cells. Colonnier (1964b) studied Golgi preparations of sections cut tangential to the pial surface in the visual cortex of the cat. He reported that in pyramidal cells the basilar dendrites are arranged in a spreading pattern according to one of the following: (a) circular, (b) right angle cross, (c) elongate oval. The apical terminations of the same cells are (a) elongate bushy or (b) circular bushy. The dendritic spread of stellate cells, when viewed in the same plane of section, is in the form of (a) elongate disks or (b) elongate cylinders that are orientated in the antero-posterior direction in the cat gyrus lateralis; the directional orientation of the long axis varies, however, in different mammals.

Colonnier (1967) studied radial sections of Golgi

preparations in the cat visual cortex and categorized three basic types of pyramidal cells according to their apical dendritic branching patterns. Cell type 1 has a relatively long apical shaft prior to its first order of branching and is found in cortical layer III. Cell type 2 has a short apical shaft which soon bifurcates and is located in the upper areas of cortical layer II. Cell type 3, found in the upper part of cortical layer I, is "deprived of its apical dendrite" and has a stellate type of dendritic arborization with numerous spines.

The structural variations of neurons in the reticular formation of the brain stem in the cat was extensively studied by Ramon-Moliner (1962a, 1962b, 1963) and by Ramon-Moliner and Nauta (1966). They observed that most of the neurons in that system have an ovoid perikaryon with approximately equal numbers of dendrite trunks. Ramon-Moliner (1962) proposed a classification scheme which is based on "dendroarchitectonics" and consists of three major groups of neurons. The major groups proposed were: (a) isodendritic, (b) allodendritic and (c) idiodendritic.

Ramon-Moliner's scheme is interesting to consider. The isodendritic cell is the most prevalent type of this scheme to be found in the brain stem regions which he studied. He observed that the dendrites of this cell have few branch sections and these are generally longer

than the trunk from which they originate. These dendrites have a pronounced tendency to form straight lines and are said to be "relatively rectilinear" (Ramon-Moliner and Nauta, 1966). As the dendrites emerge from the perikaryon they gradually taper to form a fine smooth-walled process. They intermingle freely with heavily myelinated fibre bundles. Very few spines were observed on these dendrites. The structural dendritic pattern of the isodendritic neuron in the cat was found to bear morphological similarities to neurons in the tegmentum of the dogfish shark, Squalus acanthias, and to the spinal cord of the lamprey, Petromyzon marinus. It was therefore postulated that this relatively undifferentiated neuron "represents a pool of pluripotential neurons which in the course of phylogeny have remained relatively undifferentiated and in charge of processing afferent signals of very heterogeneous origin" (Ramon-Moliner and Nauta, 1966).

The allodendritic neuron has a larger number of short dendrite branches which generally overlap each other as an open or loose reticulum. The terminal portions of the dendrites have a tendency to form wavy lines.

The idi dendritic neuron, in marked contrast to the other two groups, has a far greater number of successive branch points. The ends of the branches form a "tight reticulum" with each other as a result of wavy

and tufted terminations. The dendrites do not intermingle with axonal fibres.

Two groups of cells in the cat brain stem were reported as examples of an allodendritic nucleus; these were the dorsal and ventral tegmental nuclei of Gudden. No other dendritic nucleus was found within the brain stem from the medulla oblongata to the mesencephalon. This area within the brain stem was therefore called a "dendritic continuum".

The three-dimensional orientation of the dendritic territory of these neurons also was studied by Ramon-Moliner (1962). If the height of an imaginary linear cylinder, which could contain all the dendrites of a given neuron, were greater than its diameter then the dendritic territory of that neuron was described as having a linear (unidirectional) orientation. When the diameter of the cylinder was greater than its height, the dendritic territory was said to have a planar (bidimensional) orientation.

A new classification scheme for cortical neurons in the rabbit visual cortex was recently presented by Globus and Scheibel (1967). The scheme is based on an attempt to provide functional correlates between dendritic orientation, dendritic spine density and axonal pathway with afferent-efferent circuitry in the cortex.

Class I cells in this scheme total 80% of the

neuron population in the visual cortex; the largest portion of these (75% of total) are pyramidal, the balance (5% of total) are inverted pyramidal cells. The modular dendritic field of each of these is rigidly orientated within an elongate cylinder. The diameter of the horizontal spread of the apical arborization was reported to be the same as the basilar spread, with a maximum variance of only 15%. The dendrite territory is referred to as lying within "a cylinder of cortical tissue". A high density of dendritic spines is characteristic of Class I neurons. The spine population was expressed as number per micron and was reported to be 0.75 for the apical dendrites, 0.4 for oblique and terminal branches and 0.3 for basilar dendrites. The extracortical axonal length of these pyramidal cells below layer III was determined at a much earlier date by Golgi (1886) and Cajal (1911). Globus and Scheibel (op.cit.) have postulated that all pyramidal axons below layer II may have extracortical trajectories. The authors may not have meant to include all axon collaterals but this contentious point was neither expanded upon nor clearly stated. Sholl (1956) estimated that cortical axons which originate as collaterals outnumber the afferent fibres by three to one. Class I neurons were characterized as having long trajectory axons of extracortical length.

Class II neurons in the Globus-Scheibel scheme

comprise 20% of the cortical neurons in the rabbit visual cortex. They are represented by three cell types: stellate (10-15%), fusiform (3%), and spindle (3%). Each cell type has, in comparison with each of the others, a highly variable structural dendritic pattern; they share, however, other morphological characteristics which form the basis of the classification scheme. In contrast to the modular rigidity of Class I neurons, the dendritic field of a Class II neuron may appear in a variety of modular geometric domains. Spindle cells are circumscribed by a truncate cone, stellate cells either by an ellipsoid or by a sphere of varying size, fusiform cells by an elongate cylinder that lies vertical to the pial surface. The diameters of these domains vary from 100 to 1000 microns. Most of the Class II neurons have spineless dendrites; in a few exceptions the spines are relatively long and curved and appear to be isolated. The density of spines is approximately 0.2 per micron. All axonal lengths in Class II neurons remain intracortical; neurons in this class are therefore Golgi type II cells. The axon trajectory of one of these neurons is, in some cases, limited to the dendrite territory of its own soma while in others it may spread widely to other cortical areas.

The Globus-Scheibel scheme postulates a structure-

function correlate in which cortical neurons with large numbers of cortical afferents have, as part of their circuitry, large numbers of dendritic spines. The spines presumably increase the receptive field for functional accommodation of intra- and extracortical afferents. A criticism of this postulate is that pre-synaptic transmission need not selectively terminate on dendritic spines. The authors have therefore stated that the presence or absence of spines is more indicative of the nature of the neuronal output than the afferent input.

The tangential organization of dendrites in the auditory areas of the cat's cerebral cortex was the subject of a recent study by Wong (1967). The gyri investigated were the middle ectosylvian gyrus, posterior ectosylvian gyrus and the suprasylvian gyrus. The first two gyri have been defined as auditory areas and the latter as an association area by Woolsey (1961), using electrophysiological techniques, and by Rose (1949), who used histological techniques. Wong did not make serial sections of the entire gyri since the maximum size of the cortical tissues he ablated was 5 mm of gyrus length. Sections were prepared after the Colonnier (1964) modification of the Golgi-Kopsch method. The tangential extents of the basilar dendrites of pyramidal neurons in all layers of the gyri have

either circular or oval geometric modular fields. Apical terminations appeared oval and orientated in a vertical direction but the author reported inconclusive results due to the small number (2 specimens) studied. Dendrites of stellate neurons in all cortical layers may have either circular or oval geometric fields. In the suprasylvian gyrus the geometric domains of practically all basilar dendritic trees are circular and their mean diameter in this gyrus is smaller than corresponding geometric domains in the middle ectosylvian and posterior ectosylvian gyri. The greatest portion of basilar dendritic fields in the posterior ectosylvian gyrus are circular; in the middle ectosylvian gyrus the ratio of circular to oval fields is 6:1. The numbers of circular and oval fields of stellate neurons are approximately equal in the three gyri. The mean of the stellate dendritic field diameters in the suprasylvian gyrus is larger than for similar cells in the other two gyri.

In addition to the qualitative studies on dendrite geometric domains, several quantitative analyses have been conducted on dendrite patterns. Following is a list of the quantifiable parameters which will be discussed in this review of the literature:

- a) Mode of dendrite branching.
- b) Origin, number, length and diameter of dendrite branches.
- c) Radius of dendrite trees.
- d) Growth pattern of dendrites.

a) The mode of dendrite branching in all types of cortical neurons is by dichotomous division of the dendrite process (Sholl, 1956; Bok, 1959). There have been no reports of polychotomous branching of dendrites. The studies just cited showed that in some pyramidal neurons the main apical shaft gives off collateral branches which are obliquely directed to the linear axis of the shaft. In other types of pyramidal arborization patterns the main shaft has very few side branches of small diameter and is seen to terminate abruptly at a major point of bifurcation.

b) The origin of dendrites from the perikaryon, in all pyramidal neurons, follows a pattern that lies within narrow limits of variation. A single apical shaft emerges from the apex; basilar dendrites, which number from four to six, emerge from the sides, basilar corners and base of the triangular perikaryon. In fusiform neurons there are two main dendritic shafts which emerge from opposite poles of the perikaryon. Stellate neurons have from three to nine dendrites

which emerge randomly from the radiate points of the perikaryon (Ramon-Moliner, 1962; Mungai, 1967). A structural dendritic polarity in stellate neurons is therefore absent.

Number of dendrite branches. Bok (1936b) made several attempts to relate the number of dendrites of a neuron with the depth of its perikaryon in the cerebral cortex. He based his studies on a few drawings that had been made originally by Cajal and were from highly selected pyramidal neurons. Bok concluded that the number of dendrites is larger in neurons whose cell bodies lie in the deeper layers of the cerebral cortex than it is in neurons which are merely sub-pial in position. A study by Sholl (1953, 1955), on the visual cortex of the adult cat, was done subsequent to Bok's work. Sholl reported that in more extensive samplings there was no simple relationship between the number of branches and the depth of the perikaryon. Neither Bok nor Sholl were able to demonstrate a relationship between the number of dendrite branches and the volume or surface area of the perikaryon.

A dendrite section was defined by Bok (1936a) as that region of a dendrite between the perikaryon and its first bifurcation, between successive branch points or the region from the last branch point to its terminal end or point. Mungai (1967) has shown that

dendrite sections vary widely in their length, from 3-268 microns in pyramidal, and from 3-396 microns in stellate neurons. In the same study Mungai divided the dendritic arborization of all types of cortical neurons into three zones. In his scheme the stem zone consists of the dendrite section between the perikaryon and the first branch point, the branching zone comprises all the dendrite sections from the first to the last order of branch points and the terminal zone forms the dendrite sections from the last order of branch points to the terminal endpoints.

Mungai (op.cit.) studied the number of dendrite sections in each of the zones of neurons in the posterior sigmoid gyrus of the adult cat. The count in each zone was expressed as a percentage of the total number of dendrite sections in the neuron. The smallest percentage of the total number of dendrite sections was observed in the stem zone, a greater percentage in the branching zone, while the largest percentage was seen in the terminal zone.

Sholl (1953) introduced a new parameter for his analysis of dendrites in the visual cortex of the adult cat. A set of concentric spheres, with each sphere increasing its radius by 20 microns over its predecessor, was superimposed over camera lucida tracings of a perikaryon and its dendritic pattern. In stellate

neurons and in basilar dendrites of pyramidal neurons there is an exponential decline in the number of dendrite branches as the distance from the perikaryon increases.

One of the earliest quantitative studies on dendritic lengths was conducted by Bok (1936a, 1936b). In pyramidal cells the initial bifurcation in basilar dendrites occurs closer to the perikaryon than that found in apical dendrites. Bok therefore concluded that basilar dendrite sections in the branching zone become progressively longer as the distance from the perikaryon increases.

In the examination of five basilar dendrites from one small cerebral pyramidal neuron, Bok (1936b, 1959) concluded that the first order of bifurcation in each case occurs at a constant distance from the cell body. He claimed that the second order of bifurcation occurs at distances that are twice as far from the cell body as are the preceding branch points. Sholl (1953, 1955, 1959) was able, in a later work, to disprove Bok's claim for such a regular relationship between the length of a branch section and its predecessor.

The diameter of dendrite branches in Golgi and in Nissl preparations was not examined quantitatively by the classical neurohistologists. In Barker's (1901) review of neurohistology, dendrite diameters were reported simply as becoming successively narrower with

each branch bifurcation, until they assume a uniform diameter at the terminal area. In a thorough study of dendrites in the visual cortex of the cat Sholl (1959) was unable to find a specific relationship between the mean diameter of dendrite branches and any of the following parameters:

- i) length of dendrite sections
- ii) number of dendrite bifurcations per neuron
- iii) volume or cortical depth of the dendrites' own perikaryon.

Mungai (1967) examined the diameter of dendrite sections at the approximate midpoint between their bifurcations. He measured the diameters of basilar dendrites from pyramidal neurons and of all dendrites from stellate neurons in the three dendritic zones, stem, branching and terminal. The mean diameters in the respective zones were approximately 3.0, 2.0 and 1.0 microns for both types of dendritic tree. The mean diameters of apical dendrites of pyramidal neurons in the same respective zones were 4.5, 2.5 and 1.0 microns. Mungai referred to his measurements as "approximatelyzonal average diameters".

c) The radius of dendrite trees was studied by Bok (1936a, 1936b, 1959). A dendrite tree, as defined by Bok, consists of all the dendrites and their branches in a single neuron. The radius of a dendrite tree refers

to the mean distance between the dendritic endings of basilar dendrites and the perikaryon. Bok made camera lucida drawings of basilar dendrites from a few small pyramidal neurons in an unidentified area of the cat's cerebral cortex. Concentric spheres were placed over these drawings and the length of each dendrite section was measured. Bok concluded that the total length of a dendrite with all its sections, in each neuron, is proportional to the square of the radius of its dendrite tree.

Bok made various measurements related to the radius of the dendrite tree that are worthy of mention. On the basis of his findings Bok concluded that the surface area of the perikaryon is proportional to (a) the size of the dendrite tree and (b) to the nuclear volume of the perikaryon. Accordingly then, the radius of the dendrite tree is proportional to the nuclear volume. Bok stated this proportionality, somewhat colloquially, in the following manner: "The larger the nerve cell, the larger its dendrite tree".

(d) The growth pattern of dendrites. According to Bok (1959), the size of dendrite trees in the cerebral cortex of mammals is influenced by the linear dimension of the animal's body. The dendrite growth in different animals would therefore be expected to form

dendrite patterns of different sizes. A technique which could determine the exact nature of the growth pattern in different animals would require a comparison of homologous neurons in cortices of different animals. Since this seemed an impossible task a simplified plan of a dendrite arborization pattern was drawn and several possible variations for growth of the original plan were made. Subsequently, examinations of Golgi preparations were made of rat, mouse, guinea-pig and rabbit cortices. Three principle types of dendrite growth patterns were identified. In the first type, which was called additive growth, new and larger sections are added to the former end points. In the second type, termed proportional or isomorphic growth, all the dendrite sections in the tree are increased in linear length as the tree grows. These first two types of growth are characterized anatomically by an increase in the radius of the dendrite tree. In a third type of growth the radius of the tree remains unchanged; however, an "intensification of the ramification process" (Bok's term) occurs, which increases the number of bifurcations.

The Synapse

The classical theory that nerve cells form a histological reticulum with protoplasmic continuity was postulated by Gerlach (1871), Golgi (1885, 1890, 1891), Held (1905, 1909, 1929) and others. The alternative neuron theory was proposed by Waldeyer (1891) as a consequence of the studies by Forel (1887) on the selective atrophy of nerve cells following axon transection; the studies by His (1886, 1889) on the development of individual neuroblasts and the numerous investigations by Cajal (1888, 1890a, 1890b, 1890c) on embryonic material as well as Cajal's observations on the staining characteristics of the Golgi technique on cerebral cortical neurons.

The overwhelming evidence in favor of the neuron theory also contributed to a concept of functional continuity between neurons. Sherrington (1897) introduced the term synapse, from the Greek verb to clasp, to designate the area of functional contact between two neurons. Sherrington (1900) attributed the characteristics of the reflex arc to the unidirectional transmission of the nerve impulse at the synapse. He theorized that the one-way conduction pathway of axon to dendrite was the result of a synaptic valve-like mechanism. Cajal (1895, 1909) and Van Gehuchten (1892) theorized that the unidirectional flow was the result

of "dynamic polarization" at the synapse.

The principal structural components of the synapse consists, according to general agreement among neurohistologists, of the terminal presynaptic axoplasm and axolemma, the synaptic gap or cleft, the postsynaptic membrane and its adjoining endoplasm. Structural variations of axonal terminals form the basis of a morphological classification scheme that was proposed by Cajal (1909): Type I endings have small buds and are called synaptic boutons; Type II endings are relatively large and have neurofibrils in the form of a network; Type III endings have neurofibrils in the form of compact groups; Type IV endings are small dilations that form rings. Cajal was also able to postulate on the basis of his light microscope observations that these terminations form axosomatic, axodendritic and axoaxonic synapses. Cajal measured the size of these terminations in mammals and found them ranging from 0.5u to 7.0u in diameter (Cajal, 1909). Bodian (1942) described fish neurons having synaptic endings that are 10.0u in diameter.

The ultrafine structure of the synapse was described by Hyden (1960) in his review of the neuron. The terminal presynaptic membrane has a characteristic thickening that is about 60 \AA at the junction. The synaptic gap, or cleft, varies from 100 \AA to 300 \AA wide.

The size of the gap in the CNS is the basis of a two-type classification scheme that was proposed by Gray (1959).

Type I is found on dendritic spines and shafts; the synaptic cleft is 250-300 Å wide and most of the pre- and postsynaptic membranes adjoining the cleft are 100-150 Å thick. In Type II, found on the soma, the synaptic cleft varies from 120 to 200 Å wide and only 30-40% of the pre- and postsynaptic membranes are thickened. Gray (1967) has postulated that Type I synapses are entirely excitatory while Type II are entirely inhibitory in action. The presynaptic endoplasm is characterized by the presence of membrane-bound vesicles that range from 200 to 650 Å in diameter (de Robertis and Bennett, 1954b, 1955; Palay and Palade, 1954). These vesicles may be carriers of a mediator substance which propagates the nerve impulse at the synapse (Gray and Whittaker, 1960). The excitatory mediator is assumed to increase the permeability of the postsynaptic membrane to all extracellular ions, causing a rapid sequence of events which depolarizes the membrane and results in postsynaptic nerve impulse conduction. The inhibitory mediator is believed to increase the permeability of the postsynaptic membrane selectively to chloride and, possibly, potassium, ions. This causes the postsynaptic membrane potential to approach the equilibrium potential for these ions,

a situation which results in postsynaptic hyperpolarization (review by Eccles, 1949).

The shape of synaptic vesicles following their initial fixation by glutaraldehyde was observed by Vchizono (1965). He noted that cortical synapses which were shown by electrical studies to be of the excitatory type have round vesicles, while similarly demonstrated inhibitory synapses contain flattened vesicles. Bodian (1966) described three morphological types of cortical synaptic vesicles: type S are spheroid with an agranular content, type F are flattened with an agranular content and type G are large rounded vesicles with granular content. No structure-function studies on these structures have as yet been reported.

Electrical studies by Clare and Bishop (1955), Chang (1955) and Eccles (1955) have shown that the postsynaptic potentials induced by presynaptic activity will spread electrotonically with gradual decrement in the postsynaptic cell membrane. Coombs, Eccles and Fatt (1955) showed that the amplitude of postsynaptic potentials in dendrites are approximately halved when they reach a distance 200 microns from their point of origin. This led Eccles (1955) to postulate that dendrites of motor neurons were of secondary importance for synaptic function as the distance from the soma increases. Valverde (1961), drawing on studies made with the Golgi technique,

supported Eccles' view by claiming that the number of synapses on the dendrites of giant cells of the brain reticular formation was inversely proportional to the distance of the soma. Kositsyn (1962, 1964), using a modification of the Deinecke (1914) technique, made a similar type of study on the reticular formation of the cat. He found, in contrast to Valverde, that the number of synapses per unit area of dendritic surface remains constant to a measured distance of 400 microns from the soma even though the diameter of the dendrite had been reduced by 67%.

Cragg (1967), by means of electronmicroscopy, measured the synaptic density per cubic centimeter of cerebral cortical tissue. His method could not selectively identify dendritic synapses. Cragg observed densities of $6.5 \times 10^{11}/\text{cm}^3$ in the visual cortex of both the mouse and monkey. He found, as well, comparable densities in the motor cortex of the same two species.

Synapses of an electrical nature, which permit one-way transmission ("rectification") without the mediation of a humoral substance have been described in the crayfish (Furshpan and Potter, 1959). Hama (1961) made an electronmicroscopic study of electrical synapses in the crayfish but could find no structural correlates for the rectifying properties of such junctions. The

electrical synapse, an example of which is the type found in the crayfish, contrasts with the chemical synapse (p. 62) by exhibiting a narrow synaptic cleft of only 100 Å. The pre- and postsynaptic membranes are neither thickened nor electron-dense; synaptic vesicles and tubular structures are found in the synaptic terminations of both pre- and postsynaptic fibres.

Several types of structurally atypical synapses were found in the rat CNS and described by Hama (1966). Accordingly, he suggested new pathways of transmission consisting of soma-axonic and dendro-axonic circuits; these were based on the cytological placement of synaptic vesicles. The same worker found dendrites in very close proximity to each other in rat CNS (ibid). The space between the dendrites was estimated at about 30 Å wide and was filled with electron-dense granules. Intracellular electron-dense granules extended on either side of the plasma membranes for about 60 Å; this resulted in an overall dense layer of about 150 Å. Hama suggested that this structure might be considered as an electrical dendro-dendritic synapse.

Tightly-opposed non-vesicle synapses between two dendrites in the cerebral cortex would enable the reciprocal transmission of nerve impulses and, as well, graded depolarization between two widely separated cerebral neurons. It is possible that Hama's described dendro-

dendritic synapse is an instance of such a situation.
It is unfortunate that Hama did not specify from which
part of the rat CNS he took his illustrated example.

Cytoarchitectonics

The quantitative study of the sizes and population densities of neuronal perikarya in the cerebral cortex is known as cytoarchitectonics. The four salient parameters of the cerebral cortex that are considered in this type of study are as follows:

- 1) Total cortical volume
- 2) Variable thickness of the cortex
- 3) Total number of cortical neurons
- 4) Neuron population density in the cortex.

1) Total volume of the cerebral cortex. The fissuration and folding of the gyrencephalic brain contributes an apparent mechanical deformation of the cerebral cortex (Bok, 1929). The surface curvature of the cerebral hemispheres varies not only between individuals of the same species but also between homotopic left and right gyri in the same individual, as shown by the observation of topographical variations between such contralateral gyri (Sholl, 1955, 1956). According to Sholl (1956) the most reliable method for the determination of cortical volume in a specific individual is a planimetric technique which permits the approximate calculation of cortical surface area multiplied by the mean cortical depth. This technique requires the use of

coronal sections of brain. Some of the estimates for the cortical volume calculated by this method in a single hemisphere in the human are as follows: 290 cm³ (Donaldson, 1895), 274 cm³ (Henneberg, 1910), 289 cm³ (Jaeger, 1914), 286 cm³ (Tramer, 1916). Sholl estimated "an error amounting to 10 percent of the recorded value" for this method. This error factor may indeed be much greater since the studies by Robin et al (1956) and by Hyden (1960) have shown that histological procedures may result in an 80 percent reduction in brain volume. Pakkenberg (1966) noted that shrinkage in brain volume after fixation is 20 percent and that the final volume reduction after histological procedures is 74 percent.

2) Variable thickness of the cortex. The thickness of the cerebral cortex in an individual human brain may vary from 1400 microns in the visual cortex to 2800 microns in the precentral gyrus (van Alphen, 1945; Sholl, 1955, 1956). These studies showed also that analogous cortices in different individuals of the same species may vary in thickness by as much as 1100 microns, as has been found in the human visual cortex. Nevertheless, Sholl was able to demonstrate that the thickness of the motor cortex under a plane pial surface in any individual brain remains reasonably constant at approximately 2650 to 2800 microns. However, cortical thickness

of other regions in the same brain, measured in an identical fashion, may show considerable variation from region to region (Sholl, 1959). It is important to note here that brain tissue blocks only 3-4 mm in length were used in all previous studies that dealt with anatomical parameters of cortical examination.

3) Total number of neurons in the cerebral cortex.

The early descriptive period in the study of neurohistology, 1880-1930, was concerned also with the total number of neurons in the cerebral cortex. Recent correlative structure-function studies on the cortex have shifted the emphasis from this parameter to consideration of the extent of the field spreading between neuron territories.

The results of several studies to determine the total number of neurons in the human cerebral cortex follow: Donaldson (1895) gives a total number of 1.2×10^9 neurons, Thompson (1899) 9.3×10^9 , Berger (1921) 5.5×10^9 , Economo and Koskinas (1925) 1.4×10^{10} , Agduhr (1941) 5×10^9 , Shariff (1953) 6.9×10^9 , and Pakkenberg (1966) provides a figure of 2.6×10^9 neurons as his estimated total. Pakkenberg's studies took into account the degree of tissue shrinkage and the Abercrombie (1946) correction factor for the mean diameter of neuron nucleoli. However, the reliability of these results was probably best summed up by Sholl (1956).

"The interest in these results does not lie so much in their precision as in their order

of magnitude, for 10^9 is a very large number and difficult to visualize."

Sholl, in further evaluating the importance of these results, pointed out that a 1% removal of neurons from the cortex in an area of great redundancy will have no outwardly detectable effect, but a 1% ablation from the visual or motor cortex may lead to blindness or paralysis.

4) Neuron population density in the cerebral cortex.

Several studies have shown that the neuron packing density in the cerebral cortex may be related to a) the gross size of the brain, b) the volume of the cortex, c) the region of the cortex, d) the number of neurons in the cortex, and e) the size of the perikarya at different cortical depths. Tower and Elliott (1952) and Tower (1954) noted that the neuron population density (NPD) decreases as the size of the brain increases. They give, for example, a figure of 142.5 neurons/ 0.001mm^3 for the mouse, for guinea pig 52.5, for cat 30.8, monkey 21.5 and for human 10.5. Sholl (1956) noted that there is considerable variation in the NPD observed at different regions in the cortex within an individual brain. Klotz and Clark (1950), in a similar study, reported that analogous cortical regions in different animals of the same or different species show considerable variation in the NPD. The packing density of neurons in the visual cortex of a monkey, Macaca mulatta, has been reported as 160 neurons/ $.001\text{mm}^3$ (Chow, Bloom and

Bloom, 1950) while Sholl (1956) found the density in a cat visual cortex to be $72/\mu^3\text{mm}^3$. Sholl (1959) computed the NPD in selected cortical regions from man, cat and mouse. In man and cat the density ranged from 30 to 60 in a cortical cylinder of $400\mu^2$ bounded by the pial surface and the bottom of the cortical grey matter. The higher figure was found always in the visual cortex. The number in the mouse nonvisual cortex was about 14 for a similar cortical cylinder. The mean densities in the nonvisual area, when plotted against the relative depth of the cortex, shows a single minimum at about one-third of the cortical depth. This is followed by a single maximum at a lower depth. Although Sholl stated that the functional significance of this variation in density is unknown, he postulated that a) a low NPD would permit a greater concentration of nonperikaryal structures, for example, blood vessels, neuroglia, dendrites and axons; and that b) topological and cortical depth variations with specific connectivity patterns would alter the demands on the neuron population density.

Dendritic Spines

Spinous projections of dendrites in the cortices of the mammalian cerebrum and cerebellum were extensively described by Cajal in 1891. Later, however, Cajal (1909) and other investigators apparently came to hold the view that the observed "spines" might be the result of a staining artifact. The final acceptance that spines do in fact exist as functional entities and are partially membrane bound came in 1959 when Gray observed their presence with the aid of the electronmicroscope.

Jacobsen (1966) used both visible light and electronmicroscopy to study dendritic spines in adult rat, cat, squirrel, monkey and man. His findings confirmed those of the classical neurohistologists in that he observed spines to be abundantly present over most of the apical and basilar dendrites in cerebral cortical neurons. Spines are absent from the following regions (of the neuron): a) the perikaryon, b) the proximal portion of dendrite origin and c) the axon. According to Jacobsen those dendrites with a mean diameter of 1.4 microns have spines which consist of a) a narrow stalk 1.0 micron in length and 0.3 micron in diameter, and b) a terminal bulb whose diameter is 1.0 micron. The mean length of the entire spine is 2.0 microns. There have been no reports to this date on spine dimensions in larger dendrites. Mungai (1967)

studied the spine density on pyramidal neurons in the posterior sigmoid gyrus of the cat. In apical dendrites the lowest spine density is found in the stem zone while the highest spine density is found in the branching zone.

Gray (1959), in an electronmicroscope study of the visual cortex in the rat, observed what he has taken to be synaptic contacts at the terminal portions of dendritic spines. The granular dendroplasm of the spines which Gray observed was devoid of microtubules and neurofibrils. They did contain, however, a "spine-apparatus". The latter was described as consisting of a series of membrane-bound sacs separated by sheets or plates of dense material. The spine-apparatus has been found also in the mammalian hippocampus (Hamlyn, 1961, 1962) and in the neocortex of a number of mammalian species (Pappas and Purpura, 1961; Rosenbluth, 1962). The results of several recent studies (Gray, 1961a, b, 1962a; Boycott, Gray and Guillery, 1961) indicate that the spine-apparatus is found only in the mammalian cortex. Gray and Guillery (1963) observed that in the sensorimotor cortex of the dog there is a ribosome-like structure attached to the spine-apparatus. The apparatus is found also in dendritic trunks of the lumbar dorsal horn in cat and rat spinal cord. Gray and Guillery proposed a general theory in which the spine-apparatus "plays a special role in the activity of the postsynaptic region".

The neuronally receptive area of one neuron in comparison to another neuron may be increased by increases in the number and length of dendrite branches and of spines (Gray, 1959; Bok, 1959). An example of a quantitative study on the number of dendrite spines on a single Purkinje cell of the cerebellar cortex was made by Fox and Barnard (1957). They reported that there were, on one of these neurons, 61,000 dendritic spines whose total length of 40,700 microns gave an estimated combined receptive surface area of 222,000 square microns.

Histology of the Isolated Cerebral Cortex

The technique of the neuronally isolated cerebral cortex has become an important tool in neurophysiology (Burns, 1958). An isolated slab of cerebral cortex is without any afferent activity from surrounding fibres. The isolate affords an opportunity to determine, among many things, the properties of endogenous spontaneous neuronal activity in the cortex. Neuronal isolation of cortical tissue in situ involves fine cuts made into the brain substance (Burns, 1951; Burns and Grafstein, 1952). The nature of this thesis study, therefore, necessitates a detailed examination of the historical literature that is relevant to the histological and cytological reorganization of the cerebral cortex following surgical lesions.

Cytological preservation. The histological effects resulting from surgical lesions, usually fine scalpel wounds, in the cerebral cortex of mammalian species, was studied by several classical neurohistologists. These studies were extensively reviewed by Cajal and his conclusions and comments were published in the Spanish language in 1913 and 1914. These publications were revised, and translated into English, by R.M. May in 1928. Cajal wrote that the affected nervous protoplasm dies after the initial incision; this result

is preceded, for a short time, however, by Preservatory Necrosis, i.e. "necrosis associated with the most perfect morphological integrity".

Axon preservation. The preserved area of axons lies distal to the Zone of Corrosion. This zone is defined as the site of the scalpel wound. Initial cytological changes occur on the proximal part of the axon. The initial morphological changes are hypertrophic stumps of surviving axons with irregular dilated terminations called retraction balls. Two days after the incision the terminations from living axons will form glomeruli, hooks and, occasionally, both of these. A few of the axons, however, become pale and their axoplasm somewhat granular. Cajal noted that axon terminations which are best preserved are those which remain in the plasma exudate that forms from interstitial haemorrhage. Myelinated and unmyelinated cut axons are perfectly preserved for as long as eight days in the coagulum. Part of the same axon, situated for the same length of time in a zone free of the exudate, will show signs of cellular degeneration. Cajal stated: "In the phenomenon of preservation a great part is played by some antiautolytic principle which proceeds from the sanguineous exudate and is fixed in the protoplasm of the axon."

Dendrite preservation. Cajal observed that the proximal ends from cut apical dendrites of pyramidal

neurons appear to be little changed by the trauma after post-lesion period of several days. At the site of the incision the dendrites, in Golgi preparations, appear denser and somewhat darker. The dendritic ends become tapered out and in some instances may bend backwards for a few microns. The entire length of the dendritic distal stump undergoes atrophy and corrosion. The terminal end of the stump on the side of the perikaryon disappears. The new termination displays compact neurofibrillar bundles which are hyperchromatic to silver nitrate. Dendrite stumps in the sub-pial area are slightly tortuous and display paler neurofibrils.

Cytological degeneration.

Dendrite degeneration. There is a complete absence of retraction balls, varicosities, sprouts and the neurofibrillar reaction in degenerating dendrites. The process of Wallerian degeneration (Waller, 1852) of axons is not found in dendrites. Cajal expressed the opinion that in cerebral wounds the "lesion of the large dendrites and especially of the radial (stem zone) trunk is much more serious than that of the axon".

Axonal degeneration--Distal stump. White matter.

The distal stump refers to the axonal fibre which is separated from the perikaryon. Two regions of degeneration occur in axons of pyramidal distal stumps after an incision is made in the white matter. The necrosed

segment, the cut end of the axon, appears to be very rapidly resorbed. Two hours after the trauma the necrosed segment has disappeared. Cajal noted that in a few instances the necrosed segment was represented by a series of grains.

The degeneration segment, a few microns behind the necrosed segment, displays the initial signs of traumatic degeneration. Within a few hours of the incision the degenerative changes form retraction balls, rings, or both. The neurofibrils form a complicated reticulum within the core of the ball. A portion of the retraction ball has a clear area which was termed by Cajal as the hyaline area. Myelin sheaths remain around retraction balls and varicosities. Twenty-four hours after the incision helical structures sometimes form along the axon. Some axons, however, display granular disintegration for long distances. Soon afterwards, the distal stump dies and disappears.

Gray matter. Within the first few hours of the incision the necrotic segment of the distal stump undergoes rapid resorption. The degeneration segment may form one of several types of retraction balls. Large axons of Betz cells form retraction balls with neurofibrillar reticulae. Retraction balls of narrow axons are proportionately smaller. In some instances it was noted by Cajal that a thin and tortuous axonal thread winds out from a retraction ball towards the site

of the lesion. Certain axons have retraction balls with a dense neurofibrillar core which is capped with a hyaline area. These latter types lack extended threads. Two or three days after the incision the terminal balls become completely hyalinized. The varicose thickenings, however, persist.

Degeneration of the proximal stump. White matter and deep grey matter.

The proximal stump refers to the axonal fibre that has retained its connection to the perikaryon. The necrotic segment is very small and disappears soon after the incision. The degeneration segment in the proximal stump is much shorter than its counterpart in the distal stump. The degeneration segments of large axons are confined to retraction balls. The presence of a neurofibrillar reticulum in the terminal dilation always precedes the formation of a retraction ball. Small myelinated axons, however, form rings at their terminal ends. These rings are sometimes preceded by glomeruli and spirals.

Three days after the incision cut axons clearly display four distinctive degenerative regions:

a) Terminal retraction ball. The size of the ball is proportional to the axon diameter. Some balls undergo autotomy, i.e. free balls.

b) Varicose segment. A linear series of thickenings that extends towards the neuron.

c) Hypertrophic segment. A distinctive longitudinal swelling of the axon occurs above the varicose thickenings. The neurofibrils in this area are hyperchromatic.

d) Normal segment. The size of this segment depends upon the site of the wound, i.e. whether in grey or in white matter.

Terminal retraction balls and hypertrophic segments will form only when the lesion occurs in the grey matter distal to the level of axon collaterals. Hypertrophic segments extend up and into the last two or three uninjured horizontal collaterals.

The last pre-existing collaterals extend outwards new horizontal or oblique branches which can be followed for long distances. The new collaterals do not grow through the cortical incision. The extracortical axon is permanently lost. In consequence of the above events Golgi type I pyramidal cells are apparently transformed into Golgi type II cells. Cajal conjectured that the propagation of the nerve impulse down the mutilated axon would not be lost, but would be diverted along the collaterals and new branches.

Retraction balls and hypertrophic segments are not formed when the site of the incision occurs proximal to the level of the last collateral. Cajal believed that these cells "have suddenly been killed and preserved".

Incisions in the sub-pial region interrupt myelinated and unmyelinated axons from collaterals of Pyramidal and Martinotti cells. The proximal stump of these axons form necrotic and degeneration segments. These segments are larger than the counterparts in the deeper layers of the grey matter.

Soma alterations. According to Cajal the somata of several types of cerebral cells are affected by cerebral cortical incisions. The following descriptions include the most frequent anatomico-pathological cell types.

a) Granular neurons. These nerve cells repel silver impregnation after the incision and are then granular in appearance. The nucleus in affected cells is usually peripheral in position.

b) Hirudiform neurons. This type of cell is rare and is found only after a large incision has been made. The cells have short axon collaterals. A neurofibrillar mesh occupies the perikaryon and varicosities. These cells are usually lost seven days after the incision.

c) Vacuolated neurons. Cytoplasmic vacuolation occurs in the perikarya of large pyramidal cells whose axons have been cut distal to their collaterals. The nucleus is peripherally displaced and may bulge out into the apical dendritic shaft.

d) Pycnotic neurons. The somata of these cells are elongate and are hyperchromatic to silver impregnation. These cells have normal axons whose collaterals are unaffected by the incision.

e) Chromatolysis and Golgi fragmentation. The mutilation of the axon has a pronounced effect upon the Nissl granules and Golgi complex. The reticulum of the Golgi net becomes fragmented and granular. Complete lysis of the complex precedes the death of the cell. Chromatolysis of the Nissl granules starts from the centre of the perikaryon and rapidly spreads towards the peripheral region.

The effects of craniotomy on fibre degeneration in the cerebral cortex of rabbits and cats was reported by Harris (1960). Experimental craniotomy over the ectosylvian, suprasylvian and marginal gyri is associated with fibre degeneration. Axonal degeneration occurs in all layers of the cerebral cortex. The extent of fibre degeneration is proportional to the amount of bone and dura cut away. Harris also observed that the greatest amount of degeneration occurs when the pia mater is allowed to dry even for a few seconds. No evidence of any other degeneration or necrosis was found in the cerebral cortex. Experimental craniotomy without dura incision does not result in fibre degeneration.

Colonnier and Gray (1962) and Colonnier (1964)

studied the effects of undercutting the rat visual cortex. They examined the changes in the ultrafine structure of the bouton terminale of the cortical axons. Twenty-four hours after the incision the mitochondria become electron opaque. The cytoplasm forms granulations and appears electron dense. The synaptic vesicles are no longer present as discrete structures. Neurofilaments are not discernible. Three to five days later the pre- and postsynaptic membrane thickenings are invaginated and are invaded by the phagocytic destruction of neighboring glial processes. The latter form lamellated spirals. During the three to five day period dendrites appear normal. Colonnier noted that by the seventh to ninth day the cortical tissue no longer shows degenerating bouton terminale.

Regeneration in the cerebral cortex.

Axons. Cajal noted that three days after the incision the central stump of myelinated axons will form collateral branches. These branches are formed from the region of the degeneration segment. Collateral branches arise from axonic varicosities and on rare occasions from retraction balls. A varicosity which sends out several branches was termed by Cajal a radial or lestudinoid neoformation. A second type of collateral origin was found to arise from non-thickened regions of the axon. Collaterals which arise from pyramidal cells

are short and end in small dilations.

Dendrites. The occurrence of new dendritic branches in the CNS following anatomical interruption is rare. Cajal noted dendritic sprouting in the spinal cord of a young cat. He observed sprouting following attempts to nerve graft in the spinal cord. These dendritic neoformations were found a short distance from the necrotic segment in the anterior horn of the lumbar spinal cord. The new dendrites sprout directly from the perikaryon and form short radiate and filiform appendices. Many of these new dendrites have a small bulbous termination. Bielschowsky and Gallus (1913) reported similar results in a human brain affected by tuberoscclerosis. Pick and Bielschowsky (1911) observed signs of dendrite sprouting in human cerebral ganglia. Lafora (1914) reported that pyramidal cells of Ammon's Horn in senile dogs form new dendritic branches with dilated terminals. Lafora postulated that a growth stimulating substance is released from the cell protoplasm.

Clemente and Windle (1954) studied the effect on axonal sprouting that is exerted by agents that inhibit the formation of connective tissue. They reported that axon collaterals were able to grow over a gap 1 mm long. There was no evidence of new dendrite sprouts occurring over the treated area. Snider and Del

Cerro (1967) observed drug-induced dendrite spine growth in Purkinje cells in the adult rat cerebellum. Sodium diphenylhydantoin (Dilantin^R) was given in large intramuscular doses over a period of five weeks. The animals developed a type of muscular ataxia that is usually associated with cerebellar damage. The histological effect was observed with the aid of electronmicroscopy. Large lamellar bodies 2 to 4 microns in diameter develop in the form of sprouting dendritic spines. The internal arrangement of the sprouts has a lamellar spiral; these spirals originate from the cell membrane. It was found also that a few axonal terminals and astrocytes develop lamellar spiral bodies. The cytoplasm of the dendritic lamellar bodies is devoid of organelles such as mitochondria. Similarly, synaptic vesicles are lacking in these sprouts. Snider and Del Cerro have suggested that the "dendrites of adult Purkinje cells in the cerebellum display more morphological plasticity than is commonly believed".

Grant (1965) and Grant and Aldskogius (1967) reported on changes in dendritic organization induced by axonal transection. The peripheral portion of the twelfth cranial nerve in kittens was transected and Nauta-Laidlaw preparations were made of the hypoglossal nucleus of the medulla oblongata. The criterion which the investigators used for recognizing a degenerating dendrite was its beaded necklace-like appearance.

Retrograde dendrite degeneration was in most cases traced as far back as the stem zone. Grant and Aldskogius reported that in one specimen the degeneration extended from the middle part of the branching zone to the distal part of the terminal zone. In two other sections the degeneration was traced from the distal area of the branching zone to the ends of the terminal zone.

Globus and Scheibel (1966) noted the effects of deafferentation on the dendrites of the visual cortex in newborn rabbits. The afferent fibres from the lateral geniculate body and ipsilateral optic nerve were cut. Quantitative examinations of Golgi preparations revealed a selective reduction in the dendrite spine density. A significant falloff of spines occurred on the stem zone of pyramidal cells. However, the spine density on the oblique branches in the branching zone remained unchanged. A similar type of analysis was done in the parietal cortex after an incision of the corpus callosum. The results of the latter experiment again showed selective spine reduction. A significant loss in spine density on the oblique branches occurs after callosal incision, while the stem zone remains unchanged.

Jones and Thomas (1962) observed the effects of deafferentation on dendritic organization in the cerebral cortex of adult rats. The olfactory peduncle was obliquely incised in such manner as to separate the

olfactory bulb and tract from the ipsilateral cerebral hemisphere. It should be recalled that the ascending dendrites from the pyramidal neurons in the prepyriform cortex are the final junction for the lateral olfactory tract. The prepyriform cortex was prepared after the Golgi-Cox technique. Deafferentation of the olfactory input resulted in a marked reduction in the number of dendrite sections in the branching zone. The greatest reduction took place in the outer layer of the prepyriform cortex. There was no "obvious reduction" in the number of dendrites in the stem zone or basilar dendrites.

The data from the studies by Globus and Scheibel (1966) and Jones and Thomas (1962) established three important principles. First, structural aberrations result from presynaptic interruption. Second, the results demonstrate that the entire dendritic arborization from one neuron is divided functionally into several specific areas. Third, these findings offer an important technique for determining the specific area of afferent synaptic contact. Each area serves, presumably, for the accommodation of afferent inputs from different regions of the body. This plurality of afferent accommodation in monaxonic neurons indicates an ability for multiple codification in a single dendrite tree and soma.

Purpura and Housepian (1961) studied some of the physiological properties of the chronically isolated cerebral cortex in the immature cat. Several attempts were made to find an histological correlate for the nature of the repetitive discharges in the chronic preparation. The investigators reported that Golgi type I cells with extracortical axonal projections become altered to Golgi type II cells with intracortical axonal trajectories. These latter results confirmed earlier findings that were described by Cajal (1913-1914). Purpura and Housepian (op.cit.) also stated that the isolation "procedure did not alter the normal progression of dendritic differentiation of cells within the isolated slab". They reported further that basilar dendrites of pyramidal neurons were not altered in their maturation process. The methodology they used for their qualitative and quantitative histological determinations was, unfortunately, not published.

The effect of chronic isolation on neuron population density was studied by Cajal (1928), Sastry (1956), Echlin (1959) and by Reiffenstein (1964). All these investigators reported an overall reduction in the cell density. Cajal and Echlin pointed out that the most characteristic histological feature of chronic isolation was the complete dropout of the large Betz cells of layer V. Cajal noted that Golgi type II cells and pyramidals whose axons were severed below the level of axon collaterals survived the isolation.

3. EFFECTS of ENVIRONMENTAL MANIPULATION on MORPHOLOGY of NEURONS

Some early studies were made by Mann (1894) and by Carlson (1902-03) on the effects of sensory drive to retinal neurons. These investigators found that controlled retinal stimulation induced significant changes in retinal neuron morphology. A more recent study by Holloway (1966) showed that an enriched sensory environment increases dendrite complexity in rats' cerebral cortex. Morphological changes in nerve cells have been observed also in many studies where the experimental manipulation consisted in depriving the test animal of any stimulation from visible light. Prolonged light deprivation has been shown to produce cytological alterations in retinal neurons of mammals (Weiskrantz, 1958; Riesen, 1960). Gyllensten (1959) described perikaryal alterations in the visual cortex of mice after a period in which the animals were reared from birth to 30 days in the dark. Coleman (1965) and Coleman and Riesen (1968) studied the effects of deprivation from light on cortical dendritic fields. They observed that cats reared in the dark show significant dendritic changes in layer IV stellate cells of the visual cortex. Changes were also observed in layer III pyramidal neurons of the posterior cingulate

gyrus. The stellate cells exhibit reductions in the length of dendrites in the third order of branching. The dendrite section lengths are reduced by 22 percent of corresponding lengths measured in control preparations. Some other consequences of light deprivation were observed by Coleman and Riesen; these were: fewer dendrite branches, a small reduction in the first order of branching, larger reductions in the next two branch orders and smallest reductions in the succeeding branch orders. Coleman and Riesen used Sholl's technique of concentric circles to examine dendrite intersections (Sholl, 1956) and found that in light-deprived animals there are fewer of such intersections in the bands furthest away from the perikaryon. No changes were found in layer V pyramidal cells in the visual cortex. Valverde (1967) conducted light deprivation studies on rats. He noted a significant reduction in the number of spines per dendrite section in layer IV of the visual cortex. Globus and Scheibel (1967) conducted light deprivation studies on young rabbits. They reported that layer IV stellate neurons display shorter dendrite lengths after such deprivation but indicated, however, that the greatest morphological change that could be found was in the deformity of spines along the central three-fifths of the stem zone in apical pyramidal cells. No reduction in the number of dendritic spines was reported for the rabbit. It may be noted

finally that in all the studies just cited on the effects of light deprivation there were no reports of changes, as seen in Golgi preparations, in the neuron population density of the visual cortex.

It becomes apparent from the foregoing observations that the results of both excessive visual stimulation and of essentially complete deprivation from light tend to substantiate an important postulate. In certain mammalian species the maturation process of dendrite branching and morphology is dependent upon its past environmental experience as well as upon species inheritance factors. The maintenance of the dendritic complexity appears, also to be dependent on the ability of continued afferent input to repeat and perhaps to reinforce the animal's past experiences.

METHODS AND MATERIALS

All neurohistological tissues used in this study were prepared from adult cats of either sex, weighing from 2.5 to 5.5 kg. Thirty-two cats were used in this study. They were of unselected ancestry, Felis domestica (Linnaeus, 1758), and were not known to have any morphologic or metabolic disorders. All cats were carefully maintained in a vivarium for periods of from six days to six weeks prior to their experimental use. In the vivarium environment the cats had adequate space for exercise and normal movement; generally from 5 to 15 cats were kept in one large enclosure. At all times the animals were quite placid; they were not knowingly exposed to conditions which would normally induce rage or any other type of abnormal behavioral responses.

1. SURGICAL PROCEDURES

Intact cerebral cortex. The cats used in this experimental group were sacrificed by the intraperitoneal administration of an overdose of sodium pentobarbital; the overdose level was approximately twice the dose usually required to induce deep anaesthesia. The intraperitoneal anaesthetic dose of pentobarbital is generally taken to be 35 mg/kg (Barnes and Eltherington, 1965) so that the fatal dose given ranged between 80 and 100 mg/kg.

At the first signs of loss of consciousness in the cat it was transferred to an elevated surgical table and positioned on its ventral aspect. The head was slightly elevated and clamped in a Czermak holder (Palmer).

A midline incision of the scalp was made with a #21 scalpel blade; this separated the integument and underlying superficial fascia from the deep fascia. The anterior point of the incision was a few millimeters ahead of the junction made by the coronal and sagittal sutures and extended to about 3 cm caudad to the lambdoidal crest. The deep fascia were allowed to remain intact to the underlying temporal muscles. The temporal fascia, which serve as the origin of the temporal muscle, were cut on a line which extended over the sagittal suture and the sagittal and lambdoidal crests. The temporal fascia and underlying periosteum were then bilaterally separated from the calvarium bones. The separation proceeded ventrolaterally along the temporal fossa and finally terminated where the lambdoidal ridge joints with the zygomatic process of the temporal bone. The temporal muscles were laterally reflected and clamped just above the level of the zygomatic arch. The unattached part of the muscle was transected and removed. A rectangular area of bone about 3.0 x 1.5 cm was circumscribed over both parietal bones. The surface regional relationships of the area's borders were:

anteriorly about 3 mm from the coronal suture, dorso-medially about 3 mm from the sagittal suture, ventro-laterally about 3 mm from the squamous suture of the temporal bone. The area's internal regional relationships to the topography of the brain were: anteriorly the ansatus sulcus, medially the lateral half of the marginal gyrus, posteriorly half of the posterior lateral gyrus, laterally half of the ectosylvian gyrus, and all of the suprasylvian gyrus. A number 8 vanadium steel dental burr was used to furrow a groove into the bone on the perimeter of the circumscribed area. The furrow extended into the depth of the outer table and diploe of the calvarium. The furrow was irrigated with normal saline at 37°C in order to clear the debris and haemorrhage from the traumatized diploe. The inner table was furrowed, care being taken to prevent any trauma to the underlying dura mater. The freed bone was then lifted and removed. The area of exposed dura mater was enlarged by rongeurs. If the animal were still alive at this point extreme caution would be taken not to traumatize the sagittal sinus. Surgical exposure of the contralateral side was then completed. At this stage of surgical procedure, if the animal was still alive, an additional overdose of sodium pentobarbital was administered. The central region of the exposed dura mater was lifted and a longitudinal slit was cut with a pair of fine needlenose scissors fitted with a

blunt leading point. The free edges of the dura were reflected and the exposed pia mater was kept moist by a constant drip flow of warm saline. Several topographical landmarks of the brain (Fig. 1) were used as common guides to facilitate the identification of similar areas in all the experimental cats. The anterior landmark of the suprasylvian gyrus was defined as a line parallel to the coronal suture and passing through the crosspoint of the ansatus and lateral sulci; the posterior landmark was a line similarly defined that passed through the point at which the middle suprasylvian sulcus changed direction to form the postsylvian sulcus. The gyrus beyond the posterior landmark was cut with a tapered end in order to identify this portion during the orientation of the block for sectioning by the microtome. A number 11 scalpel blade was first thrust into the anterior landmark, and then passed along the marginal gyrus a few millimeters from the lateral sulcus, along the indicated tapered posterior end, and into the ectosylvian gyrus a few millimeters from the middle suprasylvian sulcus. The cut borders were undercut with a number 22 blade. The block was gently lifted out, without bending, by the broad end of the scalpel handle. The overall size of the block was about 28 x 12 mm and 10 mm deep. The tissue block was quickly rinsed with warm saline and placed in a brown glass jar containing

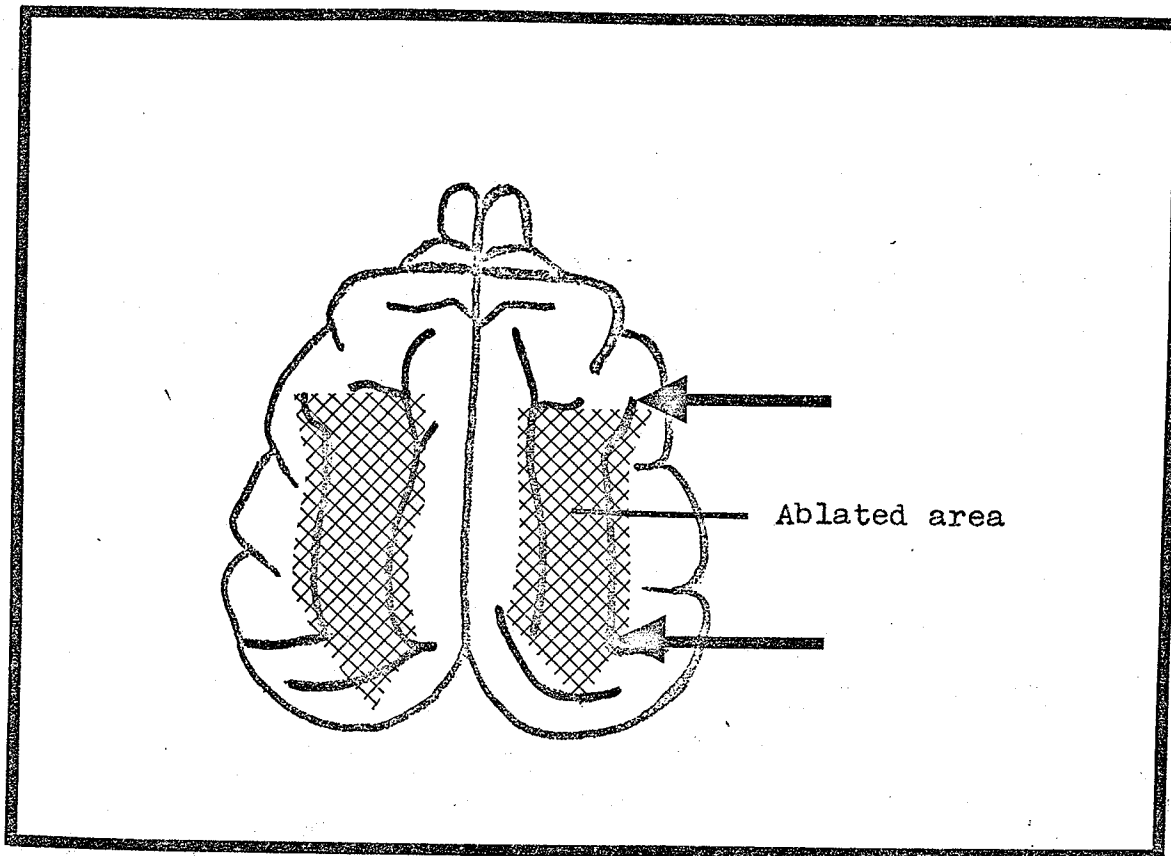


Fig. 1. Dorsal View of Cat Cerebral Hemispheres.

Anterior and posterior topographical landmarks are indicated. Ablated area indicated by cross hatch marks.

the histological fixative (see p.107). No attempt was made to perfuse the brain with saline before the cortical ablation.

Preparation of neuronally isolated slabs of cerebral cortex.

Acute isolation. Anaesthesia was induced by ether after the technique described by Brock (1967). The cat was placed in a small wooden box containing an ether-soaked pad of cotton wool. Surgical anaesthesia was attained with only a brief period of the excitement stage of anaesthesia (Goodman and Gilman, 1965, 3rd Edition). The anaesthetized cat was transferred to an operating table and placed on its back. The administration of ether was continued by the use of a nose-cone. The trachea was cannulated, the nose-cone removed and a variable-bypass ether bottle was connected which maintained surgical anaesthesia. Subsequently, a second cannula was inserted into the right femoral vein for the purpose of introducing a neuromuscular blocking agent, gallamine, and fluids. The gallamine was administered in doses of 5 mg/kg, at various intervals, in order to maintain relaxation of skeletal muscle.

The surgical procedures used for the exposure of the suprasylvian gyrus in this experimental group of cats followed very closely those techniques previously described in this chapter for the intact cerebral cortex. The salient differences were the absence of sodium

pentobarbital and the more liberal use of bone wax (beeswax with 7% phenol) to control haemorrhage resulting from trauma and exposure of the diploe of the parietal bones. Neuronally isolated slabs of cerebral cortex were cut in the cats' suprasylvian gyri by slight modifications of techniques previously described by Burns (1949, 1950), and Pinsky (1957). A 3 mm² area of pia and its superficial blood vessels at the posterior end of the gyrus was electrocauterized with a damped high frequency electrocautery device (Birtcher Hyfercator Model #703). A hole about 2 mm in diameter was aspirated through the cauterized area with a finely tapered glass tube connected to a faucet aspirator. The hole extended down into the lateral ventricle and thus provided a drainage route for the escape of excess cerebrospinal fluid. The drainage hole helped to reduce the incidence of brain swelling. A wire-knife (Pinsky, 1957), consisting of a steel wire 20 mm long with a right angle bend 4 mm long and fitted with a rounded tip was inserted into the drainage hole. The tip was manipulated to the subpial position and, through the translucent pia, was just visible to the operator. The wire-knife was gently pushed to circumscribe a rectangular area 20 mm x 5 mm, as illustrated in Fig. 2. The knife was then gently removed from the brain. A spatula stainless steel knife described by Pinsky (1957) was used as the undercutting knife. It was inserted into the

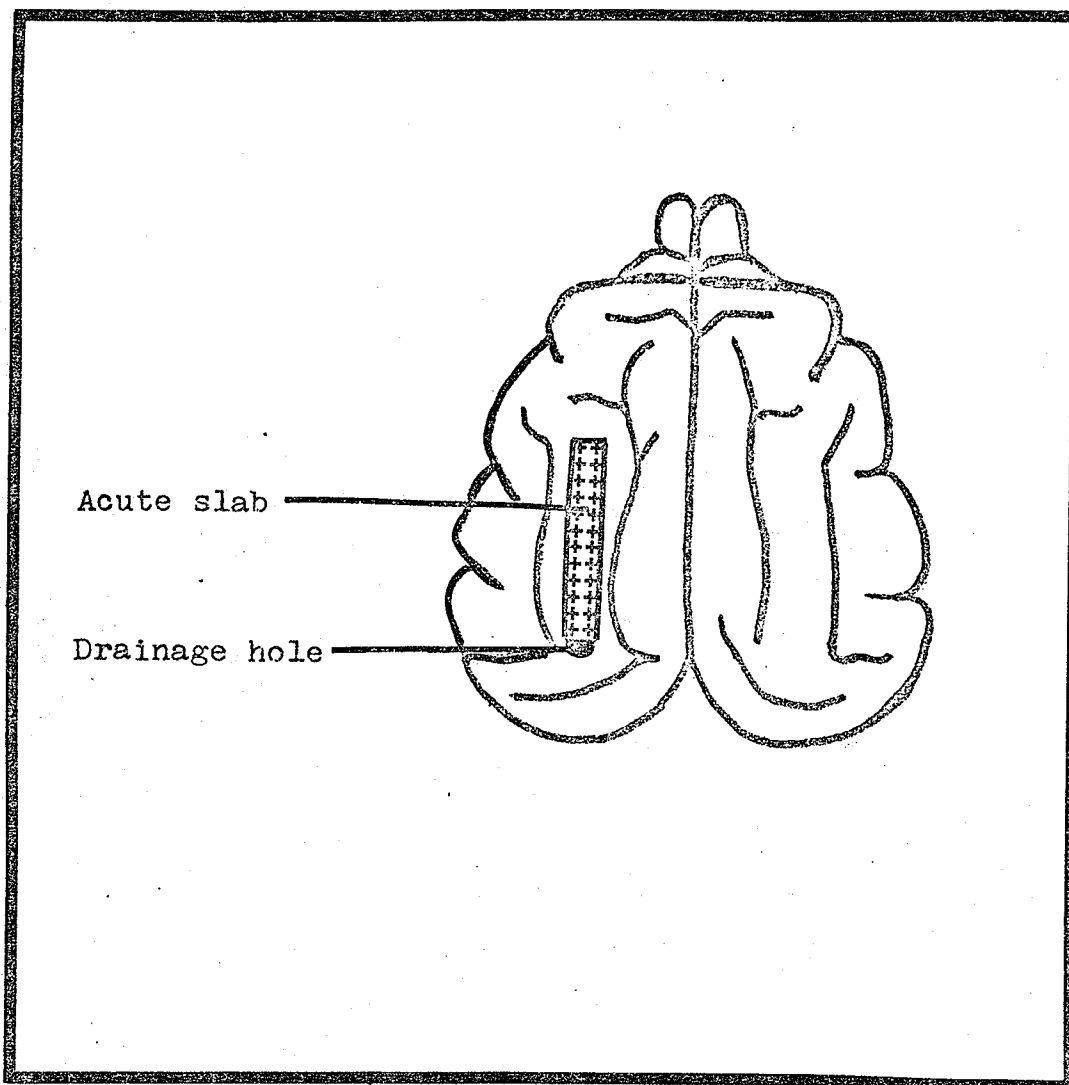


Fig. 2. Dorsal View of Cat Cerebral Hemispheres.

Rectangular area, 20 mm x 5 mm, in supra-sylvian gyrus indicates dorsal limits of acutely isolated slab.

drainage hole and gently pushed, at a depth of 5 mm below and parallel to the pial membrane, to a point just beyond the anterior end of the slab. The spatula was then rotated slightly from side to side. The rotation insured a complete undercut of cortical afferent and efferent fibres of the slab. The overlying blood vessels of the pia which supplied the isolated slab were not damaged. The surgery for the side cuts left a dark subpial line which was barely visible. The proof and the extent for the completeness of neuronal isolation was later determined by histological methods. However, the uniformity of the dark subpial line was usually indicative of neuronal isolation at the gross observation level.

Decerebration was carried out by an electrocautery loop which transected the brain stem at the midcollicular level. The tentorium cerebelli was taken as the anatomical marker in order to ascertain the regional relationship of the brain stem. The vertebral arteries, ventrally situated, were not damaged. Ether administration was discontinued and the exposed brain area was kept moist with saline. The cat was then transferred to a recording table and a respiratory pump was attached to the tracheal cannula. The free edges of the incised scalp integument were sutured to a circular iron clamp by simple knots of string. This technique formed a well over the exposed brain and surrounding bone which was filled with mineral oil at 37°C. The body temperature

of the cat was maintained at 37°C. by a rectal probe connected to a heating element which blew warm air through a perforated metal plate that supported the cat.

After a period of electrical stimulation, the nature of which is described in a later part of this chapter, the cat was transferred back to the operating table. The mineral oil was aspirated and the cat was sacrificed by a large overdose of sodium pentobarbital administered through the femoral vein cannula.

The procedure just described for sacrificing the animal was decided on because the effects of anoxia on the modified Golgi technique are not known. Therefore the cats could not be sacrificed simply by turning off the respiratory pump. Nor could death of the animal be induced by intravenous injection of saturated magnesium sulphate since high concentrations of this compound in the brain could be expected to interfere with the histological techniques.

Surgical procedures used for cortical ablation at this stage were similar to those employed for the intact cerebral cortex. In a few acute isolation experiments the edematous swelling of the brain was considered too severe for histological use. In these cases it was felt that many cytological and histological details of the cortex would have been distorted and therefore would not represent their natural relationships to each other.

Chronic isolation. Cortical slabs in this group were neuronally isolated for periods of from six to eleven months. In general, the cats gained about 1.5 kg in weight after the operation, over a period of about nine months. On the basis of their weight gain they were considered to be in better health than prior to their first operation.

The surgical procedures for the preparation of long term cortical neuronal isolation have been described by several authors (Grafstein and Sastry, 1957; Sharpless and Halpern, 1962; Gorchynski, 1964; Reiffenstein, 1964; Brock, 1967). These techniques were in some ways similar to those used in the preparation of acute neuronal isolation. The cat was anaesthetized for surgery with sodium pentobarbital (35 mg/kg intraperitoneal). It was positioned, under anaesthesia, on its ventral aspect and the head loosely clamped in a Czermak holder specified previously. The initial incision and subsequent dissection of the scalp area were carried out under clean but not aseptic conditions. The left temporal muscle was reflected from its dorsal midline origin. Great care was taken not to traumatize the reflected temporal fascia with its attached periosteum. An area of parietal bone was removed by the methods described earlier for acute isolation. The dura mater was incised on the midline of the exposure area; each half of the cut dura was then reflected. An area of

pia mater, about 4 mm in diameter, was then cauterized at the caudal end of the region intended for isolation. The brain tissue beneath this was then aspirated away to provide a drainage hole into the lateral ventricle. Neuronal isolation of a cortical slab was then done in the suprasylvian gyrus. The free ends of the dura mater were sutured to each other with fine nylon thread (Ethicon #6-0). The reflected temporal muscle and fascia were sutured to the origin of the right temporal muscle. The osteogenic layer from both the outer periosteum and from the dura mater were thus placed in apposition with each other. The reflected scalp integument was sutured on the dorsal midline with #80 cotton thread. Prophylactic antibiotics, such as streptomycin 0.5 gram, or 400,000 units of penicillin, or in some cases both, were administered one half-hour after surgery and thereafter once daily for the next three to five days. The cat was then returned to the vivarium. Burns (1958), in commenting upon the usefulness of this method, stated that "the remainder of the animal serves only as a convenient heart-lung system for perfusion of the isolated brain".

Re-exposure of the chronically isolated cerebral cortex required a slight modification from the procedures for acute isolation (Reiffenstein, 1964). The temporal muscle and fascia could not be reflected from origin in their entirety without also tearing away the newly grown

bony plaque and underlying brain tissue. Therefore, small groups of muscle fibres were teased away and electrocautery was used liberally for hemostasis of small blood vessels. The temporal muscle was then clamped near the lambdoidal ridge. A small hole was made in the parietal bone with #8 vanadium steel dental burr and gently enlarged with fine rongeurs. The underlying adhesions were cut with fine iris scissors and cauterized before the remainder of the regenerated bone was removed.

Some of the chronic cats were used for electrophysiological experiments which involved surface stimulation and recording with iridium-platinum and silk-wick electrodes. In this experimental group the procedures for anaesthesia, tracheotomy and decerebration were as previously described for acute isolation. The animals were paralyzed with gallamine triiodide (Flaxedil, Poulenc, 5 mg/kg intravenous). The cat was sacrificed, at the termination of the electrical experiments, by the intravenous injection of an overdose of sodium pentobarbital. The respiration pump was shut off slowly after this injection. In the second group of chronic cats the slabs were not stimulated; these cats were sacrificed with sodium pentobarbital. The left and right suprasylvian gyri were removed and immediately immersed in the tissue fixative.

2. HISTOLOGICAL TECHNIQUE

A highly specific histological technique was required in order to carry out the quantitative and qualitative measurements made in this study. It seems reasonable to state that the ideal staining process for cytoarchitectonic studies in gyri of intact and isolated cerebral cortex would be one that is preferential for all neurons while being achromatic towards neuroglia and blood vessels. None of the known microscopic techniques fulfills these requirements. Neurons are differentiated morphologically from glial cells by the presence of tigroid bodies. The granules are readily stained in thin paraffin sections by any of the following methods: a) methylene blue, Nissl (1894); b) cresyl violet, Keller (1945); c) thionin, Clark and Sperry (1945); d) gallocyanin, Einarson (1951). However, isolation of the cerebral cortex results in retrograde degeneration of cerebral neurons and chromatolysis of their tigroid substance (Cajal, 1928). As a result of the chromatolysis a cytoplasmic organelle stain would no longer provide a reliable method of differentiating perikarya of neurons from those of neuroglia. The Abercrombie (1946) correction factor, which is applicable only in thin microtome sections, enables an accurate count of the actual neuron nuclear population density to be made from the observable

number of nuclear fragments. In thin paraffin sections of isolated cerebral cortex it would be virtually impossible to identify separately the discrete morphological differences in nuclear fragments of neurons and of glial cells. As a result of these difficulties the correction factor could not be used in this study.

An analysis of various parameters of dendrite trees from cortical pyramidal neurons formed an important part of this study. It has long been established in neurohistological studies that cortical dendrites follow a tortuous three-dimensional pathway. Therefore patterns of dendritic arborization can be traced out only from thick microtome sections. Thick sections that have been slightly overstained will always present an extreme difficulty in the identification of a complete cortical dendrite tree from one nerve cell that is observably distinct and separate from another. On the other hand, slightly under-stained sections do not reveal enough of the smaller dendrite branches and this would lead to a biased result.

Several methods of silver impregnation with low viscosity nitrocellulose (celloidin) imbedding were tried. The Cox (1891) modification of Golgi's rapid method (Golgi, 1878) was faulty on two main points. First, the impregnation period was rather long, requiring from 3 to 5 weeks. Second, the length of the brain tissue block

could not exceed 10 mm. It was felt that there were obvious advantages in an en-block staining technique which would retain the structural integrity of the entire gyrus. A modification of Mallory's version of Golgi's rapid method (Mallory, 1938) was devised after fourteen other different trial methods had been attempted and rejected. The method finally arrived at permitted silver impregnation of relatively large blocks of cat's cerebral cortical tissue. These blocks measured 20 mm long, 8 mm wide and 6 mm deep. There are no reports in the literature of such large blocks of brain being successfully treated consistently to yield silver impregnation with uniform results throughout the tissue block.

1. Fixative. The fixative solution consisted of 40 ml of 2.5% w/v aqueous potassium dichromate ($K_2Cr_2O_7$) and 10 ml of 1% w/v aqueous osmic acid (OsO_4). Stock solutions of potassium dichromate and osmic acid were prepared but were not mixed together until required. The fixative solution was discarded after each use. Fixative and fresh brain tissue were placed in tightly stoppered dark glass bottles. The volume of fixative used was about 20 times the volume of the tissue to be fixed. Fixative time was 72 ± 3 hours with gentle agitation once every 12 hours. Fixative time was found to be highly critical.

ii. Staining. (Metallic impregnation). The stain used was 0.75% w/v silver nitrate (AgNO_3) solution. The use of this reagent has been more accurately termed a metallic impregnation technique (Davenport, Humason, 1962). Fresh solution was prepared just prior to its use and discarded after each preparation of stained tissue.

The tissue block was removed from the fixative and wrapped immediately in surgical gauze. It was washed twice in distilled water; each wash lasted only 30 seconds. Extreme caution was taken to ensure that the surface layer of each tissue block did not dry out. Prolonged washing or partial dessication invariably altered the degree of silver impregnation and gave inconsistent results. The gauze-wrapped tissue block was suspended in a stoppered dark glass bottle for 48 ± 2 hours, with gentle agitation once every 12 hours. Again, this time factor was critical for the final result. The volume of silver nitrate solution was always made 40 times the volume of tissue to be impregnated. The stain solution was discarded and replenished whenever it turned cloudy yellow after the initial immersion of the fixed tissue blocks.

iii. Dehydration. Ethyl alcohol and a final alcohol-ether mixture were used as the dehydrating

agents. The entire dehydration process was carried out under conditions of subdued light. The gauze-wrapped tissue was transferred directly from the silver nitrate solution to a graded series of ethyl alcohol-distilled water solutions (v/v) in the following manner: 30% alcohol--1 hour, 50%--2 hours, 70%--4 hours, 95%--2 changes each of 4 hours, 100%--2 changes each of 6 hours. Finally, the tissue was transferred to a 50:50 mixture of 100% absolute alcohol and anhydrous diethyl ether for 12 hours.

iv. + v. Infiltration and embedding. Low viscosity nitrocellulose (LVN, celloidin, parlloidin, pyroxylin) was used as the infiltrating agent. Initially, attempts were made to infiltrate the large tissue blocks with nitrocellulose by the methods described in several authoritative texts on microtechnique (Guyer, 1953; Davenport, 1960; Humason, 1962; Lillie, 1965). It was found that these methods never allowed more than a thin outer layer to become infiltrated even after a whole week of treatment. As a result of such incomplete infiltration it was impossible to section the tissue block core. A modified technique was consequently devised to eliminate the infiltration difficulty. Thin slices of brain tissue, a few millimeters thick, were cut away from the ventral surface of the block until the light green color of the white matter was exposed.

A #21 or #22 scalpel-blade was found useful for this procedure. The block was kept moist during this part of preparation by periodic immersion into the final alcohol-ether mixture. The tissue block was then transferred to a graded series of nitrocellulose solutions which were kept in covered Stender dishes which measured 60 mm x 30 mm. The solvent was a 50:50 mixture of 100% ethanol and anhydrous ether. The infiltration time for each of the dilutions were: 1½% celloidin in alcohol-ether solvent--1 day, 3% celloidin--2 days, 6% celloidin--1 day and saturated celloidin--1 day. The infiltration procedures were carried out in subdued light.

Infiltrated tissues were embedded in saturated nitrocellulose after a modification of the rapid method by Humason (1962). The container part of cardboard pill boxes, measuring 6.5 cm in length, 4.0 cm in width and 2.0 cm in depth, were divided diagonally by a cardboard insert to form two triangles. The triangular compartments so formed were filled with saturated nitrocellulose and a block of cortical tissue was placed in each compartment. The cortical blocks were rested on their ventral surface with the anterior end of the block directed towards the apex and the posterior end towards the base of the triangle. The compartmented boxes were transferred to a small Scheibler glass desiccator

containing 10 ml of chloroform and with the cover tightly closed. The blocks were allowed to "set" for two days or until the nitrocellulose was of gum rubber consistency. The nitrocellulose blocks were removed, properly trimmed down to sectioning size, mounted with fresh saturated nitrocellulose solution on square red fibre blocks whose surface was scored to increase adhesion. The nitrocellulose blocks were carefully orientated on the fibre blocks for future coronal sectioning with a horizontal sliding microtome. The mounted blocks were then returned to the desiccator for an additional 24 hours. At the end of this time they were immersed in 70% alcohol for a few hours or until hard enough for sectioning.

vi. Sectioning and mounting. Serial sections of the nitrocellulose-embedded tissues were cut on a horizontal clinical microtome (Sartorius). Several test sections, ranging from 30-200 microns in thickness, were carefully examined for distinctness of cytological and histological detail. A 50-micron thick section was decided on as the best compromise for the intended studies on dendrite trees and neuron population densities.

A steady pool of 70% alcohol was maintained on the top of the nitrocellulose blocks and at the edge of the knife while sectioning. Microtome knives with an

angle A or angle B cutting bevel were used. The serial orders of all sections were maintained by placing them on long strips of alcohol-moistened cigarette paper ("Chaunticlair" paper). At each millimeter interval along the length of the tissue block the central section as well as the two adjacent sections were kept for mounting purposes. Precleaned microscope slides, 25 x 75 mm, were covered lightly with a mixture containing strained egg white and a few drops of glycerol. The wet cigarette paper containing three tissue sections were cut and inverted onto the tacky slides. The sections were lightly blotted and then dehydrated with 95% alcohol for 15 minutes. This was followed by two changes, each of 10 minutes, of 100% absolute alcohol containing a few milliliters of chloroform. The sections were cleared with terpineal (Fisher) in two stages: a 50:50 mixture of terpineal and 100% absolute alcohol for 15 minutes followed by pure terpineal for 15 minutes. The slides were drained of the clearing agent and lightly blotted. They were then flooded with Fisher's Permount mounting medium and covered with Corning cover slips, #1 thickness. Finally, the slides were transferred to a drying oven at 45°C for two days.

The histological method just described, although invaluable for this type of study, was marked by one disadvantage. The tissue blocks, after being embedded with saturated nitrocellulose, could not be stored as in other

methods. The tissues had continuously to be processed up to the final coverslip stage. Nitrocellulose blocks with impregnated tissue embedded in them became darkened upon storage and the metallic stain exhibited a tendency to disperse off the dendrites onto the neighboring area. These problems were not alleviated by storage in 70% alcohol with glycerol, nor with a variety of chloroform mixtures. Storage of embedded tissues, therefore, was never permitted for specimens examined in this study.

3. ANALYTICAL METHODS

The nature of the structure-function study whose results are reported in this thesis has been determined by a simple but fundamentally important postulate. This postulate is that the CNS consists of neurons which interact with each other. The anatomical parameters that were to be quantified and examined were chosen, with this central hypothesis in mind, by making two assumptions concerning the cytology and histology of the cat's cerebral cortex. These assumptions were:

- a) that there will be a dependence of cytological density upon histological volume, i.e. that the packing density of neurons and of dendritic processes is interrelated with the total volume of available cerebral cortex;
- b) that the nature of the interaction and anatomical relationships between neurons would be altered as a result of neuronal isolation.

Two immediate effects which may be expected from neuronal isolation of the slab are: (1) structural deafferentation--loss of isogenous input stimuli upon the dendrites and perikarya; (2) axotomy--retrograde degeneration with a reduction of surviving neurons. Therefore, in attempting to examine the correlates suggested by the assumptions just stated, histological evidence of these immediate effects was sought. The following sections describe the techniques by which the

appropriate histological and cytological parameters were examined and quantified.

Measurement of histological parameters.

Intact cortex.

Dimensions of gyri and cortical depth. The histological dimensions and cortical depth of the intact suprasylvian gyri were measured from serial coronal sections, 50 microns thick, at magnifying powers of 31.25X and 200X. All observations with light-microscopy for intact and for isolated cortex were made with a Zeiss-Winkle research grade compound microscope, fitted with the following optics: planocompensating oculars of 12.5X, 15X and 20X; fluorite objectives of 2.5X, 10X, 16X, 40X and a N.A. 1.3 planapochromat 100X oil; a N.S. 1.3 substage condenser with auxiliary swingout lens; built-in illuminator with luminous-field diaphragm. Also fitted was a large rectangular mechanical stage with a movement range of 50 x 75 mm. A micrometer glass disc, ruled by a linear scale of 100 subdivisions, with every tenth line numbered, was inserted onto the ocular diaphragm. Values of the gradation intervals were calibrated by the use of a stage micrometer ruled by 100 subdivisions totalling 1.0 mm (1000u) in length, each subdivision being 0.01 mm (10u) long.

Gyrus width and cortical depth. These parameters were measured on coronal sections at 1 mm

intervals along that portion of the gyrus which had been successfully excised, stained and sectioned as described in Methods and Materials (p. 105). Measurement of distance was made to the nearest micron.

Gyrus width on any one section was taken to be the widest part of the intact gyrus, as measured by a straight line between the pial surfaces of the middle suprasylvian and lateral sulci (Fig. 3). This line frequently passed through the white matter of the gyrus. The cortical depth was measured at the midpoint of the gyrus width and thus formed a line vertical to the first (Fig. 3). The deepest part of the cortex was taken, for all measurements, as being a point just above a densely entangled hyperchromatic layer (Plates I and II). This layer consists of perikarya and processes of oligodendrocytes, astrocytes and microcytes, blood vessels and some spindle cells. The lower side of this layer was indistinct to a depth of about 30 microns and for this reason it was not included in the measurement. It was felt that the deliberate omission of this layer increased the reproducibility of measurement and hence increased the accuracy of the estimation of cortical depth.

The results of these measurements were plotted to show the variations in cortical depth and gyrus width along the length of the gyrus. The results were examined to determine any correlation between the cortical depth

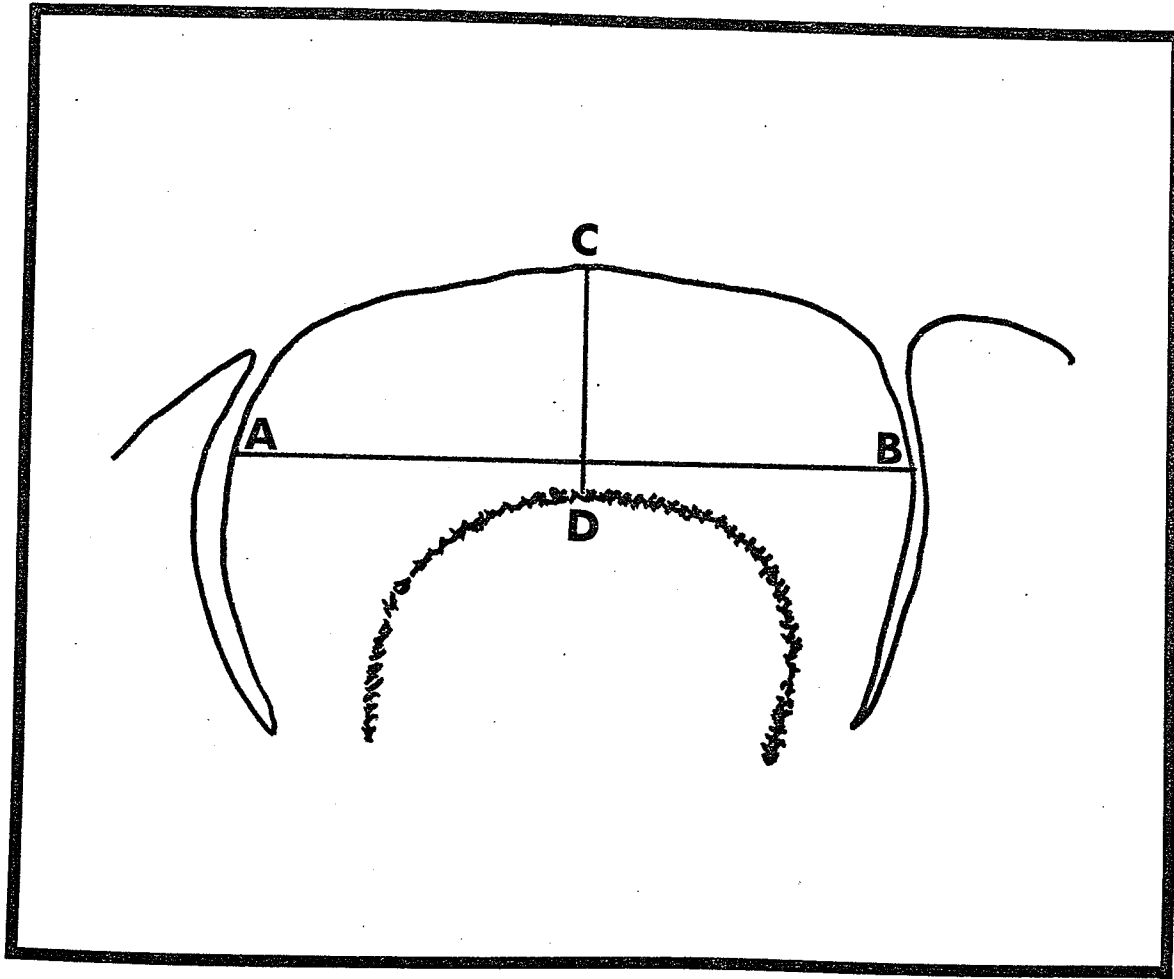


Fig. 3 Diagram of Coronal Section in the Left Intact Gyrus

A-B Maximum width of gyrus

C-D Cortical depth at midpoint of gyrus width

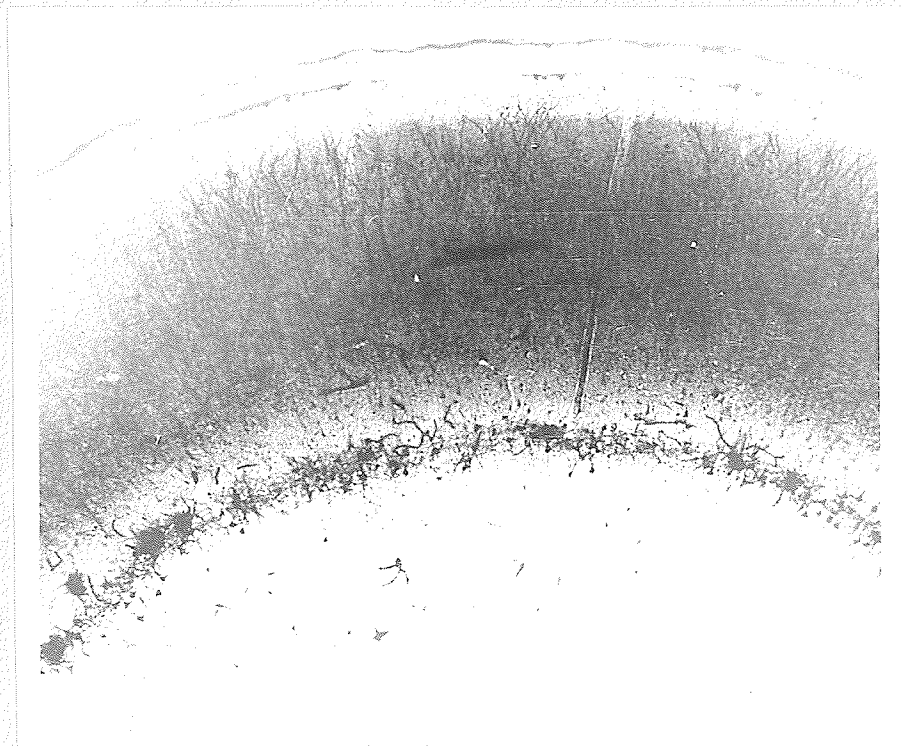


Plate I. Coronal Section, Intact Gyrus, 12.5X

Continuous hyperchromatic "glial line"
demarcates gray from white matter.

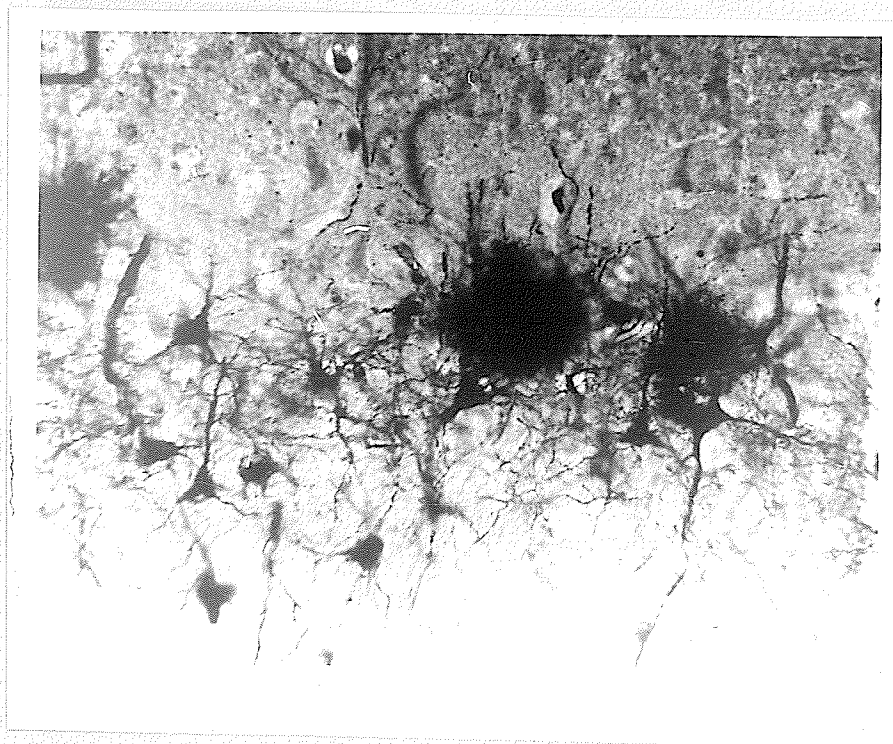


Plate II. High Magnification of Glial Line, 500X

Interwoven processes from neuroglial and neuronal cells. Perikarya from both types of cells are indistinguishable in this layer.

and the gyrus width. These parameters were measured at 1 mm intervals along the length of the gyrus.

Neuron population density. A specific area of the intact cortex was selected for studies on neuron population density. This area corresponded to those in other cats from which acute and chronically isolated slabs were prepared. Measurement of neuron population density was done with the aid of two ocular micrometer inserts superimposed upon each other in the microscope. The first insert was a net micrometer glass disc, 10 x 10 mm, ruled by 100 squares with every line on the two adjacent sides numbered. This insert was calibrated against a stage micrometer. The second insert was the previously described linear scale micrometer of 100 subdivisions.

That portion of the coronal section which was chosen for the population density studies consisted of an area which extended 1500 microns on either side of the midpoint of the gyrus width and was further bounded by the pial surface and by the upper surface of the hyperchromatic layer described in the previous subsection. The manner in which this area was subdivided is illustrated in Fig. 4. The cortical depth was divided into two equal halves with the upper half subdivided into four equal parts. Each one of these six subdivisions will be referred to, throughout this study, as a cortical segment. This method of cortical sub-

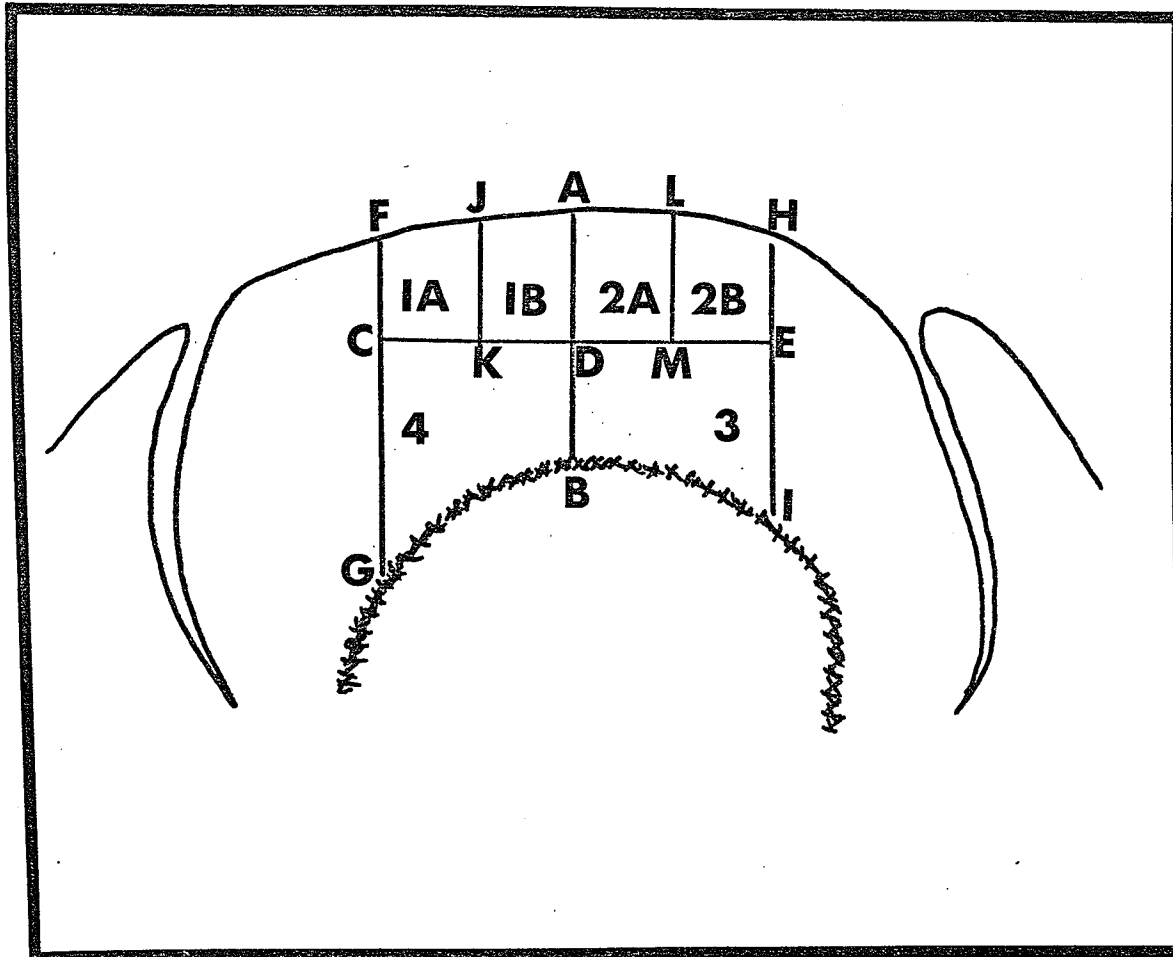


Fig. 4 Diagram to Show Subdivision of Intact Cerebral Cortex into Segments

Legend for Fig. 4

- A-B Midline of gyrus width
- C-E Division of cortical depth into upper and lower halves
- C-D 1,500 microns distance from A-B and equal to D-E
- F-G, H-I Side limits of demarcated area and parallel to A-B
- J-K, L-M Vertical subdivision of upper cortical half into 4 equal parts
- C-K, K-D, D-M, M-E All distances equal to each other each distance 750 microns
- 1A, 1B, 2A, 2B, 3,4 Titles for each segment in subdivided cortex

division permitted a study to be made of differences between neuron population densities in regions of the cortex separated by only small distances.

Neuron population densities were determined at one millimeter intervals for the entire length of the gyrus. The determinations made for each segment were a) the number of ocular micrometer squares and b) the number of observable neuron cell bodies. The volume of cortical tissue in each segment was calculated from the known thickness of the section and from the number of squares in the segment. The following example will illustrate the necessary calculations:

dimensions of micrometer square = 70u on an edge

thickness of tissue section = 50u

∴ volume of cortical tissue contained

in each observed square = 70u x 70u x 50u

$$= 245 \times 10^3 u^3$$

Where there are "n" squares per segment,

the volume, "V", of the segment is calculated from

$$V = \frac{n \text{ squares}}{\text{segment}} \times \frac{245 \times 10^3 u^3}{\text{square}} \times \frac{1.0 \text{ mm}^3}{10^9 u^3}$$

$$\therefore V = n \times 245 \times 10^{-6} \text{ mm}^3.$$

The neuron population density, "D", in a segment may be calculated from the formula

$$D = (n/V) \frac{\text{observable cells}}{\text{mm}^3}$$

n = no. of observable cells in the

cortical segment and

V = volume of the segment, in mm^3 , as
explained above.

For calculations from the raw data "D" was calculated from

$$D = \frac{\text{no. of observable cells per segment}}{\text{no. of squares per segment} \times 245 \times 10^{-6}}$$

The units of this parameter are observable cells/ mm^3 .

Cytoarchitectonic studies by Sholl (1956) have shown conclusively that the Golgi Rapid Method impregnates with silver approximately 2 percent of the available neurons in cat's cerebral cortex. Therefore, $D \times 50$ will approximately equal the number of neurons per mm^3 in the cortical tissues taken from the specimens of cat's intact suprasylvian gyrus used in this study.

Acutely isolated cortex.

Dimensions of gyri, isolated slabs and cortical depth.

Serial coronal sections, 50 microns thick, were made from acutely isolated slabs in cats' suprasylvian gyri. The following parameters were measured: a) gyrus width, b) slab width at pial surface, c) slab depth including white matter, d) slab cortex depth, e) depth of intact cortex adjacent to lateral sulcus, f) distance between suprasylvian sulcus and apex of slab, g) cortical width at base of slab. These parameters are illustrated in Fig. 5.

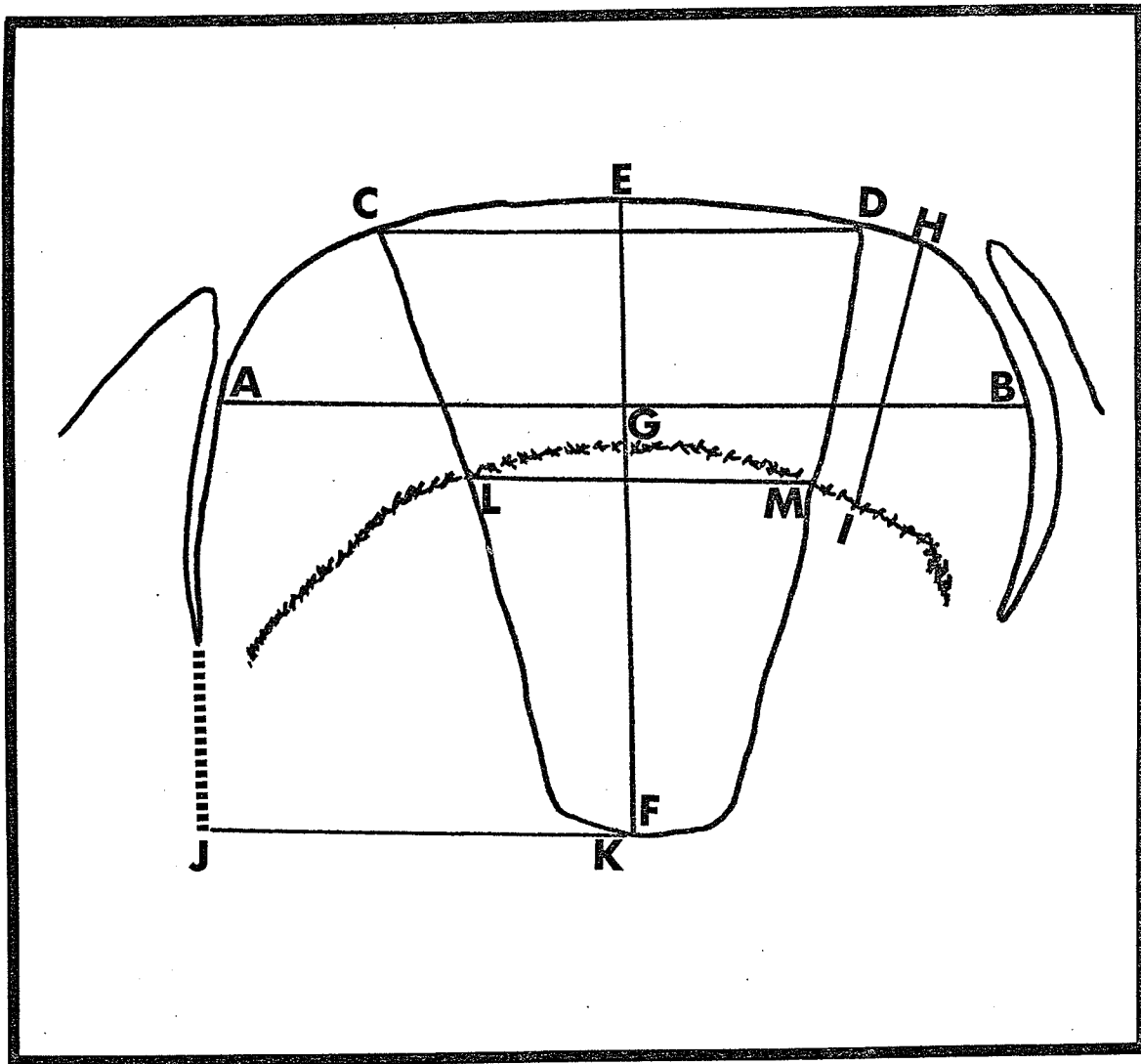


Fig. 5 Coronal View of Gyrus with Acutely Isolated Slab

Legend for Fig. 5

- A-B Maximum width of gyrus, measured as for intact gyrus
- C-D Slab width at pial surface
- E-F Slab depth including white matter
- E-G Slab cortex depth
- H-I Intact cortex depth, measured at right angle from spindle line to pial surface
- J-K Distance of suprasylvian sulcus to left margin of apex
- L-M Cortical width at base of slab

These histological parameters were used in several specific studies. First, they provided an opportunity to extend the correlative studies of cortical depth and population densities of neurons. This area of investigation paralleled the study in intact cortex. Second, the measurements afforded an opportunity for additional examination of discrete histological differences which were observed to exist between closely spaced regions in cat cerebral cortex. Third, histological observations on the effects of short term isolation were recorded and analyzed. Special attention was given to ascertain the extent of shrinkage and compression of isolated cortex throughout the entire length of the slab. Also, an attempt was made to ascertain whether the tightly interwoven basal layer of spindle cells and neuroglia contributed to the architectural integrity of the tissue. Finally, an observation that had been made early in this study was extended in the analysis of the acutely isolated tissue. The early observation had suggested that the apex of slabs in chronic and acute isolation exhibited a preferential geometric orientation. The parameter J-K in Fig. 5 permitted a more extensive analysis of this observation.

Neuron population density. The parameters which subdivided the acutely isolated slabs for cell density studies were similar to those which were pre-

viously described in the subdivision of the intact cortex. The methods used to calculate cortical volume in mm^3 for all cortical segments, for the enumeration of neurons and for the expression of neuron population density, were the same as those previously described for the intact cortex. The subdivision of the acutely isolated cortex is illustrated in Fig. 6.

Several attempts were made to determine whether a regular relationship existed between each of:

(a) cortical volume, (b) gyrus width, (c) cortical depth and (d) neuron population density.

Chronically isolated cortex.

Slab and gyrus dimensions, cortical depth.

Cerebral cortical tissue could be expected to undergo considerable histological alteration and, possibly, reorganization after long term isolation. The predominance of nerve tracts in the white matter contrasts with the more cellular character of the cortex. The preparation of isolated slabs always included an area of white matter which was greater in depth than the cortical depth. The degree of shrinkage and compression in each of these two areas within the same slab might differ from adjacent areas outside of the slab but lying within the same gyrus. The geometric orientation of the slab apex was measured as for acutely isolated slabs. The parameters measured in coronal sections of chronically

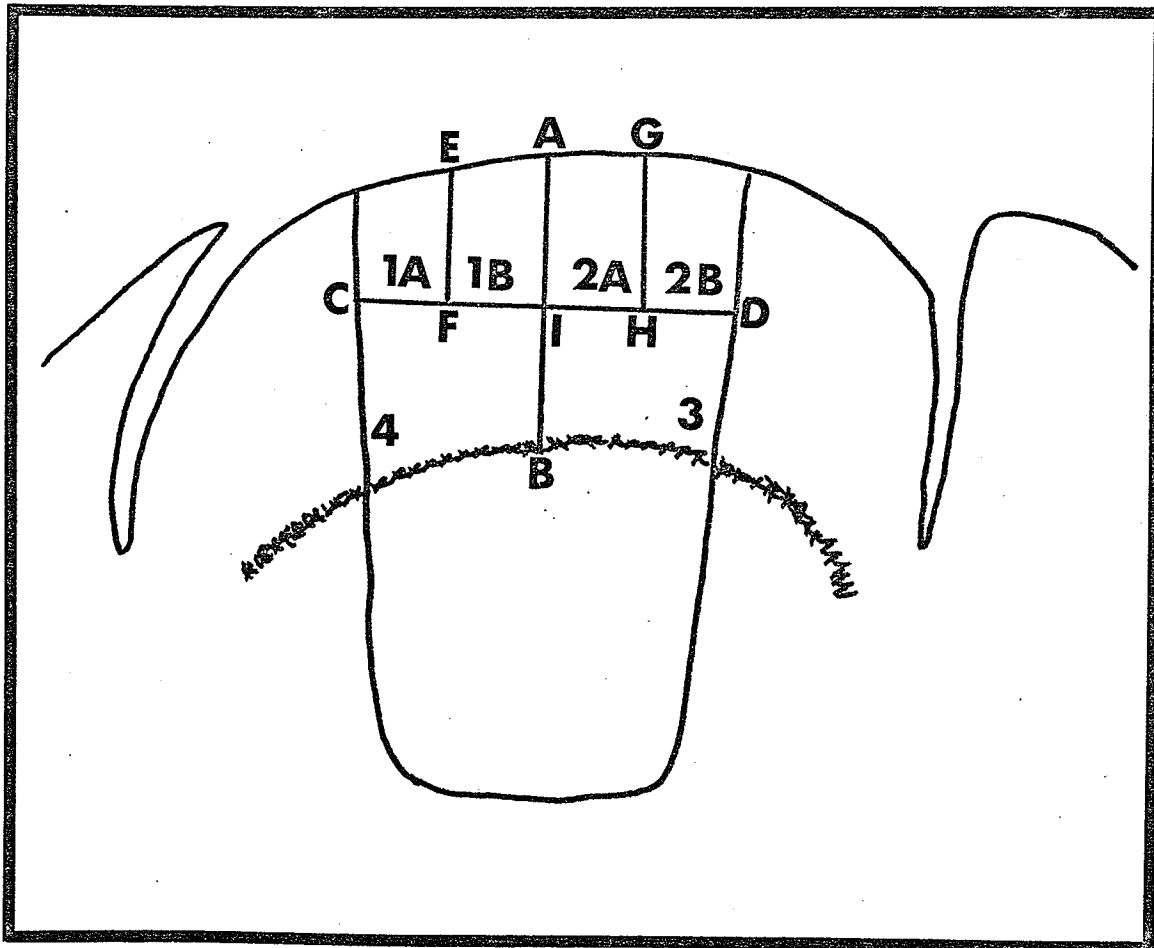


Fig. 6 Coronal View of Acutely Isolated Slab Showing Cortical Subdivision into Segments for Neuron Population Density Studies

Legend for Fig. 6

- A-B Midline of slab width
- C-D Division of slab cortical depth into upper and lower halves
- E-F, G-H Equal subdivision of each quadrant in upper half to yield a total of six segments in the cortical section

The subdivisions are expressed as:

C-F, equal to F-I

I-H equal to H-D

A localized compression or shrinkage along a side cut was expressed as an unequal subdivision between C-F and F-I to I-H and H-D.

isolated slabs were as follows: a) width of gyrus, b) width of slab at pial surface, c) depth of slab from pial surface to apex at midpoint of slab width, d) depth of slab cortex at midpoint of slab width, e) depth of intact cortex on left side, f) depth of intact cortex on right side, g) distance between slab apex and suprasylvian sulcus. These parameters are illustrated in Fig. 7.

Neuron population density. The cerebral cortex in chronic isolation was subdivided (Fig. 8) by the methods previously described for acute isolation. Cortical volume and density determinations were as described for acute isolation.

Measurement of cytological parameters. The analytical studies done by Bok (1936, 1959) have demonstrated conclusively that there are at least as many cytological parameters in a cortical dendrite tree as there are cortical histological parameters. The selection of the cytological parameters examined in this study was influenced primarily by results from several electrophysiological studies on isolated cerebral cortex (Burns, 1949, 1950, 1951, 1954, 1958; Pinsky, 1957, 1961, 1963, 1967; Grafstein and Sastry, 1957; Halpern, 1960; Purpura and Housepian, 1961; Purpura, 1961; Pinsky and Burns, 1962; Reiffenstein, 1964; Sanders and Pinsky, 1967). These studies deal mainly

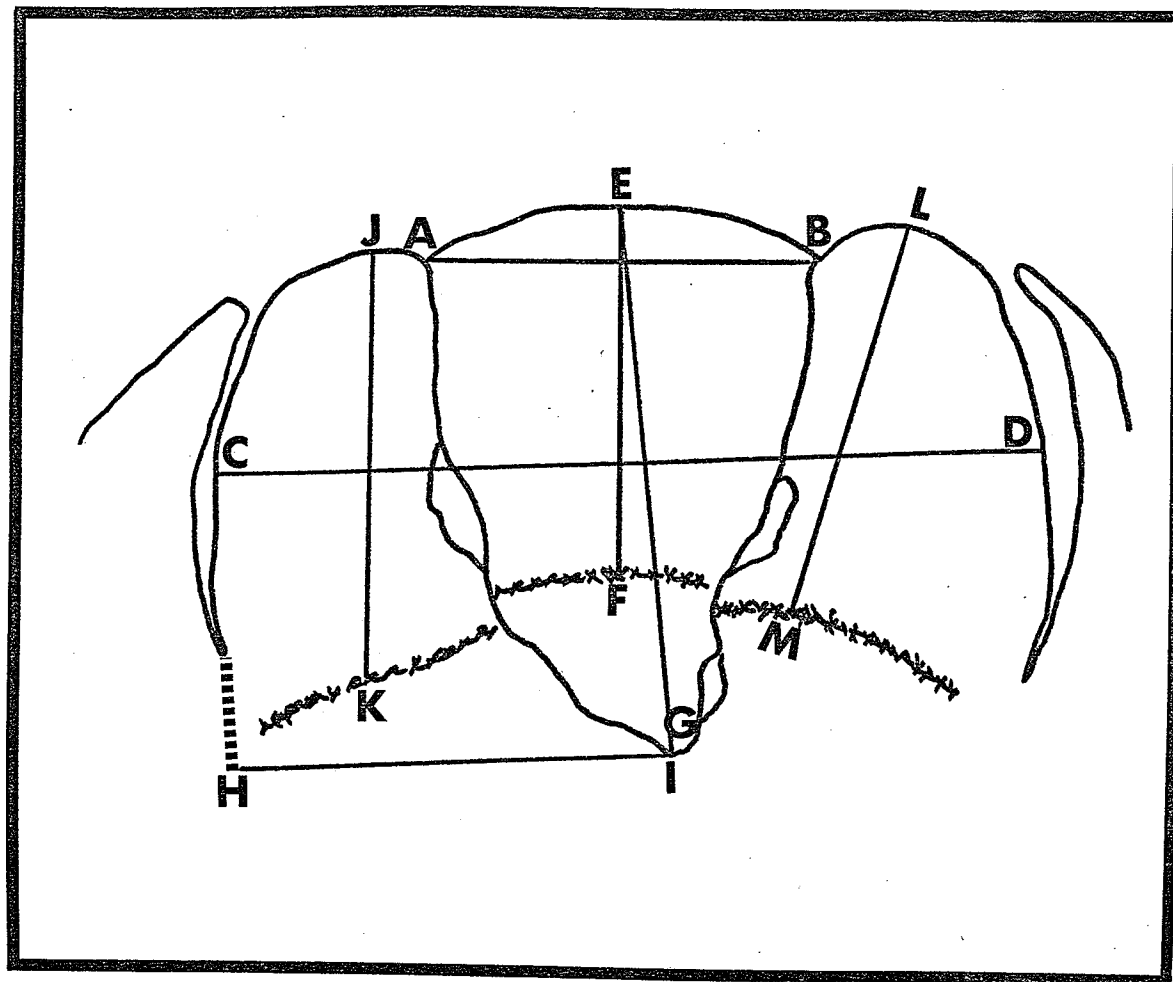


Fig. 7 Coronal Section of Gyrus with Chronically Isolated Slab

Legend for Fig. 7

- A-B Width of slab at pial surface
- C-D Width of gyrus
- E-F Depth of slab cortex at midpoint of slab width
- E-G Depth of slab at pial midpoint to apex
- H-I Distance between suprasylvian sulcus and slab apex
- J-K Depth of intact cortex on left side measured parallel to E-F
- L-M Depth of intact cortex on right side, measured at right angle from spindle layer to pial surface

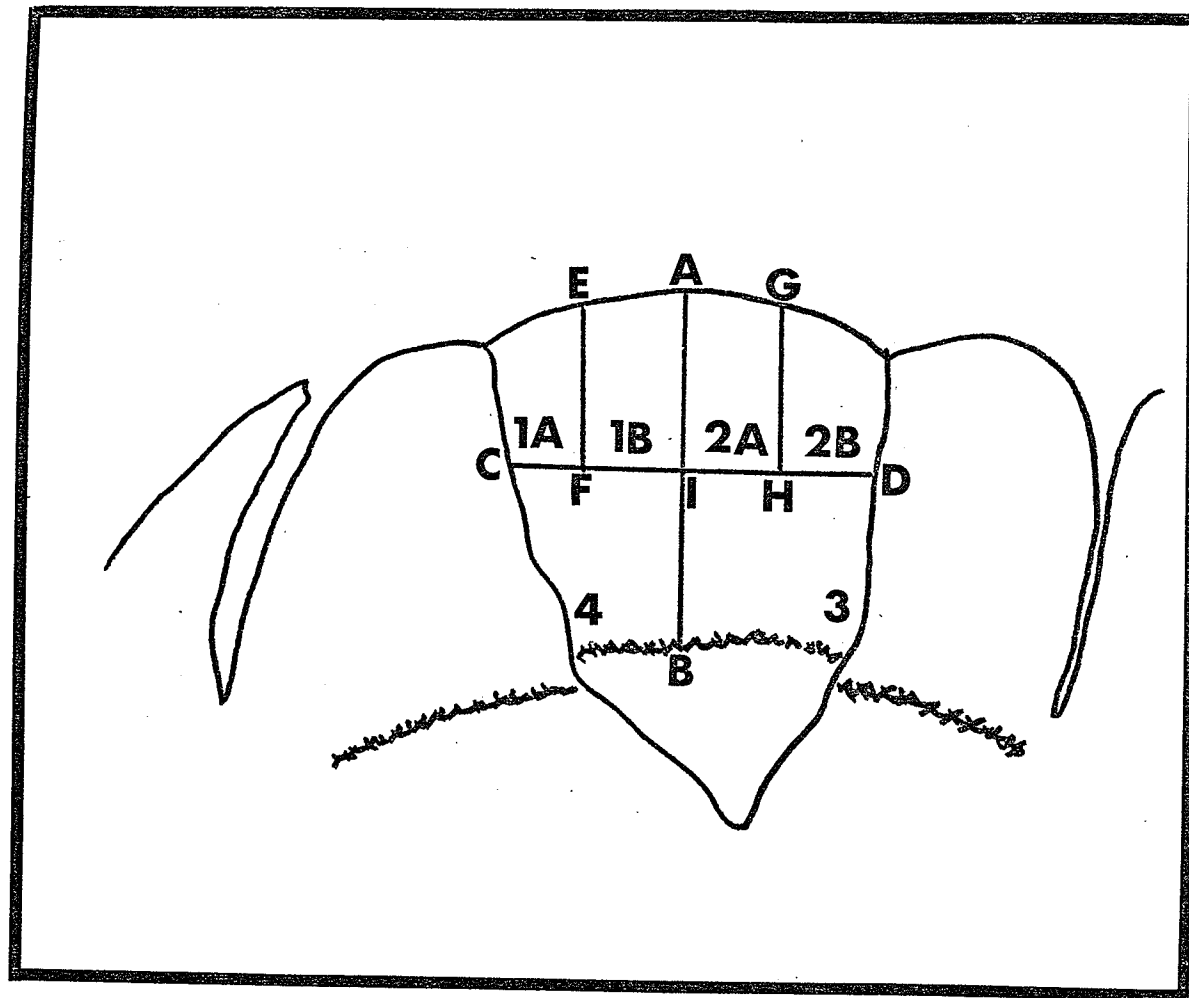


Fig. 8 Coronal Section of Chronically Isolated Slab
Showing Subdivisions for Neuron Population Density

Legend for Fig. 8

A-B Midline of slab width

C-D Division of slab cortical depth into upper
and lower halves

E-F, G-H Equal subdivision of each quadrant
in upper half

with the responses obtained when isolated slabs of cat's cerebral cortex are stimulated electrically at their pial surface.

Coronal sections from suprasylvian gyri were observed through a camera lucida instrument attached to the Zeiss-Winkle microscope. A drawing tube of the Treffenberg type (Model SZ8321) was supplied by Wild Heerbrugg Ltd., Switzerland. The drawing tube projected a real image of the drawing paper in the intermediate picture plane. The paper image, therefore, was not mirror-reversed. The drawing tube was attached on the one side to the binocular inclined tube and on the other side to the objective rotator cone of the microscope. This system permitted the continued and simultaneous use of multiple ocular inserts. One of the oculars was fitted with a 15X ocular goniometer having a 360° etched rotator on crossed hairs. It was used in direct microscopic observation. The other ocular was fitted with two superimposed micrometer disc inserts which were earlier described. Both micrometer discs were recalibrated against a stage micrometer. The extension of the microscope tube by the drawing apparatus resulted in a 1.25X multiplying factor. Two rotating polarization light filters were separately fitted beneath the sub-stage condenser. By selective filter rotation the viewer was able to vary independently the image brightness of the microscope slide and of the drawing paper.

Intact cortex. An area, corresponding to the region previously chosen for studying histological parameters in the intact cortex, was subdivided into four segments as illustrated in Fig. 9. The cortical segments designated 1 and 2 extended down to Brodmann's layers I, II, III and part of IV. The combined width of segments 1 and 2 was 3000 microns, the mid-point, (A-B in Fig. 9), passed through the middle of the gyrus width. The depth of the segments was half the cortical depth at the mid-point of the gyrus width. Segments 3 and 4 included Brodmann's layers IV and V. This method of subdivision helped to rule out errors due to variations between different cortical regions.

Analysis of cytological changes was confined to patterns of arborization in apical dendrites. Camera lucida drawings were made from those nearly complete dendrite trees which had an observable soma. A representative dendrite tree was chosen from different cortical segments at 1 mm intervals, as illustrated in Fig. 9. The sequence of segments chosen followed a linear spiral in which segment 1 was selected for the first millimeter, segment 2 for the second millimeter and so on, i.e., 12341234. This selection pattern usually enabled each segment to be represented three times in each gyrus. It was necessary to pinpoint the exact regional relationships of the selected soma within the intact cortex. The soma distances from the

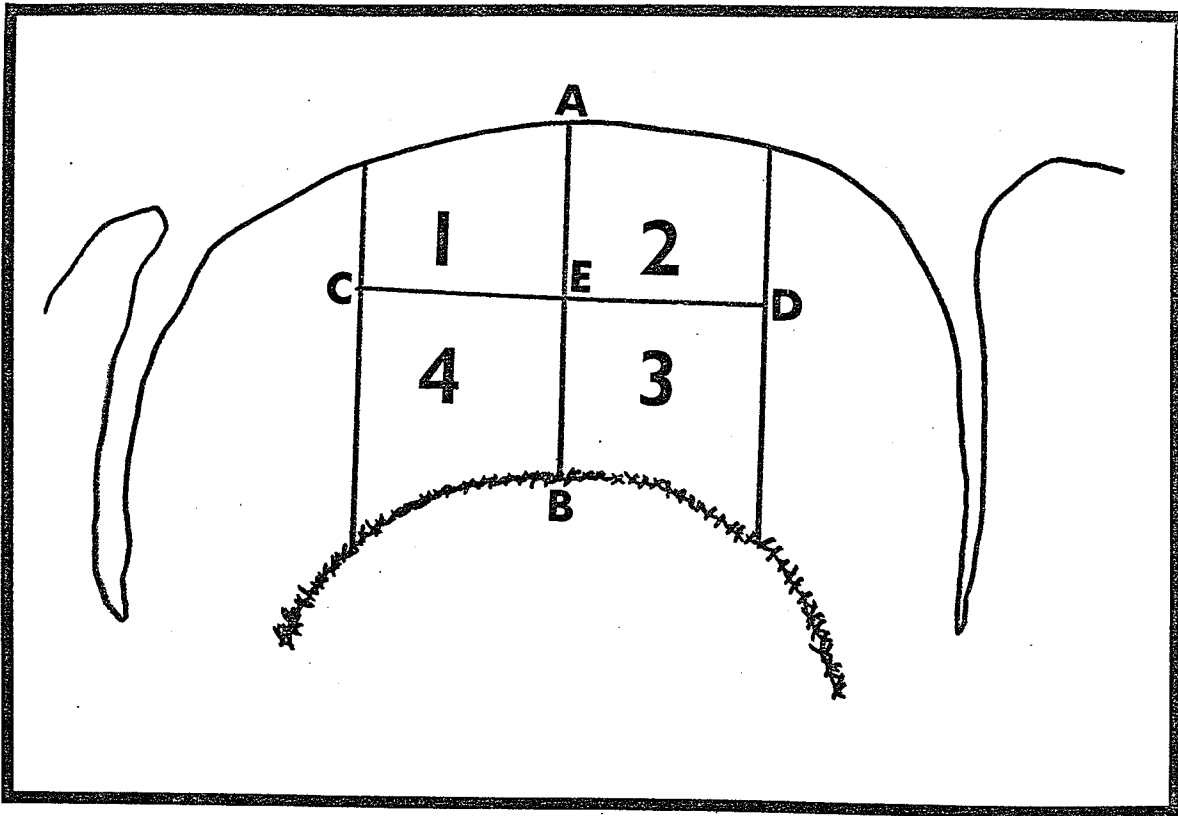


Fig. 9 Coronal View of Intact Cortex with Subdivision of Cortex into 4 Quadrants for Measurements of Cytological Parameters

Legend for Fig. 9

- A-B Midpoint of gyrus width drawn through cerebral cortex
- C-D Total width of segments 1 and 2 at base line and equal to 3,000 microns
- C-E Total distance 1,500 microns and equal to G-D
- A-E One-half the cortical depth and equal to G-B

dorsal pial membrane and the lateral sulcus were measured and recorded. These parameters helped to identify the exact locus of the soma in relation to the Ansatz sulcus as well as to the closest pial surface. The soma diameter may be measured by several methods; in this study the soma diameter was considered as the widest horizontal plane which lay vertical to the apical shaft. Dendrite trees, with the exception of their spines, were traced out as exactly as possible from slides which were observed at 750X magnification. All discrete and tortuous pathways of the dendrite branches, including V-shaped wedges (Results, p234), were followed. In some instances it was almost impossible to distinguish the difference between a branch bifurcation and two closely separated dendrites whose angle of crossover was less than 45° . In such cases the oculars were changed to 20X KPL and the objective to an oil-immersion 100X planapochromat. Although this power was above the effective magnification range for these optics it nevertheless enabled the viewer to make the required distinction.

Bok (1959) reported a positive correlation between the size of the perikaryon and the size of the dendrite tree. In this present study the dendrite arborization was divided arbitrarily into zones, each of which measured 10 times the diameter of the neuron's own soma. Thus the size of the dendrite tree zones

was related to the size of the soma; this permitted the data from neurons with differing dendrite tree sizes to be pooled. Each bifurcation in the dendrite tree, referred to throughout this study as a branch point, was assigned an encounter number which commenced from the clockwise direction. The first branch point encounter along the apical shaft was designated as the first order of branching. Each branch point from succeeding branch sections was then designated a single numerical increase in branch order (Fig. 10). The number of branch points and V-shaped wedges in each zone were recorded. A branchlet was defined as a dendrite section whose linear length is less than twice the soma diameter and which emerges only from the primary apical shaft in the stem zone. Such branchlets were not enumerated in this study. The distance between the distal part of the observable tree and the dorsal pial surface was measured and recorded.

An ocular goniometer was used under direct microscopic observation to measure the angles at branch points. On a few occasions the two branch sections immediately following a branch point were not in the same plane of focus. In such instances the two branch sections can be compared to an angle rotated around one of its arms. In consequence the observed angle must always be less than the real angle. The correction factor which was used to calculate the real angle

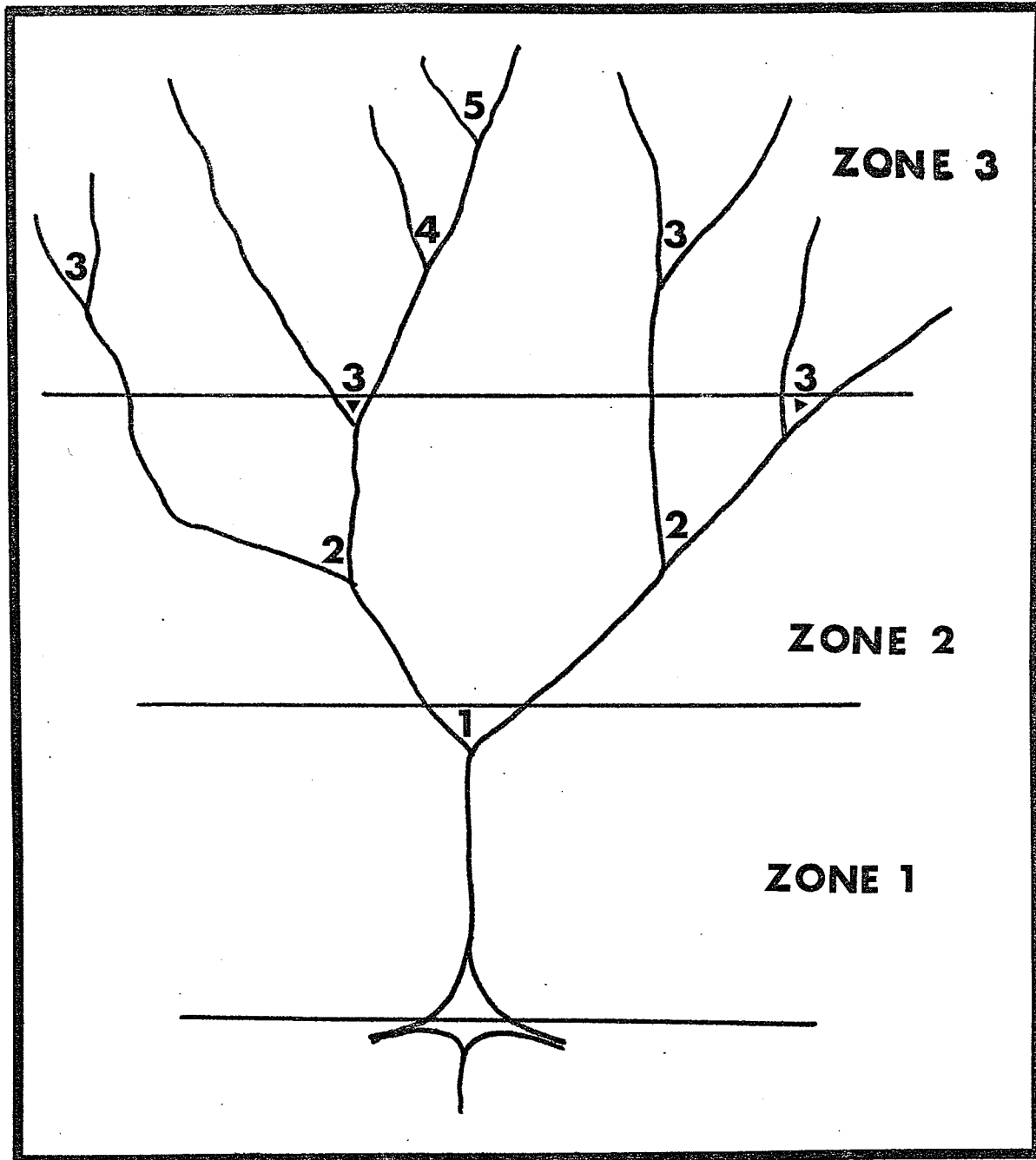


Fig. 10 Diagrammatic Presentation of Apical Dendritic Tree Showing Zone Distribution and Designation of Branch Order

Each zone measures 10 times the diameter of the neuron's own soma.

required the measurements from the following parameters:

a) The observed angle, b) the vertical distance between the two branch sections at loci 5 microns from the branch point. The trigonometric basis for this calculation is given in the appendix of this thesis.

Isolated cortex. The cytological reorganization of apical dendrites was analyzed in acute and in chronically isolated cerebral cortex. Most of the analytical methods described earlier for the intact cortex were applied also to the isolated slabs. The histological location of the perikaryon was determined in relation to the side cuts of the slab and not to the pial membrane of the middle suprasylvian sulcus. This parameter pinpointed the distance between the soma and the area of surgical deafferentation.

There are several techniques by which histological parameters can be measured. The direct method, which is the most reliable technique, obtains measurements under direct microscopic observation. Instrumental loss of resolution in this technique is limited only by the optical system of the microscope. The indirect methods involve the use of photomicrographs, camera lucida drawings and projections of microscopic images on a screen or through a television monitor. These techniques utilize both optical and non-optical systems each of which has its own characteristic loss of resolution.

The single use or coupling of any of these techniques results in a significant reduction in optical resolution and spatial orientation for observing and for measuring cortical cellular components. In the present study all histological and cytological measurements were obtained by the direct microscopic technique.

4. DISCUSSION of METHODS

Non-neuronal cerebral cortical cells. In this study the neuroglia were neither qualitatively nor quantitatively analyzed. Histo- and cytomorphological differences between neuroglial and neuronal cells were determined before any analyses were made of the histological sections. Neuroglia identifications were made on the basis of the following: a) size and shape of soma, b) morphology of processes, c) histological and cytological relationships. Currently standard neuroanatomy texts recognize four basic types of glial cells in the CNS: a) fibrous astrocytes, b) protoplasmic astrocytes, c) oligodendrocytes, and d) microcytes. Hortega (1920) and Polyak (1965) considered microcytes as a "false neuroglia" which belong to the reticulo-endothelial system. Their views were based upon the mesodermal origin of microcytes which is in contrast with the ectodermal origin of astrocytes and of oligodendrocytes.

Polyak (1965), in his review on the light microscopy study of neuroglia, noted that metallic impregnation was the only reliable technique for the study of glial morphology. However, some glial cells, such as fibrous astrocytes, do not exhibit consistent morphological characteristics with modifications of the metallic technique. The Golgi method impregnates the cell body and its processes, the Cajal method clearly demonstrates

perivascular end-processes, while the Hortega method preferentially exhibits gliofibrils. Ramon-Moliner (1957, 1961) reported that microcytes and oligodendrocytes stained well in fresh tissue only when the fixative contained a mixture of formaldehyde, dichromate and chloral hydrate. The modified Golgi-Rapid method used to impregnate dendrites for this study gave inconsistent staining of neuroglia. Therefore, in order to distinguish accurately between neuronal and neuroglial cells, this study took into account the morphological characteristics of neuroglia after different impregnation techniques.

Protoplasmic astrocytes are confined, with few exceptions, to the gray matter of the brain and spinal cord. They are found in abundance, attached to the undersurface of the pia. The soma, which is mononuclear, is either stellate or multipolar in shape and gives rise to several processes. The astrocytic soma and nucleus are larger than counterparts found in oligodendrocytes and microcytes (Smart and Leblond, 1961). The nucleoplasm contains fine chromatin granules which are closely packed at the nuclear membrane. The cytoplasm contains a centrosome although no mitotic figures have been found (Ham, 1965). Other cytoplasmic inclusions include dark granular gliosomes, which, together with numerous gliofibrils, extend throughout the length of the processes (Penfield, 1932). Lipochrome pigments and a nucleolus

are present but each requires a specific nonmetallic staining technique for detection.

The somata give rise to numerous wavy processes which branch freely. These processes are considered to be cytoplasmic extensions which lie between axons and dendrites. Astrocytic processes do not ensheath neuronal processes (Penfield, 1932). Palay (1958) and Palay et al (1962) observed, with the aid of the electronmicroscope, that astrocytic processes formed a major portion of a CNS neuropil. Modified cerebral cortical astrocytes with a mixture of protoplasmic and fibrous processes were noted by Held (1909). Plasmatofibrous astrocytes found at the boundary between cortical gray and white matter also bear a mixture of processes (Bloom and Fawcett, 1965). The protoplasmic type extend into the gray matter while the fibrous type run into the white matter. Protoplasmic processes are directionally orientated either to a neuronal perikaryon or to cortical blood vessels. The vascular contacts are formed by means of terminal dilations which Cajal termed perivascular end-feet.

Hortega (1943) recognized three types of protoplasmic astrocytes: (a) Neuronal satellite--the astrocytic soma lies flattened in close apposition to a neuron body, (b) Interneuronal--the soma is non-specific in location while the processes are perineuronal and perivascular, (c) Vascular satellite--the astrocytic soma

lies in contact with the wall of a blood vessel.

Superficial injuries to the brain and spinal cord are accompanied by structural changes to the subpial astrocytes (Palay, 1958; Bunge et al, 1961). The number of fibrous processes soon increases and these contribute, in part, to the formation of CNS scar tissue.

Fibrous astrocytes are generally confined to the white matter of the CNS. The soma morphology is similar to that for somata of the protoplasmic astrocyte.

Fibrous processes, in contrast with the protoplasmic type, are narrow in diameter and have very few branch points (Penfield, 1932). Several fibrous processes bear terminal dilations which form perivascular feet. The remainder of the fibrous processes run between and parallel to myelinated fibres.

Oligodendrocytes are the most abundant type of glial cell found in the gray matter and to a lesser number in the white matter of the brain and spinal cord (Penfield, 1932). The oval soma, which is smaller than its astrocytic counterpart, contains either an oval or a round nucleus. A nucleolus is present; however, it can be demonstrated only with a specific nonmetallic staining technique. Cytoplasmic chromatin granules, which coexist as both coarse and fine types, are closely packed near the nuclear membrane. Palay (1958) noted that ultra-fine nucleoprotein granules and vacuoles were present in the cytoplasm. Gliofibrils, which are a

common feature of the astrocyte, are not present in the soma or in processes of the oligodendrocyte. In the gray matter the oligodendrocytic soma usually lies as a satellite of either a neuron cell body or a blood vessel. The oligodendrocytes in the white matter are commonly distributed in rows that lie between myelinated fibres.

The oligodendrocytic processes, which are few in number, originate directly from the soma. The processes are long and slender and have very few branch points. The modified Golgi-Rapid method employed in this study often resulted in periodic dilatations along the attenuated oligodendrocytic processes. The terminations of processes from oligodendrocytes do not form perivascular contacts. Penfield (1932) and Luse (1956), as well as other investigators, have noted that oligodendrocyte processes are associated with the myelination of nerve fibres.

Hortega (1928) recognized four morphological types of oligodendrocytes:

Type I--were found to be abundant in the gray matter of the forebrain, cerebellum and spinal cord. These cells were distributed around blood vessels, neurons and fibre tracts. The type I cell body, which is 15 to 20 microns in diameter, is either spherical or slightly polygonal. Several processes emerge from the cell body, and then branch to form elongate delicate processes which

become directionally orientated towards nerve fibres. Type I correspond to Robertson's (1900a) mesoglia cells.

Type II--were found only in the white matter. The soma, 20 to 40 microns in diameter, has a somewhat cuboid shape and is larger than the type I soma. The processes are fewer and thicker than type I and are usually closely wrapped around nerve fibres. According to Polyak (1965) type II cells were previously referred to as Cajal's apolar cells.

Type III--were found mainly in the spinal cord, cerebellar and cerebral peduncles. The soma, irregular in shape, gives rise to 3 or 4 relatively thick processes which cover a wide area of nerve fibres. These cells corresponded to Paladino's (1892) neuroglial cells.

Type IV--were found only in the white matter. The cell body, which lies in apposition to nerve fibres, is either mono or bipolar in shape.

Penfield (1932) has suggested that oligodendrocytes, in addition to their involvement with myelin formation, are in some way associated with the elimination of debris during secondary degeneration of nerve fibres. Truex and Carpenter (1964) have theorized that perineuronal oligodendrocytes are probably responsible for neuronophagia, the removal of dying nerve cells.

Microcytes are commonly found in the gray matter of the spinal cord and brain. They are also found, in lesser numbers, in the white matter lying between

myelinated nerve fibres. The microcytic soma, smallest of all the neuroglial cells, is either perineuronal or perivascular in position (Smart and Leblond, 1961). Microcytes, as a mesodermal derivative, originate from the pia mater and usually accompany blood vessels into the brain and spinal cord. Cerebral cortical microcytic soma, when stained with hematoxylin and eosin, appear elongate and oval. When impregnated by the Golgi method the soma form a stellate outline (Penfield, 1932). The nucleoplasm contains uniformly distributed coarse and fine granules within an oval or rounded nucleus (Smart and Leblond, 1961). Gliosomes and gliofibrils are not present in the cytoplasm.

The microcytic processes are relatively thick with several small branch sections which bear short spines. The terminations of the processes do not form perivascular end feet.

Lacerations of brain tissue are accompanied by an enlargement of adjacent microcytes, termed Compound Granular Corpuscles, or Gitter cells, which become phagocytic in activity (Ransom and Clarke, 1959).

RESULTS

1. GROSS APPEARANCE

Intact gyrus. The surface topography of the suprasylvian gyrus in adult cats exhibits subtle gross morphogenic variations at both anterior and posterior ends (Papez, 1929). The ansatus sulcus was taken arbitrarily as the landmark which would demarcate the anterior end of the suprasylvian gyrus. In the majority of cats examined the ansatus sulcus formed an approximate angle of 115° from an attached vertical axis formed by the lateral sulcus (Appendix, Fig. 3). However, in some cats the angle is larger than 145° , resulting in the placement of the ansatus sulcus in the posterior sigmoid gyrus. A variation of this type did not clearly identify the morphological distinction between the anterior end of the suprasylvian gyrus and the posterior end of the coronal gyrus. In such cases the anterior end of the suprasylvian gyrus was taken arbitrarily to be at the coronal plane which passed through the junction of the ansatus and lateral sulci. Morphogenic variations of sulci in the occipital area necessitated the choice of an arbitrary landmark which would identify the posterior end of the suprasylvian gyrus. The angle between the posterior sylvian and middle

suprasylvian sulci usually forms a right angle. However, in some cats where the angle was greater than 90° the posterior termination of the suprasylvian gyrus was somewhat indefinite. The demarcation between these two latter gyri was taken to be the coronal plane which passed through the junction of the posterior suprasylvian and the middle suprasylvian sulci. In addition, the posterior lateral sulcus was not always continuous with the lateral sulcus. This resulted in a noticeable gap, 2-3 mm wide, of cortex between the marginal and suprasylvian gyri. An ipsilateral morphogenic variation was not necessarily repeated on the contralateral homotope gyrus. The suprasylvian gyrus in all cats examined had a slight curve whose concave surface always faced the mid-sagittal plane.

Surgical procedures employed for bilateral craniectomy and removal of the dura mater did not cause any undue swelling of the brain. The pial membrane and its containing blood vessels appeared quite normal following surgery.

Acute gyrus. The gross morphogenic variations described earlier for intact gyri were found also in cats used for acute neuronal isolation. The blood vessels lying between the intima pia and epipial layer (Key and Retzius, 1875; Millen and Woollan, 1961, 1962) showed no evidence of luminal collapse in either the

acute or the chronic type of preparation. The occasional slight swelling of the suprasylvian gyrus following surgery subsided after a couple of hours. However, in two acute preparations, the brain was discarded because of excessive edematous swelling; it was felt that cytological distortion would have occurred within the cerebral cortex of those two preparations.

The isolated slab could be identified, at the gross level, by a subpial rectangular dark line which corresponded to the cortical side cuts.

Chronic gyrus. Newly regenerated bone in the chronic animal was thin and very delicate. It had a mottled outer surface which contrasted with the smooth plane surface of the old parietal bone. Fibrous connective tissue adhesions were formed between the new bone and the sutured dura mater. Subdural adhesions developed fibrous attachments with the underlying epiplial membrane. Surgical detachment of the adhesions did not injure the cerebral cortex. There was no gross evidence of hypoxia or anoxia in the area. All gyri in the area were pinkish in color. In gross examination the suprasylvian gyrus with the chronically isolated slab appeared slightly sunken in relation to the height of adjacent intact ectosylvian and marginal gyri. The dorsal periphery of the slab was outlined by a continuous

dark line which was formed from subpial cortical scar
tissue.

2. HISTOLOGY of CORTICAL PREPARATIONS

Intact cortex. Coronal sections from intact suprasylvian gyri were initially examined at 25X. Observations of "0" mm section revealed that cortical morphogenic development in this gyrus could be categorized into three basic histological patterns (Plates III, IV, V).

(i) Type I--Continuous arch. The cerebral cortex is horizontally arched between the two adjacent gyri. The glial line appears to extend continuously across the ectosylvian, suprasylvian and marginal gyri; however, the line is interrupted by invaginations of the intima pia from the middle suprasylvian and lateral sulci.

(ii) Type II--Partial arch. The glial line is unilaterally continuous with its counterpart in an adjacent gyrus. The contralateral part of the glial line curves inwards and is directed towards the white matter. It therefore has an intragyral termination.

(iii) Type III--Intragyrar arch. In this type the glial line is bilaterally directed towards the white matter and does not exhibit spatial continuity with the glial line of adjacent gyri. Two modified forms of the three basic types are shown in Plates VI and VII. The gyrus shown in Plate VI exhibits a papilla-like evagination of white matter extended into the cerebral cortex.

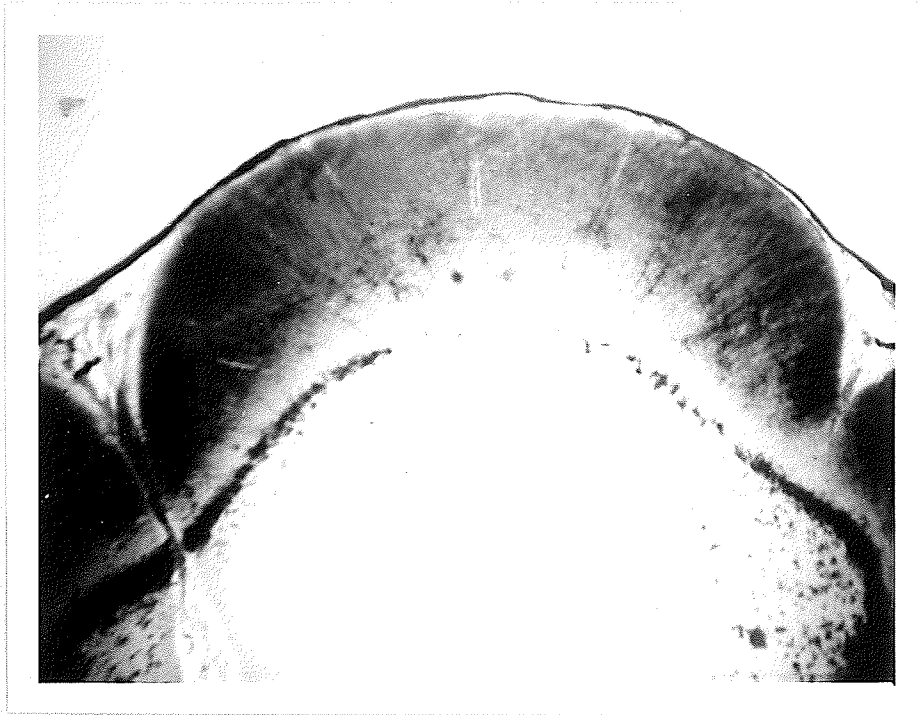


Plate III. Coronal Section of Acute Gyrus, 12.5X

Histological pattern type I. Continuous

Arch

Glial line appears to extend continuously across ectosylvian, suprasylvian and marginal gyri.

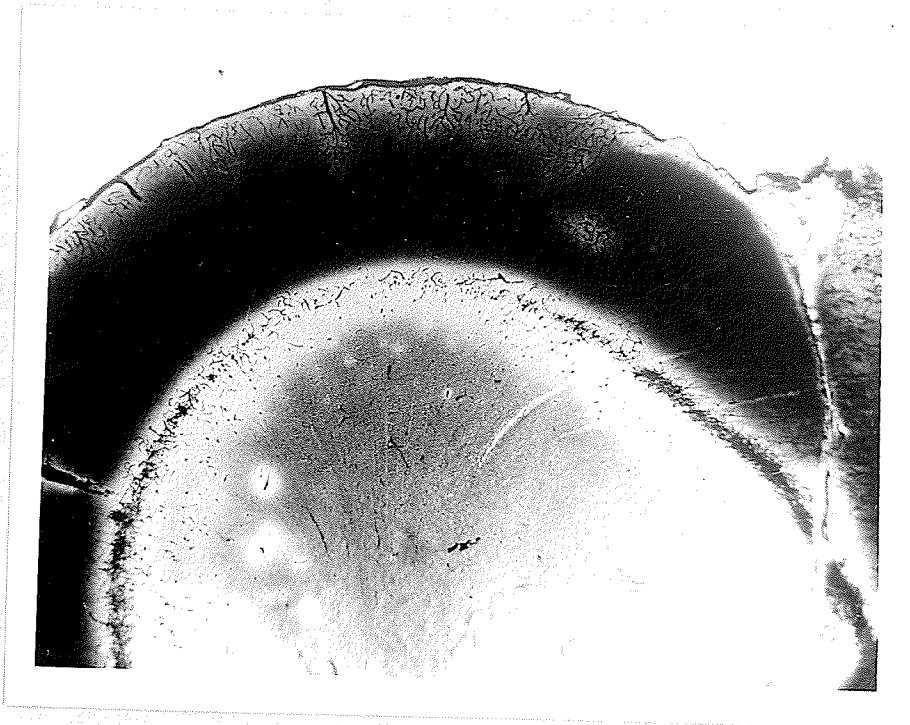


Plate IV. Coronal Section of Intact Gyrus, 12.5X

Histological pattern type II. Partial Arch
Glial line is intragyral on one side.

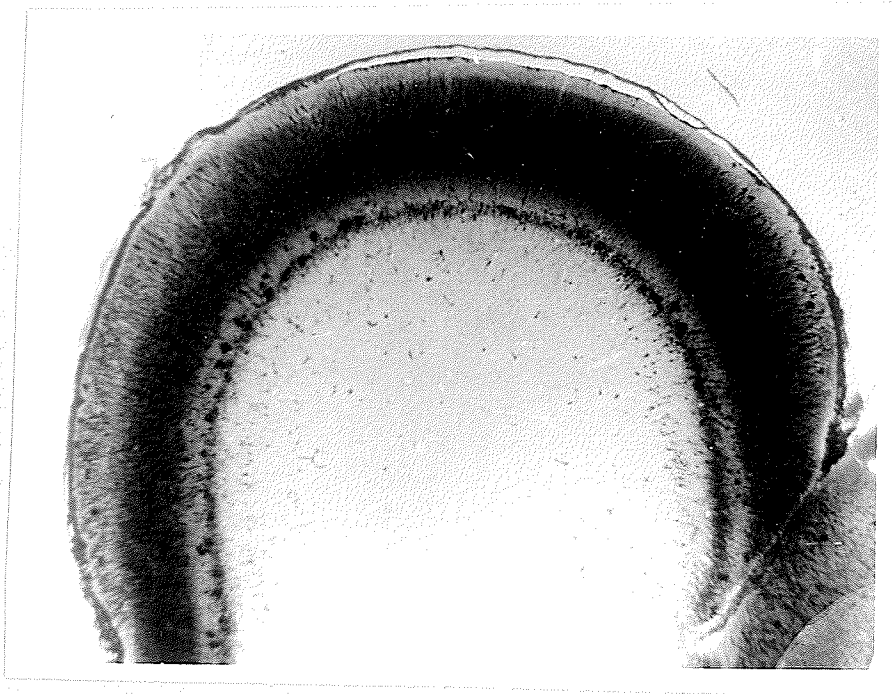


Plate V. Coronal Section of Intact Gyrus, 12.5X

Histological pattern type III. Intragyrar Arch

Glial line is bilaterally directed towards
white matter.



Plate VI. Coronal Section of Intact Gyrus, 12.5X

Note papilla evagination of white matter
extending into cerebral cortex.

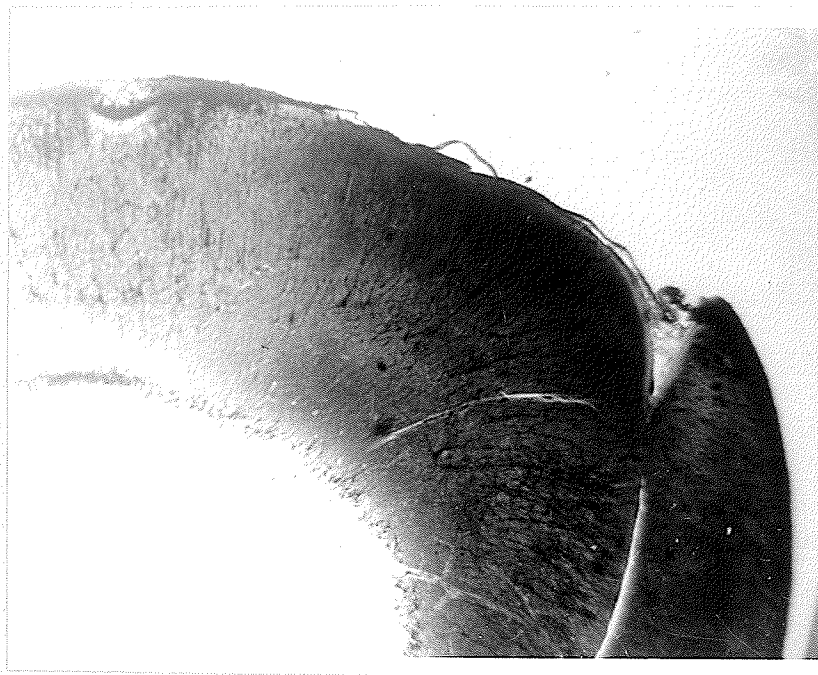


Plate VII. Coronal Section of Intact Gyrus, 12.5X

Note extensive overlapping of marginal gyrus
on right side, cortex thin and elongate.

Plate VII shows an elongate arch on one side and partial overlapping of the dorsal surface.

The en-bloc staining technique used in this study gave, for the most part, consistently good results. However, in one intact preparation, the cortex from the left and from the right homotope gyrus was not impregnated. Unaccountable overstaining of two other intact gyri resulted in the cortex being rendered useless for cytological study.

It was calculated that approximately 2% of the neurons and their processes were impregnated with silver. These results are in accord with those reported earlier by Sholl (1956). The perikarya, apical and basilar dendrites appeared black against a yellowish background. However, on epilumination the neurons appeared greyish in color. A few protoplasmic astrocytes and oligodendrocytes were found scattered throughout the section. Dendritic spines were well impregnated and were easily discerned. In almost all sections examined the lumen and cellular walls of blood vessels were not impregnated. The cross section and longitudinal section of cortical blood capillaries showed up as optically light areas which accounted for vacuolar-like areas throughout the section (Plate VIII).

Apical dendrites in the terminal zone sometimes showed a beaded effect (Plate IX). The perikarya of these dendrites could be found in either layer III or

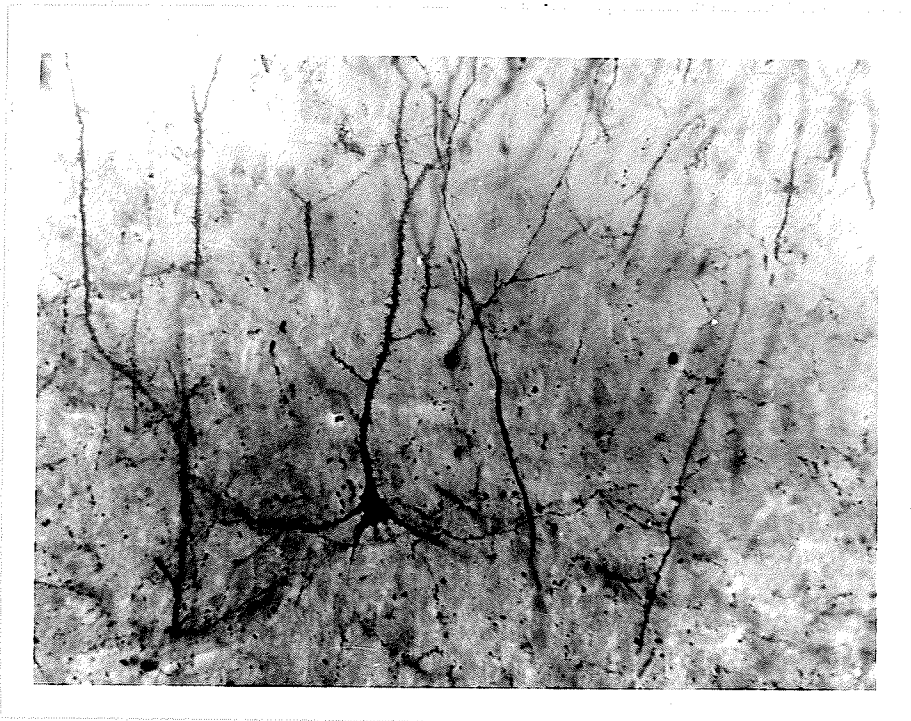


Plate VIII. Intact Cortex, 200X

Irregular patterns of optically light areas
are dispersed throughout the cortex.

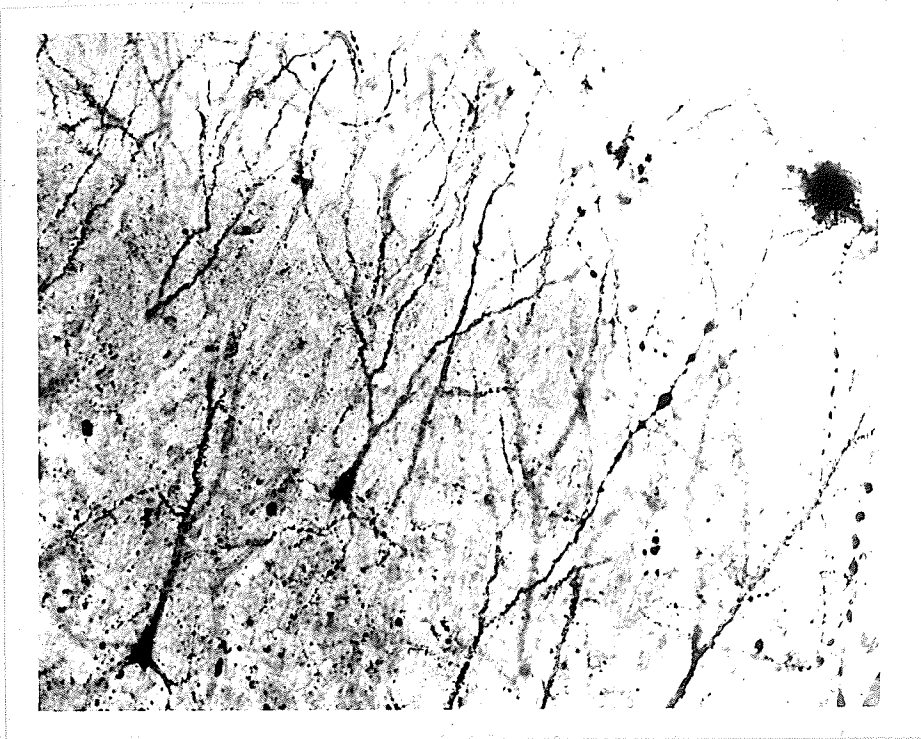


Plate IX. Intact Upper Cortical Region, 125X

Some dendritic sections in terminal zones
end as dendritic dilatations

layer V. Dendritic dilatations, when present, were found only in the subpial area of the suprasylvian gyrus. They were never present in the cortical areas of the two adjacent ectosylvian and marginal gyri. These results are in contrast with the results of an earlier study of "dendritic bulbous dilatations" by Mungai (1967). The significance of the two contrasting results will be presented in the Discussion section of this thesis.

Acute cortex. The side cuts within the cortex were readily identified by two dark scar lines that extended from the pial surface to the glial line. The cuts in the white matter, though discernible, were less pronounced (Plates X and XI). Small cyst formations which contained a mixture of clear fluid and blood cells were observed at the base of the slab within the first four hours of acute isolation. Blood plasma exudate and blood cells were noted also to occupy the entire depth of the side cuts. The impregnation of acutely isolated cortex was very similar, generally, to that of intact cortex. Two acute slabs were electrically stimulated for short periods of time with 1.0 m Sec pulses at a frequency of 30 per sec and pulse amplitudes of approximately 10 volts. These slabs appeared, on strictly subjective observation, to be more heavily impregnated with silver than were the unstimulated preparations.

The glial line between the side cuts was

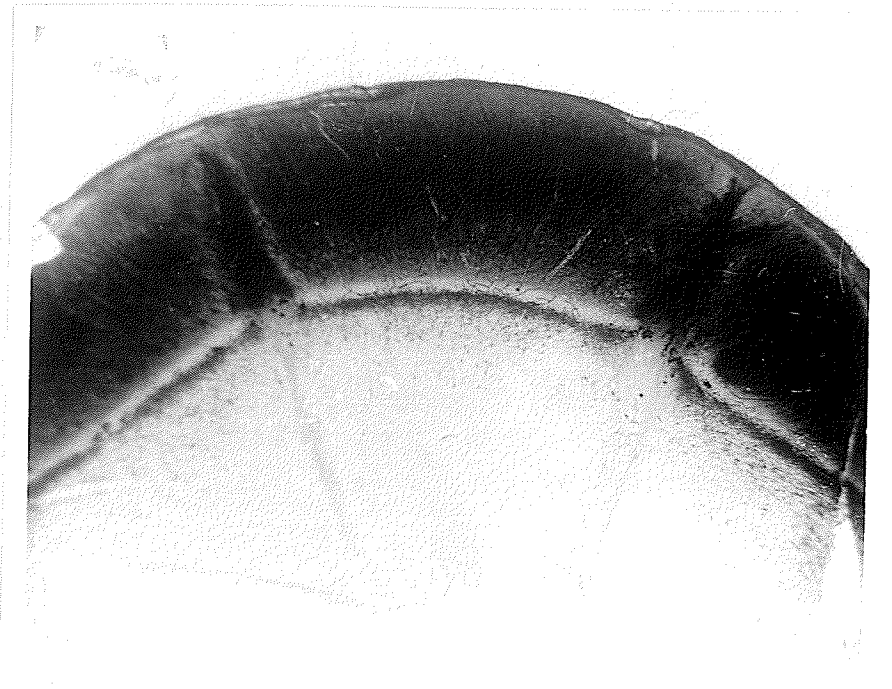


Plate X. Coronal Section, Gyrus with Acute Slab, 12.5X

Side cuts in cortex marked by two dark lines.
Cuts in white matter less discernible.

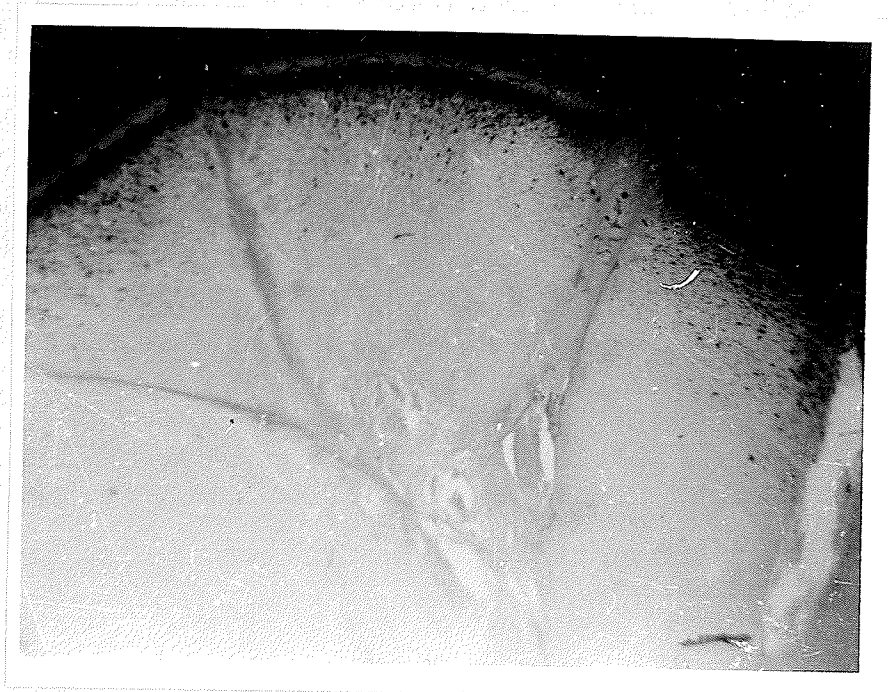


Plate XI. Coronal Section, White Matter of Acute Slab, 25X

White matter of slab shows evidence of bilateral shrinkage after six hours of isolation.

elevated for a few microns into the cortical area. The underlying white matter, after only a few hours of isolation, showed structural evidence of bilateral compression and concurrent shrinkage (Plate XI).

The photograph on Plate XII shows part of a coronal section of an acute preparation two hours after isolation. The initial form of the acute slab was a rectangle and no evidence of compression was seen. Such a result indicates that the wire isolating knife had been inserted parallel to the height of the cortex and that the undercutting knife was at right angles to this. The photograph on Plate XI reveals the presence of bilateral compression after six hours of isolation. In this example a six-hour isolation period resulted in a reduction of the width of the slab at the base of the cortex compared with the slab's subpial width. The form of the slab, therefore, becomes that of a rhomboid after periods of isolation that are six hours or greater. This eventual rhomboid shape may be deduced from the extensive series of measurements which are summarized in Table 2 and Fig.12 of the next section.

Preparations examined after 13 hours of isolation showed evidence of the slab having undergone considerable tissue deformation (Plate XIII). The isolated cortex became shallower than its adjacent intact cortex in the same gyrus. Cyst formations at the base and along the sides of the slab apex were larger than in the slab

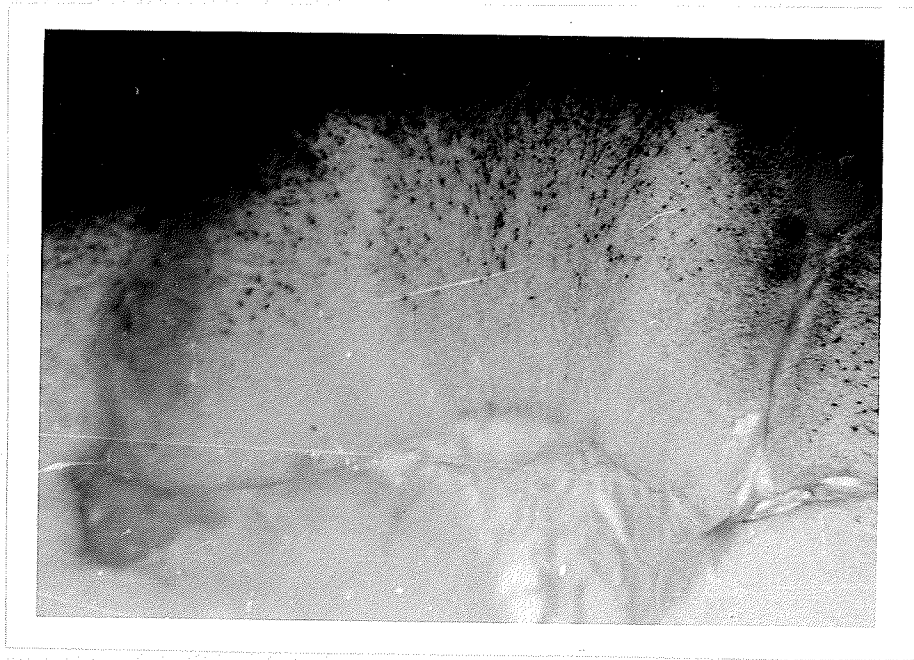


Plate XII. Coronal Section, White Matter of Acute Slab, 25X

No evidence of shrinkage or tissue distortion after two hours of isolation. Cyst formations filled with blood cells and clear fluid.

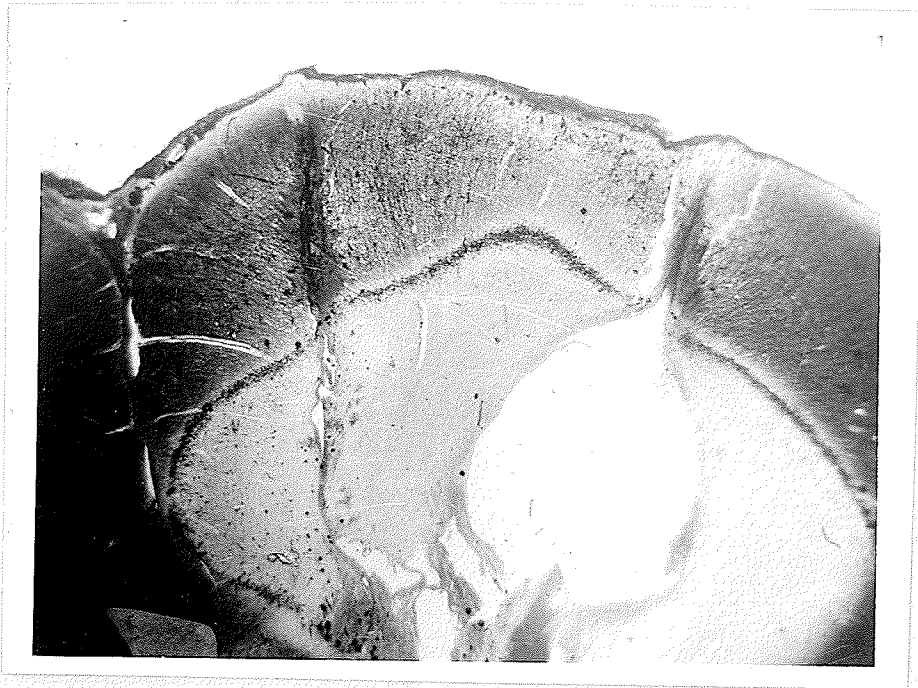


Plate XIII. Coronal Section of Gyrus with Acute Slab, 12.5X

Preparation after 13 hours isolation showing
extensive cortical deformation.

examined only a few hours after isolation.

Chronic cortex. The histological effect of long term chronic isolation is shown in Plate XIV. After 6 to 11 months of chronic isolation the slab exhibited considerable tissue deformation and shrinkage. In coronal sections the original rectangular isolate was transformed into a triangular shaped mass with the apex directed towards the white matter. The pial surface of the gyrus had three convex curves; two dimples on the pial surface corresponded in position and were attached to the underlying cortical scar tissue. The lower two-thirds of the slab was surrounded by large clear cysts which were notably devoid of any cellular constituents. Chronic slabs were not as intensely impregnated as intact or acute cortical preparations; however, perikarya and their dendritic arborization patterns were clearly defined and later analyzed.

In only one chronic preparation did neuroglial scar tissue completely fill the cortical area of the slab. This type of metaplasia was also found in the immediate adjacent intact cortex of the same gyrus.

Arterioles and venioles lying within the pia mater were found to be filled with blood cells. Blood capillaries were abundantly present in cortical and subcortical areas.

Chronic slabs, in contrast with intact and acute



Plate XIV. Coronal Section, Gyrus with Chronic Slab, 12.5X

Chronic slab after 11 months isolation.

Pial surface has 3 convex curves with 2 invaginations at point of side cut. Cyst formations are large and void of any cellular components.

preparations, showed a total increase in the number of observable impregnated protoplasmic astrocytes in the cortex. The glial line appeared dissociated and had lost its normal histological integrity. Most of the observable astrocytes were found in the lower cortical areas. Reiffenstein (1964) reported a fourfold increase in the number of astrocytes in chronic slabs.

Evidence for dendritic sprouting, which has been described by Pick and Bielschowsky (1911), Cajal (1913), Bielschowsky and Gallus (1913) and Lafora (1914), was not found in this study. Dendrites were not observed to extend across the cortical scar lines. Numerous small cells, probably microcytes, were found on either side of the cortical cuts (Plate XVI). In almost all chronic slabs examined the neuronal isolation extended for the entire depth of the cortex. In two chronic slabs it was observed that incomplete separation had occurred in the subpial area. This cortical continuity between the chronic slab and adjacent intact cortex was 75 microns in depth (Plate XVII). An explanatory note which might account for this continuity will be given in the Discussion.



Plate XVI. Chronic Slab, Upper Cortical Region, 35.5X

Chronic slab after 11 months of isolation.

No evidence of axons or dendrites across side cut.

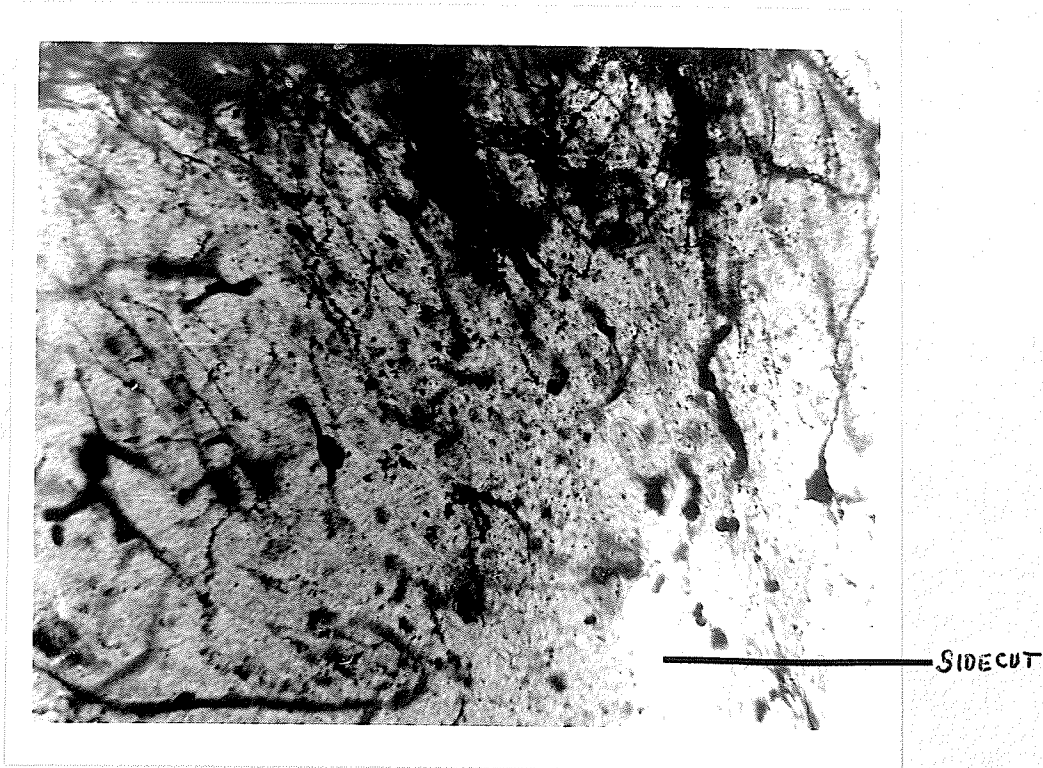


Plate XVII. Chronic Slab, Subpial Region, 500X

Cortical continuity between chronic slab cortex and adjacent intact cortex measured about 75 microns in depth.

3. HISTOLOGICAL DIMENSIONS

Intact gyrus. The quantifiable parameters of gyrus width and cortex depth were measured from coronal sections of five intact left and five homotopic gyri. Small variations in these dimensions were found at each millimeter interval throughout the entire length of every gyrus. The mean dimensions of gyrus width and cortex depth from five cats are shown in Table 1. The maximum variation in the mean gyrus width on the left side ranged from a low of 6031u to a high of 6639u; the mean cortical depth ranged from 1559u to 1690u; these results represent a maximum range of 10% in both of the histological parameters. The mean dimensions from intact homotopic gyri were within the same range of variations as those of the left side. The mean width of the homotopic gyrus ranged from a low of 5929u to a high of 6295u; the mean cortical depth of the homotope ranged from 1537u to 1727u; the maximum range for both parameters was 7% and 12% respectively.

Table 1 shows that there are no significant differences between the mean dimensions at each millimeter interval throughout the lengths of intact left and homotopic gyri. However, an examination of the measurements from the individual gyri showed that in eight out of ten gyri the cortical depth and gyrus width were slightly greater at the anterior and posterior

Table 1. Mean Dimensions of Five Intact Left Gyri and Five Homotopes

Dist. From "0" Section in mm	Left Gyrus Width Microns	Left Cortex Depth Microns	Right Gyrus Width Microns	Right Cortex Depth Microns
6 Ant. End	6412 \pm 230	1690 \pm 98	6240 \pm 128	1727 \pm 131
5	6170 \pm 172	1668 \pm 98	5973 \pm 91	1690 \pm 117
4	6031 \pm 120	1610 \pm 102	6046 \pm 142	1610 \pm 106
3	6170 \pm 142	1588 \pm 102	6156 \pm 168	1581 \pm 98
2	6207 \pm 109	1581 \pm 106	6156 \pm 124	1544 \pm 113
1	6203 \pm 117	1592 \pm 142	6097 \pm 120	1588 \pm 109
0	6222 \pm 139	1573 \pm 113	6002 \pm 172	1537 \pm 109
1	6258 \pm 150	1559 \pm 117	5929 \pm 201	1566 \pm 102
2	6368 \pm 230	1603 \pm 106	6200 \pm 175	1603 \pm 113
3	6295 \pm 226	1595 \pm 95	6295 \pm 157	1573 \pm 102
4	6295 \pm 193	1617 \pm 102	6192 \pm 183	1581 \pm 102
5	6368 \pm 219	1617 \pm 95	6185 \pm 252	1581 \pm 120
6 Post. End	6639 \pm 256	1647 \pm 98	6112 \pm 285	1551 \pm 120

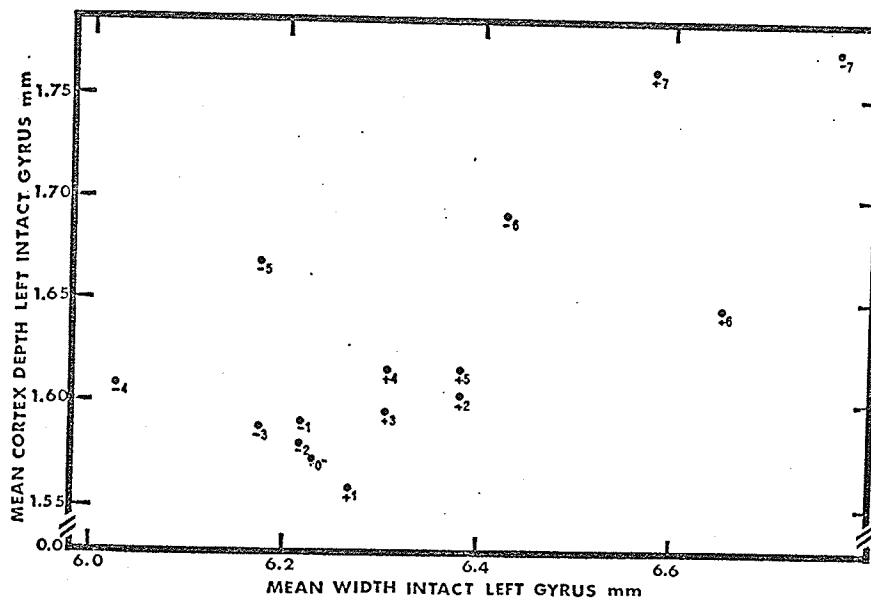


Fig. 11 Mean Gyrus Width Plotted Against Mean Cortex Depth from 5 Intact Left Gyri

No simple relationship is shown.

Note: Sections anterior to midsection "0" are designated as + mm; sections posterior to midsection "0" are designated as - mm.

range of these measurements at each millimeter interval was comparable with those just described for the intact gyri (Tables 1 and 2). However, the overall widths of gyri in which acutely isolated slabs had been prepared in left and right hemispheres were significantly greater than comparable parameters for intact gyri ($p \leq 0.001$).

Variations in slab width were examined along the length of the slab in order to determine whether there was a distinctive pattern of shrinkage at the pial surface of slabs in the left hemisphere. The result of plotting the mean widths and their standard error from Table 2 are shown in Fig. 12. No significant differences were found, in five acute preparations, between the mean slab width at any of the 1.0 mm sections for a distance of 6.0 mm on either side of the "0" section.

Such results indicate that the isolating cuts had been made with uniform spacing. There is, however, an unmistakable tendency for the middle of the slab to be narrower than any other region; an examination of the data from each individual gyrus showed that "0" mm section was always the narrowest part of the slab between -5 mm to +5 mm sections.

The depth of cortex in the acutely isolated slab was always shallower at the same locus than the adjacent intact cortex within the same gyrus (Table 2). The shallowest parts of the cortex in the means of six acute slabs were found to be at the slab midsection area of

Table 2. Mean Dimensions of Five Acute Isolated Gyri and Four Homotopes (Microns)

Dist. From "0" Section in mm	Left Slab Width	Left Gyrus Width	Left Slab Cortex Depth	Left Intact Cortex Depth	Left Slab Width at Cortex Base
6 Ant. End	3864±124	6463±201	1903±157	1888±164	2287±237
5	4355±146	6661±135	1833±124	1917±142	2766±402
4	4377±124	6906±201	1694±106	1895±139	2964±329
3	4304±146	6997±204	1701±102	1793±124	3154±292
2	4260±150	7016±241	1639±124	1749± 91	3184±230
1	4260±162	6880±256	1603±120	1749± 95	3286±157
0	4194±175	6954±256	1474±131	1712±106	3345±186
1	4289±157	7045±256	1493±117	1705±109	3425±252
2	4370±175	6943±237	1504±142	1778±113	3425±256
3	4406±204	6778±230	1592±120	1808±109	3484±292
4	4465±183	6650±248	1701± 95	1888± 98	3440±314
5	4479±219	6789±256	1844± 69	1961±102	3250±300
6 Post. End	4051±248	6990±201	1994±117	2020±131	2496±146

Dist. From "0" Section in mm	Right Slab Width	Right Gyrus Width	Right Slab Cortex Depth	Right Intact Cortex Depth	Right Slab Width at Cortex Base
4 Ant. End	4684±585	7173±366	1464± 95	1647±201	3403± 36
3	4743±622	7268±234	1474±139	1595±168	3806±219
2	4889±512	7294±340	1438±117	1610±150	3897±128
1	4941±622	7356±289	1464±135	1632±128	4135±183
0	4831±585	7341±366	1449±157	1595±124	4099±292
1	4853±475	7330±402	1522±183	1632± 95	4026±183
2	4878±549	7305±366	1537±201	1621±113	3971±128
3	4853±549	7232±322	1610±256	1647±150	3897±180
4	4475±402	6954±329	1705±274	1756±164	3513±329
5 Post. End	4135±366	6734±475	1683±259	1830±201	3092±329

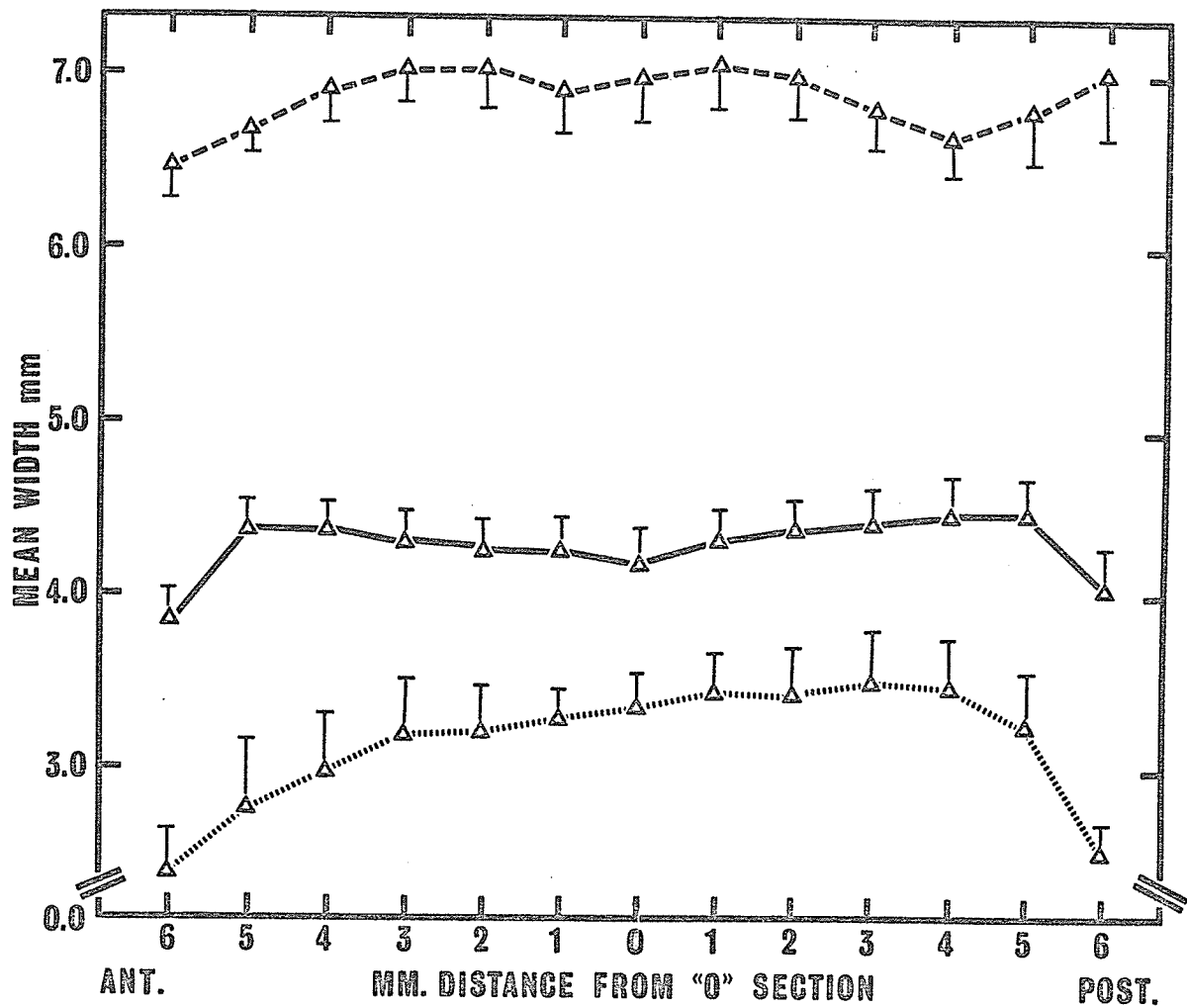


Fig. 12 Mean Widths in 5 Acute Left Gyri and their Slabs

- Δ— — — — Δ— — — — Δ represents mean left gyrus width in 5 acute gyri (illustrated in Fig. 5 as A-B)
- Δ— — — — Δ— — — — Δ represents mean left slab width at pial region (illustrated in Fig. 5 as C-D)
- Δ ······· Δ ······· Δ represents mean left slab width at cortex base (illustrated in Fig. 5 as L-M)

-2 mm to +2 mm sections. The mean slab cortex depth of this region was 1518 ± 115 microns. The maximum depth in this region was 1903 ± 140 microns. The gyrus cortex depth was compared to the slab cortex depth in the mid-region of the slab, from section -2 mm to +2 mm. A paired comparisons test showed the gyrus cortex depth to be significantly greater than the slab cortex depth over this distance ($p \leq 0.01$). There were, however, no significant differences between the slab and gyrus cortex depths at the ends of the slab, (-6 to -4 and +6 to +4 mm sections). These data are presented in graphical form in Fig. 13.

Data from Table 2 reveal the rhomboidal shape which the isolated slab assumes after periods of isolation lasting six hours or more. This is graphically illustrated in Fig. 12 where the slab width at the pial surface is seen to be always larger than the slab width at the base of the cortex throughout the entire length of the slab.

Chronically isolated gyrus. The anterior two-thirds of each chronic gyrus was almost entirely of uniform width while the posterior end was noticeably narrower and tapering (Table 3 and Fig. 14). These figures show that the mean width of six chronic gyri at "+5" mm section was 15% less than the mean width at "0" mm section.

Table 3. Mean Dimensions of Six Chronic Isolated Gyri and Three Homotopes (Microns)

Dist. From "0" Section in mm	Left Slab Width	Left Gyrus Width	Left Slab Cortex Depth	Left Intact Cortex Depth	Left Slab Depth	Lateral Sulcus to Slab Apex
6 Ant. End	2287±113	5167± 91	1317± 80	1507±128	1782±274	2324±475
5	2536±113	4567±164	1365± 58	1614±124	2181± 98	2232±208
4	2602± 80	4494±212	1427± 73	1548±117	2236± 62	2393±146
3	2745± 76	4523±223	1390± 73	1540±113	2217± 84	2444±150
2	2862± 76	4794±150	1354±109	1485± 98	2196±146	2357±117
1	2847±102	4487±256	1394±109	1511± 91	2152±131	2217±146
0	2821±128	4487±256	1339±109	1449± 43	2071±139	2100±153
1	2766±146	4432±274	1291± 91	1438± 36	2067±124	1954±120
2	2745±164	4505±274	1262± 98	1474± 62	2031±139	1855± 87
3	2690±128	4384±201	1237± 91	1529± 87	1943±139	1756±102
4	2562±150	3989±219	1174±102	1566±109	1833±146	1745± 87
5	2474± 73	3843±109	1281± 91	1676±146	1632±183	1464± 73
6 Post. End	2525± 73	3733±109	1354± 91	1775±146	2013± 36	1317±146

Dist. From "0" Section in mm	Right Gyrus Width	Right Intact Cortex Depth
6 Ant. End	6075±402	1592± 36
5	5965±402	1573± 18
4	5877±146	1518± 54
3	5903±146	1500± 62
2	5819±117	1511± 73
1	5903± 65	1438±128
0	6002± 36	1449±139
1	6331± 62	1427±139
2	6514±128	1464±117
3	6463±102	1522±128
4	6196± 21	1522±102
5	6002± 36	1628± 18
6 Post. End	5801± 18	1665± 18

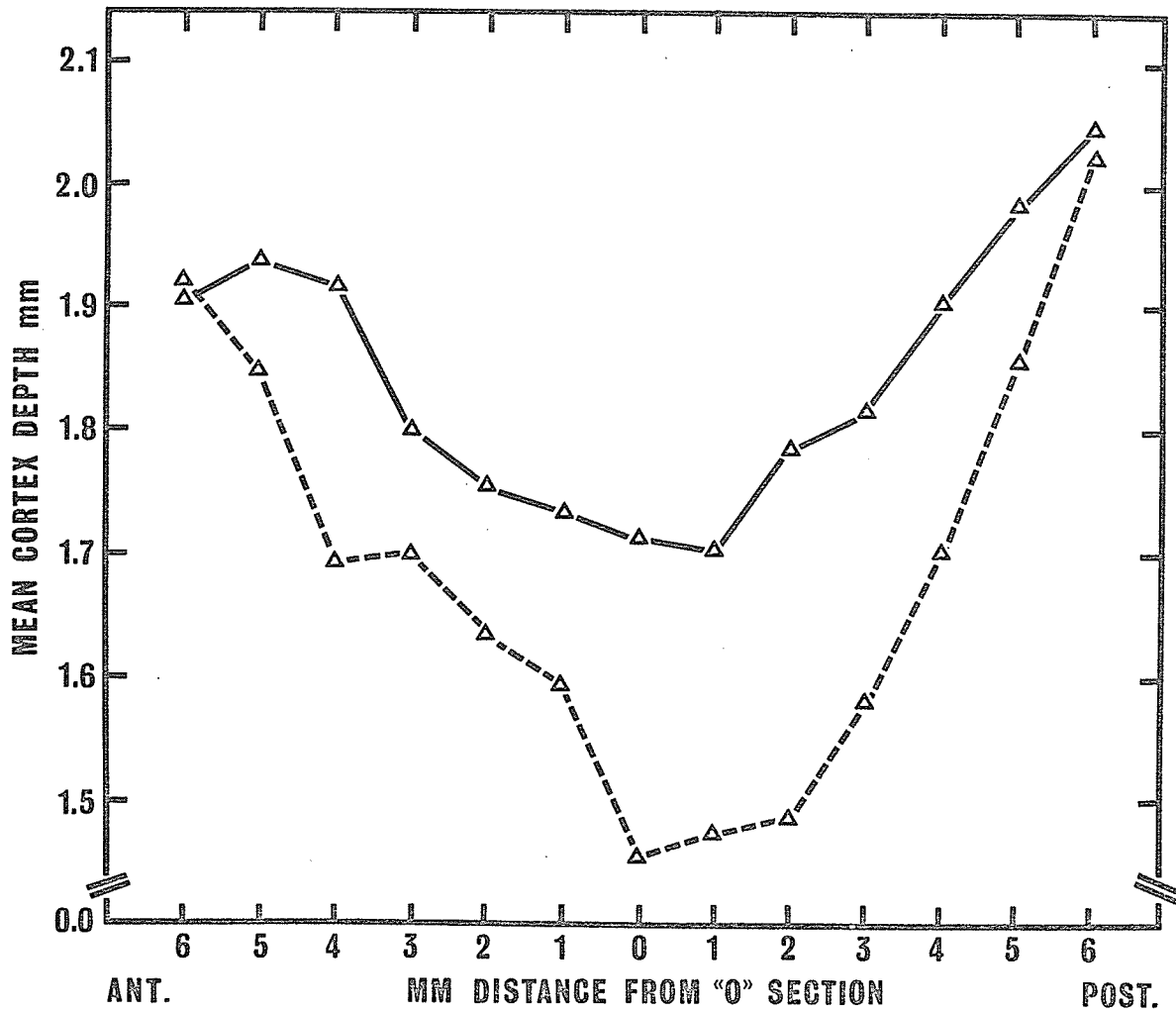


Fig. 13 Mean Cortex Depths in 5 Left Acutely Isolated Gyri and their Slabs

△—△—△ represents mean cortex depth in 5 acute left slabs (illustrated in Fig. 5 as E-F)

△.....△.....△ represents mean cortex depth in 5 acute left gyri (adjacent intact cortex, illustrated in Fig. 5 as H-I)

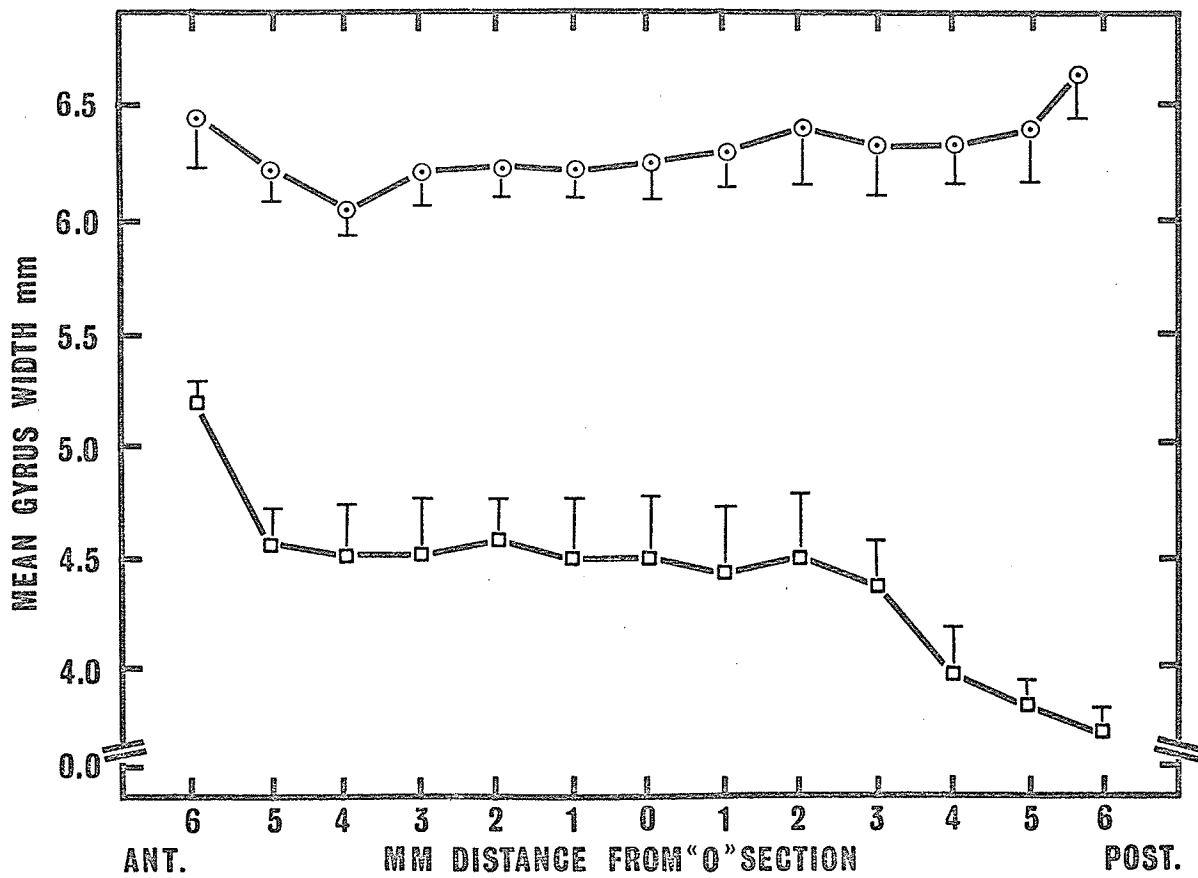


Fig. 14 Mean Widths of 6 Chronic Left Gyri and 5 Intact Left Gyri

○—○—○ represents mean width of 5 intact left gyri (illustrated in Fig. 3 as A-B)

□—□—□ represents mean width of 6 chronic left gyri (illustrated in Fig. 7 as C-D)

The widths of three gyri in which chronic slabs had been prepared was compared to the nonoperated homotopic gyri in the same animals. A paired comparisons test showed that chronic isolation causes a significant ($p \leq 0.001$) reduction in gyrus width in the gyral region alongside the isolated area. The mean width of the three chronic gyri, in central region (-2 to +2 mm section), was 4794 microns and the mean width of their homotopes in the central region of the gyrus was 6112 microns. This reduction of 22% in mean gyrus width seemed to be a feature of all six chronic gyri examined, as may be seen from comparing the data in Columns 3 and 8 of Table 3.

After 6-11 months of chronic isolation the subpial widths of the chronic slabs were significantly less than corresponding parameters in acute slabs ($p \leq 0.001$). The mean widths of six chronically isolated slabs when compared at "0" mm section were only 65% of the ipsilateral mean widths of five acutely isolated slabs (Tables 2 and 3) at the corresponding "0" mm section. In contrast with acute slabs the widest region of the chronic slabs was at their central region. The terminal ends of the chronic slabs, which were badly scarred, tapered markedly to a width of about 100 microns. The means of slab and gyri widths from six chronic gyri were plotted against each other in order to ascertain whether any regular relationship existed between the

shrinkage factors of these two parameters (Fig. 15). A straight line relationship was found between the two parameters. The only significant deviations from the relationship were at "-4" mm and "-5" mm sections which were adjacent to the drainage hole.

Both the chronic slab cortex depth and the chronic gyrus cortex depth were uniform at the anterior end of the slab ("-6" to "0" mm). The mean cortex depths of six chronic slabs were always shallower at the same locus than that occupied by the adjacent intact cortex within the same gyrus (Table 3 and Fig. 16). Significant differences (p ranging from ≤ 0.01 to ≤ 0.001) were found by paired comparisons test between chronic slab and cortex depth throughout the entire length of the chronic slab.

The mean depths of non-isolated cortex in each of the three types of gyri and their homotopes were calculated from the data obtained at all sections along the length of the slabs. These data are presented below and are shown graphically in Fig. 17.

Intact Left	1698 \pm 18 microns
Intact Homotope	1701 \pm 14 microns
Acute Left	1690 \pm 29 microns
Acute Homotope	1647 \pm 40 microns
Chronic Left	1606 \pm 32 microns
Chronic Right	1588 \pm 11 microns

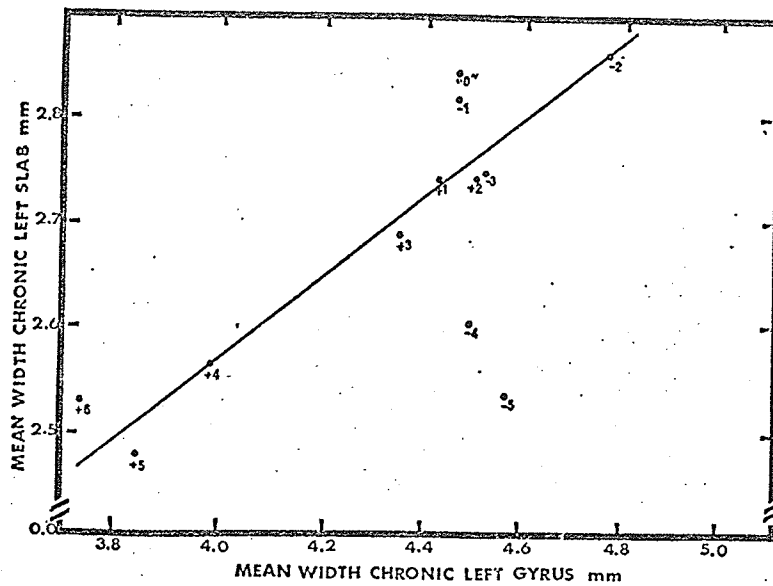


Fig. 15 Mean Slab Width Plotted Against Mean Gyrus Width from 6 Chronic Gyri

A straight line relationship is shown between the two parameters.

Note: Sections anterior to midsection "0" are designated as + mm; sections posterior to midsection "0" are designated as - mm.

Ordinates -4 and -5 are adjacent to posterior drainage hole; these may be taken as invalid.

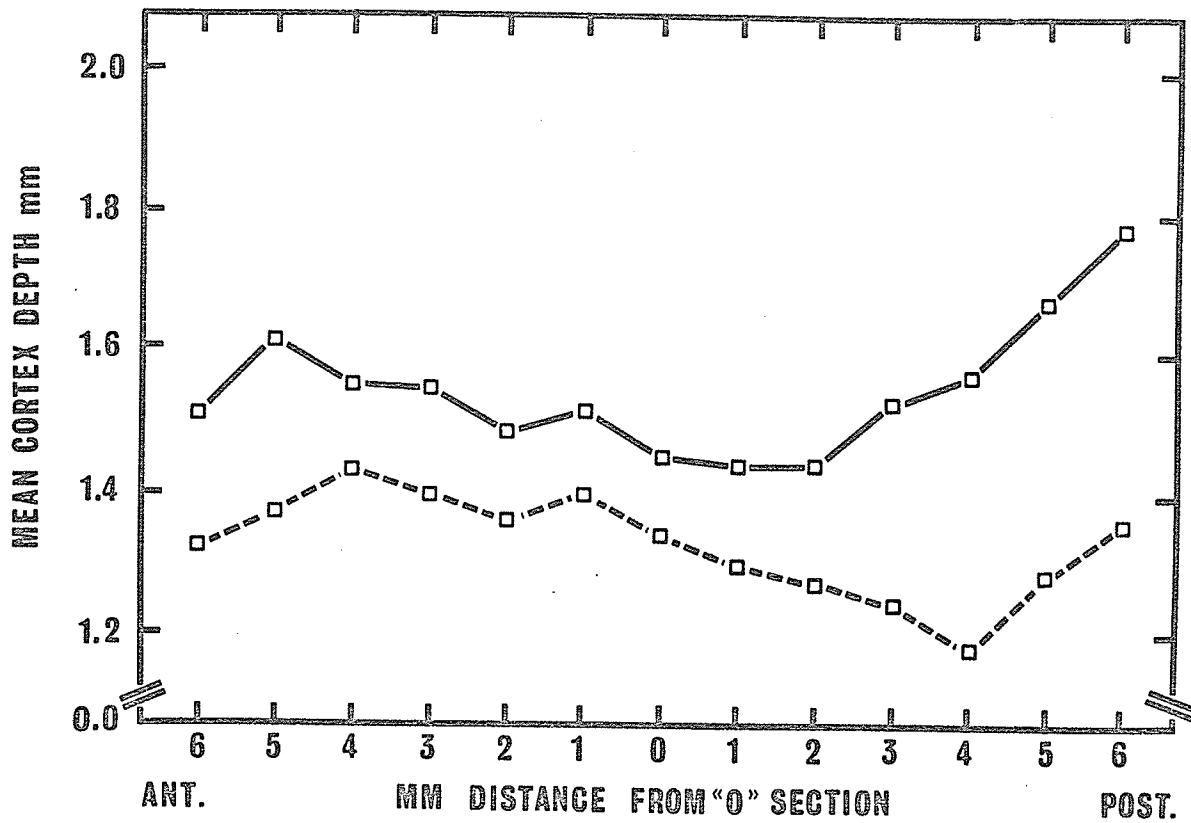


Fig. 16 Mean Cortex Depth of 6 Chronic Slabs

- represents mean cortex depth in chronic left gyrus (adjacent intact cortex, illustrated in Fig. 7, L-M)

- represents mean cortex depth in chronic left slab (illustrated in Fig. 7, E-F)

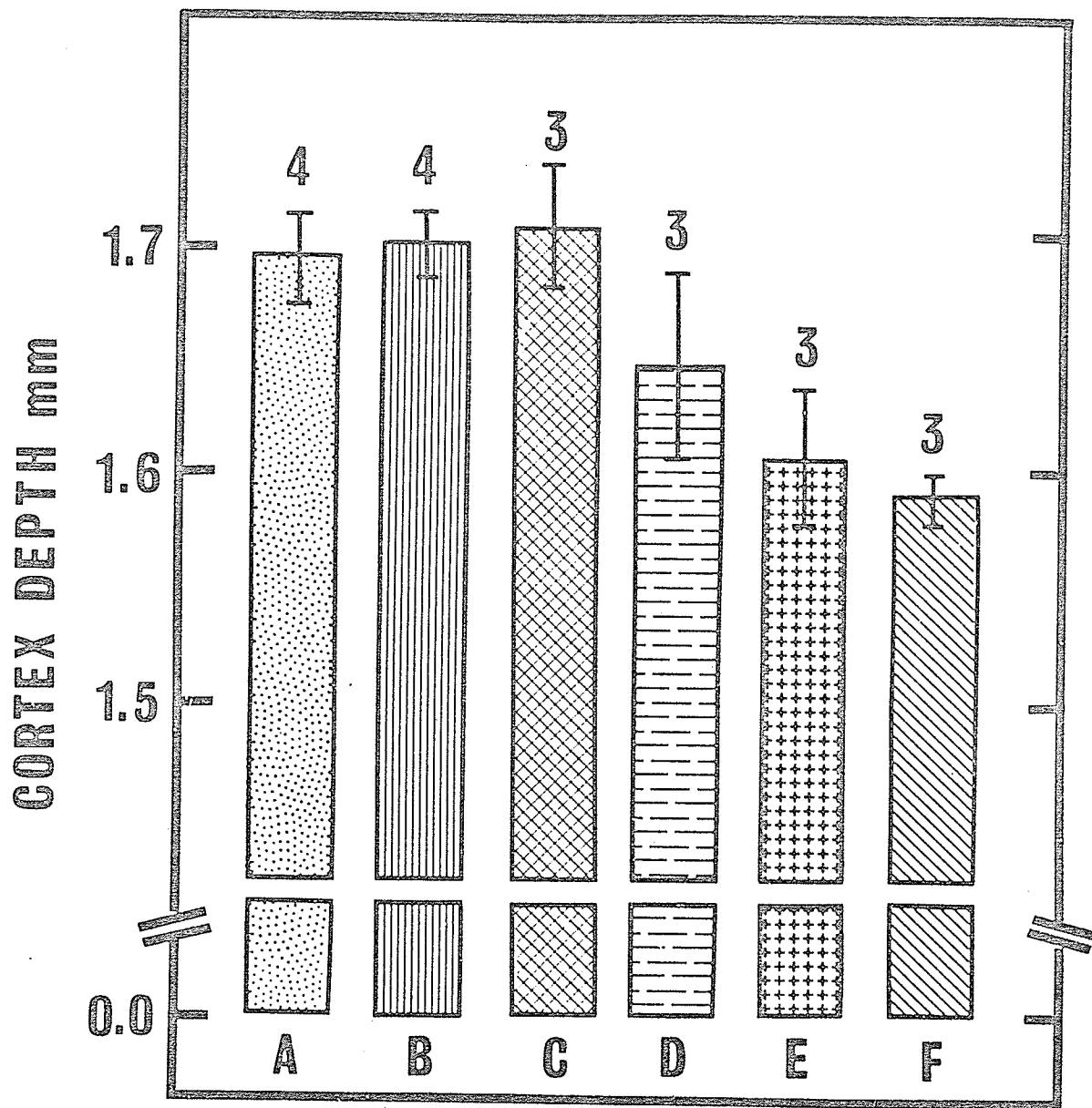


Fig. 17 Mean Depths of Non-Isolated Cortex in each of the 3 Types of Gyri and their Homotopes

- A = Intact left gyrus
- B = Intact right gyrus
- C = Acute left gyrus
- D = Acute right gyrus
- E = Chronic left gyrus
- F = Chronic homotope gyrus

No significant differences were found between the mean depth of cortex in the intact left gyri and their homotopes, nor between the mean of this parameter in the acute left gyri and their homotopes. A significant difference does exist between the mean cortex depth of intact left gyri and chronic left gyri ($p \leq 0.01$); also there is a significant difference between the mean cortex depth of the intact homotope gyri and chronic homotope gyri ($p \leq 0.001$).

4. NEURON POPULATION DENSITY

Earlier cytoarchitectonic studies on neuron population densities in the cerebral cortex were concentrated on two structurally spatial parameters. The first parameter was a measure of the differences in packing densities which were found at different cortical depths within a small region of the same brain; the second parameter measured packing densities in different hemispheric regions of the same brain without regard to variations at different cortical depths (Lashley and Clarke, 1946; Klotz and Clarke, 1950; Bailey and von Bonin, 1951; Sholl, 1956, 1959). These early results showed that there were considerable variations in population densities within any small part from any region of the cerebral cortex; for example, cat visual cortex and sensori-motor cortex, man striate area and precentral gyrus. The data from these measurements were taken from relatively few sections cut from tissue blocks only about 3 mm long. In contrast, histological techniques developed for the present study permitted continuous investigations of neuron population densities at regular intervals from tissue blocks 15 mm long. Quantitative results on neuron population densities were obtained from the three types of gyri preparations and their homotopes.

Intact cortex. During the period of experimentation in this study the histological time procedures did not enable a larger number of samplings from gyri with intact cortices. The mean population density of observable neurons per mm^3 of cortex in the cortical segments was calculated and is shown in Columns 1 and 2 in Table 4. Since the estimated neuron impregnation rate was 2% of available neurons (Sholl, 1956), the number of observable neurons per mm^3 as shown in this table may be multiplied by a factor of 50 in order to calculate the actual neuron population density.

Table 4. Mean Neuron Population Density of Observed Neurons per mm³.

	(1) Intact Left	(1) Intact Homotope	(5) Acute Left	(4) Acute Homotope	(5) Chronic Left	(1) Chronic Homotope
1A	263±34	394±68	180±14	151±21	117±18	207± 7
1B	255±30	401±33	211±10	221±12	200±34	297±47
2A	222±29	256±46	197± 7	229±16	195±21	249±36
2B	286±51	375±52	162±16	118±17	168±20	227±14
3	362±49	410±43	394±16	388±30	292±26	288±66
4	508±61	453±78	462±28	501±30	280±15	400±90
$\bar{\Sigma}$	316±42	381±27	267±51	268±60	208±27	278±28

The data from each of six cortical segments (see inset, Fig. 18) were paired in each tissue section for the entire length of the gyrus for compared comparisons tests in the following manner:

1A with 2B

1B with 2A

4 with 3.

When treated in this manner the data showed no significant differences in neuron population densities between each of the paired upper cortical segments and no significant differences between each of the paired lower cortical segments in the intact left and homotopic gyri. Nevertheless, there are genuine differences in population density between these paired segments in any one section, and also between any one of these segments and its counterpart in any other section. This is graphically illustrated in Figs. 18 and 19.

The mean neuron population densities for the entire upper half of the cortex were compared with the means for the entire lower cortical half at 2 mm interval sections; paired data were used from left and homotopic gyri. A significant difference ($p \leq 0.01$) exists in neuron population density between the two compared cortical depths throughout the entire lengths of intact gyri.

The mean neuron population density with standard error for each cortical segment from all available

INTACT LEFT

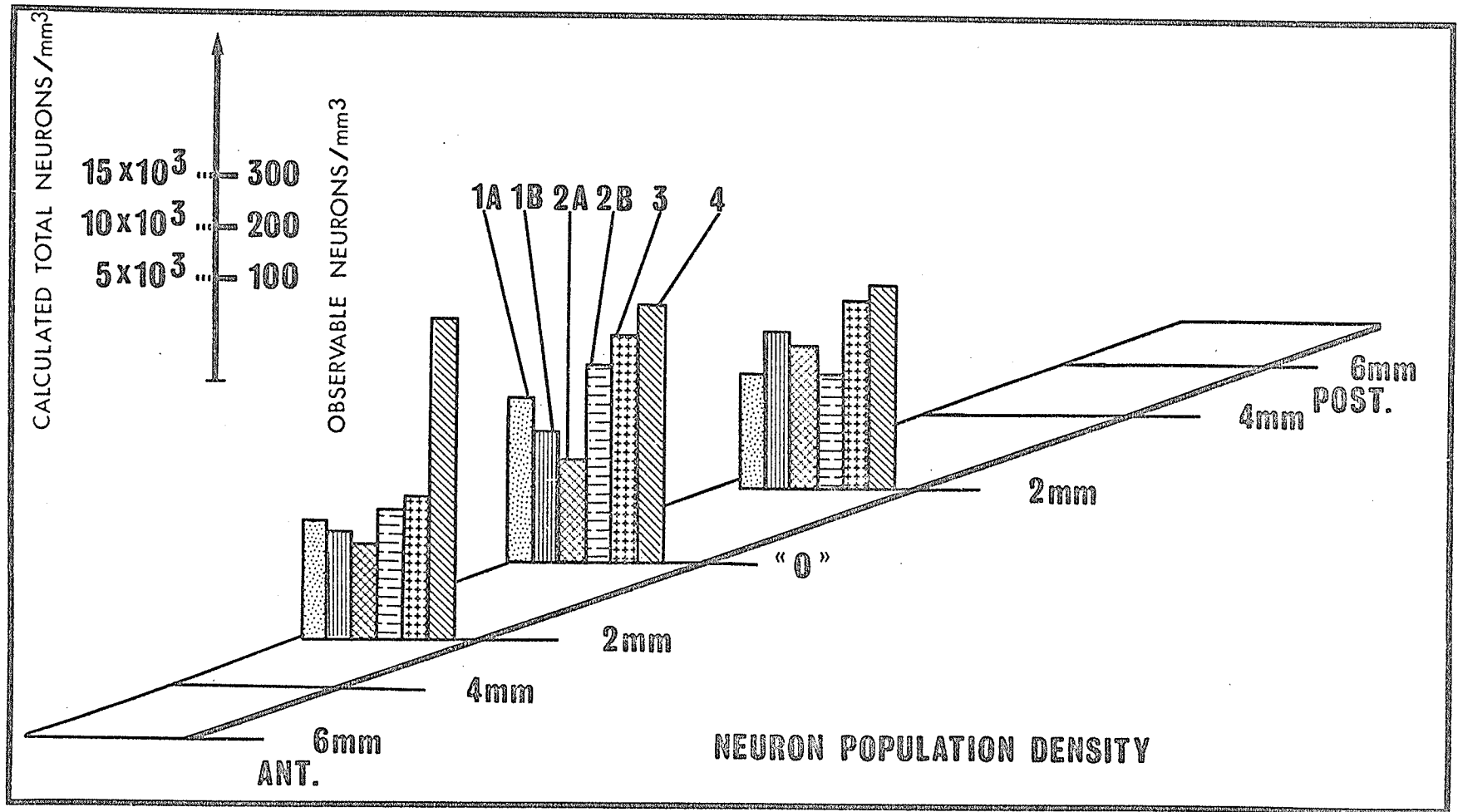


Fig. 18 Neuron Population Density in 1 Intact Left Gyrus

1A, 1B, 2A, 2B, 3 and 4 represent cortical segments in intact left gyrus (subdivision illustrated in Fig. 13).

INTACT HOMOTOPE

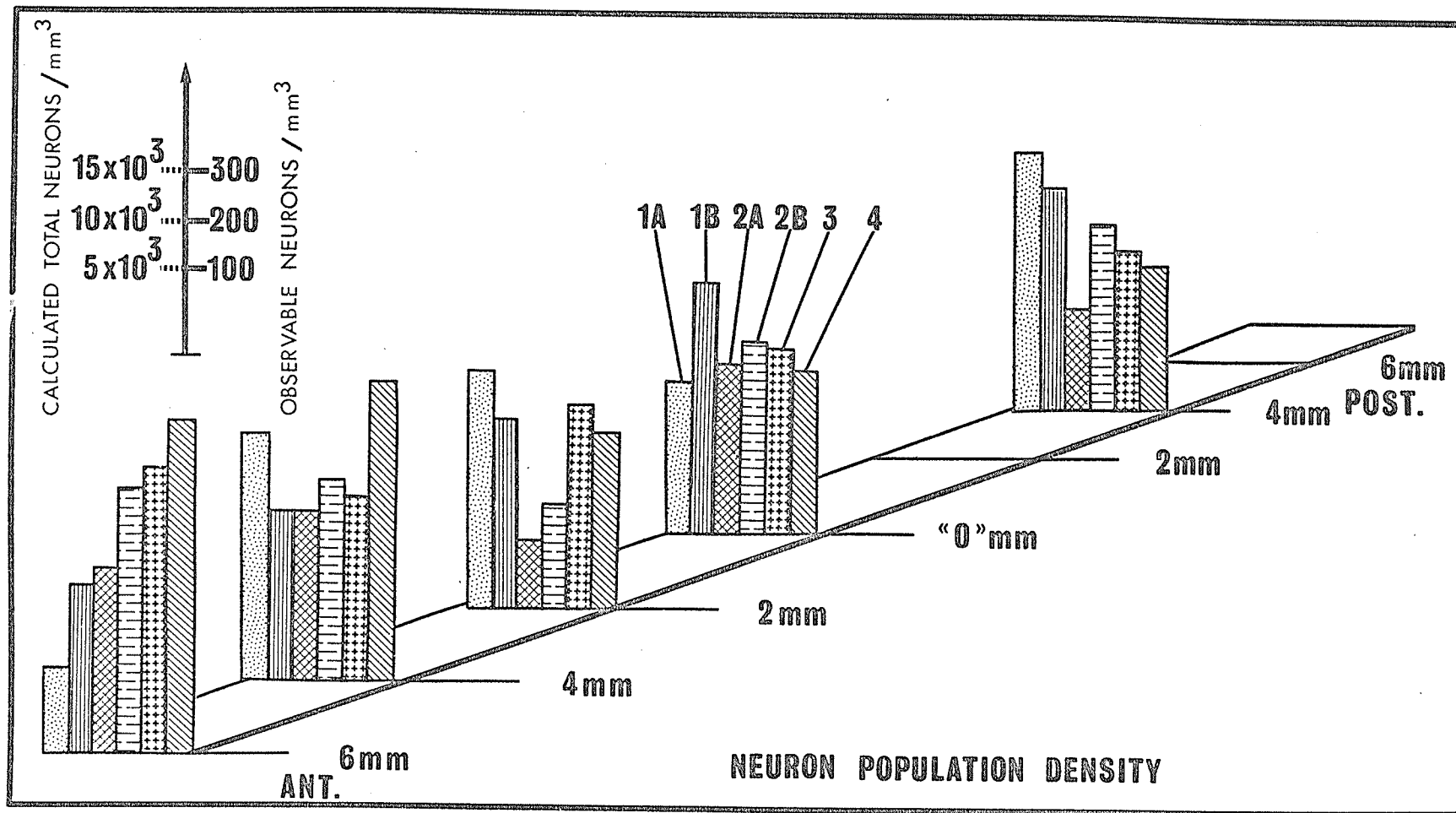


Fig. 19 Neuron Population Density in 1 Intact Homotopic Gyrus

1A, 1B, 2A, 2B, 3 and 4 represent cortical segments in intact right gyrus (subdivision illustrated in Fig. 13).

sections in intact left and homotopic gyri are shown in Figs. 20 and 21. The data presented in this form serve the purpose of showing a representative coronal section with those cortical volume and cellular parameters which could be found in a classical Golgi preparation and in the modification developed for this study. The mean density (expressed as observed neurons/mm³) in the upper cortical half of the cortex ranges from a low of 222 ± 29 to a high of 401 ± 33 ; the range in the lower cortical half extends from a low of 362 ± 49 to a high of 508 ± 61 . The data are also shown in histogram profiles in Figs. 22 and 23. The results show that variations in neuron population densities in intact gyri occur even between two closely spaced parameters in all spatial orientations of length, width and depth.

Acutely isolated cortex. The neuron population densities from nine acute left and homotopic gyri in each of six cortical segments were compared. Population densities in the different segments were compared according to the scheme on p. 192. As well, a paired comparison was made between the acute left gyri and their homotopes.

The results of these tests showed that no significant differences exist between each of the paired upper cortical segments in the left and homotopic gyri. However, significant differences are found between

Dorsal Pial Surface

$d = 263 \pm 34$ $\Sigma N = 18$ $\Sigma V = 0.070$ $D = 13,150$ 1A	$d = 255 \pm 30$ $\Sigma N = 22$ $\Sigma V = 0.086$ $D = 12,750$ 1B	$d = 222 \pm 29$ $\Sigma N = 20$ $\Sigma V = 0.089$ $D = 11,100$ 2A	$d = 286 \pm 51$ $\Sigma N = 18$ $\Sigma V = 0.066$ $D = 13,600$ 2B
$d = 508 \pm 61$ $\Sigma N = 94$ $\Sigma V = 0.185$ $D = 25,400$ 4		$d = 362 \pm 49$ $\Sigma N = 66$ $\Sigma V = 0.182$ $D = 18,100$ 3	

Fig. 20 Coronal Section of Intact Left Cortex
 Mean of 1 Slab(3 sections only)

d = Density of Observed Neurons/ mm^3

ΣN = Total Number of Observed Neurons

ΣV = Total Volume in mm^3

D = Estimated Neuron Population Density/ mm^3

Σ Neurons Observed for 1 Slab = 239

Σ Volume of Cortex Examined = 0.678mm^3

Neuron Impregnation Rate = 2%

Dorsal Pial Surface

$d = 394 \pm 68$ $\Sigma N = 44$ $\Sigma V = 0.114$ $D = 19,700$ 1A	$d = 401 \pm 33$ $\Sigma N = 61$ $\Sigma V = 0.152$ $D = 20,050$ 1B	$d = 256 \pm 46$ $\Sigma N = 39$ $\Sigma V = 0.152$ $D = 12,800$ 2A	$d = 375 \pm 52$ $\Sigma N = 50$ $\Sigma V = 0.133$ $D = 18,750$ 2B
$d = 453 \pm 78$ $\Sigma N = 133$ $\Sigma V = 0.293$ $D = 22,650$ 4		$d = 410 \pm 43$ $\Sigma N = 121$ $\Sigma V = 0.295$ $D = 20,500$ 3	

Fig. 21 Coronal Section of Intact Homotopic Cortex
 Mean of 1 Slab (5 Sections)

d = Density of Observed Cells/ mm^3

ΣN = Total Number of Observed Neurons

ΣV = Total Volume in mm^3

D = Estimated Neuron Population Density/ mm^3

Σ Neurons Observed for 1 Slab = 448

Σ Volume of Cortex Examined = 1.139mm^3

Neuron Impregnation Rate = 2%

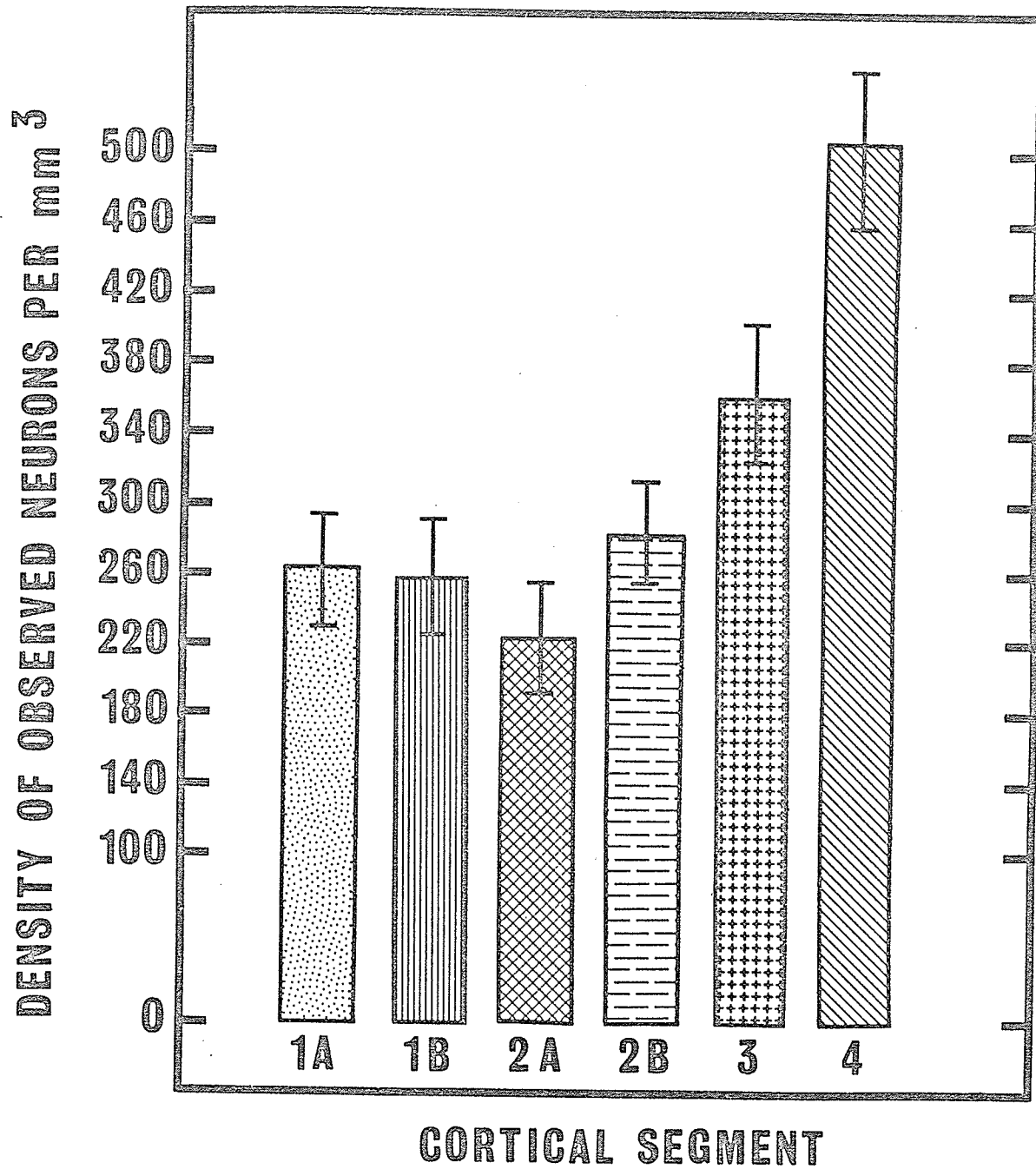


Fig. 22 Mean Neuron Population in 1 Intact Left Gyrus

1A, 1B, 2A, 2B, 3 and 4 represent cortical segments (subdivision illustrated in Fig. 4)

Σ Observed neurons = 239

Σ Cortical volume examined = 0.678 mm³

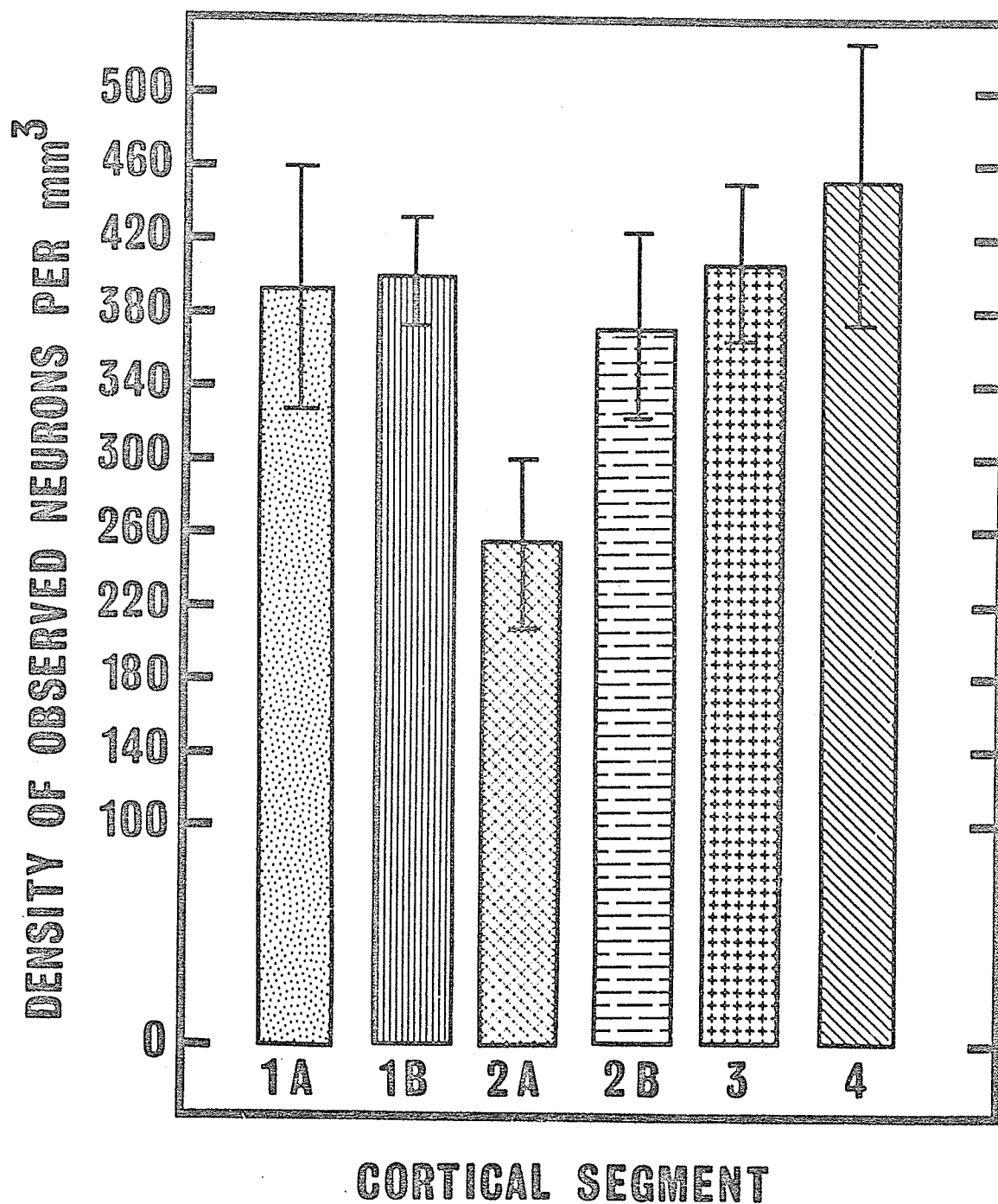


Fig. 23 Mean Neuron Population Density in 1 Intact Right Gyrus.

1A, 1B, 2A, 2B, 3 and 4 represent cortical segments (subdivision of segments illustrated in Fig. 4

Σ Observed neurons = 448

Σ Cortical volume examined = 0.139 mm^3

the two lower cortical segments in both the left and homotopic gyri ($p \leq 0.05$ in both hemispheres). A greater packing density is found in the lower lateral cortical segment, designated in this study as #4, than in the adjacent medial segment (#3). Segment #4 lies adjacent to the tract association area of the ectosylvian gyrus. The similarities in density profiles of coronal sections at regular intervals throughout the lengths of acute left and acute homotopic gyri are shown graphically in Figs. 24 and 25.

The data from population densities in cortical segments from every 2 mm interval section in acute left slabs was compared to the data from similarly defined cortical segments in acute homotopic slabs. No significant difference exists between the densities of paired cortical segments in left and homotopic gyri.

A highly significant difference exists in neuron population densities between upper and lower cortical depths in both acute left ($p \leq 0.001$) and homotopic ($p \leq 0.001$) slabs. No significant differences in densities were found, at 2 mm interval sections, in the following: in the upper cortical half, between the mean densities of acute left slabs and their homotopic slabs; in the lower cortical half, between mean densities in acute left slabs and their homotopic slabs.

Significant differences in population density are not always found between different segments when these are

ACUTE LEFT SLABS

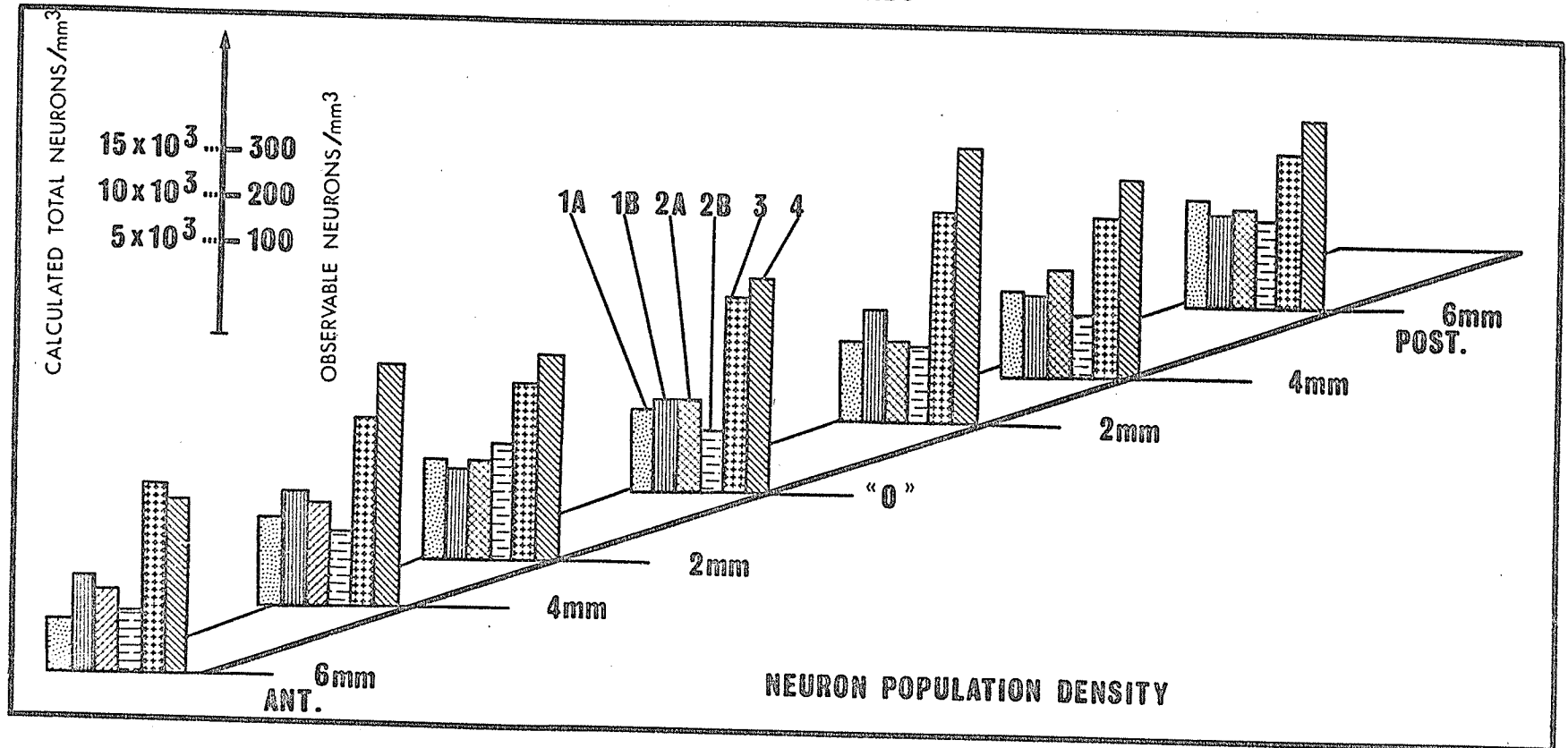


Fig. 24 Neuron Population Density in 5 Acute Left Slabs

1A, 1B, 2A, 2B, 3 and 4 represent cortical segments in acute left slabs (subdivision illustrated in Fig. 15).

ACUTE HOMOTOPE SLABS

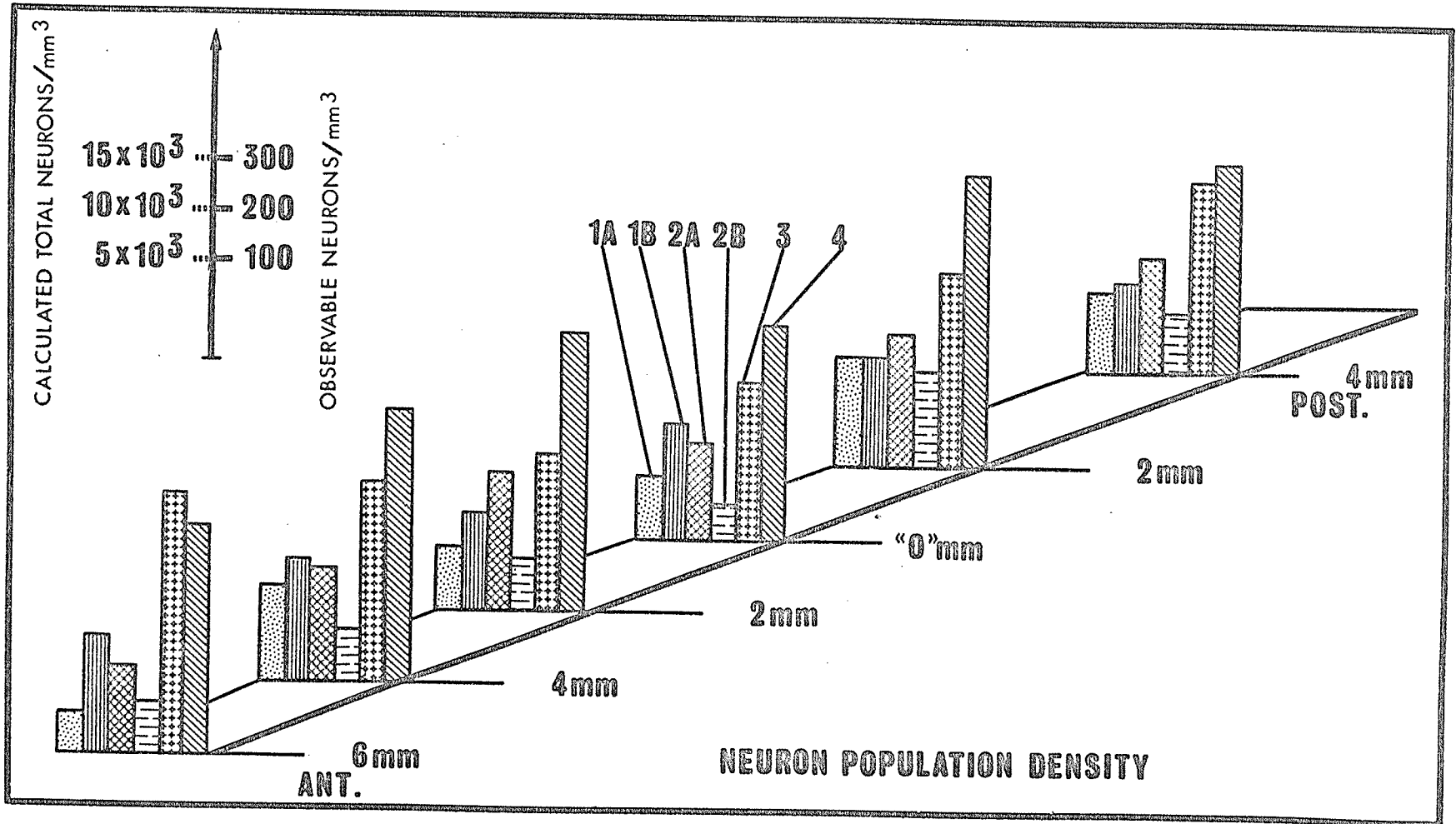


Fig. 25 Neuron Population Density in 4 Acute Homotopic Slabs

1A, 1B, 2A, 2B, 3 and 4 represent cortical segments in acute right slabs (subdivision illustrated in Fig. 15).

tested by paired comparisons in several slabs. Nevertheless the results show that genuine differences do exist between individual segments along the entire length of acutely isolated slabs. These results are shown graphically in Figs. 24 and 25.

A representative coronal section of mean densities for cortical segments from nine acute and homotopic gyri are shown in Figs. 26 and 27. The upper central cortical segments, i.e., 1B and 2A, have the highest population densities in the upper cortical half. The non-homogeneity of packing density in the cortex of the slabs is graphically demonstrated in histogram profiles in Figs. 28 and 29. A distinct profile of population density may be discerned in the upper and lower halves of both acute left and homotopic slabs. The characteristic of this profile is that, in both hemispheres, the two outer segments in the upper half are smaller than the two central segments; the two lower segments are markedly larger than any of the upper segments.

Chronically isolated cortex. Paired comparison tests of neuron population density were made between various combinations of six cortical segments from five chronic left gyri. The densities between each of the six cortical segments from five chronic left slabs were paired

Dorsal Pial Surface

$d = 180 \pm 14$ $\Sigma N = 162$ $\Sigma V = 0.900$ $D = 9,000$	$d = 211 \pm 10$ $\Sigma N = 243$ $\Sigma V = 1.151$ $D = 10,550$	$d = 197 \pm 7$ $\Sigma N = 229$ $\Sigma V = 1.164$ $D = 9,850$	$d = 162 \pm 16$ $\Sigma N = 162$ $\Sigma V = 1.002$ $D = 8,100$
1A	1B	2A	2B
$d = 462 \pm 28$ $\Sigma N = 981$ $\Sigma V = 2.122$ $D = 23,100$		$d = 394 \pm 16$ $\Sigma N = 760$ $\Sigma V = 1.931$ $D = 19,700$	
4		3	

Fig. 26 Coronal Section of Acute Left Slab Cortex
 Mean of 5 Acute Slabs

d = Density of Observed Cells/ mm^3

ΣN = Total Number of Observed Neurons

ΣV = Total Volume in mm^3

D = Estimated Neuron Population Density/ mm^3

Σ Neurons Observed for 5 Slabs = 2,537

Σ Volume of Cortex Examined = 8.270 mm^3

Neuron Impregnation Rate = 2%

Dorsal Pial Surface

$d = 151 \pm 21$ $\Sigma N = 96$ $\Sigma V = 0.635$ $D = 7,550$ 1A	$d = 221 \pm 12$ $\Sigma N = 196$ $\Sigma V = 0.883$ $D = 11,050$ 1B	$d = 229 \pm 16$ $\Sigma N = 213$ $\Sigma V = 0.928$ $D = 11,450$ 2A	$d = 118 \pm 17$ $\Sigma N = 78$ $\Sigma V = 0.661$ $D = 5,900$ 2B
$d = 501 \pm 30$ $\Sigma N = 843$ $\Sigma V = 1.681$ $D = 25,050$ 4		$d = 388 \pm 30$ $\Sigma N = 738$ $\Sigma V = 1.902$ $D = 19,400$ 3	

Fig. 27 Coronal Section of Acute Homotopic Cortex
 Mean of 4 Slabs

d = Density of Observed Cells/ mm^3

ΣN = Total Number of Observed Neurons

ΣV = Total Volume in mm^3

D = Estimated Neuron Population Density/ mm^3

Σ Neurons Observed for 4 Slabs = 1,558

Σ Volume of Cortex Examined = 6.690mm^3

Neuron Impregnation Rate = 2%

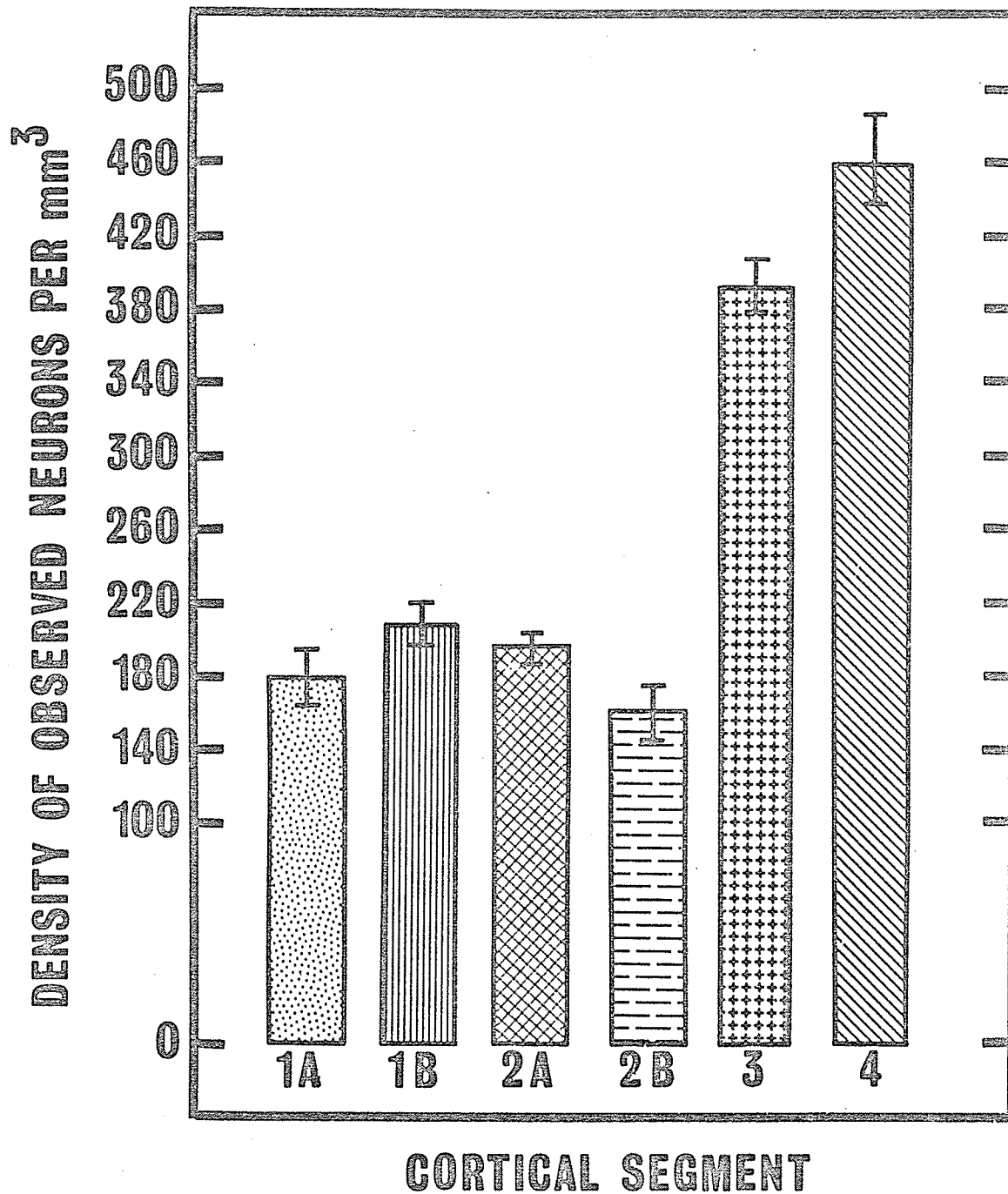


Fig. 28 Mean Neuron Population Density in 5 Acute Left Slabs

1A, 1B, 2A, 2B, 3 and 4 represent cortical segments (subdivision of segments illustrated in Fig. 6)

Σ Observed neurons = 2537

Σ Cortical volume examined = 8.270 mm³

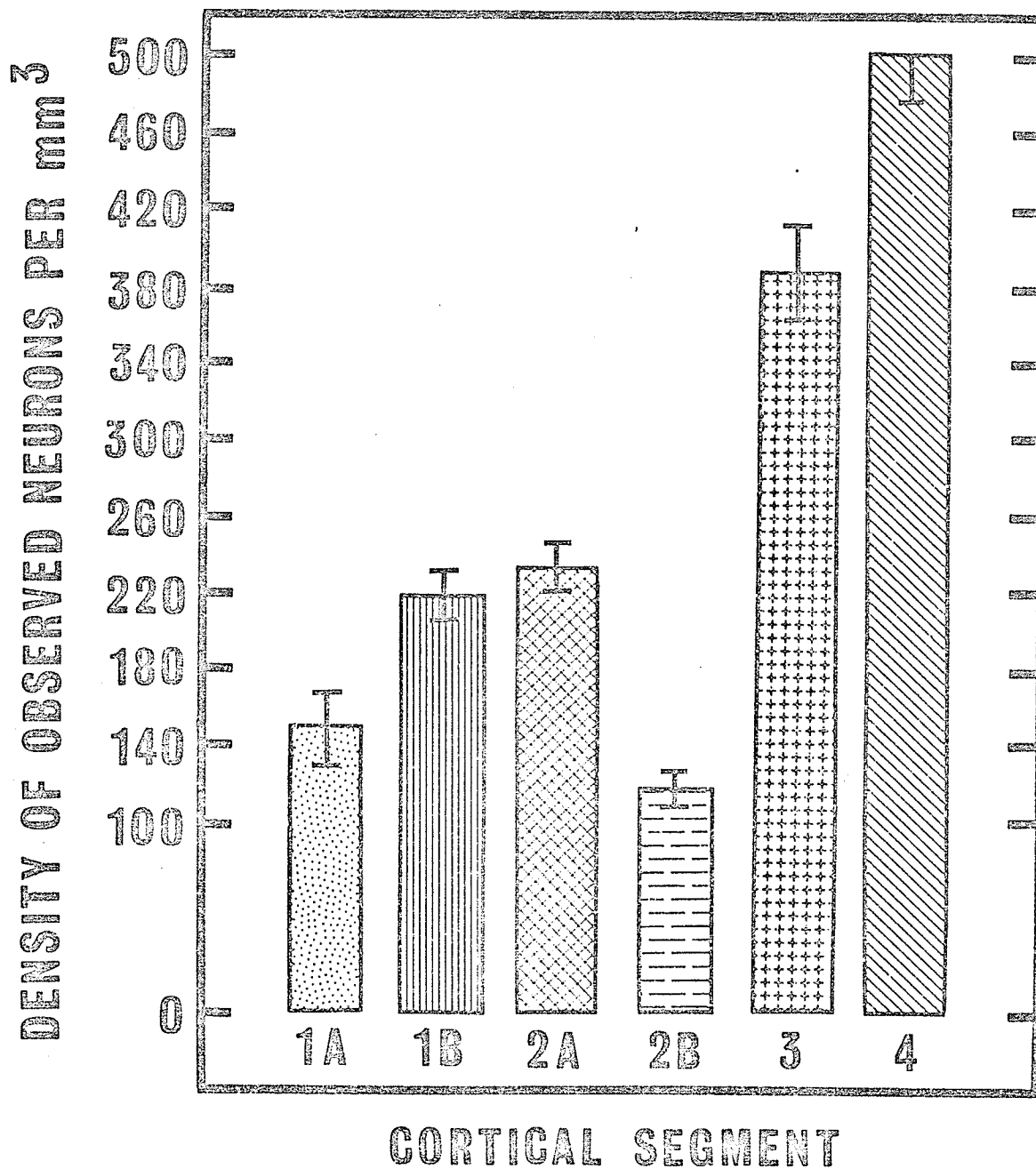


Fig. 29 Mean Neuron Population Density in 4 Acute Right Slabs

1A, 1B, 2A, 2B, 3 and 4 represent cortical segments
(subdivision of segments illustrated in Fig. 6)

Σ Observed neurons = 1558

Σ Cortical volume examined = 6.690 mm³

as previously described in the schemes for intact and acute preparations (p. 192). There are no significant differences between the paired segments in the upper cortical half ($p \leq 0.10$); nor are there any significant differences between the segments in the lower cortical half ($p \leq 0.70$). A paired comparison test of mean densities between the upper and lower cortical half in the chronic slab shows significant differences ($p \leq 0.001$).

Histograms were prepared to show the profiles of mean neuron population densities for each of the six cortical segments in the chronic slabs. Figs. 34 and 35 clearly demonstrate that density profiles which were observed with acute left and homotopic slabs are still present. They are, however, considerably flattened and with peaking less pronounced. The histograms along the length of chronic slabs also show an unmistakable tendency for the neuron population density in the upper cortical half to become slightly less towards the posterior region of the slab (Fig. 30). This tendency was not observed in the histogram profiles of intact, acute left and homotopic gyri (Figs. 18, 19, 24 and 25).

Variations in mean neuron population densities for each of the six cortical segments along the lengths of five chronic slabs are shown in Table 4. The results show that the central upper cortical segments, i.e., 1B and 2A, maintain slightly higher densities than the two adjacent cortical areas. However, a t-test for two samples

CHRONIC LEFT SLABS

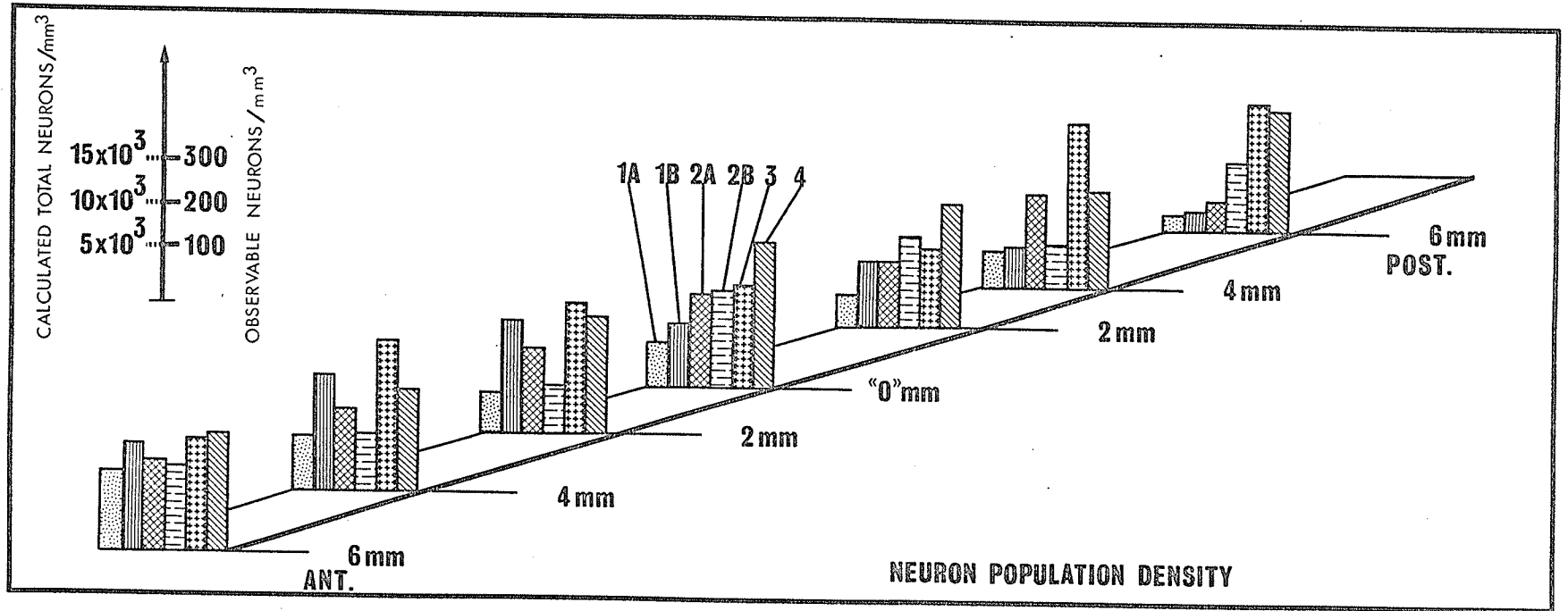


Fig. 30 Neuron Population Density in 5 Chronic Left Slabs

1A, 1B, 2A, 2B, 3 and 4 represent cortical segments in chronic left slabs (subdivision illustrated in Fig. 17).

CHRONIC HOMOTOPE

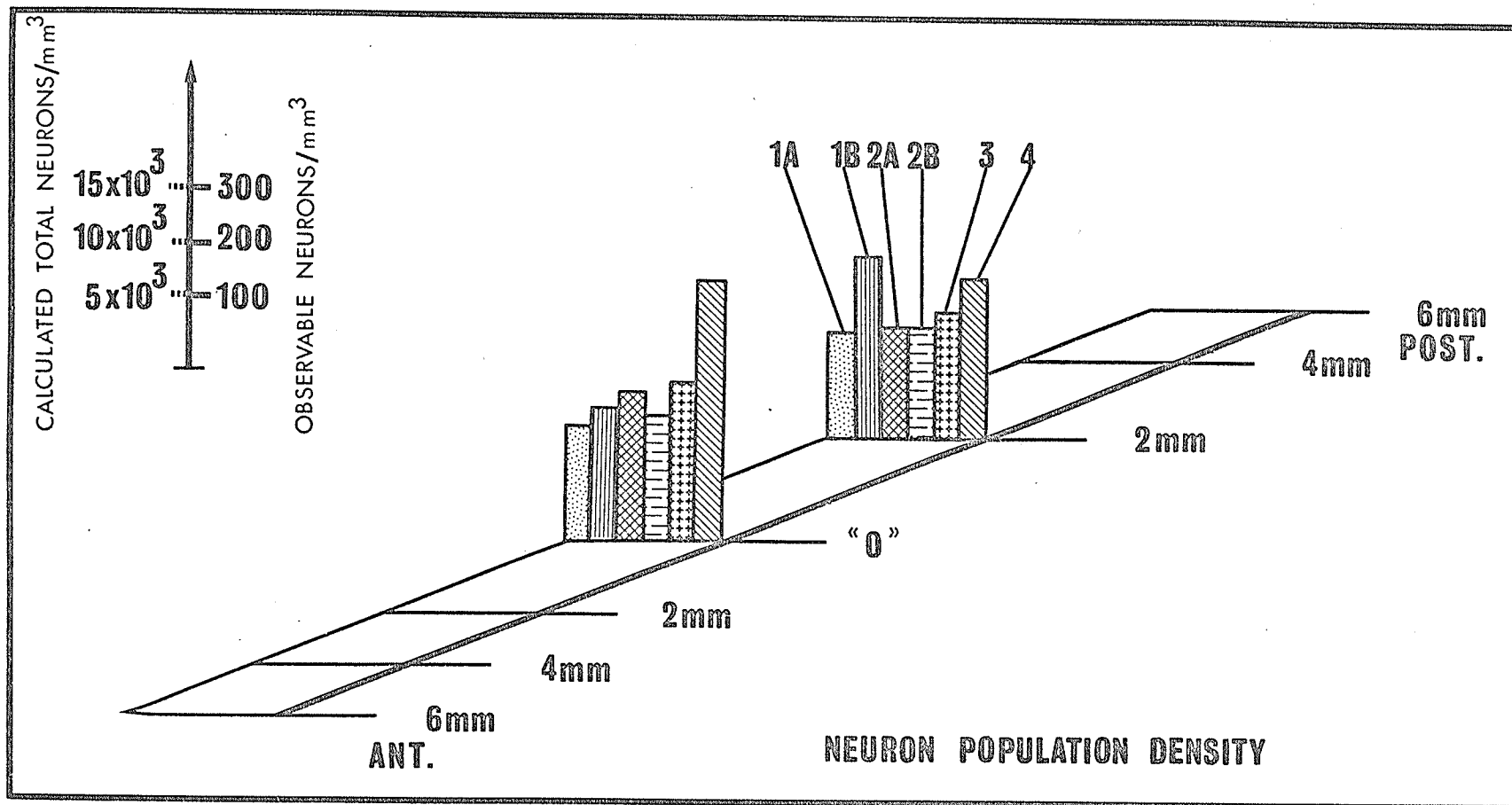


Fig. 31 Neuron Population Density in 1 Chronic Homotopic Gyrus

1A, 1B, 2A, 2B, 3 and 4 represent cortical segments in chronic homotopic gyrus (subdivision illustrated in Fig. 13).

Dorsal Pial Surface

$d = 117 \pm 18$ $\Sigma N = 54$ $\Sigma V = 464$ $D = 5,850$	$d = 200 \pm 24$ $\Sigma N = 135$ $\Sigma V = .675$ $D = 10,000$	$d = 195 \pm 21$ $\Sigma N = 134$ $\Sigma V = .688$ $D = 9,750$	$d = 168 \pm 20$ $\Sigma N = 78$ $\Sigma V = 464$ $D = 8,400$
1A	1B	2A	2B
$d = 280 \pm 15$ $\Sigma N = 314$ $\Sigma V = 1.120$ $D = 14,000$		$d = 292 \pm 26$ $\Sigma N = 326$ $\Sigma V = 1.116$ $D = 14,600$	
4		3	

Fig. 32 Coronal Section of Chronic Left Cortex
 Mean of 5 Chronic Slabs

d = Density of Observed Cells/ mm^3

ΣN = Total Number of Observed Neurons

ΣV = Total Volume in mm^3

D = Estimated Neuron Population Density/ mm^3

Σ Neurons Observed for 5 Slabs = 1,041

Σ Volume of Cortex Examined = 4.527 mm^3

Neuron Impregnation Rate = 2%

in chronic slabs which lumped all the densities in cortical segments 1A and 2B did not show any significant difference from the lumped densities in 1B and 2A.

The homotopic gyri were not available for neuron population studies. However, a chronic homotopic gyrus with an intact cortex, whose chronic left slab was not studied, was analyzed for neuron population density. The data from this homotopic gyrus was compared with that from intact left and right gyri, using a t-test for two sample means whose population variances are unknown. No significant differences were found between population densities in the various cortical segments in the chronic homotope and their counterparts in the intact gyri from animals where slabs had never been prepared (Figs. 19 and 31).

The mean neuron population densities for each of the six cortical segments from five chronic slabs and the one homotopic gyrus are represented as typical coronal sections in Figs. 32 and 33.

A visual comparison of the six illustrations (Figs. 22, 23, 28, 29, 34, 35) which show the means for each of the six cortical segments in the three types of cortical preparations gave the impression that the neuron population density in the upper cortical half was hardly affected by varying periods of neuronal isolation.

Accordingly then, several t-tests for two samples were made on densities in each of the six cortical segments

Dorsal Pial Surface

$d = 207 \pm 7$ $\Sigma N = 7$ $\Sigma V = 0.034$ $D = 10,350$ 1A	$d = 297 \pm 47$ $\Sigma N = 16$ $\Sigma V = 0.053$ $D = 14,820$ 1B	$d = 249 \pm 36$ $\Sigma N = 15$ $\Sigma V = 0.061$ $D = 12,450$ 2A	$d = 227 \pm 14$ $\Sigma N = 13$ $\Sigma V = 0.062$ $D = 11,350$ 2B
$d = 400 \pm 90$ $\Sigma N = 48$ $\Sigma V = 0.124$ $D = 20,000$ 4		$d = 288 \pm 66$ $\Sigma N = 14$ $\Sigma V = 0.104$ $D = 14,400$ 3	

Fig. 33 Coronal Section of Chronic Homotopic Cortex
 Mean of 1 Gyrus (2 Sections only)

$d =$ Density of Observed Cells/ mm^3

$\Sigma N =$ Total Number of Observed Neurons

$\Sigma V =$ Total Volume in mm^3

$D =$ Estimated Neuron Population Density/ mm^3

Σ Neurons Observed for 1 Slab = 113

Σ Volume Cortex Examined = 0.438 mm^3

Neuron Impregnation Rate = 2%

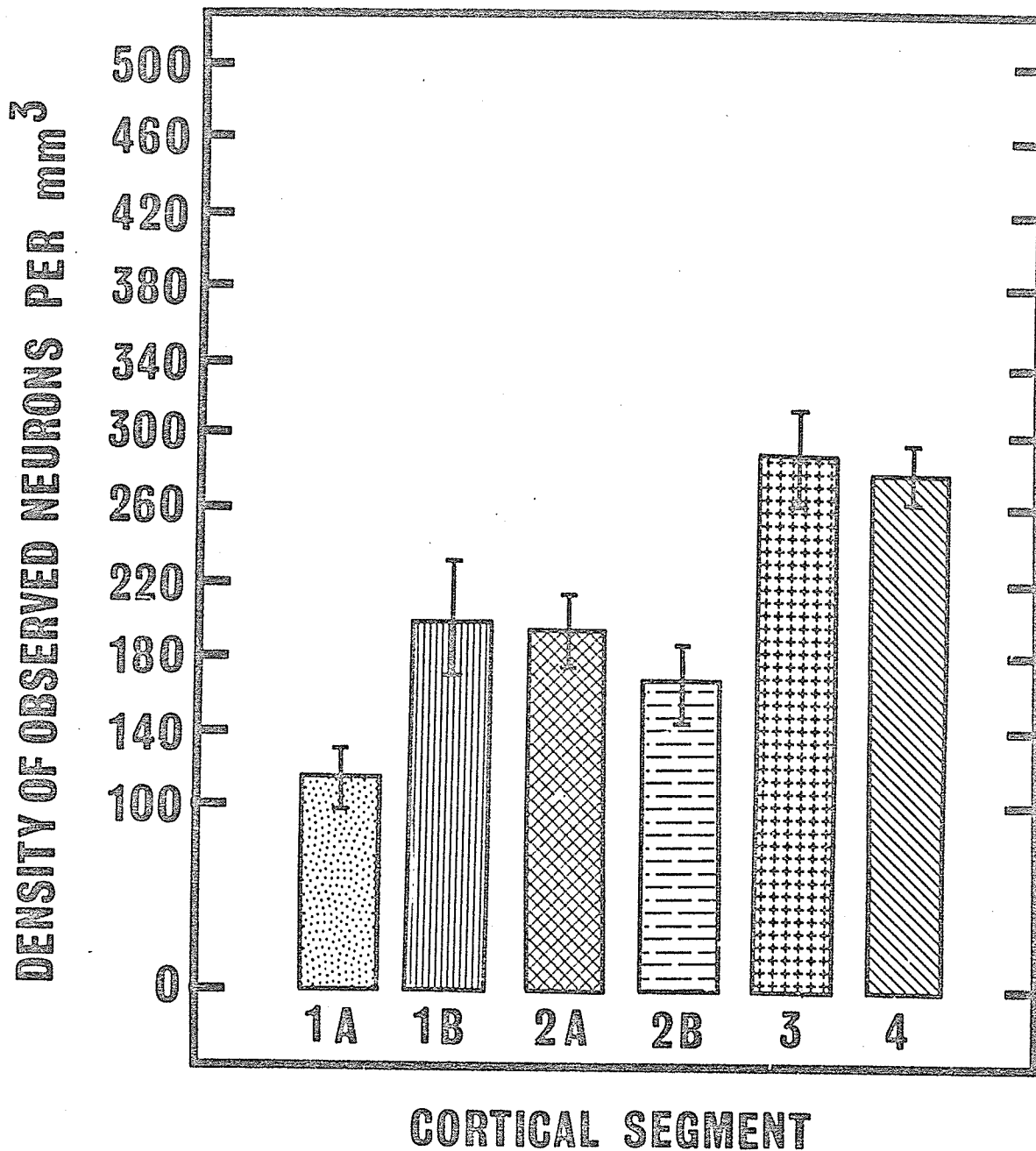


Fig. 34 Mean Neuron Population Density in 5 Chronic Left Slabs

1A, 1B, 2A, 2B, 3 and 4 represent cortical segments (subdivision of segments illustrated in Fig. 8).

Σ Observed neurons = 1041

Σ Cortical volume examined = 4.527 mm³

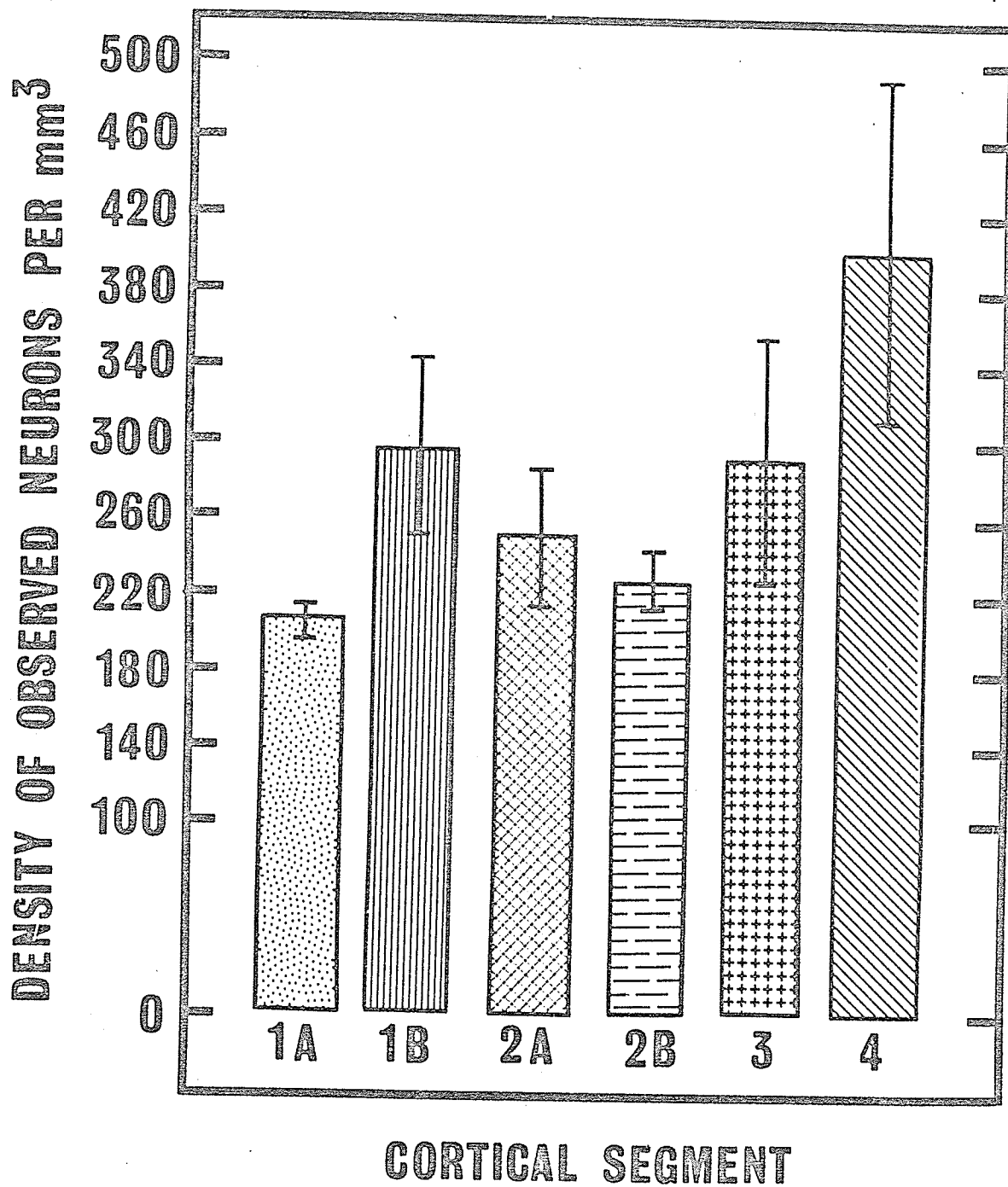


Fig. 35 Mean Neuron Population Density in 1 Chronic Homotopic Gyrus

1A, 1B, 2A, 2B, 3 and 4 represent cortical segments (subdivision of segments illustrated in Fig. 4)

Σ Observed neurons = 113

Σ Cortical volume examined = 0.438 mm³

between chronic slabs and acute slabs, and also between chronic slabs and intact gyri. Data from each of the cortical segments 1B and 2A were lumped ($=1B + 2A$) as representing a surgically-protected area in the upper cortical half; 1A and 1B were lumped ($=1A + 2B$) as representing equally traumatized upper segments; 3 and 4 were lumped as representing equally traumatized lower segments. The results of the t-tests show that NO significant differences exist between the following:

- (1B + 2A) on chronic slabs vs. (1B + 2A) on acute slabs;
- (1B + 2A) on chronic slabs vs. (1B + 2A) on intact gyri;
- (1A + 2B) on chronic slabs vs. (1A + 2B) on acute slabs.

A highly significant difference was found to exist between (1A + 2B) on chronic slabs and (1A + 2B) on intact gyri ($p \leq 0.001$). The differences in neuron population densities between lumped segments (3 + 4) in chronic slabs and in acute slabs were also highly significant ($p \leq 0.001$). Fig. 36 is a histogram profile on the mean neuron population density for each category of cortical preparation. This type of graphical presentation shows the tendency for chronic isolation to lessen the neuron population density in the cerebral cortex.

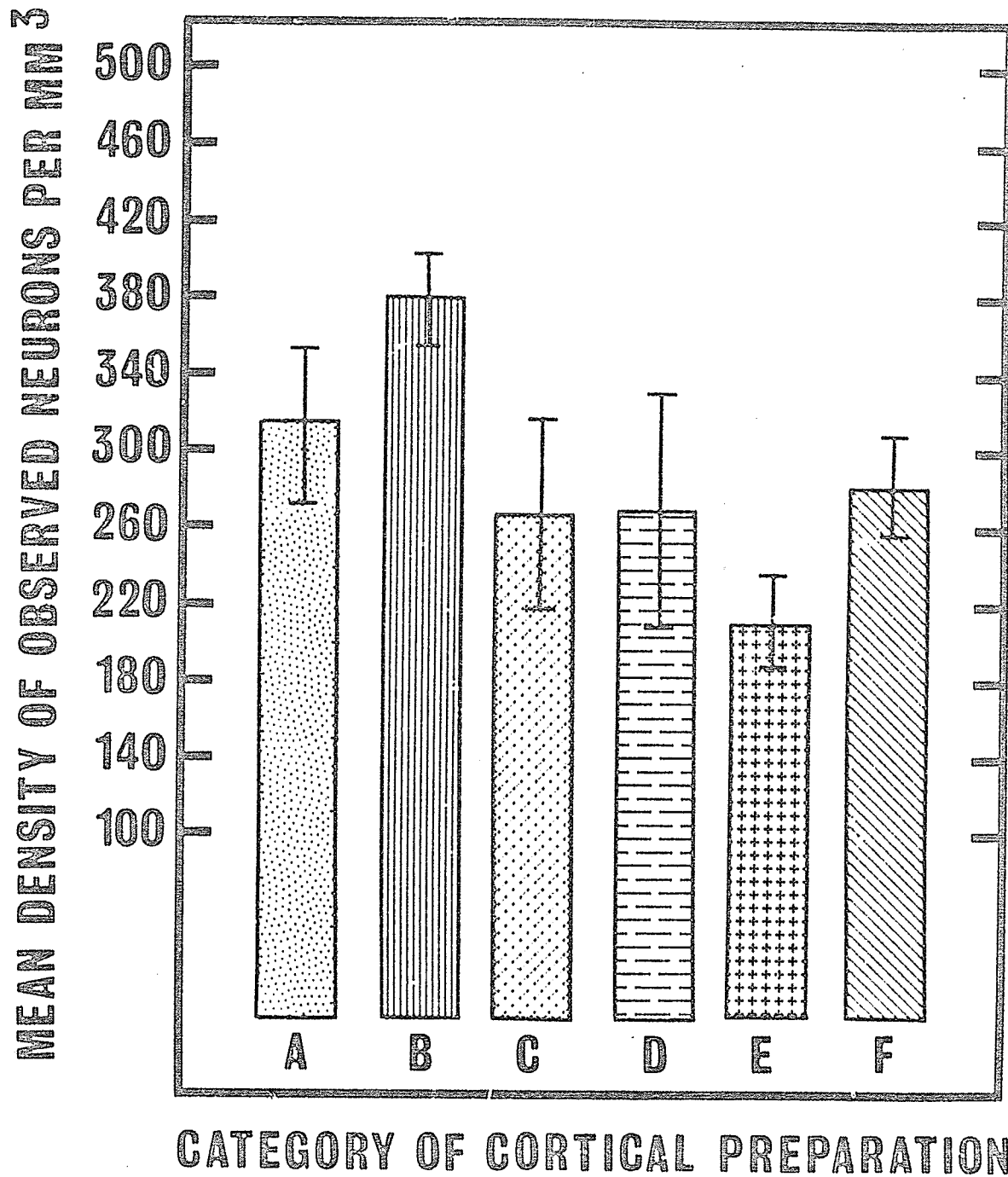


Fig. 36 Mean Neuron Population Density for each Category of Cortical Preparation

- A = Intact left gyrus
- B = Intact right gyrus
- C = Acute left slab
- D = Acute right slab
- E = Chronic left slab
- F = Chronic homotopic gyrus

5. ANALYSIS OF DENDRITES

Analysis of cytological changes was confined to the apical dendritic trees of pyramidal cells as observed from coronal sections. The mean dendrite density was calculated from the number of dendrite sections lying within a tree zone. The diameter of each zone was correlated to the diameter of the neuron's own soma (Methods, p. 140). No attempt was made to analyze dendrite distribution in each of the cortical stratification layers by techniques previously described by Ramon-Moliner (1961) for the postcruciate gyrus in the cat.

The parameters of cortical dendrites which were measured and analyzed were: a) the number of apical dendrites per pyramidal cell in the intact and in the isolated cortex, b) the extent of dendrite branching in both horizontal and vertical spreading patterns and c) the number of spines as a partial indication of afferent circuitry. These measurements and numerous other recorded neurocytological observations permitted also data to be obtained toward the following objectives: a) to examine and to quantitate the structural changes in dendritic trees after varying periods of neuronal isolation, b) to ascertain the extent to which tissue compression and shrinkage might contribute to structural changes in cortical dendrites and c) to possibly contribute to the knowledge of classical neurocytology which might be discovered in the cat cerebral cortex.

Distribution of dendrite density. Small numbers of nearly complete dendritic trees with attached soma were observed in each tissue section. Several factors determined the selection of a tree for analysis: a) the biased selectivity of the stain in favor of certain neurons by factors which are, as yet, unknown; b) dendritic trees which lay within a geometric pattern which would permit most of the dendrites to remain intact and not be sectioned by the microtome knife; c) the bias of the investigator in favor of those trees found within "clear" areas which were discernible from adjacent structures.

The distribution of dendrite density was expressed as the number of dendrite branch points per tree zone. The data for each of the three types of cortex is presented in Table 5 and, graphically, in the histograms of Figs. 37 and 38. The results show that in intact and acute gyri the largest dendrite density is found in those neurons whose soma is situated in the upper cortical halves (Table 5, Fig. 37). No differences were found in dendrite densities between neurons in each of the two upper quadrants or between neurons in each of the two lower quadrants of intact and of acute gyri. In chronic slabs the neurons in each of the four cortical quadrants have essentially similar dendrite densities.

Fig. 38 provides a graphical summary of the effects which varying periods of neuronal isolation

Table 5. Distribution of Dendrite Density

		Quad. 1	Quad. 2	Quad. 3	Quad. 4	Mean
INTACT	Σ Branch Points	28	19	42	37	
LEFT	Σ Cortical Zones	8	5	17	15	
GYRUS	Branch Points/Zone	3.5	3.8	2.4	2.4	3.0 \pm 0.3

		Quad. 1	Quad. 2	Quad. 3	Quad. 4	Mean
ACUTE	Σ Branch Points	49	51	16	12	
LEFT	Σ Cortical Zones	19	19	12	9	
SLAB	Branch Points/Zone	2.5	2.6	1.3	1.3	1.9 \pm 0.3

		Quad. 1	Quad. 2	Quad. 3	Quad. 4	Mean
CHRONIC	Σ Branch Points	20	15	15	20	
LEFT	Σ Cortical Zones	13	15	13	20	
SLAB	Branch Points/Zone	1.5	1.0	1.1	1.0	1.1 \pm 0.1

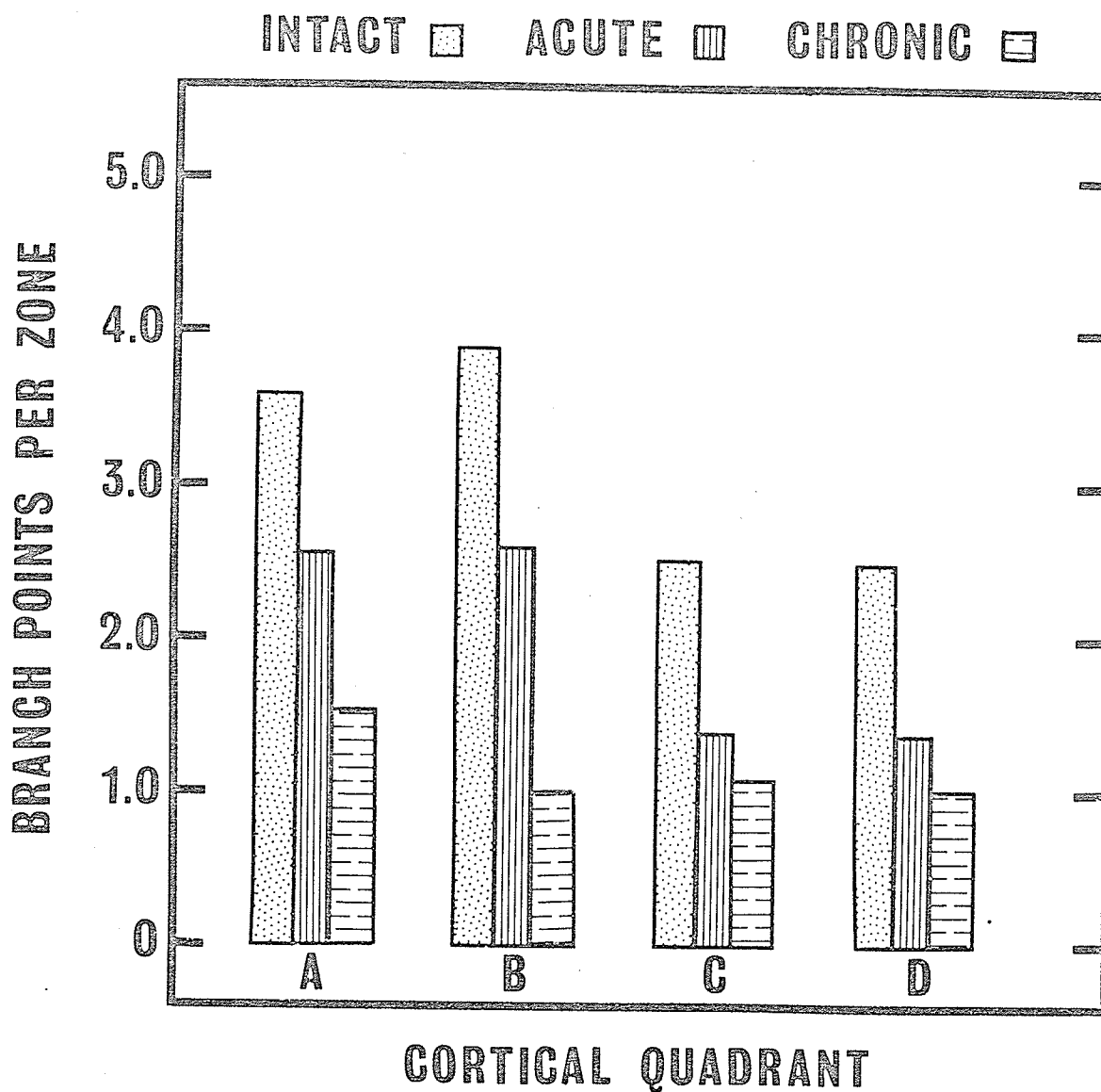


Fig. 37 Comparison of Branch Points Per Zone in Intact Left Gyrus, Acute Left Slab and Chronic Left Slab

A, B, C and D represent cortical quadrants (subdivision illustrated in Fig. 9)

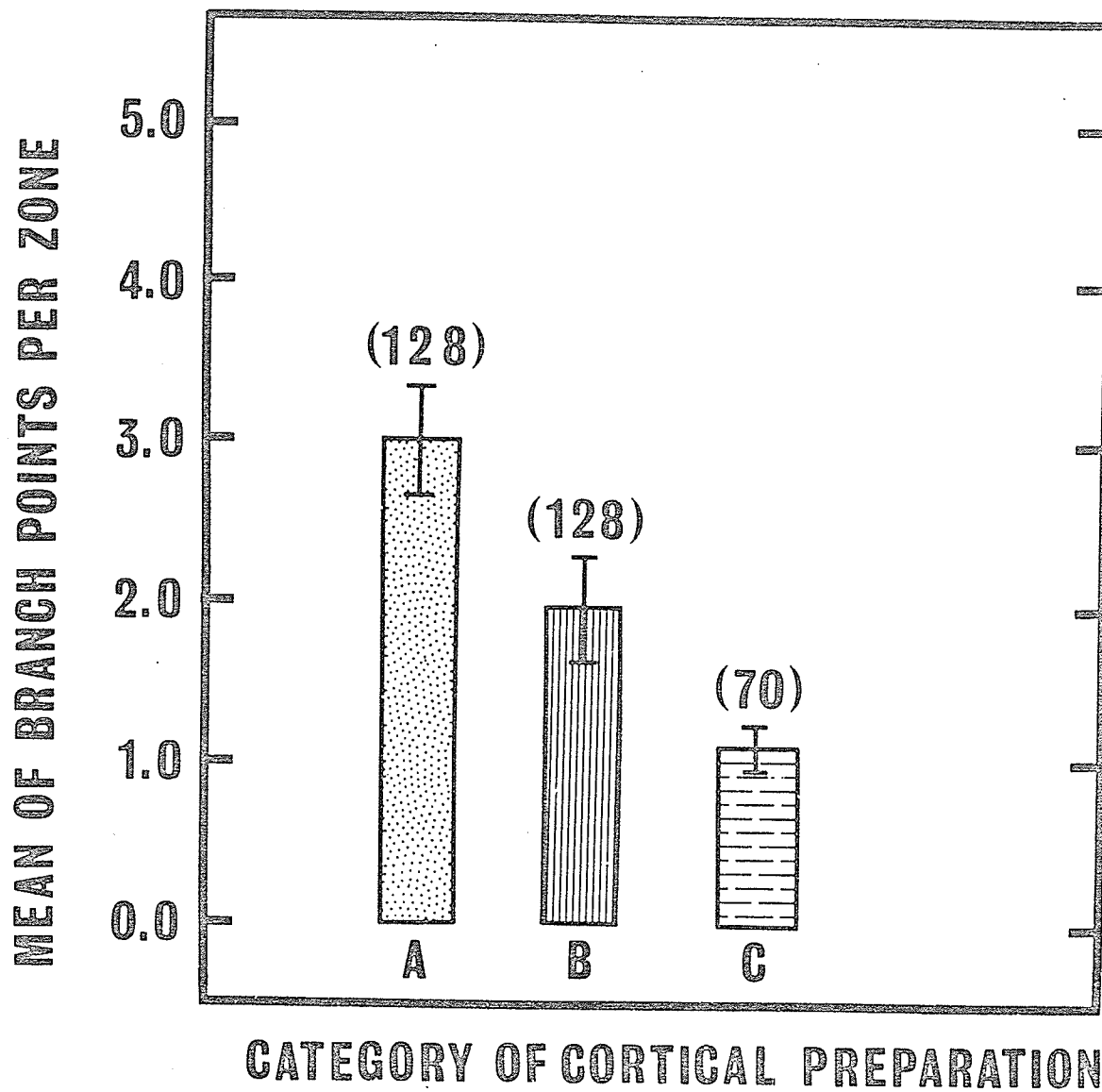


Fig. 38 Mean Dendritic Density, Averaged from all 4 Quadrants in the 3 Different Kinds of Cortical Preparation

A = Intact left gyrus

B = Acute left slab

C = Chronic left slab

have on mean dendritic density, averaged from all four quadrants, in the three different kinds of preparation. The greatest change is seen to occur after long term isolation.

The data from each of the three types of cortex was tested for significance by the t-test for two samples. The results show a highly significant difference ($p \leq 0.001$) was found between intact gyri and chronic slabs. No significant differences in dendrite densities exist between intact gyri and acute slabs or between acute and chronic slabs. However, an examination of the data from individual neurons clearly suggests that the dendrite differences found between the three types of gyri shown in Table 5 and Fig. 38 are a biological fact.

Two examples of camera lucida drawings of dendritic trees used in this study are presented on Plate XVIII.

The absence of impregnated and optically resolvable dendrites in the superficial layer was a histological artifact, probably characteristic of this silver technique, found in most tissue sections. The drawings show clearly that horizontal extensions and branchings of dendrites in this layer were not enumerated. Their omission from this study is not meant to infer that horizontal dendrites were no longer considered to be an important part of the circuitry in the cerebral cortex.

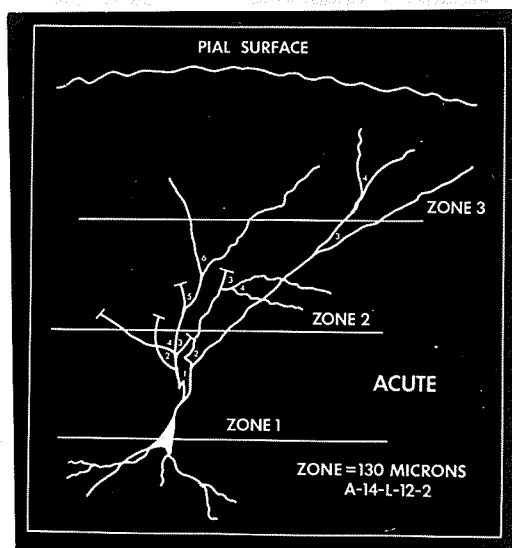
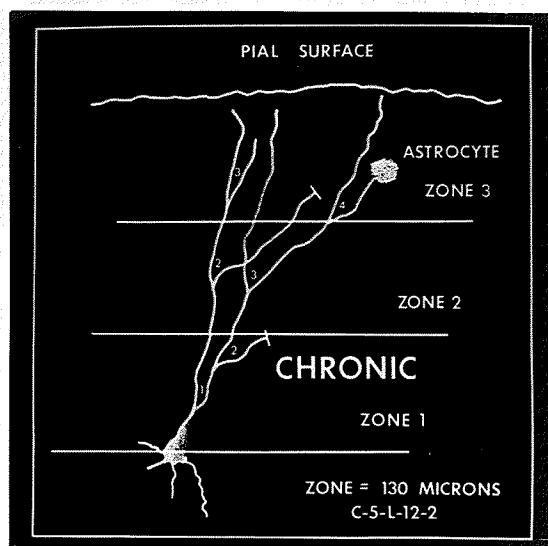


Plate XVIII. Camera lucida drawings of two apical dendritic trees.

Top photograph from chronically isolated slab.

Lower photograph from acutely isolated slab.

Angulation at branch points.

Initial inspection of the impregnated neurons gave the impression that the magnitude of angulation at branch points was smaller in the chronic slabs than in acute slabs and intact gyri. An ocular goniometer was used under direct microscopic observation to measure angles at branch points. A trigonometric correction factor (Appendix, p.331) was applied in order to convert the observed angle to the real angle when the two dendritic arms of the branch point were not in the same plane of focus.

The distribution of mean angles at branch points is shown in Table 6. Measurements were made from apical dendritic trees whose perikarya were situated in one of the four cortical quadrants. Very small differences in the mean angulation were found between each of the quadrants in intact gyri and acute slabs. The ranges in mean angulation with their standard errors were as follows: intact gyri varied between $50.4 \pm 2.6^{\circ}$ to $46.3 \pm 3.3^{\circ}$; acute slabs varied between $57.0 \pm 5.3^{\circ}$ to $43.4 \pm 2.3^{\circ}$. In chronic slabs the mean values for each cortical quadrant were notably smaller where the ranges varied between $35.7 \pm 2.9^{\circ}$ to $45.0 \pm 3.7^{\circ}$. The results show also that in the three types of cortex the maximum and minimum mean values were not repeatedly confined to any one cortical quadrant.

Paired comparisons tests in intact gyri and acute and chronic slabs showed that no significant differences in angulation exists between any of the four cortical quadrants in each type of preparation.

Table 6. Mean Angle at Branch Points per Quadrant

INTACT	Quad.1	Quad.2	Quad.3	Quad.4	
LEFT GYRUS	Mean Angle at Br.Pts./Quad.	46.3±3.3	46.9±3.5	50.4±2.6	48.2±2.8

ACUTE	Quad.1	Quad.2	Quad.3	Quad.4	
LEFT SLAB	Mean Angle at Br.Pts./Quad.	51.6±2.1	43.4±2.3	48.5±4.9	57.0±5.3

CHRONIC	Quad.1	Quad.2	Quad.3	Quad.4	
LEFT SLAB	Mean Angle at Br.Pts./Quad.	35.7±2.9	41.0±3.4	45.0±3.7	39.0±2.7

Several t-tests for two samples were made for significance of differences between data pooled from all quadrants in intact gyri and acute slabs, and between similar data from intact gyri and chronic slabs. The results of the tests showed that no significant differences in pooled angulation exist between intact gyri and acute slabs ($p \leq 0.40$) or between intact gyri and chronic slabs ($p \leq 0.10$). However, there is a significant difference ($p \leq 0.05$) between the means of the angles measured in quadrant 1 of chronic slabs and intact gyri, and also between the means of angles measured in quadrant 4 of chronic slabs and intact gyri; the mean angulation in the chronic slab is reduced from that in the intact gyrus.

All t-tests were repeated using the data from uncorrected observed angles in order to ascertain whether shrinkage and distortion in the chronic slab had altered the geometry of the dendritic tree. The results of these tests showed no change in the p values for the upper cortical quadrants in all three kinds of preparation. This implies that chronic isolation does not induce rotation of dendritic trees in the upper quadrants. However, the p values for the lower cortical quadrants in chronic slabs changed from $p \leq 0.10$ to $p \leq 0.40$. The altered p values found only for chronic slabs indicates that the partial rotation of the apex, observed in chronic slabs in this study, (Parameter H-I

in Fig. 7 and Column 6 in Table 3), also affects the geometric plane of apical dendritic trees. A paired comparison test was made between corrected and uncorrected angles in intact gyrus, acute and chronic slabs. No significant differences were found in the intact gyrus and acute slab. However, a highly significant difference was found in the chronic slab ($p \leq 0.001$). These results lend greater support to the evidence for rotation of dendritic geometric domains in chronic slabs.

Fig. 39 illustrates in histogram form the mean angle at branch points for each quadrant in the three types of cortical preparation. The profiles show that chronic isolation resulted in a reduction of mean angulation in all cortical quadrants examined when chronic slabs were compared to intact gyri and acute slabs. This decrease in branch angulation appears to be generally distributed throughout the chronic slab.

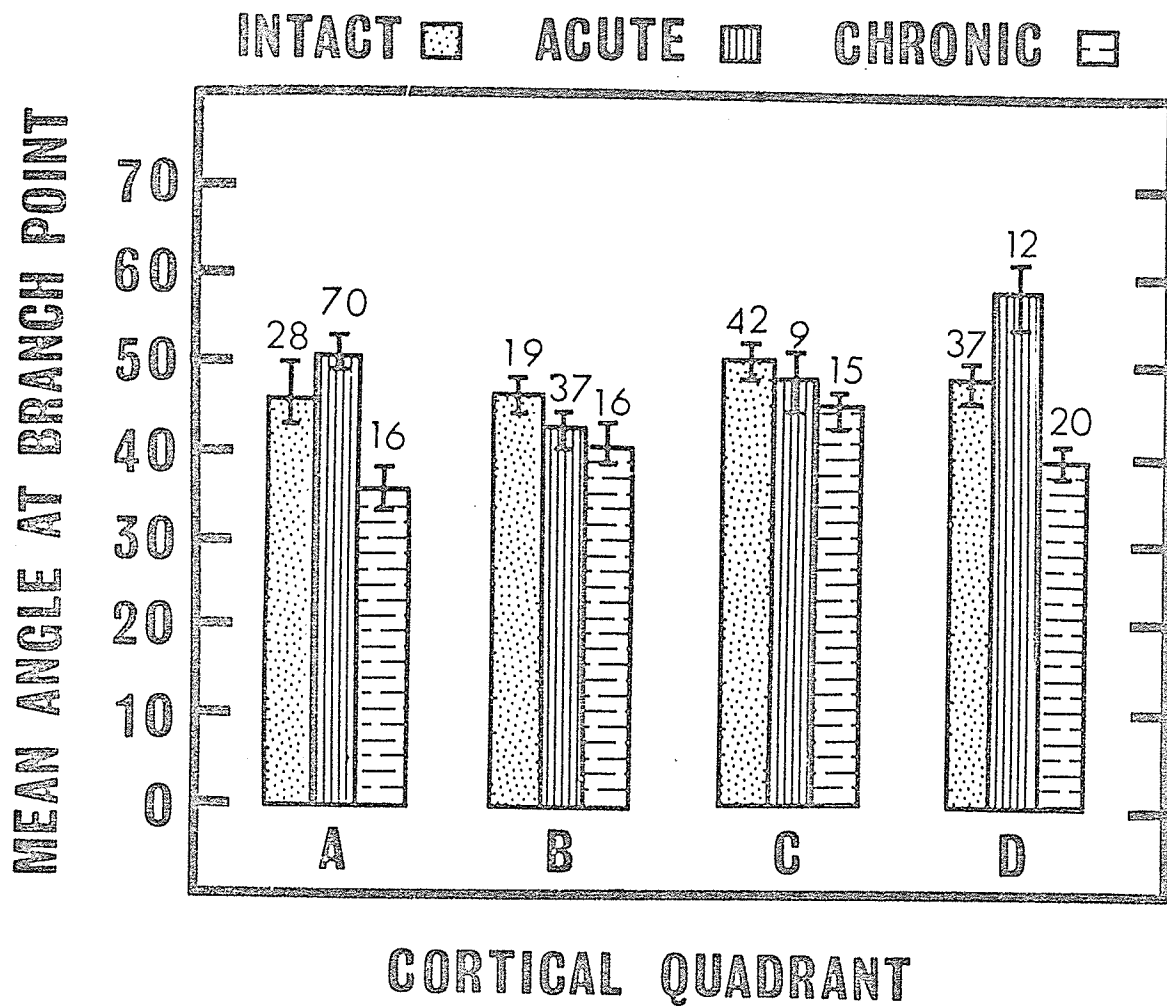


Fig. 39 Mean Angle at Branch Points for each Quadrant in the 3 Types of Cortical Preparation

A, B, C and D represent cortical quadrants (subdivision illustrated in Fig. 9)

Dendritic spine density.

The spine density was expressed as the number of observable dendritic spines found per micron length of dendrite section. Separate density calculations were made in each of the stem, branching and terminal zones which are found in a dendritic tree. Neurons were categorized into one of two groups: a) soma of pyramidal neurons situated in layer III as representing the upper cortical half, and b) soma of pyramidal neurons in layer V as representing the lower cortical half. This technique of neuron grouping was based upon recent results of studies on cortical circuitry by means of environmental deprivation (Globus and Scheibel, 1967; Valverde, 1967; Coleman and Riesen, 1968). The acute left slab chosen for this part of the study involved surface stimulation and recording with iridium-platinum and silk-wick electrodes. The pulses were 2 milliseconds in duration, the pulse amplitude ranged from 10-25 volts and the slab was stimulated at 30 pulses per second for periods of 1 to 2 seconds. Intact gyrus and chronic slabs were left unstimulated for this part of the study.

Three dendritic trees in each of the cortical halves were analyzed for spine density. Dendritic spines were not found on any parts of neuronal somata in density studies on 36 dendritic trees. The dendritic spine density in the three kinds of cortical preparation are shown in Table 7. The results showed that the least spine density is usually found in the stem zone while the greatest spine density was consistently found in the branching zone. These results indicate that the largest afferent region of the dendritic tree is the intermediate area which was designated as the branching zone; this agrees with the observations of Mungai (1967).

Table 7. Dendrite Spine Density

	INTACT LEFT GYRUS		INTACT HOMOTOPE GYRUS	
	Upper Half	Lower Half	Upper Half	Lower Half
STEM ZONE	1.3±0.06	1.4±0.2	1.1±0.08	1.2±0.1
BRANCHING ZONE	6.0±1.0	7.3±0.3	6.5±0.1	5.5±0.4
TERMINAL ZONE	2.6±0.06	1.2±0.1	1.0±0.03	Not Avail.

	ACUTE LEFT SLAB Stimulated		ACUTE HOMOTOPE SLAB	
	Upper Half	Lower Half	Upper Half	Lower Half
STEM ZONE	1.7±0.23	3.2±1.4	1.3±0.16	1.2±0.14
BRANCHING ZONE	6.1±0.5	8.1±0.4	7.2±0.9	6.1±0.20
TERMINAL ZONE	6.1±0.7	4.7±0.3	2.4±0.3	Not Avail.

	CHRONIC LEFT SLAB		CHRONIC HOMOTOPE GYRUS	
	Upper Half	Lower Half	Upper Half	Lower Half
STEM ZONE	1.5±0.1	1.5±0.1	2.5±0.6	1.9±0.3
BRANCHING ZONE	4.1±0.2	4.8±0.5	6.8±0.5	5.6±0.5
TERMINAL ZONE	1.3±0.4	0.6±0.08	3.0±0.6	Not Avail.

Note: All preparations were unstimulated except for the acute left slabs.

233a

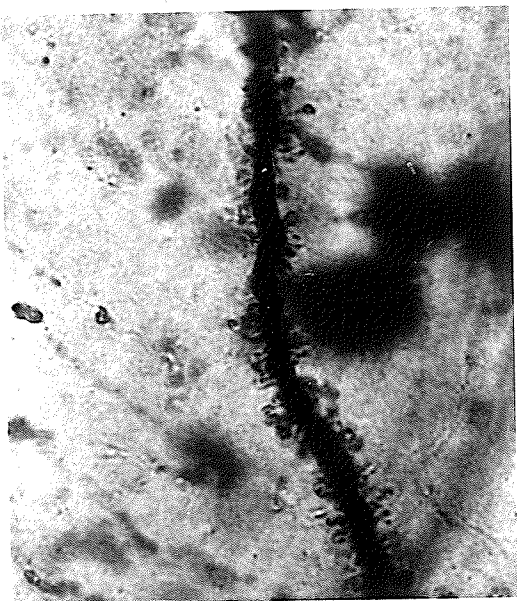


Plate XXXI. Apical Dendrites from Layer III Neurons. 1250X.

Upper photograph from chronically isolated slab.

Lower photograph from stimulated left acutely
isolated slab.

Paired comparison tests were made to test for significant differences in spine densities between similar zones in intact left gyrus and homotopic gyrus, acute left slab and homotopic slab, chronic left slab and homotopic gyrus. No significant differences in densities were found between the left and homotopic preparation. Several t-tests for two samples were made for significance in spine densities between similar zones in the three kinds of cortical preparation. The results showed no significant differences in spine densities between the three homotopic preparations. Significant differences were found in spine densities between upper cortical terminal zones in intact left gyrus and acute left slab ($p \leq 0.02$); highly significant differences were found between lower cortical terminal zones in intact left gyrus and acute left slab ($p \leq 0.001$). Similar significant values were found in the terminal zones between acute left slabs and chronic left slabs. These results would appear to indicate that repetitive reinforcement of electrical activity on the pial surface of the slab significantly increases spine density in subpial dendrites. The fall-off in spine density in unstimulated chronic slabs, as noted in Table 7, supports the theory that the apparent "dis-use" of dendrites results in partial loss of their structural integrity. Plate XXXI illustrates the differences in spine density in the terminal zones between acute left slabs and chronic left slabs.

Dendrite wedges. In the present study, dendritic wedges were found regularly in intact gyri, in both acute and chronic slabs. Plate XIX shows a photomicrograph of cerebral cortex from an intact gyrus with three incomplete dendritic trees whose somata are situated in layer III. Dendritic wedges are distributed in both stem and branching zones. Wedges found in acute slabs are illustrated in Plate XX. Dendritic wedges were found also in chronic slabs.

In some instances dendritic wedges from several adjacent neurons were grouped in pairs (Plates XX and XXI). Plate XXI, which is a high magnification of the area seen in Plate XX, three pairs of dendritic wedges are shown. The results obtained from the silver technique used here does not preclude the possibility that other dendrites might also be present between the paired wedges.

Dendritic wedges were studied for angular redirection beyond the "V" configuration. The results showed that in the examination of 82 dendritic wedges the post-wedge direction of dendrite sections was usually within 10° of the pre-wedge pathway. It was found that the narrow range of angular pathways was maintained for distances up to 350 microns.

Observations of dendritic wedges at high magnification sometimes show the transverse section of a

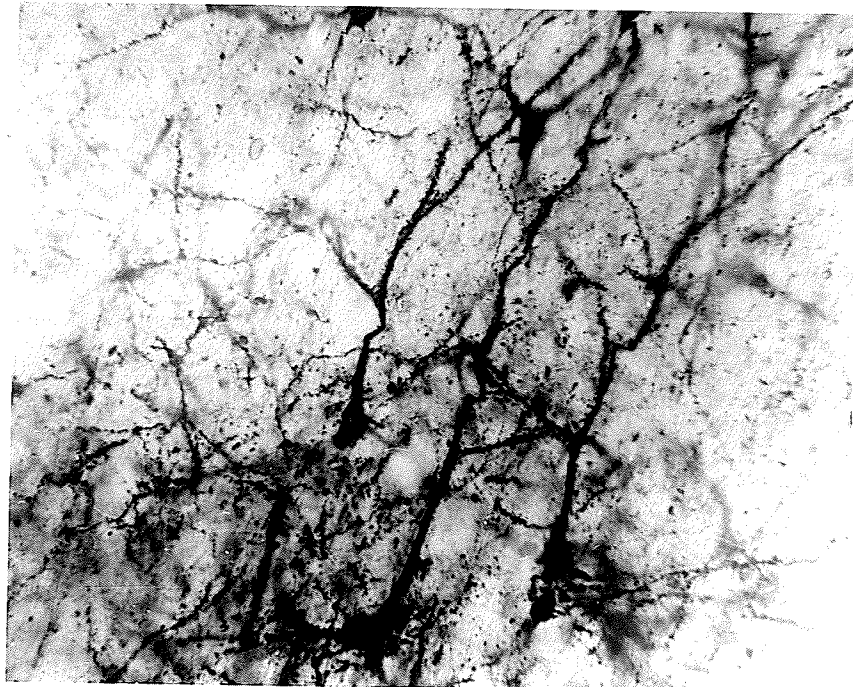


Plate XIX. Intact Cortex, Upper Cortical Half, 200X

Pyramidal neurons of Layer III with apical dendritic trees. Dendritic wedges are shown in both stem and branching zones.

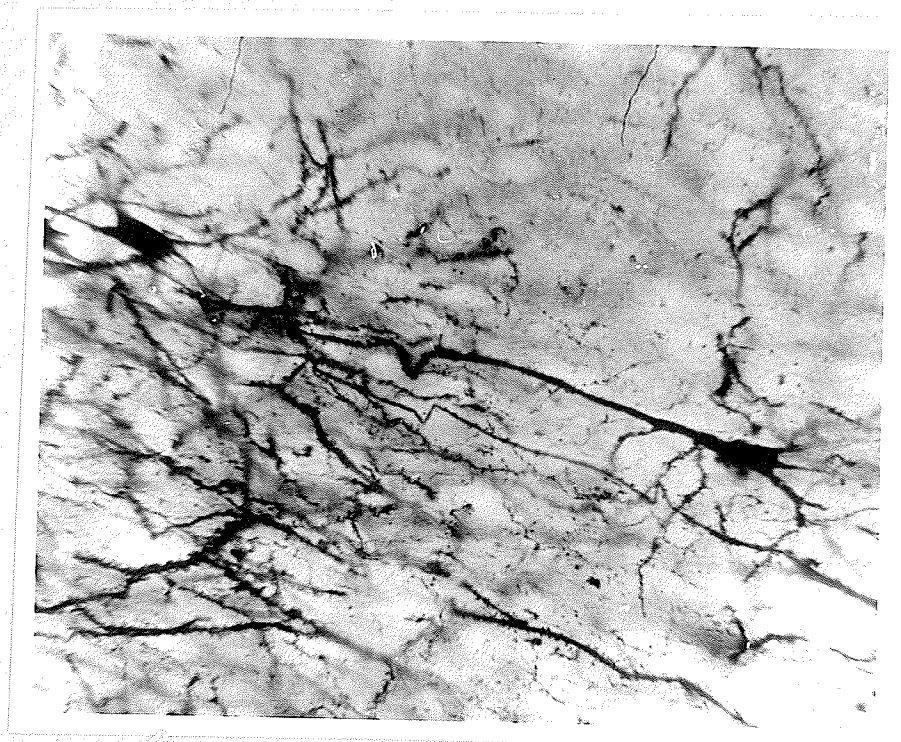


Plate XX. Acute Slab, Lower Cortical Half, 200X

Dendritic wedges from several adjacent
neurons are grouped in pairs.

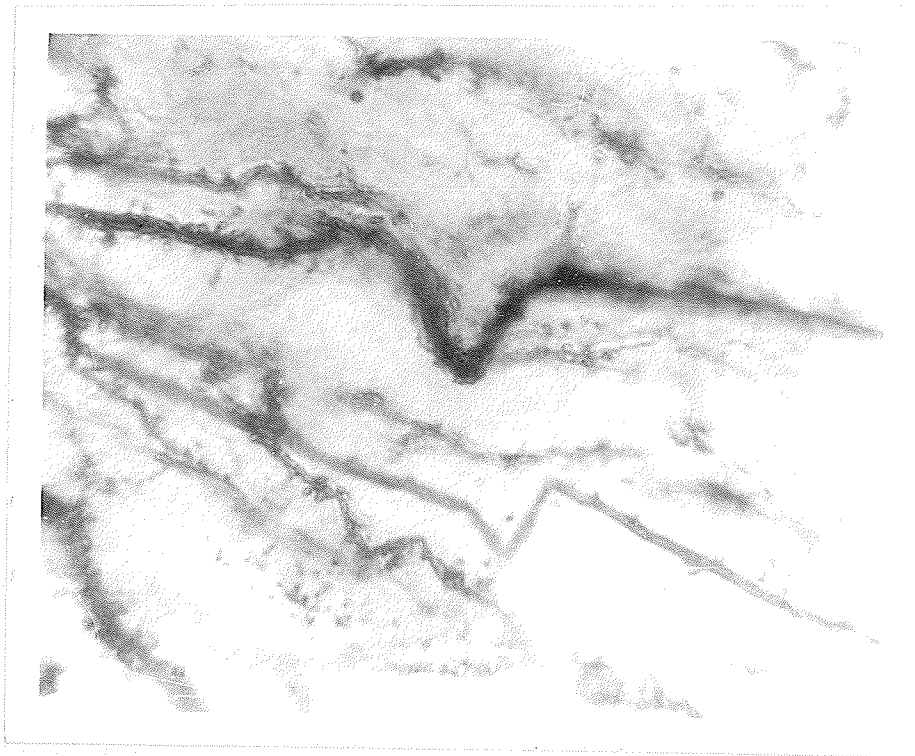


Plate XXI. High Magnification of Wedge Area Shown in Plate XX

Three pairs of dendritic wedges from adjacent neurons. Note large number of dendritic spines in upper dark wedge.

blood vessel lying within the acute angle of the wedge (Plate XXII). It will be noted that the dendrite section, instead of assuming a new tangential direction, follows the circumference of the blood vessel and thereby maintains its pre-wedge direction. Such results suggest that the directional growth of apical dendrites may be influenced, in part, by toxic factors found in the subpial region.

The distribution of dendritic wedge density, in terms of the total number of wedges found in each dendritic tree, were calculated. The results for intact left gyri, acute left slabs and chronic left slabs are summarized in Table 8. No statistical tests were made to test for significant differences between the different preparations. However, the results demonstrate an unmistakable tendency towards a reduction in the numbers of wedges per dendrite tree after long term isolation.

Basilar dendrodendritic pathways. An early observation made during the course of this study revealed a possible dendrodendritic junction between two pyramidal neurons, via their basilar dendrites. This observation was regarded with extreme caution, realizing that light microscopy alone could not provide cytological evidence for any of the following: the ultimate structural characteristic of the junction, whether or not this kind of junction is physiological, whether

Table 8. Distribution of Dendritic Wedge Density

Mean Density Dendritic Wedges, (Wedges/Tree) Preparation	Intact Left Gyrus	Acute Left Slabs	Chronic Left Slabs
Upper Cortical Half	2.6	1.3	1.4
Lower Cortical Half	3.5	4.5	2.4
Mean of Upper and Lower Halves	3.1	2.9	1.9

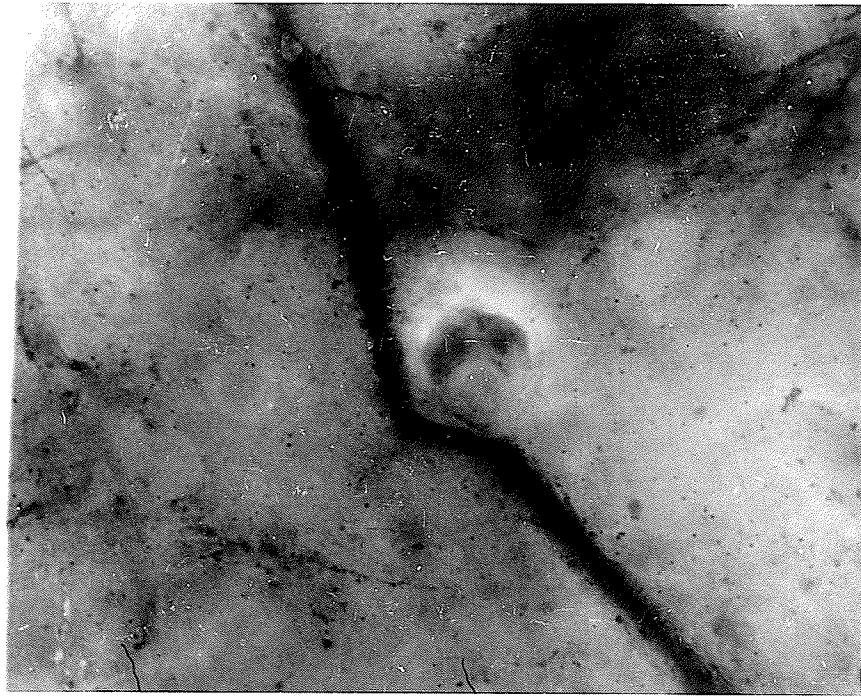


Plate XXII. Acute Slab, Dendrite Wedge, 600X

Dendrite section follows circumference of
blood vessel and maintains its pre-wedge direction.

the junction is an artifact peculiar to this stain technique. Taking note of these cautions the cortex from the three kinds of tissue were examined for further evidence of such basilar dendrodendritic junctions. In Plate XXIII taken from an intact gyrus, the centre of the field of view, observed at 200x, shows two pyramidal neurons in Layer III. An examination of the basilar dendrites between the perikarya, observed at 1250x oil with a N.A. of 1.3, failed to reveal any separation along the dendrite or at the perikarya. In Plate XXIV two pyramidal neurons in Layer III from a chronic slab shows another such possible communication between two perikarya via a basilar dendrodendritic pathway. It was impossible to ascertain by means of optical microscopy whether this basilar pathway consisted of a single dendrite from one perikaryon (dendrosomatic) or two dendrites joined at a given point between the two cells (dendrodendritic). In Plates XXV and XXVI a basilar dendrodendritic pathway is shown to extend from a Layer III neuron to a Layer V neuron. The two photographs are composites made from a consecutive series of photographs, each of which was taken at a different plane of focus.

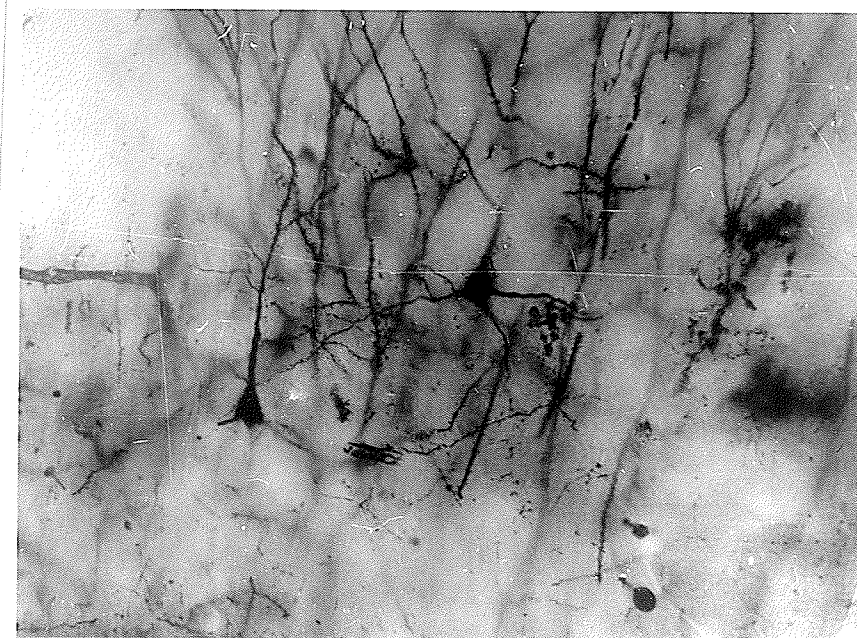


Plate XXIII. Intact Gyrus, Upper Cortical Half, 200X

Two pyramidal neurons in Layer III show an
apparent basilar dendrodendritic pathway.

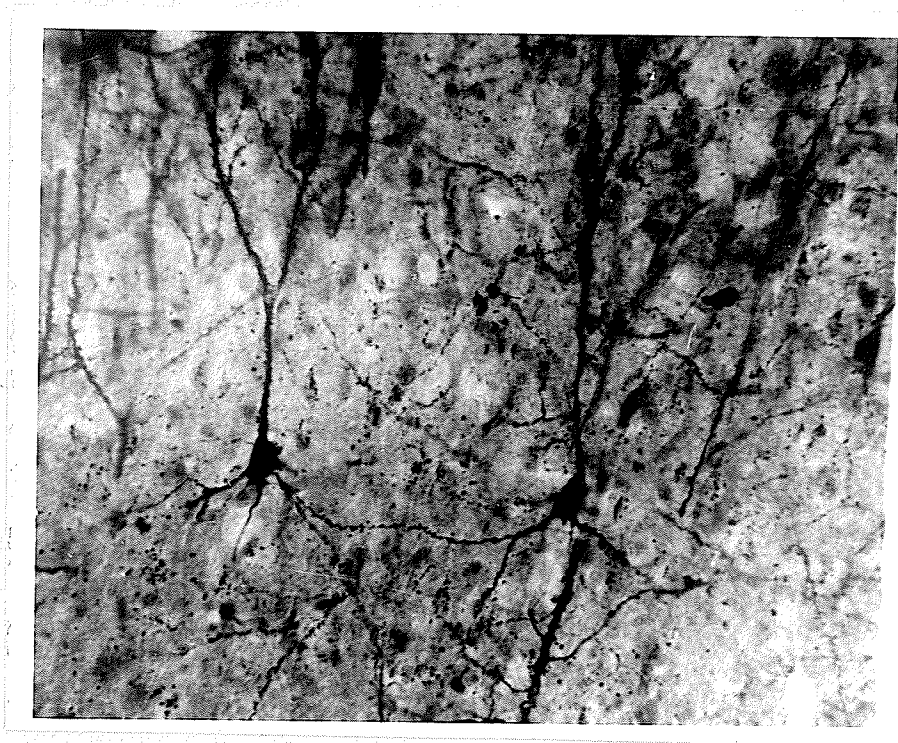


Plate XXIV. Chronic Slab, Upper Cortical Half, 200X

Two pyramidal neurons in Layer III show additional evidence in support of a possible basilar dendrodendritic pathway.

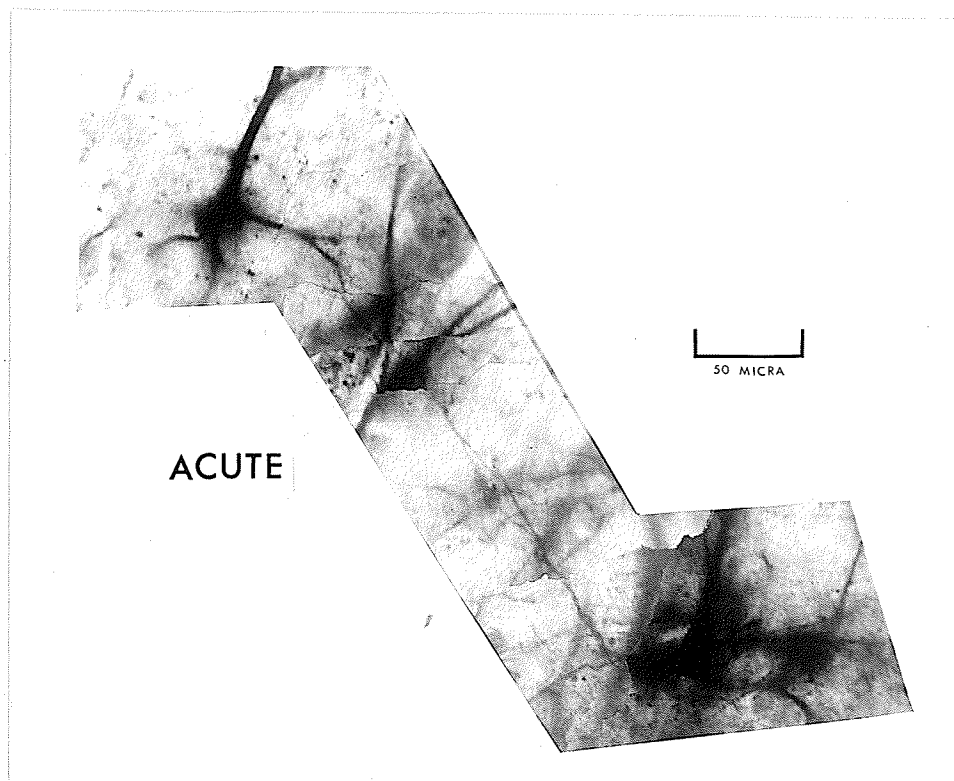


Plate XXV. Acute Slab, Composite Photograph, 1250X

A possible basilar dendrodendritic pathway is shown to extend from a Layer III neuron to a Layer V neuron.

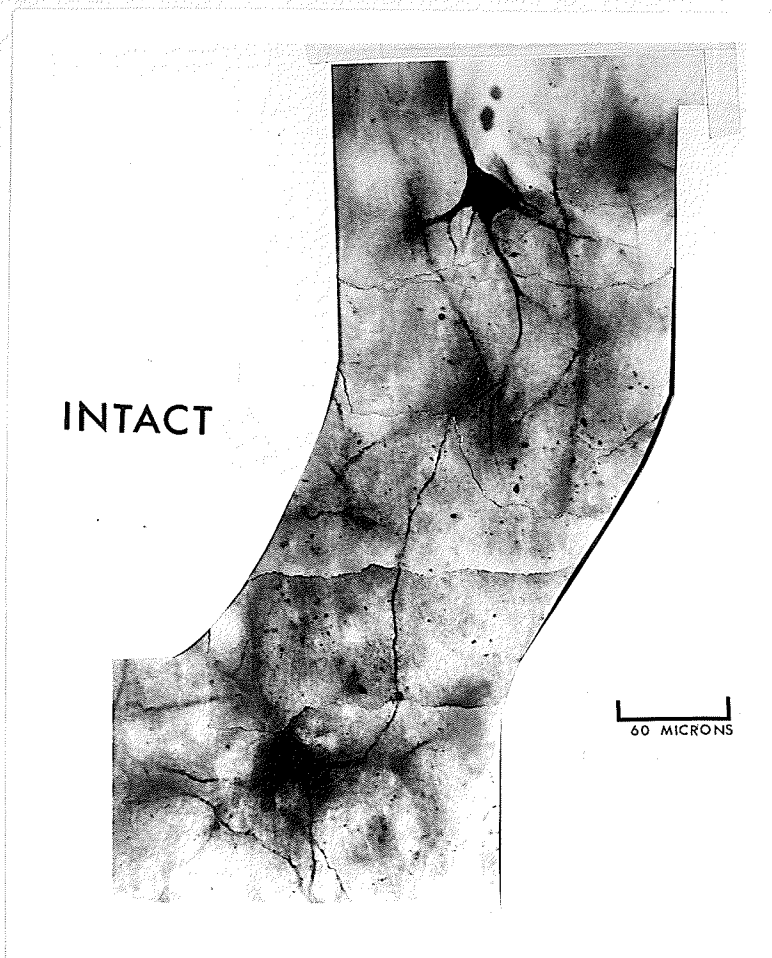


Plate XXVI. Intact Gyrus, Composite Photograph, 1250X

A possible basilar dendrodendritic pathway is shown to extend from a Layer III neuron to a Layer V neuron.

Trifurcated branch point. Localized failure in development of the gray matter was observed in the mid-region of one intact left suprasylvian gyrus (Plate XXVII). The anterior and posterior regions, in contrast to the abnormal mid-region, appeared quite normal in development. The corresponding contralateral gyrus appeared to be entirely normal. A reasonable assumption would be that abnormal development occurred during the fetal agyri stage (Truex and Carpenter, 1964) and was maintained into the period of postnatal growth. It would be reasonable also to assume that the initial development and subsequent growth of dendrites during the postnatal period was influenced by the same unknown factors which influenced the abnormal development of the gray matter. This gyrus was, therefore, deliberately omitted from the analytical data reported in the earlier parts of this thesis.

An examination of the cortex at 200x in the medial half of the abnormal gyrus showed a type of Layer III pyramidal neuron not previously described here or in the literature (Plate XXVIII). The termination of the apical dendritic shaft is marked by a trifurcated branch point. Additional observations at 1250x (Plate XXIX) and at 1500x revealed clearly that three dendrite sections, each directed towards the pial region, emerged from this branch point. Each of the three dendrite

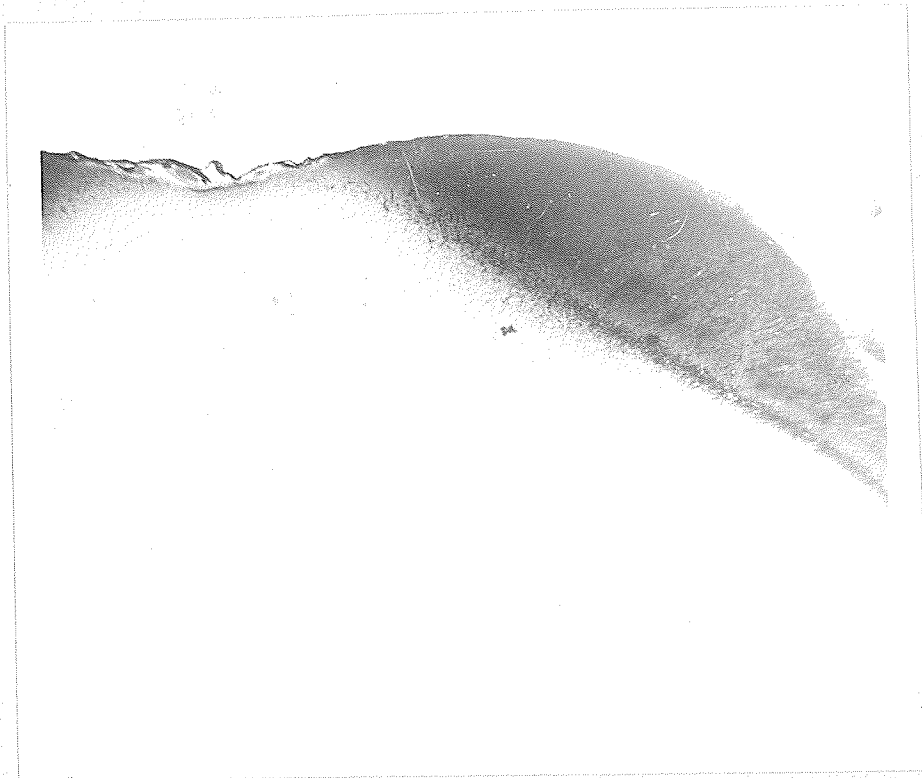


Plate XXVII. Coronal Section, Intact Left Gyrus, 25X

Localized failure in development of gray matter in the mid-region of a suprasylvian gyrus.

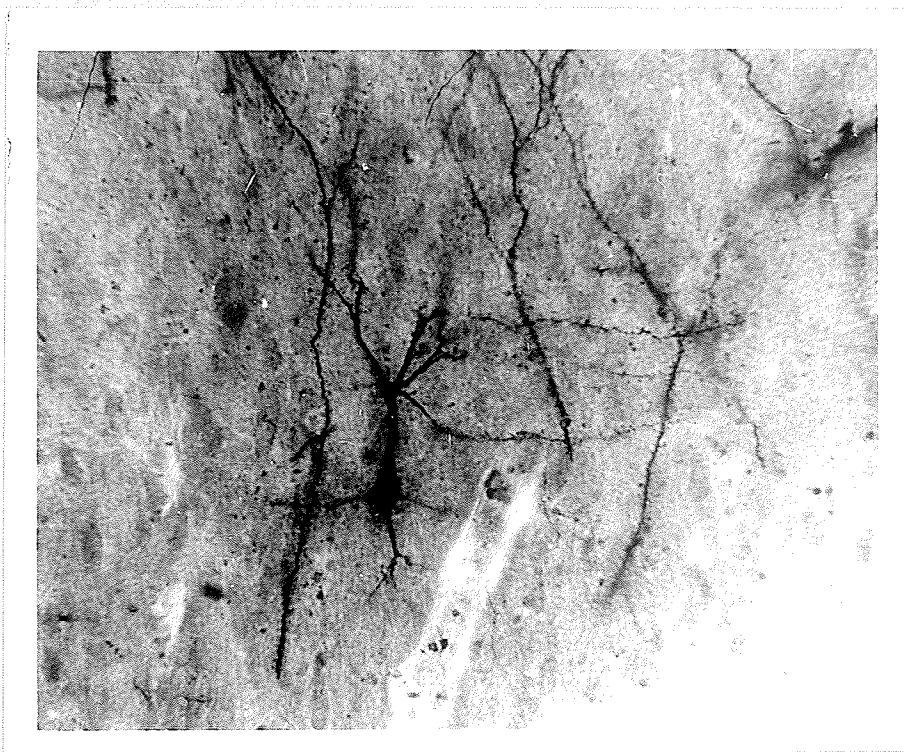


Plate XXVIII. Upper Cortical Half, Right Side from
Plate XXVII, 200X

Type of Layer III pyramidal neuron with apical
dendritic shaft marked by a trifurcated branch point.

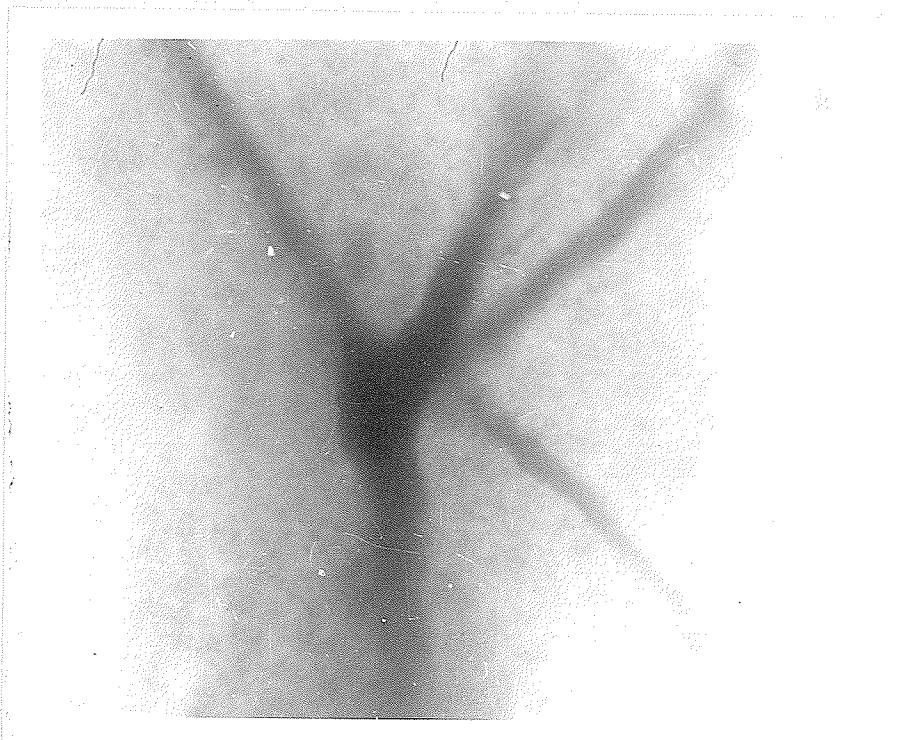


Plate XXIX. High Magnification of Trifurcated Branch Point, 1250X

Lower right dendrite section is not a structural part of the trifurcation (determined by fine optical adjustments).

sections was found to lie in a different plane of focus as if in a bouquet arrangement; however, the continuity from the branch point was identified for each section.

Structural variations and electrical stimulation.

Two acute left slabs examined in this study were electrically stimulated by surface stimulating electrodes. The amplitude of the stimulating voltage was between 10 and 25 volts, the pulse duration was 30 pulses per second in periods of 1 to 2 seconds and the pulse duration was 0.2 msec. The electrodes were applied to the pial surface at about the mid-region of the slab. The examination of the anterior ends of both slabs showed an unusually large number of apical dendritic shafts, each of which were apparently cut off from their own perikaryon by the microtome knife. Similar cortical areas in intact gyri and non-stimulated acute slabs showed, by subjective observations, a greater number of dendritic apical shafts which were attached to their own perikaryon. The histological relationship of a dendritic shaft to its perikaryon in a coronal section of stimulated slabs was similar to that of a hair shaft to its hair root in a vertical section of mammalian skin. The apical dendritic tree from the midpoint of the apical shaft to the terminal zone may have "bent" towards the stimulated point. These observations were neither analyzed nor tested for significant differences between stimulated

and non-stimulated slabs. However, it is interesting to theorize that exogenous electrical stimulation may have exerted some sort of taxic influence on geometric domains of dendritic trees.

Dendritic spines in stimulated acute left slabs appeared much longer when compared to similar structures in the non-stimulated cortex (Plate XXX). The longest spines appeared in the subpial region of the stimulated slabs. These observations were neither analyzed nor tested for significant difference.



Plate XXX. Acute Left Slab, Dendrite Section, 1500X

Acute left slab electrically stimulated by surface stimulating electrodes. Spines appeared much longer in stimulated slabs when compared to non-stimulated cortex.

DISCUSSION

1. HISTOMORPHOLOGICAL CHANGES FOLLOWING NEURONAL ISOLATION

A major aim of this study, as stated in an earlier section of this thesis, was to determine whether there are histomorphological changes in chronically isolated slabs which could account for any of the known alterations in the electrical activity of such a preparation. Any attempt to form such structure-function correlations from data in the neuronally isolated cortex must consider, as a priori, those physicochemical factors which may have contributed to the distortion of the tissue and the loss of cerebral cortical volume. The cerebral cortex is subjected to considerable trauma by the extensive surgery of the sidecuts and undercut. The surgery required for craniotomy can, by itself, be reasonably expected to cause some form of microscopic disturbance to the underlying cerebral cortex. Experimental craniotomy accompanied by dura incision over an intact area of ectosylvian, suprasylvian and marginal gyri is associated with fibre degeneration in the underlying cerebral cortex (Harris, 1960). Surgery in the cortex and in the underlying white matter results in extensive intracortical hemorrhage, axotomy, dendrite fractionation and gliosis (Cajal, 1928).

The loss of cortical volume and tissue deformation were anatomical features that were noted in all acutely and chronically isolated slabs. Cortical volume loss might, theoretically, be due to several mechanisms which act in combination to produce the results observed in the experimental data from this study. Among such mechanisms three possibilities are most prominently suggested by the data acquired in this study; these are: a) tissue shrinkage from loss of perivascular fluid, b) tissue compaction from loss of all other extracellular spaces, c) loss of intracellular fluid from neurons and neuroglia.

In the cerebral cortex the amount of intercellular fluid appears to be inversely dependent upon the density of cortical vascularity and cell population density. Blood vessels from the subarachnoid space and pia course into the underlying cortex via perivascular channels that are lined by a cellular continuation of the intima pia (Weed, 1922). Perivascular channels are, in turn, continuous with pericapillary spaces lying in the deeper recesses of the cerebral cortex. Cerebrospinal fluid from the cerebral ventricles diffuses, via the ependymal epithelium, into cortical perivascular and pericapillary spaces (Millen and Woollan, 1961, 1962) which act as absorption routes for cerebrospinal fluid in the cerebral hemispheres (Adams, 1951; Maas and Adams, 1951;

Sweet, Talland and Ervin, 1959; Browsher, 1957). A low neuron population density implies greater interneuronal spaces that are available for blood vessels, neuroglia nerve processes (Sholl, 1959). This hypothesis of Sholl appears to have been confirmed by Ramon-Moliner (1961) who reported that in the postcruciate gyrus of the cat neuroglial population densities show variations with the cortical depth and the region examined. Variations in vascular density in the cerebral cortex were reported by Dunning and Wolff (1936, 1937). A direct relationship between cortical capillarization and neuropil density was observed by Lorente de No (1927), Campbell (1937) and Drummond (1944). Blood capillary density in the cerebral cortex is highest in cortical layers III, IV and V (Campbell, 1939). Variations in neuron population densities throughout entire lengths of suprasylvian gyri were reported earlier in this study and are shown graphically in Figs. 18, 19, 24, 25, 30 and 31. The histological parameters of acutely and chronically isolated gyri presented in Tables 2 and 3 in this study show conclusively that changes in the slabs' distortion and shrinkage occurs at 1 mm intervals throughout the entire length of the isolate. It may be concluded from the foregoing discussion that intracortical surgery cuts off numerous cortical blood vessels from their surrounding tortuous routes; this in turn shuts off perivascular

channels that serve as an important intracortical route for cerebrospinal fluid. The inferences that may be deduced are twofold: first that cortical shrinkage may be attributable to a loss of cerebrospinal fluid, and second that the variations in neuron population densities and neuroglial population densities implies inverse ratios of vascular densities with perivascular channels for cerebrospinal drainage. The latter accounts for the variations in amounts of tissue shrinkage due to fluid loss along the length of the slab.

Several unsuccessful attempts have been made to induce an experimental in vivo condition of brain oedema by water overload (Gerschenfeld, 1959). Tight junctions in glial cells form occluding zones that reduce the intercellular gap to about 50 \AA (Farquhar and Palade, 1963). These occluding zones were offered as a possible area of fluid impermeability. De Robertis and Gerschenfeld (1961) reported that the size of extracellular spaces in the gray matter of the CNS ranged between 100 \AA and 250 \AA . Their in vivo studies, obtained during brain oedema of brain slices, showed that no increase occurred in the size of the extracellular space during oedema. However, they noted also that astrocytic somata and their processes were significantly swollen. De Robertis (1965) considered this as proof against the concept of extracellular oedema in the gray matter of the CNS. Astrocytes were considered

also as constituting important pools for CNS water and electrolytes. De Robertis hypothesized that some part of the blood-brain barrier mechanism would pump the excess fluid back into the blood capillaries.

In considering the foregoing in relation to the observations in the present study there seems to be good reasons to assume that the sizes of intercellular spaces in the cerebral cortex will not vary to any great extent as a result of various experimental procedures. Cortical segments 2A and 1B in the chronically isolated slabs here represent areas of surgical protection. The observed number of cells in these segments were approximately 40% less than corresponding segments in acute slabs (Figs. 26 and 32). The volume of these cortical segments in the chronic slabs were generally reduced by almost 40% when compared to similar segments in acute slabs (Figs. 26 and 32). It will be noted that the neuron population densities in these chronic cortical segments were not increased. It seems reasonable to assume that if cortical volume reduction was due to primarily tissue compaction through a loss of intercellular spaces then the neuron population densities in chronic slabs would increase rather than remain comparable to their acute counterparts. In considering the evidence against the possibility of variations in sizes of intercellular spaces presented by De Robertis, Gerschenfeld and Farquahar, and the results of neuron

population density studies it seems reasonable to propose that cortical volume reductions in chronic slabs is not due to tissue compaction. Indeed, it is tempting to postulate that an increase in tissue compaction in the cerebral cortex is not possible. It must therefore be concluded that loss of cerebral cortical fluid and cell fall-off are the primary factors for reductions in cerebral cortical volume.

In a previous anatomical study on neuronally isolated cerebral cortex Reiffenstein (1964) measured gyrus width, slab depth and cortical depth from one small undetermined area of the suprasylvian gyrus. In the present study serial measurements were made of histological parameters of gyrus width and cortical depth in isolated gyri. Measurement was made to within an accuracy of the nearest micron at each millimeter interval. These measurements were then compared to similar parameters taken from intact gyri. Previously it was not known whether there was any regular pattern in the occurrence of discrete changes in width along the length of the suprasylvian gyrus, either within a single cut or as a general structural pattern in different cats. Sholl (1956) reported that large variations in the depth of the visual cortex were found to occur normally in different mammals. It was not known whether similar variations in cortex depth would be found in the suprasylvian gyrus of different cats.

The widest gyrus observed in this study was 6771 microns (from data used to compile Table I) and the narrowest was 5416 microns. This 25% difference between these two gyrus widths (1355 microns) was statistically significant ($p \leq 0.001$). It is of considerable interest to find that, although the gyrus width in any one animal varies at each millimeter interval, these variations are not statistically significant when compared to the mean gyrus width on that same animal. The discrete variations in width do not recur as a regular structural pattern within the same gyrus. These results imply that for each individual cat the suprasylvian gyrus has, within a narrow range, an approximate width that represents a stable parameter for that cat. The mean width of five intact gyri at each millimeter interval is shown in Table 1. No significant differences were found between the mean widths at the different millimeter intervals for all the gyri measured. The stability of this parameter around a mean width is shown graphically in Fig. 11. It is therefore suggested that it would be appropriate to refer to a mean approximate width to describe the mean for the gyrus width from several different cats. By this suggestion, then, the suprasylvian gyrus in each individual animal has an approximate width while there is a mean approximate width of

gyrus for a population of animals. It must, therefore, be noted that no single absolute measurement in the width of this gyrus can be considered as an exact representative for the same gyrus or any other gyrus in other cats. This circumstance was not taken into account by various earlier investigators from the classical descriptive period.

An analysis of cortex depth in the intact suprasylvian gyrus leads to similar conclusions to those just described for intact gyrus width. The difference found between the deepest cortex in one cat and the shallowest intact cortex of another cat was 805 microns (70% difference). This difference in cortex depth between the two compared gyri was statistically significant ($p \leq 0.001$). No significant differences were found in cortex depth between the depths at each millimeter interval within the same gyrus. Also, no significant differences in mean cortex depth were found between each millimeter interval in the mean of 5 intact left and homotopic gyri (Table 1). It must therefore be concluded that the depth of the cerebral cortex in the suprasylvian gyrus for each individual cat should be represented only by its own approximate depth. Similarly, in referring to a population of gyri, a mean approximate depth must be considered as representative for the gyri. These conclusions are in agreement with an earlier study by Sholl (1953, 1956) on the visual cortex in cats. In Sholl's study the brains

from 12 cats were perfused with formol saline and subsequently embedded in paraffin. Sholl stated that it is probably expedient to consider the relative, rather than the absolute, depth of the individual animal's cortex.

The mean values of cortex depth and gyrus width were plotted against each other (Fig. 11). No simple relationship exists between these two parameters. These results are of particular interest in that they demonstrate the presence, in the cerebral cortex, of two separate parameter determining mechanisms; one mechanism influences the extent of gyrus width while the other the extent of cortex depth. The extent of gyrus width might very well be related to a foetal mechanism that determines the formation of gyrencephalism by invaginating the closely investing pia mater. The extent of cortex depth would appear to be related to those specific mechanisms associated with the histogenesis (neuronal, neuroglial and vascular) of the cerebral cortex. Although both these mechanisms are exerted initially during the developmental stage it seems most reasonable to assume that these mechanisms are not necessarily interdependent. In considering the stabilization of both parameters in each gyrus it is apparent that each mechanism bears uniform influences throughout the length of the gyrus.

The depth of cortex in acute slabs was consistently less at the same locus than in the adjacent intact cortex within the same gyrus (Table 2). However, the results have shown that significant differences between the two compared depths occur only at the slab mid-region. These results have shown also (Figs. 18 and 19) that no appreciable difference in neuron population density occurs between the mid-region and terminal region in intact gyri. It can therefore be inferred that the significant loss of cortical depth in this region is attributable to cortical shrinkage after the effects of surgical trauma in a region of greater cerebral capillary density.

In the procedures used in this study the posterior drainage hole, which extends from the pia mater to the lateral ventricle, can be expected also to contribute to the partial deformation of the gyrus with an acute slab.

It is reasonable to assume that the escape of ventricular cerebrospinal fluid would enter the undercut lesion and lift the entire neuronal slab. An examination of Plates X and XI would tend to substantiate this conclusion. The cerebrospinal fluid would also contribute to the extensive cyst formations found within the undercut lesion.

The width of the acute slab at its lowest depth within the cortex was found to be consistently narrower than its subpial width (Table 2, columns 1 and 5). The analysis of that data, provided in the previous section, has indicated that the two side cuts of the slab were almost parallel to each other at the time of their preparation. This significant loss of width, which was confined to the slab base, would thus suggest that the investing pia mater contributes, in some degree, to the structural integrity of the cerebral cortex. The loss of perivascular fluid and collapse of blood vessels at the site of the side cut suggest that either bilateral compression or tissue shrinkage had taken place. The results have shown that neuron population density was not increased in the lower cortical segments in acute slabs. Had there been a significant increase in population density then a compression mechanism would have been indicated as more likely than shrinkage. The adjacent intact cortex in the same gyrus did not exhibit the same degree of volume loss as that found within the slab (Table 2, column 4). This area of intact cortex maintained a vascular supply from three different sources: a) dorsal pial blood vessels, b) pial blood vessels from the adjacent sulcus, c) collateral capillarization from the underlying white matter. Vascular supply within the acute and chronic slabs were maintained from only one source, the dorsal pial blood vessels.

The anterior and posterior ends of the acute slabs did not exhibit any appreciable loss in subpial width relative to the middle regions of the slab. This was in contrast with the significant loss in subpial slab width found at the ends of chronic slabs (Tables 2 and 3). Any attempt to explain these differences must consider two mechanisms: a) fluid flow of cerebrospinal fluid along the pathway of the undercut lesion and b) the accumulation of a congealed mass of haemorrhagic exudate. It has been noted in an earlier section that the contents of the cyst formations in acute slabs contained a mixture of clear fluid and blood cells. It seems most likely that congealed exudate accumulated at the ends of the slab would provide some measure of protection against an excessive fluid loss and shrinkage. It is therefore possible that these protective measures were not encountered equally at the pial surface and at the base of the cortex in the acute slab. One possible explanation for this is that the intima pia of the pia mater contributes to the structural integrity in this area of the cortex where shrinkage is also evident.

Long term chronic isolation of cortical slabs was characterized by a structural pattern of bilateral and dorsoventral reductions in size when compared to short term (acute) isolation (Tables 2 and 3). The large surface area of exposed ends of blood vessels would naturally lead to an area of great shrinkage. Chronicity

was also associated with cyst formations which had surrounded the apex of the slab. These cysts were now acellular and had contained a clear fluid. It can therefore be concluded that extensive phagocytosis had taken place along the side walls of the slab.

The greatest change in the width of chronic slabs occurred at the posterior region (Fig. 14 and Table 3). The analysis of the data suggests that the cortical tissue surrounding the posterior drainage hole had collapsed into the area of the hole. It should also be noted that the neuron population density in the posterior region of chronic slabs showed a pronounced tendency to be decreased with respect to the mid-region of the slab (Fig. 30). This falloff in the number of neurons can be expected to contribute to the reduction in slab dimension. Therefore, there seems no reason to believe that the mechanisms which influenced fluid loss at the posterior region were any different from those which influenced the rest of the slab.

Beritoff (1965) reported that cats with bilateral ablation of the suprasylvian gyrus suffered a distinct loss of spatial orientation. With Beritoff's technique no part of either suprasylvian gyri was left in neuronal communication with the rest of the CNS. The approximate dorsal surface area of the gyrus, without the sulcal region, may be estimated from surface topography to be approximately 25 mm x 8 mm or approximately 200 mm². In

this present study the extent of chronic isolation encompassed a surface area approximately 20 mm x 6 mm or approximately 120 mm². Thus, in the animals used to obtain the data for this thesis, some 30-35 percent of the gyrus on the operated hemisphere was left intact and in neuronal communication with the rest of the CNS; the contralateral gyrus was totally intact. It is interesting that the ablation produced by the isolation procedures was insufficient to cause any discernible loss of spatial orientation or of sensory awareness in the operated animals.

Surface stimulation of the intact suprasylvian gyrus in the cat has been reported to be associated with a rage response (Kaada, 1951). In the present study chronic isolation of the gyrus did not appear to affect the usual placid or timid character of the cats.

Association tracts running from the ectosylvian gyrus to the suprasylvian gyrus have long been established. Recently, association tracts from the visual cortex and geniculate nuclei have been reported by Wilson and Cragg (1967), Wilson (1968) and Dubner and Brown (1968). In the cats studied here no obvious loss of hearing or sight, nor inability to perceive simple sounds, could be discerned in the cats with chronic neuronal isolation.

2. NEURON POPULATION DENSITY

Earlier studies on cytoarchitectonics (cf. literature review) reported that the thickness of the cerebral cortex varied considerably from one gyrus to another within the same individual. Indeed, the data from the present study has shown that small, though statistically not significant, differences in cortical thickness occur normally along the length of an individual gyrus. Sholl (1959), in a study on neuron population densities in the cerebral cortex of mouse, cat and human, took into account the varied cortical thickness in different individuals of the same species. The cortex, with the exception of the subpial neuron-free zone, was divided into ten strips of equal depth. The neuron density was then calculated for each area of relative depth. No corrections were made for cortical shrinkage caused by the histological procedures. The neuron population density in the cat cruciate gyrus can be calculated from Sholl's published data (1959) and was compared with the results obtained in the present study. Sholl's results on density studies must be considered in relation to those specific techniques that he employed. His calculated neuron population density for the upper cortical half of the cruciate gyrus was approximately $21,000/\text{mm}^3$. In this present study the calculated density for a comparable area of intact cortex in the supra-

sylvian gyrus was approximately $16,000/\text{mm}^3$ (calculated from Figs. 20 and 21). The density given by Sholl for the lower cortical half of the cruciate gyrus was approximately $15,000/\text{mm}^3$; in the results the comparable area in the intact suprasylvian gyrus was approximately $21,500/\text{mm}^3$. Sholl reported also on density studies for the cat visual cortex. His data showed that the neuron packing density in the upper cortical half was approximately $40,000/\text{mm}^3$ and in the lower cortical half it was approximately $35,000/\text{mm}^3$. Sholl reported also that the neuron population density varied from section to section in the same region of a single brain. The data from Sholl's study and the present study are not necessarily in conflict with each other. No serious suggestion has ever been made in the literature that the neuron population densities for all gyri in the same individual or in different individuals of the same species must be the same. Therefore it may be suggested that the calculated neuron population densities expressed in the present study lie within an acceptable range.

It has been largely established in the literature that the cat visual cortex is purely "sensory" while the cruciate gyrus is "sensori-motor". In contrast, the suprasylvian gyrus has been variously described as an association area, a determinant area for spatial orientation, an area which when electrically stimulated pro-

duced a rage response, and finally as a "silent area" (cf. literature review). It may therefore be possible that variations in neuron population density, as an anatomical characteristic, are in some way correlated with the variations of physiological responses.

Ramon-Moliner (1961) studied the neuron population density in the cat postcruciate gyrus. He divided the cortical depth into 20 equal strips and clearly demonstrated the necessity of taking into account a tissue linear shrinkage factor as well as shrinkage factors for perikarya both in neurons and in neuroglia. The present study, which did not calculate shrinkage factors, does not infer that the actual neuron population density has been calculated. Rather, an aim of the present study is emphasized in that it provides a comparison for determining relative measures for neuron packing densities which are present in the three categories of brain tissue, a) intact cortex, b) acutely and c) chronically isolated cortex.

A self-sustaining mechanism which influences neuron population density appears to be present in cats' suprasylvian gyri. The individual differences in neuron population density in the various sections along the length of the gyrus are real and genuine. However, the analysis of the data showed that there were no significant differences in neuron population densities between upper cortical halves in any of the

following five types of gyri: intact left gyrus, intact right gyrus, acute left gyrus, acute homotopic right gyrus and the chronic homotopic gyrus. Neither were any significant differences found between the lower cortical halves in these same five types of gyri. The large differences in neuron population densities at different cortical depths in the same gyrus have been thoroughly analyzed and discussed in a previous section.

These results most strongly suggest that in the cat suprasylvian gyrus, irrespective of cortical volume, a mechanism exists which maintains distinctive patterns of neuron population density for specific areas in the cerebral cortex. There is a significant difference in neuron population density between the upper and lower cortical halves in all gyri of any one kind. Some specific mechanism must be responsible for this. Therefore, it is possible to suggest that this same mechanism results also in the maintenance of a basic density profile that is fundamentally operative along the length of the suprasylvian gyrus. The coupling of the above results with the conclusions just enunciated further suggests a plausible similarity in all of these gyri of an intracortical structural organization for the establishment of communication pathways.

Cajal (1928) noted that axotomy was associated with retrograde degeneration of neurons. It was considered of particular importance to ascertain, from an

analysis of the data in this study, whether there was any evidence of such degeneration in the neuron population density in the upper cortical half of chronically isolated slabs. Is axotomy or deafferentation, or a combination of both, the cause of a falloff in neuron population density? It is interesting to note that in chronically isolated cortex no significant differences were found in neuron population density between the lumped densities of the protected upper central cortical segments 1B + 2A and the adjacent non-protected segments 1A + 2B (Fig. 34). In order for axotomy to cause the death of the cell by means of retrograde degeneration the axon would have to be cut at a proximal point to the first collateral branch (cf. literature review). These results do not provide evidence in favor of retrograde degeneration by axotomy. The same results showed also that there were no significant differences in density between the upper protected segments of chronically isolated cortex and acutely isolated cortex nor between similar segments in chronically isolated cortex and the non-operated cortex. A similar lack of difference was found in comparisons between the traumatized upper cortical segments in the chronically isolated and in the acutely isolated cortex. However, there was a highly significant difference between chronic and intact cortex in the lumped neuron population densities of the unprotected segments 1A + 2B

($p \leq 0.001$; t-test for two samples). It should be noted, however, that the degrees of freedom "n" for the tests between chronic and acute were 26; the degrees of freedom "n" between chronic and intact were only 14, with 4 samples from 2 intact sections contributing to this test. That t-test included data from only 2 sections in that specific intact area and therefore some degree of reservation should be exercised in placing any reliance on that particular t-test. An analysis of the data in the chronically isolated cortex shows unmistakably a tendency towards a decrease in neuron population density in the upper cortical half with respect to acutely isolated slabs. However, the fact that this difference is not statistically significant is strongly suggestive that axotomy may not be the only causal relationship to the reduction of neuron density in this area. Evidence in favor of degeneration by axotomy would have likely resulted in a significant difference in neuron population density in the non-protected cortical segments as compared to the protected segments. This statement is substantiated further by the results from an analysis of the data in the lower cortical half.

The present study has demonstrated convincingly that only when there is extensive axotomy in chronically isolated slabs does the falloff in neuron population density reach a statistically significant level. The proof for this lies in the conclusions drawn from an

analysis of the data from the lower cortical half. No significant difference was found in the neuron population densities between the two lower cortical segments in all the non-operated gyri or between the two lower cortical segments in chronically isolated cortex. No significant difference was found in the lumped neuron population density of cortical segments 3 + 4 between non-operated intact cortex and acutely isolated cortex; a highly significant difference was found in density in lower cortical halves between chronic slabs and acute slabs. These results are suggestive of extensive axotomy. The results showed that a significant difference was always found in neuron population density between upper and lower cortical halves in the non-operated intact cortex as well as in the acutely isolated cortex. It is important to note that the results show also that even after long-term neuronal isolation in chronic slabs with extensive undercut axotomy a significant difference is still observed between the neuron densities in the upper and lower cortical halves. Therefore if axotomy had been a major factor in the falloff of neurons in the upper cortical half in chronically isolated slabs then the differences in neuron density between the upper and lower halves of the slab would have been greatly diminished. Axotomy contributes to a significant difference in neuronal density in lower cortical halves between short term and long term neuronal isolation periods.

Non-anatomical factors might be closely related to the neuron falloff in the upper cortical half of chronic slabs. An important physiological effect associated with the side-cut is the complete loss of extracortical afferent input following surgical deafferentation. In considering the manner in which surgical deafferentation and environmental deafferentation significantly affects dendritic density (cf. literature review), it is tempting to postulate that the loss of continuous afferent reinforcements may have less effect in a more chemically dynamic area of the neuronal perikaryon. Perikaryon chromophilia and chromophobia, which are the result of cytochemical factors, have been successfully used as an indicator of neuron activity (cf. literature review). It seems probable then that the result of surgical deafferentation would therefore contribute to a genuine though non-significant falloff of neurones in the upper cortical half of chronic slabs. The marked difference in electrical behavior between chronic slabs and acute slabs with regard to responses elicited from the upper cortical half might be attributed to a combination of changes in the pattern of humoral mediators and dendritic architecture. The development and maintenance of a neuron population density for specific areas of the brain that is species constant would appear to be interdependent, then, upon both genetic inheritance and constant physiological reinforce-

ment.

Some physiological mechanisms appear to influence the maintenance of density profiles at various sections along the length of acute and chronic slabs (Figs. 20 and 30). However, chronic slabs to some extent lose their profile at their posterior region. This area corresponds to the highly traumatized surgical drainage hole where the greatest neuron falloff can be expected to occur.

3. DISTRIBUTION of DENDRITE DENSITY

The greatest decrease in dendrite density following neuronal isolation was found to occur in the upper cortical half of the slab. In contrast, this is where the least change in neuron population density occurs. It must be concluded, therefore, that the reduction in dendrite density is a result due primarily to the neuronal isolation itself, and not necessarily related to degenerative changes in the neuronal somata. Corroborative evidence for this conclusion may be found in the following results of other physiological and anatomical studies.

Several detailed studies on dendrite density in cerebral cortex were reported by Bok (1936, 1959), Sholl (1953, 1955, 1956) and Ramon-Moliner (1961). Sholl was able to conclude from his studies that in pyramidal cells of motor and visual cortex there was no simple relationship between the total number of a neuron's dendrites and the depth of its soma below the surface of the pia. He was able to show that neuronal somata which were situated deeply in the cerebral cortex did not have fewer branches or shorter dendrites than neurons found in the upper area of the cortex. Sholl (1956) rejected a hypothesis by Bok that there is a constant number of dendrite branch points at any given radial distance from the soma of large pyramidal neurons (Bok, 1936, 1959).

The studies of Ramon-Moliner (1961), which have shown the presence of three peaks of dendrite density in the cat's postcruciate gyrus, are discussed in a subsequent section of this thesis.

In the present study chronic slabs showed only slight evidence of cytoarchitectonic disorganization of its layers while no discernible disorganization was evident in the intact or acutely isolated preparations. As a result the analysis of dendritic trees in all three types of preparation was a representative sample of most types of pyramidal neurons which are normally found in cortical layers.

An analysis of the data on dendritic density per tree zone in the three types of preparation might, from the argument put forward at the beginning of this subsection, reasonably be expected to demonstrate changes in the neuron's afferent pathway. The largest dendritic density per tree zone in intact and acute gyri were found in neurons whose somata were situated in the upper cortical quadrants. No significant differences in dendrite densities were found between each of the quadrants. It seems reasonable to suppose, then, that there must have been little difference in the amount of afferent input to the neurons in each of the quadrants in the intact preparation. A comparison between dendrite densities in the upper quadrants of intact cortex and of chronically isolated cortex showed a highly significant reduction of

dendrite density in the chronic preparation. These results indicate a marked reduction in afferent flow into the chronic cortex. The consideration of dendritic spine density, which follows in the succeeding subsection, provides further evidence that the extent of reduced afferent flow is in proportion to the statistically significant loss of dendritic density.

The analysis of the data in Table 5 shows that chronic slabs have neurons with similar dendrite densities in all four cortical quadrants. This factor would tend to equalize the likelihood of impulses travelling with equal facility between upper and lower regions in the chronic slab. This might be related to the ability of the chronic slab to sustain very long lasting epileptiform afterdischarges (Grafstein and Sastry, 1957; Sharpless and Halpern, 1962; Pinsky, Halpern, personal communication). Electrical models of neurons with branching dendritic trees show that there will be less decrement in the conduction of subthreshold activity from the dendritic periphery to the soma in those neurons which have least branches (Pinsky, 1967--Bremer Meeting). Both these structure-function relationships can possibly account, in part, for the fact that chronically isolated cortex responds to strong electrical stimulation with epileptiform afterdischarges which can last for several hours. This response contrasts with the afterdischarges of only 10 second duration which can be induced in acutely

isolated cortex with a greater dendritic density.

The results on the falloff in dendrite density are in accord with other studies on the morphology of pyramidal trees. Mungai (1967), in a study of dendritic trees in pyramidal neurons, reported that the stem zone had 9 percent of the total, the branching zone had 36 percent of the total and the terminal zone had 55 percent of the total number of dendrite sections in the neuron. Jones and Thomas (1962) have shown that surgical deafferentation results in a significant loss of dendrite sections from the peripheral areas of the tree without any reduction of dendrite sections from the stem zone.

4. ANGULATION at BRANCH POINTS

It has been shown in these studies that the chronically isolated slab undergoes partial rotation of the apex (p. 228). Definitive evidence was presented to show that such rotation of the slab affected the geometric plane of apical dendritic trees. A significant difference in the mean angulation was found between corrected angles of dendrites in intact cortex and chronic slabs. The dendrite branches in chronic slabs run closer to the main axis of the apical shaft than in intact cortex and acutely isolated cortex. The two factors of a loss in dendritic density and smaller angulation in chronic slabs would tend to confine electrotonic excitatory stimuli between upper and lower regions of the slab.

5. DENDRITIC SPINE DENSITY

Dendritic spine density is regarded as a relative and quantitative measure of the neuron's afferent input (cf. literature review). Spine density is known to be highest in branching and terminal zones of dendritic trees and least in the stem zone. Reduction of spine density by environmental deprivation as a type of deafferentation has already been thoroughly dealt with in the literature review. It was therefore not surprising to find that, in the present study, the surgical deafferentation consequent on neuronal isolation had significantly reduced spine density in the outer zones of dendritic trees in unstimulated slabs. It is of considerable interest that a significant increase in spine density was found in stimulated slabs when compared to non-stimulated cortex. It would appear that those structural components which form the main afferent pathway in a neuron require repetitive reinforcement for their maintenance. On the other hand an increase of exogenous electrical activity which is probably far greater than that resulting from normal physiological drive results in an endogenous growth stimulus or factor which increases spine density. These results would appear to be in agreement with the findings of Marin-Padilla (1967). He reported that apical dendritic spine density in motor neurons increased in the newborn human being in amounts

which roughly corresponded to an increase in the infant's awareness and motor discharge.

6. DENDRITE WEDGES

An examination of drawings made by Cajal on dendritic trees will show clearly that the occasional dendrite section has a V-shaped wedge. Camera lucida drawings made during the course of studies by several other neurohistologists of the classic school have also demonstrated the presence of dendritic wedges. Ward (1961) proposed a theory that chronic depolarization of dendrites could be initiated by dendritic wedges. Ward presumed that the wedges observed in his study were formed by the direct action of lesions which were induced by aluminum hydroxide.

The tendency towards a reduction in the number of wedges per dendrite tree in chronic slabs seems to be intimately related to the rotation of the slab around its apex. Alterations to the dendritic geometric domain would appear to affect the structure of the wedge.

It is postulated that angular redirection of dendrites beyond the wedge structure is indicative of toxic factors that may be found in the subpial region. Extreme examples of this possibility may be seen where the dendrite section follows the periphery of a blood vessel and then resumes its original course (Plate XXII).

7. BASILAR DENDRODENDRITIC PATHWAYS

Quantitative histological pathways of basilar dendrites from cortical pyramidal cells were studied by Lorente de No (1934), Sholl (1953), Bok (1959) and Ramon-Moliner (1961). Lorente de No observed that branches of apical shafts and basilar dendrites were short and generally horizontal in their direction. He reported also that some basilar dendrites from Layer III pyramidal perikarya descend into Layer IV. Basilar dendrites from pyramidal neurons in Layer IV reach down to the lower limit of Layer IV but never reach Layer V. Lorente de No reiterated Cajal's observations that Layer V basilar dendrites remained exclusively within the vertical range of Layer V. In J.F. Fulton's authoritative textbook "Physiology of the Nervous System" (3rd Ed. 1949, pp. 274-301) Lorente de No concluded that dendrites "fractionate the vertical section of the cortex into several strata of more or less horizontal dendrites crossed by vertical shafts".

Dendritic horizontal lamination in the cat cortex was analyzed by Ramon-Moliner (1961) who reported that dendritic densities occur in three peaks. The first peak was found to occur in the subpial region; the second peak, which was due to basilar dendrites, was found in Layer V; the third peak was due to horizontal dendritic plexuses of spindle cells and was deeply situated in the cortex.

He noted, however, that a very small number of dendrites do leave the level of Layer V.

Sholl (1953) reported that basilar dendrites of one pyramidal cell could possibly spread over a cortical area which would contain between 2,000 and 4,000 perikarya. In a literature review by Ramon-Moliner (1961) on the importance of dendritic distribution Van der Loos (1956) was reported to have demonstrated that dendrodendritic synaptic junctions occurred only at regular distances from the perikaryon. The maximum neuronal communication possible via basilar dendrites would therefore be a certain percentage of the area encompassed by the basilar spread.

Colonnier (1966, 1967) presented evidence from studies on axodendritic contacts to show an anatomical correlate of the physiological columns previously described in sensory cortex by Mountcastle (1957) and Hubel and Wiesel (1962), and in motor cortex by Hubel and Wiesel (1965). The basilar dendrodendritic circuits described in this study would thus provide a columnar dendritic pathway for physiological reinforcement of those afferent columns described by Colonnier.

The demonstration of functional basilar dendrodendritic pathways would tend to establish new principles of neurophysiological significance. Basilar pathways between two neurons in the same layer or between two neurons of different layers would increase the number of neurons and processes lying within the reach of the

receptive field of one neuron. This would tend to contribute to the pluripotential capabilities of a single cortical neuron. A basilar dendrodendritic circuit that would consist of two dendrites would also establish the concept of afferent dendrites which are physiologically antidromic within the cerebral cortex.

8. TRIFURCATED BRANCH POINT

The development of the human telencephalon in the first few months of gestation is characterized by surfaces which are both smooth and non-convoluted (Truex and Carpenter, 1964). Rapid growth of the cerebral hemispheres during the sixth and seventh months of gestation results in the development of surface involutions which develop convoluted gyri, shallow sulci and deep furrowed fissures. It would be reasonable to postulate that the gyrencephalic brain of the cat develops also in a similar way.

A malformed intact suprasylvian gyrus in which the gray matter had developed only along the lateral regions of the gyrus was observed (Plate XXVII). In this abnormal cortical region an apical dendritic shaft was noted to bear a trifurcated branch point (Plates XXVIII and XXIX).

Several theories, some teleological in thought, might be offered to explain the function of a trifurcated branch point in a malformed cerebral cortex. An increased number of dendrites in an area marked by a low density of neuronal perikarya would have the net effect of increasing the functional load of each trifurcated neuron to accommodate the afferent input. A trifurcated neuron may demonstrate plasticity of form in order to meet a specific functional requirement.

9. STRUCTURAL REGRESSION OF CHRONIC SLABS

The development of spontaneous activity in the neocortex of the newborn kitten was studied by Grossman (1955). He observed that the spontaneous activity recorded at the cortical surface at birth does not exhibit spiking or rhythmic oscillations; at 5 days of age oscillations with a few very low-level spikes occur at the rate of 6 to 7 per second. At 13 days of age the spontaneous activity of the neocortex exhibits low level spikes followed by large smooth waves which occur at a frequency of 1 to 1.5 per second. The 10 week old kitten, in contrast, develops a self-sustaining spontaneous activity which consists of rapid and repetitive spikes with only intermittent small waves. The unstimulated chronically isolated cortex in the adult cat shows spontaneous activity in surface recordings, which consists of intermittent spiking, followed by slow waves and short bursts of high frequency activity (Sharpless and Halpern, 1962; Vasquez, Krip and Pinsky, 1969). This spontaneous activity in the chronic slab of the adult cat thus resembles that seen in the immature cortex of the neonate kitten.

The histogenesis of the suprasylvian gyrus was studied by Conel (1947). He reported that the larger neurons in the lower cortical half develop earlier than the smaller neurons in the upper cortical half. The

development of cortical spontaneous activity characteristic of the adult cat thus coincides with extensive growth and development of dendritic arborization patterns with interneuronal connections (Grossman, 1955).

An epileptogenic area within the cortex shows cellular destruction that has regressed histologically and physiologically to the immature cortex (*ibid.*). The three peaks of dendritic density at different cortical depths in adult cerebral cortex, as reported by Ramon-Moliner (1961), would therefore be lacking within the epileptic focus. This is consistent with the finding in the present study that chronically isolated slabs, known to be epileptogenic, showed no significant differences in dendritic density between upper and lower cortical halves.

It is therefore postulated that the structural regression of chronic slabs to primal histological features is correlated with the slab's regression of spontaneous activity to the level of the immature cortex.

SUMMARY

As early as the latter part of the 19th century Franz Nissl initiated the technique of the undercut cerebral cortex in an attempt to find correlations between histomorphology and function in this type of tissue. Further studies by Cajal and others have since given detailed descriptions of chromatolysis, axon-collateral sprouting and changes in cytoarchitectonics that result from neuronal isolation. The techniques used in the aforementioned studies were extended and applied to the present correlative study.

All neurohistological tissues used in this study were prepared from 32 adult cats of either sex. A modification of Mallory's (1938) version of Golgi's Rapid Method was especially developed for the quantitative and qualitative measurements made in this study. Coronal serial sections 50 microns in thickness were made of the entire length from suprasylvian gyri from intact gyri, and from gyri in which an acutely isolated and chronically isolated slab had been prepared.

The quantifiable parameters of gyrus width and cortex depth were measured from coronal sections from five intact left and homotopic gyri. No significant differences were found between the mean dimensions at

each millimeter interval throughout the lengths of the gyri. These results imply that for each individual cat the suprasylvian gyrus has, within a narrow range, an approximate width and an approximate cortex depth, that represents a stable parameter for that cat. No simple relationship was found to exist between cortex depth and gyrus width. The depth of cortex in the acutely isolated slab was always shallower at the same locus than the adjacent intact cortex within the same gyrus. A paired comparisons test showed that chronic isolation causes a significant ($p \leq 0.001$) reduction in gyrus width in the gyral region alongside the isolated area. The mean cortex depths of six chronic slabs were always shallower at the same locus than that occupied by the adjacent intact cortex within the same gyrus. Significant differences (p ranging from ≤ 0.01 to ≤ 0.001) were found by paired comparisons test between the compared cortex depths. These results indicate that long term neuronal isolation by surgical techniques employed in the present study significantly reduced the volume of the isolated cerebral cortex.

A significant difference ($p \leq 0.01$) was found to exist in neuron population density between the upper and lower cortical halves for each of the three types of tissue examined. However, in each type of tissue no significant differences in neuron population densities

were found at each 2 mm interval section. No significant differences in neuron density were found in the upper cortical halves between intact gyri, acute and chronic slabs. However, a highly significant difference ($p \leq 0.001$) in neuron population density in lower cortical halves was found between chronic and acute slabs. These results demonstrate convincingly that the significant reduction in neuron population density in the lower cortical half of chronic slabs was caused by extensive axotomy.

The analysis of apical dendrites showed that in intact gyri and acute slabs the largest dendritic density was found in those neurons whose soma was situated in the upper cortical halves. A t-test for two samples showed a highly significant difference ($p \leq 0.001$) in dendrite densities between intact gyri and chronic slabs. In chronic slabs the neurons in the upper and lower cortical halves had essentially similar dendrite densities. This factor would tend to equalize the likelihood of impulses travelling with equal facility between upper and lower regions in the chronic slab.

An ocular goniometer was used under direct microscopic observation to measure angles at branch points. A trigonometric correction factor was used to convert the observed angle to the real angle when the two dendritic arms were not in the same plane of focus. Paired comparison tests in intact gyri and acute and chronic

slabs showed that no significant differences in angulation exist between the upper and lower parts of the cortex in each type of preparation. A paired comparison test was made between corrected and uncorrected angles in intact gyrus, acute and chronic slabs. No significant differences were found in the intact gyrus and acute slab. However, a highly significant difference was found in the chronic slab ($p \leq 0.001$). Dendrite branches in chronic slabs run closer to the main axis of the apical shaft and would tend to confine electrotonic excitatory stimuli between upper and lower regions of the slab.

The spine density was expressed as the number of observable dendritic spines found per micron length of dendrite section. The least spine density was found in the stem zone while the largest spine density was consistently found in the branching zone. No significant differences in spine densities were found in the three homotopic preparations. A highly significant difference in spine density was found between terminal zones of lower neurons in unstimulated intact left gyri and electrically stimulated left acute slabs ($p \leq 0.001$). The significant increase in spine density in stimulated slabs would appear to have activated an endogenous growth stimulus or factor which influenced spine development.

New observations. The present study has presented several observations which form the basis of this author's claims to originality; these are as follows:

- (1) A modification of Golgi's Rapid Method was developed for this work. The resulting technique has enabled a study to be made of qualitative and quantitative parameters from serial sections taken continuously from the entire length of the suprasylvian gyrus in the adult cat brain.
- (2) The histomorphology of the suprasylvian gyrus in adult cats, Felis domestica (Linnaeus, 1758), may vary widely with respect to cerebral cortical histology between adjacent sulci.
- (3) The gyral width and depth along the entire length of the suprasylvian gyrus is relatively constant for any individual cat and represents a stable parameter for that cat.
- (4) Chronic neuronal isolation after surgical procedures results in a significant loss of cortical volume with a consistently observable twisting of the slab's apex.
- (5) In chronically isolated cortical slabs the depth of slab cortex is significantly less than that of the adjacent intact cortex lying within the same gyrus.
- (6), Dendritic bulbous dilatations on apical terminal dendrites appear to be artifacts of histological processing procedures. No evidence was found to substantiate the claim that they form regular cytological features of dendrites.

- (7) The neuron population densities at similar cortical depths throughout the length of intact gyri and acute slabs between two closely spaced sections seem to show differences, but these are not statistically significant.
- (8) A tendency towards a reduction in neuron population density was observed in those areas of chronic slabs which were protected from axotomy and anoxia.
- (9) Short term neuronal isolation--12 hours--results in a tendency towards a reduction in dendrite density of apical arborization trees.
- (10) In chronically isolated slabs the neurons in the upper and lower cortical halves had essentially similar dendrite densities.
- (11) Chronic neuronal isolation results in a reduction in angulation at dendritic branch points so that the dendrite branches run closer to the main axis of the apical shaft.
- (12) Electrical stimulation of acutely isolated slabs resulted in a statistically significant increase in dendritic spine density when compared to non-stimulated slabs. * (see reference p. 295)
- (13) Dendrodendritic pathways can apparently occur between pyramidal neurons via their basilar dendrites. One such possible pathway extended between two neurons whose somata lay in Layer III; another such pathway extended between Layer III and Layer V somata.
- (14) Structural regression of chronic slabs to primal

histological features is correlated with the slab's regression of spontaneous activity to the level of the immature cortex.

* Since the publication of this thesis, Schapiro and Vukovich (Science, Jan. 16, Vol. 167, 1970) reported their observations on the effects of increased sensory experience on the dendritic spine density in infant rats. Dendritic spine density was significantly increased in the environmentally stimulated rats when compared to non-stimulated rats of the same age group. It was postulated that the increase of afferent input had a direct effect upon the development of dendritic spines. The results reported by Schapiro and Vukovich appear to confirm the findings in the present study. Exogenous electrical stimulation, as a method of increasing afferent input to the brain, significantly increases dendritic spine density.

BIBLIOGRAPHY

- ABERCROMBIE, M. (1946). Estimation of Nuclear Population from Microtome Sections. *Anat. Rec.* 94: 239-247.
- AGDUHR, E. (1941). A contribution to the technique of determining the number of nerve cells per unit of tissue. *Anat. Rec.* 80: 191-202.
- ALPHEN, G.W.H.M. van. (1945). Kernmetingen in de Neocortex van de Mens. Leiden, Ijdo.
- AITKEN, J.T. and J.E. BRIDGER (1961). Neuron size and neuron population density in the lumbosacral region of the cat's spinal cord. *J. Anat.* 95: 38-53.
- ALTSCHUL, R. (1938). cited by Hyden. *Arch. Pathol. Anat. u. Physiol. Virchow's.* 301: p. 273.
- ALZHEIMER, A. (1910). cited by Hyden. *Histol. u. histopathol. Arb. Grosshirnrinde* 3: p. 401.
- AMANO, S. (1957). The structure of the centrioles and spindle body as observed under the electron and phase microscope. A new extension-fibre theory concerning mitotic mechanism in animal cells. *Cytologia*, 22: 193-212.
- APATHY von S. (1897). Das leitende Element des Nerven-systems. *Mitt. a.d. Zool. Stat. in Neapel.* 12: p. 495.
- AREY, L.B. (1965). Developmental Anatomy. Philadelphia: Saunders.
- BAILEY, P. and G. von BONIN (1951). The Isocortex of Man. University of Illinois.
- BAILLARGER, J.G.F. (1840). Recherches sur la structure de la couche corticale des circonvolutions du cerveau. *Mem. Fac. Med. Paris.* 8: 149-183.
- BARDEEN, C.R. (1903). The growth and histogenesis of the cerebrospinal nerves in mammals. *Am. J. Anat.* 2: p. 231.

- BARKER, L.F. (1899). The Nervous System and its Constituent Neurons. New York.
- BARKER, L.F. (1901). Histology of Brain. Reference Handbook of the Medical Sciences. 2: 322-365.
- BARR, M.L., BERTRAM, L.F. and H.A. LINDSAY (1950). The morphology of the nerve cell nucleus according to sex. Anat. Rec. 107: 283-297.
- BARTELMEZ, G.W. and H.M. EVANS (1926). Development of the human embryo during the period of somite formation, including embryos with 2 to 16 pairs of somites. "Contr. Embryol.", No. 85. Carnegie Inst. Washington.
- BEHEIM-SCHWARZBACH, D. (1955). cited by Hyden. J. Hirnforsch. 2: p. 1.
- BENDA (1898). Mitochondria. Cited in The Cell (1951), by C. Swanson. Philadelphia: Saunders.
- BENSLEY, R.R. (1951). Facts versus artifacts in cytology; the Golgi apparatus. Ex. Cell Res. 2: p. 1.
- BENSLEY, R.R. and HOERR, N.L. (1934). cited by De Robertis. Anat. Rec. 60: p. 251.
- BERGER, H. (1921). Untersuchungen uber den Zellgehalt der menschlichen Grosshirnrinde. Z. ges. Neurol. Psychiat. 69: 46-59.
- BERITOFF, J.S. (1965). Neural Mechanisms of Higher Vertebrate Behavior. Boston: Little, Brown.
- BETHE, A. (1903). Allgemeine Anatomie und Physiologie des Nervensystems. Leipzig: Thieme.
- BETHE, A. and FLUCK, M. (1937). cited by Hyden. Z. Zellforsch. u. mikroskop. Anat. 27: p. 211.
- BIELSCHOWSKY, M. (1904). Die Silberimpragnation der Neurofibrillen. J. Psychol. u. Neurol. 3: p. 169.
- BIELSCHOWSKY, M. (1928). Handbuch der mikroskopischen Anatomie des Menschen. Vol. IV. Berlin: Springer.
- BIELSCHOWSKY, M. and GALLUS (1913). cited by Cajal. Degeneration and Regeneration. Cajal (1928). London: Oxford.

- BISHOP, G.H. and J.M. SMITH (1964). The Sizes of Nerve Fibres Supplying Cerebral Cortex. *Ex. Neurol.* 9: 483-501.
- BLOOM, W. and D.W. FAWCETT (1965). Textbook of Histology. Philadelphia: Saunders.
- BODIAN, D. (1936). A new method for staining nerve fibres and nerve endings in mounted paraffin sections. *Anat. Rec.* 65: 89-97.
- BODIAN, D. (1937). The staining of paraffin sections of nervous tissue with activated Protargol. The role of fixatives. *Anat. Rec.* 69: 153-162.
- BODIAN, D. (1942). Cytological aspects of synaptic function. *Physiol. Rev.* 22: 146-169.
- BODIAN, D. (1962). The generalized vertebrate neurone. *Science* 137: 323-326.
- BODIAN, D. (1966). Synaptic types on spinal motoneurons: an electron microscopic study. *Bull. J. Hopkins Hosp.* 119: 16-45.
- BOK, S.T. (1929). Der Einfluss der in den Furchen und Windungen auftretenden Krümmungen der Grosshirnrinde auf die Rindenarchitektur. *Z. ges. Neurol. Psychiat.* 121: 682-750.
- BOK, S.T. (1934). A quadratic relation between the volumes of the nucleus and body of ganglion cells of different sizes. *Psychiat. Neurol. Bladen*, 38: 318-325.
- BOK, S.T. (1936a). A quantitative analysis of the structure of the cerebral cortex. *Proc. Kon. Ned. Akad. Wetenschap, Afdel. Natuurk, Sect. II.* 35: 1-55.
- BOK, S.T. (1936b). The branching of the dendrites in the cerebral cortex. *Proc. Kon. Ned. Akad. Wetenschap.* 39: 1209-1218.
- BOK, S.T. (1939b). Cephalization and the boundary values of the brain-and body sizes in mammals. *Proc. Kon. Ned. Akad. Wetenschap.* 42: 515-525.
- BOK, S.T. (1939b). A method of measuring the surface of a body from a series of parallel sections. *Acta. Neerl. Morphol.* 2: 280-292.

- BOK, S.T. (1959). Histonomy of the Cerebral Cortex. Amsterdam: Elsevier.
- BOK, S.T. and M.J. KIP (1939a). The size of the body and the size of the cerebral cortex. Acta. Neerl. Morphol. 2: 293-321.
- BOK, S.T. and M.J. KIP (1939b). The size of the body and the size and the number of the nerve cells in the cerebral cortex. Acta. Neerl. Morphol. 3: 1-22.
- BONNIN, G.V. (1950). Essay on the Cerebral Cortex. Springfield: Thomas.
- BOYCOTT, B.B., E.G. GRAY and R.W. GUILLERY (1961). Synaptic structure and its alteration with environmental temperature: a study by light and electron microscopy of the central nervous system of lizards. Proc. Roy. Soc. 154: 151-172.
- BRACHET, J. and A.E. MIRSKY (1959). The Cell. ed. by Brachet and Mirsky. 5 vol. New York: Academic Press.
- BREEMAN, van V.L. (1961). Ultrastructure of the parietal cell of the human gastric gland. Anat. Rec. 139: p. 324.
- BREMER, F. (1935). Quelques proprietes de l'activite electrique du cortex cerebrale "isole". C.R. Soc. Biol. Paris. 118: 1241-44.
- BROCK, J.R. (1967). Neuronal Interaction in the epileptiform afterdischarge. M.Sc. Thesis. University of Manitoba, Winnipeg.
- BROCA, P. (1878). Anatomie comparee circonvolutions cerebrales. Le grand lobe limbique et la scissure limbique dans la serie des mammiferes. Rev. Anthropol. Ser. 2, 1: 384-498.
- BRODMANN, K. (1905). Bertraege zur histologischen lokalisation der Grosshirnrinde. J.F. Psychol. u. Neurol. 4: 177-226.
- BRODMANN, K. (1909). Vergleichende Lokalisationslehre der Grosshirnrinde in ihren Prinzipien dargestellt auf Grund des Zellenbaues. J.A. Barth. pp. 324.
- BRUNO, G. (1931). Sulla struttura e su alcune proprietate fisiche della fibra nervosa midollata. Arch. Ital. Anat. e Embrial. 29: p. 1.

- BUNGE, M.B., R.P. BUNGE and H. RIS (1961). Ultrastructural study of remyelination in an experimental lesion in adult cat spinal cord. J. biophys. biochem. Cytol. 10: 67-94.
- BURNS, B.D. (1949). Some properties of the cat's isolated cerebral cortex. J. Physiol. 110: p. 9.
- BURNS, B.D. (1950). Some properties of isolated cortex in the unanaesthetized cat. J. Physiol. 112: 156-175.
- BURNS, B.D. (1954). The production of after bursts in isolated unanaesthetized cerebral cortex. J. Physiol. 125: 427-446.
- BURNS, B.D. (1958). The Mammalian Cerebral Cortex. London: Arnold.
- CAJAL - see Ramon y Cajal, S.
- CAMPBELL, A.C.P. (1937). The relative vascularity of different areas of the mammalian brain. J. Ment. Sci. 83: 510-511.
- CAMPBELL, A.C.P. (1939). Variation in vascularity and oxidase content in different regions of the brain of the cat. Arch. Neurol. Psychiat. 41: 223-242.
- CAMPBELL, A.W. (1903). Histological studies on cerebral localization. Proc. Roy. Soc. Lond. 72: p. 488.
- CAMPBELL, A.W. (1905). Histological studies on the localization of cerebral function. Cambridge.
- CARLSON, A.J. (1902-03). Changes in the Nissl's substance of the ganglion and the bipolar cells of the retina of the Brandt cormorant Phalacrocorax pencillatus during prolonged normal stimulation. Amer. J. Anat. 2: 341-347.
- CASPERSSON, T. (1950). Cell Growth and Cell Function. New York: Norton.
- CHANG, H.T. (1955). Cortical response to stimulation of medullary pyramid in rabbit. J. Neurophysiol. 18: 332-353.
- CHOJA, N. (1936). cited by Hyden. Mitt. med. Akad. Kiota. 17: p. 18.

- CHOW, K.L., J.S. BLOOM and R.A. BLOOM (1950). Cell ratios in the thalamo-cortical visual system of Macaca mulatta. *J. comp. Neurol.* 92: 227-240.
- CLARE, M.H. and G.H. BISHOP (1955). Properties of dendrites; apical dendrites of the cat cortex. *Electroenceph. clin. Neurophysiol.* 7: 85-98.
- CLARKE, G. (1945). A simplified Nissl stain with thionin. *Stain Tech.* 20: 23-24.
- CLEMENTE, C.D. and W.F. WINDLE (1954). Regeneration of severed nerve fibres in the spinal cord of the adult cat. *J. Comp. Neurol.* 101: 691-732.
- COLEMAN, P.D. (1965). Effects of rearing in the dark on dendritic fields of stellate cells in visual cortex. A.A.A.S. Meeting at California.
- COLEMAN, P.D. and A.H. RIESEN (1968). Environmental effects on cortical dendritic fields. I Rearing in the dark. *J. Anat.* 102: 363-374.
- COLONNIER, M. (1964b). The structural design of the neocortex. Brain and Conscious Experience. Rome Meeting.
- COLONNIER, M. (1964). Experimental degeneration in the cerebral cortex. *J. Anat. Lond.* 98: 47-53.
- COLONNIER, M. (1966). Fine Structural Arrangement of the Cortex. *Trans. A. Neurol. Assoc.* p. 173.
- COLONNIER, M. (1967). The fine structural arrangement of the cortex. *Arch. Neurol.* 16: 651-657.
- COOMBS, J.S., J.C. ECCLES and P. FATT (1955). The electrical properties of the motoneurons membrane. *J. Physiol.* 130: 291-325.
- COWDRY, E.V. (1912). Mitochondria and other cytoplasmic constituents of the spinal ganglion cells of the pigeon. *Anat. Rec.* 6: p. 33.
- COWDRY, E.V. (1914). The comparative distribution of mitochondria in spinal ganglion cells of vertebrates. *Am. J. Anat.* 17: p. 1.
- COX, W.H. (1891). Impragnation des centralen Nervensystem mit Quecksilberzalzen. *Arch. Mikr. Anat.* 37: 16-21.
- CONEL, L.J. (1947). Cortex of the 3-month infant, in the postnatal development of the human cerebral cortex. Cambridge: Harvard U. Press. 3: p. 147.

- CRAGG, B.G. (1967). The density of synapses and neurones in the motor and visual areas of the cerebral cortex. *J. Anat.* 101: 639-654.
- DAVENPORT, H.A. (1960). Histological and Histochemical Technics. Philadelphia: Saunders.
- DAVID, G.B., A.W. BROWN AND K.B. MALLION (1961). On the identify of the 'neurofibrils', 'Nissl complex', 'Golgi apparatus' and 'Trophospongium' in the neurons of Vertebrates. *Quart. J. mic. Sci.* 102: 481-493.
- DEHLER, A. (1895). Bertrag zur Kenntnis vom feineren Bau der sympathischen Ganglienzelle des Frosches. *Arch. f. mikr. Anat. Bd.* 46: p. 724.
- DEL RIO HORTEGA, P. (1920). Neuroglia, in Progress in Brain Research. Vol. 15. Amsterdam: Elsevier.
- DEL RIO HORTEGA, P. (1943). Neuroglia, cited in Progress in Brain Research. Vol. 15. Amsterdam: Elsevier.
- DEMPSEY, E.W. (1956). Variations in the structure of mitochondria. *J. Biophys. and Biochem. Cytol.* 2: Suppl.4: 305-312.
- DE ROBERTIS, E. (1954a). cited by Hyden. *J. Histochem. and Cytochem.* 2: p. 341.
- DE ROBERTIS, E.D.P. and H.S. BENNETT (1954b). Submicroscopic vesicular component in the synapse. *Fed. Proc.* 13: p. 35.
- DE ROBERTIS, E.D.P. and H.S. BENNETT (1955). Some features of the submicroscopic morphology of synapses in frog and earthworm. *J. biophys. biochem. Cytol.* 1: 47-58.
- DE ROBERTIS, E. and F.H. RAFFO (1957). cited by De Robertis in Cell Biology 1966. *Exp. Cell Res.* 12: p. 66.
- DONALDSON, H.H. (1895). The Growth of the Brain. Chicago.
- DUBNER, R. and F.J. BROWN (1968). Response of Cells to Restricted Visual Stimuli in an Association Area of Cat Cerebral Cortex. *Ex. Neurol.* 20: 70-86.

- DUNNING, H.S. and H.G. WOLFF (1936). The relation between function and vascularity in the nervous system. *Trans. Amer. Neurol. Assoc.* 62: 150-154.
- DUNNING, H.S. and H.G. WOLFF (1937). The relative vascularity of various parts of central and peripheral nervous system of cat and its relation to function. *J. Comp. Neurol.* 67: 433-450.
- ECCLES, J.C. (1964). The Physiology of Synapses. New York: Academic Press.
- ECKLIN, F.A. (1959). The supersensitivity of chronically, partially isolated cerebral cortex as a mechanism in focal epilepsy and lobotomy. *A.M.C. Arch. Neurol. Psychiat.* 75: 659-660.
- ECONOMO, C. von and G.N. KOSKINAS (1925). Die Cytoarchitektonik der hirnrinde des erwachsenen Menschen. Berlin.
- EDINGER, L. (1908). Vorlesungen über den Bau der nervösen Centralorgane des Menschen und der Thiere. Leipzig: Vogel.
- EDSTROM, J.E. (1956a). cited by Hyden. *J. Neurochem.* 1: p. 159.
- EDSTROM, J.E. and D. EICHNER (1958b). cited by Hyden. *Z. Zellforsch. u. mikroskop. Anat.* 48: p. 187.
- EDSTROM, J.E. and H. HYDEN (1954). cited by Hyden. *Nature* 174: p. 128.
- EDSTROM, J.E. and A. PIGON (1958). cited by Hyden. *J. Neurochem.* 3: p. 95.
- EINARSON, L. (1951). On the theory of gallocyanin-chromalum staining and its application for quantitative estimation of basophilia. *Acta. Patholog. et Microbio.* 28: 82-102.
- EINARSON, L. and E. KROGH (1955). cited by Hyden. *J. Neurol. Neurosurg. Psychiat.* 18: p. 1.
- ELLIOTT, H.D. (1963). Textbook of Neuroanatomy. Philadelphia: Lippincott.
- ELLIOT-SMITH, G. (1902). The primary subdivisions of the mammalian cerebellum. *J. Anat.* 36: p. 381.

- ERNSTER, L. (1956). The enzymatic organization of mitochondria and its role in the regulation of metabolic activities in animal tissues. Diss. Almqvist and Wiksell, Uppsala.
- ESTABLE, C. and J.R. SOTELO (1951). cited by Hyden. Publ. inst. invest. cienc. biol. 1: p. 105.
- FARQUHAR and DE ROBERTIS (1963). Neuroglia, cited in Progress in Brain Research. Vol. 15. Amsterdam: Elsevier.
- FARQUHAR, M.G. and J. WELLINGS (1957). cited by Hyden. J. Neuropathol. Exptl. Neurol. 16: p. 18.
- FERNANDEZ-MORAN, H. (1950). Sheath and axon structures in the internode portion of vertebrates myelinated nerve fibres, an electron microscope study of rat and frog sciatic nerves. Ex. Cell Res. 1: 309-337.
- FERNANDEZ-MORAN, H. (1957). Electron microscopy of nervous tissue. In Metabolism of the Nervous System. 1956. Denmark: Pergamon.
- FERNANDEZ-MORAN, H. (1962). cited by De Robertis in Cell Biology 1966. Circulation 26: p. 1039.
- FINEAN, J.B. (1957). cited by Hyden. Acta. Neurol. Psychiat. Belg. 57: p. 462.
- FOREL, A. (1887). Einige hirnanatomische Betrachtungen und Ergebnisse. Arch. Psychiat. Nervenkr. 18: 162-198.
- FOX, C.A. and J.W. BARNARD (1957). A quantitative study of the purkinje cell, dendritic branchlets and their relationship to afferent fibres. J. Anat. 91: 299-313.
- FULTON, J.F. (1949). Physiology of the Nervous System. 3rd Ed. Philadelphia: Saunders.
- GATENBY, J.B. (1953). cited by Hyden. J. Roy. Microscop. Soc. 73: p. 61.
- GASSER, H.S. and H. GRUNDFEST (1939). Axon diameters in relation to the spike dimensions and the conduction velocity in mammalian A fibres. Am. J. Physiol. 127: 393-414.
- GEHUCHTEN, van A. (1891). La structure des centres nerveux. La Cellule 7: p. 81.

- GEHUCHTEN, van A. (1892). La structure des lobes optiques chez l'embryon de poulet. *La Cellule* 8: 1-43.
- GELLHORN, E. (1953). The physiological basis of emotion. Physiologic Foundation of Neurology and Psychiatry. Minneapolis: Univ. of Minn. Press.
- GEREN, B.B. (1954). The formation from the Schwann cell surface of the myelin in peripheral nerves of chick embryos. *Exper. Cell Res.* 7: 558-562.
- GERLACH, J. (1871). Von dem Rückenmarke. In *Handbuch der Lehre von den Geweben.* 2. Stricker.
- GERSCHENFELD. (1959). Neuroglia, in Progress in Brain Research Vol. 15. Amsterdam: Elsevier.
- GLEES, P. (1961). Experimental Neurology. London: Oxford.
- GLOBUS, A. and SCHEIBEL (1966). Loss of dendritic spines as an index of pre-synaptic terminal patterns. *Nature* 212: 463-465.
- GLOBUS, A. and A.B. SCHEIBEL (1967). Pattern and Field in Cortical Structure: The Rabbit. *J. Comp. Neurol.* 131: 155-172.
- GLOBUS, A. and A.B. SCHEIBEL (1967). The effect of visual deprivation on cortical neurons: A Golgi study. *Ex. Neurol.* 19: 331-345.
- GOLDBY, F. and R.J. HARRISON (1961). Recent Advances in Anatomy. Ser. 2. Chap. 7, 247-273. Boston: Little, Brown.
- GOLGI, C. (1875). Sulla fina anatomia dei bulbi olfactori. Reggio-Emilia.
- GOLGI, C. (1878). Un nuovo processo di tecnica microscopia. *Rend. Inst. Lombardo Sci. e Let.* 12: p. 5.
- GOLGI, C. (1878). Di una nuova reazione apparentemente nera della cellule nervose cerebrali. *Archivio per le sc. med.* V. 3. No. 11.
- GOLGI, C. (1885). Sulla minuta anatomia degli organi centrali del sistema nervoso. Milano 1.
- GOLGI, C. (1890). Uber den feineren Bau des Rückenmarkes. *Anat. Anz.* 5: 372-396.

- GOLGI, C. (1891). Methode suivie dans les recherches histologiques. Arch. ital. Biol. 15: 434-463.
- GOLGI, C. (1894). Untersuchungen ueber den feineren Bau des centralen und peripherischen Nervensystems. Jena: Fischer.
- GOLGI, C. (1898). Intorno allei struttura delli cellule nervose. Boll. d. Soc. med. chir., Pavia. F. 1. 16 pp.
- GONZALES-RAMIREZ, J. (1963). Considerations on nucleolar physiology. In Cinemicrography in Cell Biology. New York: Academic Press.
- GOODMAN, L.S. and A. GILMAN (1965). The Pharmacological Basis of Therapeutics. 3rd Ed. New York: Macmillan.
- GOTHLIN, G.F. (1917). Relation entre le fonctionnement et la structure des elements nerveux. Conference faite devant la faculte de medecine d'Upsal. 1917. 13: Upsala Lakare forenings Forkandingar.
- GRANT, G. and H. ALDSKOGIUS (1967). Silver impregnation of degenerating dendrites, cells and axons central to axonal transection. I. A Nauta study on the Hypoglossal Nerve in Kittens. Ex. Brain Res. 3: 150-162.
- GRAY, E.G. (1959). Axo-somatic and axo-dendritic synapses of the cerebral cortex: an electron microscope study. J. Anat. Lond. 93: 420-433.
- GRAY, E.G. (1961a). Ultrastructure of synapses of the cerebral cortex and of certain specialisations of neuroglial membranes. In Electron Microscopy in Anatomy. London: Arnold.
- GRAY, E.G. (1961b). The granule cells, mossy synapses and Purkinje spine synapses of the cerebellum: light and electron microscopic observations. J. Anat. Lond. 95: 345-356.
- GRAY, E.G. (1962a). Electron microscopy of synaptic organelles of the central nervous system. IV. Int. Cong. Neuropath. Stuttgart: Thieme.
- GRAY, E.G. (1967). The synapse. Science Journal 3: 5.

- GRAY, E.G. and V.P. WHITTAKER (1960). The isolation of synaptic vesicles from the central nervous system. *J. Physiol. (Lond.)* 153: 35-37.
- GRAY, E.G. and R.W. GUILLERY (1963). A note on the dendritic spine apparatus. *J. Anat. Lond.* 97: 389-392.
- GRIMM, U. (1949). *Über die Grossenbeziehung zwischen Kern und Nucleolus menschlicher Ganglienzellen.* Diss. Bern. cited by Hyden.
- GROSSMAN, C. (1955). Electro-Ontogenesis of Cerebral Activity. *A.M.A. Arch. Neurol. Psychiat.* 74: 186-202.
- GUILLERY, R.W. (1967). A light and electron microscopical study of neurofibrils and neurofilaments at neuro-neuronal junctions in the dorsal, lateral geniculate nucleus of the cat. *Am. J. Anat.* 120: 583-604.
- GYLLENSTEIN, L. (1959). Postnatal development of the visual cortex in darkness (mice). *Acta morphol. neerl.-scand.* 2: 331-345.
- HALPERN, L.M. (1960). The effects of some antiepileptics on neuronally isolated supersensitive cerebral cortex. *The Pharmacologist.* 2: p. 77.
- HAM, A. (1965). Textbook of Histology. Philadelphia: Lippincott.
- HAMLIN, L.H. (1961). Electron microscopy of mossy fibre endings in Ammon's Horn. *Nature, Lond.* 190: 645-646.
- HAMLIN, L.H. (1962). The fine structure of the mossy fibre endings in the hippocampus of the rabbit. *J. Anat. Lond.* 96: 112-120.
- HAMMARBERG, C. (1895). *Studies oefver idotens Klinik och patologi jaemte undersocksinger of hjaebarkens normalis anatomi.* Akademish afhandling. Upsala.
- HARRIS, W.G. (1960). Fibre degeneration in the cerebral cortex of the cat and rabbit following experimental craniotomy. *J. Anat.* 94: 216-223.
- HARTMANN, J.F. (1948). cited by Hyden. *Anat. Rec.* 100: p. 49.

- HARTMANN, J.F. (1949). cited by Hyden. Anat. Rec. 103: p. 541.
- HARTMANN, J.F. (1953). cited by Hyden. J. Comp. Neurol. 99: p. 201.
- HARTMANN, J.F. (1956). Electron microscopy of mitochondria in the central nervous system. J. Biophys. & Biochem. Cytol. 2: Suppl. 4. 373-378.
- HEIDENHAIN, M. (1911). Handbuch der Anatomie des Menschen. Plasma und Zelle, vol. 2. p. 687. Fischer, Jena.
- HELD, H. (1896). cited in H.H. Donaldson (1901). Arch. L. Anat. u. Physiol. Anat. Abth. Leipzig.
- HELD, H. (1897). cited in Hyden. Zweite Abhandl. Arch. Anat. Physiol., Anat. Abt. p. 396.
- HELD, H. (1905). Zur Kenntniss einer neurofibrillaren Continuitat im Centralnervensystem der Wichelthiere. Arch. Anat. Physiol. Lpg. 55-78.
- HELD, H. (1909). Die Entwicklung des Nervengewebes bei den Wirbeltieren. Leipzig: Barth.
- HELD, H. (1929). Die Lehre von den Neuronen und vom Neurencytium und ihr heutiger Stand. Fortschr. naturwiss. Forsch. N.F. H. 8.
- HENNEBERG, R. (1910). Messung der Oberflachenausdehnung der Grosshirinde. J. Psychol. Neurol. 17: 144-158.
- HERTWIG, R. (1903). cited by Hyden. Biol. Centre. 23: p. 49.
- HERWERDEN, van M.A. (1913). cited by Hyden. Arch. Zellforsch. 10: p. 431.
- HESS, W.R. (1948). Die Funktionelle Organisation des Vegetativen Nervensystems. Basel: Schwabe.
- HESS, W.R. (1954). Diencephalon. London: W. Heinemann.
- HESS, W.R. (1956). Hypothalamus und Thalamus. Stuttgart: Thieme.

- HIBBARD, H. (1945). Current status of our knowledge of the Golgi apparatus in the animal cell. *Quart. Rev. Biol.* 20: p. 1.
- HIS, W. (1886). Zur Geschichte des menschlichen Rückenmarks und der Nervenwurzeln. 1. Leipzig.
- HIS, W. (1889). Die Neuroblasten und deren Entstehung im embryonalen Marke. *Abh. math.-physik. Kl. sacks. Akad. Wiss.* 15: 311-372.
- HOERR, N.L. (1936). Cytological Studies by the Altmann-Gersh Freezing-drying Method. *Anat. Rec.* 66: 81-90.
- HOLLOWAY, R.L. (1966). Dendritic branching: some preliminary results of training and complexity in rat visual cortex. *Brain Res.* 2: 393-396.
- HUBEL, D.H. and T.N. WIESEL (1962). Receptive fields, binocular interaction and functional architecture in the cat's visual cortex. *J. Physiol. Lond.* 160: 106-154.
- HUBEL, D.H. and T.N. WIESEL (1965). Receptive fields and functional architecture in two non-striate visual areas (18-19) of the cat. *J. Neurophysiol.* 28: 229-289.
- HUBER, G.C. (1927). Experimental observations on peripheral nerve repair. U.S. Gov. Print. Off. Wash.
- HUMASON, G.L. (1962). Animal Tissue Techniques. San Francisco: Freeman.
- HYDEN, H. (1959). The Neuron. In The Cell, vol. IV. ed. by Brachet and Mirsky. New York: Academic Press.
- HYDEN, H. and B. LINDSTROM (1950). Microspectrographic studies on the yellow pigment in nerve cells. *Discussions Faraday Soc.* 9: 436-441.
- HYDEN, H. and S. LARSSON (1956). cited by Hyden. *J. Neurochem.* 1: p. 134.
- JAEGER, R. (1914). Inhaltsberechnungen der Rinden und Marksubstanz des Grosshirns durch Planimetrische Messungen. *Arch. Psychiat.* 54: 261-272.

- JONES, W.H. and D.B. THOMAS (1962). Changes in the dendritic organization of neurons in the cerebral cortex following deafferentation. *J. Anat. Lond.* 96: 375-381.
- KAADA, B. (1951). Somatomotor, autonomic and electrocorticographic responses to electrical stimulation of "rhinencephalic" and other structures in primates, cat and dog. *Acta Physiol. Scandinav.* 24: Suppl. 83.
- KAADA, B., J. JANSEN and P. ANDERSEN (1953). Stimulation of the hippocampus and medial cortical areas in unanaesthetized cats. *Neurology*, 3: 844-857.
- KAPPERS, C.V.A., G.C. HUBER and E.C. CROSBY (1936). The Comparative Anatomy of the Nervous System of Vertebrates Including Man. 2 vols. New York: Macmillan.
- KELLER, G.J. (1945). A reliable Nissl stain. *J. Tech. Methods* 25: 77-78.
- KEY, A. and G. RETZIUS (1875). Studien in der Anatomie des Nervensystems und des Bindegewebes. Stockholm: Samson and Wallin.
- KLEBS, E. (1865). cited by Hyden. *Arch. pathol. Anat. u. Physiol. Virchow's* 32: p. 168.
- KLOTZ, D.A. and G. CLARK (1950). An attempt at graphic cytoarchitectonic description. *J. Comp. Neurol.* 92: 215-225.
- KLUVER, H. (1951). Functional differences between the occipital and temporal lobes. In Cerebral Mechanisms in Behavior. p. 147. New York: Wiley.
- KOGAN, A. (1949). Electrophysiological investigation of central mechanisms of some compound reflexes. Moscow: Medgit.
- KOLLIKER von, A. (1904). Ueber die Entwicklung der Nervenfasern. *Verhandl. d. anat. Gesellsch* 18: p. 7.
- KOSITZYN, N.S. (1964). Axo-dendritic Relations in the Brain Stem Reticular Formation. *J. Comp. Neurol.* 22: 9-17.

- KOSITZYN, N.S. (1964). Certain peculiarities in the inner organization of the brain stem reticular formation. Dokl. Akad. Nauk. SSSR. 145: 920-921.
- KRASS, M.E., PINSKY, C. and F.S. LA BELLA (1968). Glucose metabolism in the neuronally isolated cerebral cortical slab of the cat. J. of Neurochem. 15: 1381-1382.
- LA FORA, G.R. (1914). Neoformaciones dendriticas en las neuronas y alteraciones de la neuroglia en el perro senil. Tra. del Lab. de Investig. Biol. t. 12. fasc. 1.
- LASHLEY, K.S. and G. CLARK (1946). The cytoarchitecture of the cerebral cortex of Ateles: a critical examination of architectonic studies. J. Comp. Neurol. 85: 223-305.
- LEHNINGER, A.L. (1962). Water uptake and extrusion by mitochondria in relation to oxidative phosphorylation. Physiol. Rev. 42: p. 467.
- LENHOSSEK, von M. (1895). Der feinere Bau des Nervensystems im Lichte neuester Forschungen, zweite Auflage. Berlin, 1895.
- LEWIS, W.B. (1878). On the comparative structure of the cortex cerebri. Brain, 1: 79-96.
- LEWIS, W.H. and M.R. LEWIS (1924). Behavior of cells in tissue cultures. Sect. 7 General Cytology, ed. Cowdry. U. of Chic. Press.
- LITTLEFIELD, J.W. and E.B. KELLER (1957). cited by Hyden. J. Biol. Chem. 224: p. 13.
- LORENTE DE NO, R. (1927). Ein Bertrag Zur Kenntniser der Gefassverteilung in der Hirnrinde. J. Psychol. Neurol. 35: 19-27.
- LORENTE DE NO, R. (1934). Studies on the structure of the cerebral cortex. I. The area Entorhinalis. J. Psychol. Neurol. 45: 381-438.
- LORENTE DE NO, R. (1949). Cerebral cortex: Architecture, Intracortical Connections, Motor Projections. In Fulton's Physiology of the Nervous System. London: Oxford.

- LUSE, S.A. (1956). Formation of myelin in the central nervous system of mice and rats, as studied with electron microscope. *J. biophys. biochem. Cytol.* 2: 777-784.
- LUSE, S.A. (1956). Electron microscopic observations on the central nervous system. *J. biophys. biochem. Cytol.* 2: 531-542.
- MALLORY, F.B. (1944). Pathological Technique. Philadelphia: Saunders.
- MANN, G. (1894). Histological changes induced in sympathetic, motor and sensory nerve cells by functional activity. Meeting of Scottish Micr. Soc.
- MARIN-PADILLA, M. (1967). Number and Distribution of the Apical Spines of the Layer V Pyramidal Cells in Man. *J. Comp. Neur.* 131: 475-490.
- MARIN-PADILLA, M. (1968). Cortical axo-spinodendritic synapses in man: a Golgi study. *Brain Res.* 118: 227-248.
- MARTINOTTI, C. (1889). Contributo allo studio della corteccia cerebrale, ed all'origine centrale dei nervi. *Ann. di freniat. e Sc. aff. d. R. Manicomio di Torino*, 1: p. 314.
- MATSUMATO, T. (1920). The granules, vacuoles, and mitochondria in the sympathetic nerve fibres cultivated in vitro. *Bull. Johns Hopkins Hosp.* 31: p. 91.
- MEYNERT, T. (1867). The Brain of Mammals. In Stricker's Manual of Histology, 1872. New York: Wood.
- MICHAELIS, L. (1900). cited in The Cell, Vol. 1. Brachet and Mirsky. *Arch. Mikroskop. Anat. u. Entwicklungsmech.* 55: p. 558.
- MILLEN, J.W. and D.H.M. WOOLLAM (1961). Observations on the nature of the pia mater. *Am. J. Physiol.* 170: 682-689.
- MILLEN, J.W. and D.H.M. WOOLLAM (1962). The Anatomy of the Cerebrospinal Fluid. pp. 90-102. New York: Oxford.
- MITRA, N.L. (1955). A quantitative analysis of cell types in mammalian neo-cortex. *Anat. Rec.* 118: p. 333.

- MIVART, S. (1874). The Cat; its History, Anatomy, Psychology and Origin, an Introduction to the Study of Backboned Animals, especially Mammalia. London.
- MOORE, K.L. and M.L. BARR (1953). Cited in Hyden. J. Comp. Neurol. 98: p. 213.
- MOORE, K.L. and M.L. BARR (1955). Smears from the oral mucosa in the detection of chromosomal sex. Lancet, 2: 57-58.
- MOUNTCASTLE, V.B. (1957). Modalities and topographic properties of single neurons of cat's sensory cortex. J. Neurophysiol. 20: 408-434.
- MUHLMANN, M. (1900). cited by Hyden. Verhandl. deut. path. Ges. 3: p. 148.
- MUHLMANN, M. (1901). Die Veränderungen der Nervenzellen in verschiedenem Alter beim Meerschweinchen. Anat. Anz., Bd. 19: S. 377.
- MUNGAI, J.M. (1967). Dendritic patterns in the somatic sensory cortex of the cat. J. Anat. 101: 403-418.
- NISSL, F. (1884-5). Naturforscherversamml. z. Strassburg.
- NISSL, F. (1894). Methylene Blue Stain. Cited by Humason. Animal Tissue Techniques, 1962. San Francisco: Freeman.
- NISSL, F. (1903). Die Neuronenlehre und ihre Anhänger. Jena, Fischer.
- NURNBERGER, J.A., A. ENGSTROM and B. LINDSTROM (1952). Cited by Hyden. J. Cellular Comp. Physiol. 39: p. 215.
- OBERSTEINER, H. (1903). Cited by Hyden. Arb. Neurol. Inst. Wien. Univ. 10: p. 245.
- OBERNDORFER, M. (1921). Cited by Hyden. Z. ges. Neurol. Psychiat. 72: p. 105.
- OLZEWSKI, J. (1947). Zur morphologie und Entwicklung des Arbeitskerns unter besonderer Berücksichtigung des Nervenzelkerns. Biol. Zbl. 66: 265-304.

- OWEN, R. (1868). On the Anatomy of Vertebrates. 3 vols. London: Longmans Green.
- PAKKENBERG, H. (1966). The number of nerve cells in the cerebral cortex of man. *J. Comp. Neur.* 128: 17-20.
- PAL, J. (1887). Ein Beitrag zur Nervenfarbtechnik. *Zschr. wissen. Mikr.* 4: 92-96.
- PALADE, G.E. (1952). Cited by Hyden. *Anat. Rec.* 114: p.427.
- PALADE, G.E. and S.L. PALAY (1954). Electron microscopic observations of interneuronal and neuromuscular synapses. *Anat. Rec.* 118: p. 335.
- PALADINO, G. (1892). De la continuation de la nevroglie dans le squelette myelinique des fibres nerveuses et de la constitution pluricellulaire du cylinderaxe. *Arch. ital. de biol.* 1893. 19 p.26.
- PALAY, S.L. (1958). An electron microscopical study of neuroglia. In Biology of Neuroglia. Springfield: Thomas.
- PALAY, S.L. and G.E. PALADE (1955). The fine structure of neurons. *J. Biophys. & Biochem. Cytol.* 1: 69-88.
- PAPPAS, G.D. and D.P. PURPURA (1961). Fine structure of dendrites in the superficial neocortical neuropil. *Exp. Neurol.* 4: 507-530.
- PAPEZ, J.W. (1929). Comparative Neurology. New York: Crowell.
- PAPEZ, J.W. (1937). A proposed mechanism of Emotion. *Arch. Neurol. Psychiat.* 38: 725-743.
- PENFIELD, W.G. (1921). The Golgi apparatus and its relationship to Holmgren's trophospongium in nerve cells. Comparison during retispersion. *Anat. Rec.* 22: p. 57.
- PENFIELD, W.G. (1920). Alterations of the Golgi apparatus in nerve cells. *Brain*, 43: p. 290.
- PENFIELD, W.G. (1932). Neuroglia, normal and pathological. In Cytology and Cellular Pathology of the Nervous System. Vol. 11. New York: Hoeber.

- PETERS, A. (1960). The formation and structure of myelin sheaths in the central nervous system. *J. Biophys. Biochem. Cytol.* 8: 431-446.
- PICK, A. and M. BIELSCHOWSKY (1911). Cited by Cajal. *Degeneration and Regeneration* (1928). London: Oxford.
- PILCZ, A. (1895). Cited by Hyden. *Arb. Neurol. Inst. Wien. Univ.* 3.
- PINSKY, C. (1957). The physiology of the paroxysmal afterdischarge. M.Sc. Thesis, McGill University, Montreal.
- PINSKY, C. (1961). Mechanisms of the paroxysmal afterdischarge. Ph.D. Thesis, McGill University, Montreal.
- PINSKY, C. (1963). Paroxysmal afterdischarges and differential repolarization in cat's cerebral cortical neurones. *Fed. Proc.* 22: p. 395.
- PINSKY, C. (1967). Bremer Symposium on the Cerebral Cortex. University of Montreal, Montreal.
- PINSKY, C. and B.D. BURNS (1962). Production of epileptiform afterdischarges in cat's cerebral cortex. *J. Neurophysiol.* 25: 359-379.
- PLENK, H. (1934). Cited in Hyden. *Z. mikroskop.-anat. Forsch.* 36: p. 191.
- POLYAK, S. (1957). The Vertebrate Visual System. Chicago: U. of Chicago Press.
- PORTER, K.R. (1953). Cited by De Robertis. *J. Exp. Med.* 97: p. 727.
- PORTER, K.A., A. CLAUDE and E.F. FULLAM (1945). Cited by De Robertis. *J. Exp. Med.* 81: p. 233.
- PROSSER, C.L. (1959). *Evolution of Nervous Control from Primitive Organisms to Man*. A.A.A.S.
- PURPURA, D.P. (1961). An analysis of axodendritic synaptic organizations in immature cerebral cortex. *Ann. N.Y. Acad. Sci.* 94: 604-654.
- PURPURA, D.P. and E.M. HOUSEPIAN (1961). Morphological and Physiological Properties of Chronically Isolated Immature Neocortex. *Ex. Neurol.* 4: 377-401.

- RAMON-MOLINER, E. (1957). A chlorate-formaldehyde modification of the Golgi method. *Stain Tech.* 32: 105-116.
- RAMON-MOLINER, E. (1958). A tungstate modification of the Golgi-Cox method. *Stain Tech.* 33: 19-29.
- RAMON-MOLINER, E. (1961). The histology of the post-cruciate gyrus in the cat. I. Quantitative Studies. *J. Comp. Neur.* 117: 43-62.
- RAMON-MOLINER, E. (1961). The histology of the post-cruciate gyrus in the cat. II. A statistical analysis of the dendritic distribution. *J. Comp. Neur.* 117: 63-76.
- RAMON-MOLINER, E. (1962a). An attempt at classifying nerve cells on the basis of their dendritic pattern. *J. Comp. Neur.* 119: 211-227.
- RAMON-MOLINER, E. (1962b). The distribution of non-specific dendritic patterns in the brain stem (abstract). *Anat. Rec.* 142: p. 270.
- RAMON-MOLINER, E. (1963). Dendritic patterns of the cat's brain stem. *Anat. Rec.* 145: p. 366.
- RAMON-MOLINER, E. (1966). The isodendritic core of the brain stem. *J. Comp. Neur.* 126: 311-336.
- RAMON y CAJAL, S. (1888). Estructura de los centros nerviosos de los aves. *Rev. trim. de Histologia normal y patologica* p. 1.
- RAMON y CAJAL, S. (1889). Textura del sistema nerviosa. Madrid. p. 121. Cited by Barker, 1901.
- RAMON y CAJAL, S. (1890a). Sur les fibres nerveuses de la couche granuleuse du cervelet et sur l'evolution des elements cerebelleux. *Int. Mschr. Anat. Physiol.* 7: 12-31.
- RAMON y CAJAL, S. (1890b). Sur l'origine et les ramifications des fibres nerveuses de la moelle embryonnaire. *Anat. Anz.* 5: 85-95.
- RAMON y CAJAL, S. (1890c). Response a Mr. Golgi a propos des fibrilles collaterales de la moelle epiniere, et de la structure generale de la substance grise. *Anat. Anz.* 5: 579-587.

- RAMON y CAJAL, S. (1891). Sur la structure de l'ecorce cerebrale de quelque mammiferes. La Cellule 7: 124-176.
- RAMON y CAJAL, S. (1895). Les nouvelles idees sur la structure du systeme nerveux chez l'homme et chez les vertebres. Paris: Reinwald.
- RAMON y CAJAL, S. (1899). Textura del sistema nervioso del hombre y de los vertebrados. Estudios sobre et plan estructural y composicion histologica de los centros nerviosos adicionados de consideraciones fisiologicas fundadas en los nerevos descubrimientos. 2 vols. Libreria of Nicolas. Moya, Madrid.
- RAMON y CAJAL, S. (1904). Variaciones morfologicas normales y patologicas del reticulo neurofibrilar. Trab. d. Lab. de invest. biol. Univ. de Madrid, 3: p. 9.
- RAMON y CAJAL, S. (1909, 1911). Histologie du Systeme Nerveux de l'Homme et des Vertebres. Vol. I, 1909; vol. II, 1911. Paris: Maloine.
- RAMON y CAJAL, S. (1911). Histologie du Systeme Nerveux de l'Homme et des Vertebres. Madrid, C.S.I.C.
- RAMON y CAJAL, S. (1928). Degeneration and Regeneration of the Nervous System. London: Oxford.
- RANSOM, S.W. and S.L. CLARK (1959). The Anatomy of the Nervous System. Philadelphia: Saunders.
- RANVIER, M.L. (1874). Traite technique d'histologie. Paris: Savy.
- RANVIER, M.L. (1878). Lecons sur l'histologie du systeme nerveux. Vols. I-II. Paris: Savy.
- REICHEL, W., J. HOLLANDER, J.H. CLARK and B.L. STREHLER (1968). Lipofuscin pigment accumulation as a function of age and distribution in rodent brain. J. Geront. 23: 71-78.
- REIFFENSTEIN, R.J. (1964). Denervation Supersensitivity in the Cortex: a Possible Basis for Focal Epilepsy. Ph.D. Thesis, University of Manitoba, Winnipeg.

- REIGHARD, J. and H.S. JENNINGS (1951). Anatomy of the Cat. New York: Henry Holt.
- RHODIN, J.A.G. (1963). An Atlas of Ultrastructure. Philadelphia: Saunders.
- RIESEN, A.H. (1960). Effects of stimulus deprivation on the development and atrophy of the visual sensory system. *Amer. J. Orthopsychiat.* 30: 23-26.
- ROBERTSON, J.D. (1955). Ultrastructure of adult vertebrate peripheral myelinated nerve fibres in relation to myelinogenesis. *J. Biophys. and Biochem. Cytol.* 1: 271-278.
- ROBERTSON, J.D. (1958). The ultrastructure of Schmidt-Lantermann clefts and related shearing defects of the myelin sheath. *J. Bioph. & Biochem. Cytol.* 4: 39-46.
- ROBERTSON, J.D. (1959). The ultrastructure of cell membranes and their derivatives. *Biochem. Soc. Symp.* 16: 3-43.
- ROBINS, E., D.E. SMITH and K.M. EYDT. (1956). The quantitative histochemistry of the cerebral cortex. *J. Neurochem.* 1: 54-67.
- ROSE, J.E. (1949). The cellular structure of the auditory region of the cat. *J. Comp. Neurol.* 91: 409-439.
- ROSENBLUTH, J. (1962). Subsurface cisterns and their relationship to the neuronal plasma membrane. *J. Cell Biol.* 13: p. 405.
- SANCHEZ, M. (1916). Recherches sur le reseau endocellulaire de Golgi dans les cellules de l'ecorce du cervelet. *Tral-d. lab. de invest. biol. Univ. de Madrid* 14: p. 87.
- SANDERS, F.K. (1948). Cited by Hyden. *Proc. Roy. Soc.* 135: p. 323.
- SASTRY, P.B. (1956). The functional significance of acetylcholine in the brain. Ph.D. Thesis. McGill University, Montreal.
- SCHADE, J.P. and D.H. FORD (1965). Basic Neurology. Amsterdam: Elsevier.
- SANDERS, H.D. and C. PINSKY (1967). Facilitation in spatial summation in neurons considered with epileptiform afterdischarges in the isolated cerebral cortex of the cat. *Can. J. Physiol. & Pharmac.* 45: p.965.

- SCHMITT, F.O. and R.S. BEAR (1937). Cited by Hyden. J. Cellular Comp. Physiol. 9: p. 261.
- SCHMITT, F.O. R.S. BEAR and K.J. PALMER (1941). X-ray diffraction studies on the structure of the nerve myelin sheath. J. Cell. & Comp. Physiol. 18: 31-42.
- SCHULTZE, M. (1871). Allgemeines uber die Strukturelemente des Nervensystems. In Stricker's Handbuch der Lehre von den Geweben des Menschen und der Thiere. Leipzig: Engelmann.
- SHARIFF, G.A. (1953). Cell counts in the primate cerebral cortex. J. Comp. Neur. 98: 381-400.
- SHERRINGTON, C.S. (1897). The central nervous system. Vol. 3, in A Text-Book of Physiology. London: Macmillan.
- SHERRINGTON, C.S. (1900). The spinal cord. In A Text-Book of Physiology. Vol. 2, 782-883. London: Caxton.
- SHOLL, D.A. (1953). Dendritic organization in the neurons of the visual and motor cortices of the cat. J. Anat., Lond. 87: 387-406.
- SHOLL, D.A. (1955). The organization of the visual cortex in the cat. J. Anat., Lond. 89: 33-46.
- SHOLL, D.A. (1956). The Organization of the Cerebral Cortex. London: Methuen.
- SHOLL, D.A. (1959). A comparative study of the neuronal packing density in the cerebral cortex. J. Anat. 93: 143-158.
- SIEBERT, G., O. HEIDENREICH, R. BOHMIG and K. LANG (1955). Cited by Hyden (1960). 42: p. 156. Naturwissen.
- SIEKEVITZ, P. and G.E. PALADE (1958). Cited by De Robertis. J. Biophys. Biochem. Cytol., 2: p. 417.
- SJOSTRAND, F.S. (1953). The lamellated structure of the nerve myelin sheath as revealed by high resolution electron microscopy. Experientia (Basel) 9: 68-69.

- SJOSTRAND, F. (1956). Cited by Hyden. Intern. Rev. Cytol. 5: p. 456.
- SMART, T. and C.P. LEBLOND (1961). Evidence for division and transformations of neuroglia cells in the mouse brain, as derived from radioautography after injection of thymidine- H^3 . J. Comp. Neurol. 116: p. 349.
- SNIDER, R.S. and M.P. DEL CERRO (1967). Drug induced dendritic sprouts on purkinje cells in the adult cerebellum. Ex. Neurol. 17: 466-480.
- SOSA, J.M. (1935). Modificaciones de la Red Neurofibrilar en Correlacion on la Accumulacion Pigmentaria (Lipofuscina) en las Neuronas. Arch. Soc. de Biol. de Montevideo 6: 124-236.
- SOSA, J.M. (1952). Aging of Neurofibrils. J. Geront. 7: 191-195.
- SPEIDEL, C. (1933). Studies of living nerves. II. Activities of amoeboid growth cones, sheath cells and myelin segments, as revealed by prolonged observations of individual nerve fibres in frog tadpoles. Am. J. Anat. 52: p. 1.
- STEIN, W.D. (1955). Cited by Hyden. Nature 175: p. 256.
- STRAUS-DURCKHEIN, H.A. (1845). Anatomie descriptive et comparative du chat, type des mammiferes en general, et des carnivores en particulier. 2 vols. Paris.
- SWEET, W.H., G.A. TALLAND and F.R. ERVIN (1959). Loss of memory following section of the fornix. Tr. Am. Neurol. 84: 76-82.
- TAYLOR, G.W. (1940). Cited by Hyden. J. Cell. Comp. Physiol. 15: p. 363.
- TAYLOR, G.W. (1941a). Cited by Hyden. J. Cell. Comp. Physiol. 18: p. 233.
- TAYLOR, G.W. (1941b). Cited by Hyden. Anat. Record 81: p. 41.
- TENNYSON, V.M. (1962). Electron microscopic observations of the development of the neuroblast in the rabbit embryo. In Int. Cong. Elect. Mic. Vol. 11. New York: Academic Press.

- TEWARI, H.B. and G.H. BOURNE (1962a). Histochemical evidence of metabolic cycles in spinal ganglion cells of rat. *J. Histochem. Cytochem.* 10: 42-64.
- TEWARI, H.B. and G.H. BOURNE (1962b). The histochemistry of the nucleus and nucleolus with reference to nucleic-cytoplasmic relations in the spinal ganglion neurone of the rat. *Acta Histochem.* 13: 323-350.
- THOMAS, O.L. (1947). Cited by Hyden. *Quart. J. Microscop. Sci.* 88: p. 445.
- THOMAS, O.L. (1948). Cited by Hyden. *Quart. J. Microscop. Sci.* 89: p. 333.
- THOMPSON, H. (1899). The total number of functional nerve cells in the cerebral cortex. *J. Comp. Neur.* 9: 113-140.
- TOWER, D.B. (1954). Structural and functional organization of mammalian cerebral cortex: the correlation of neurone density with brain size. *J. Comp. Neur.* 101: 19-52.
- TOWER, D.B. and K.A.C. ELLIOTT (1952). Activity of the acetylcholine system in cerebral cortex of various unanesthetized animals. *Am. J. Physiol.* 168: 747-759.
- TRAMER, M. (1916). *Über Messung und Entwicklung der Rindenoberfläche des menschlichen Grosshirns.* *Arb. himanat. Inst., Zurich.* 10: 5-57.
- TRUEX, R.C. and M.B. CARPENTER (1964). Human Neuroanatomy. Baltimore: Williams and Wilkins.
- UCHIZONA (1965). Shape of synaptic vesicles. Cited by Jacobsen (1966).
- UZMAN, B.G. and G. NOGUEIRA-GRAF (1957). Electron microscopic studies of the formation of nodes of Ranvier in mouse sciatic nerves. *J. Biophys. Biochem. Cytol.* 3: 589-598.
- VALVERDE, F. (1961). Reticular formation of the pons and medulla oblongata. A Golgi study. *J. Comp. Neur.* 116: 71-99.

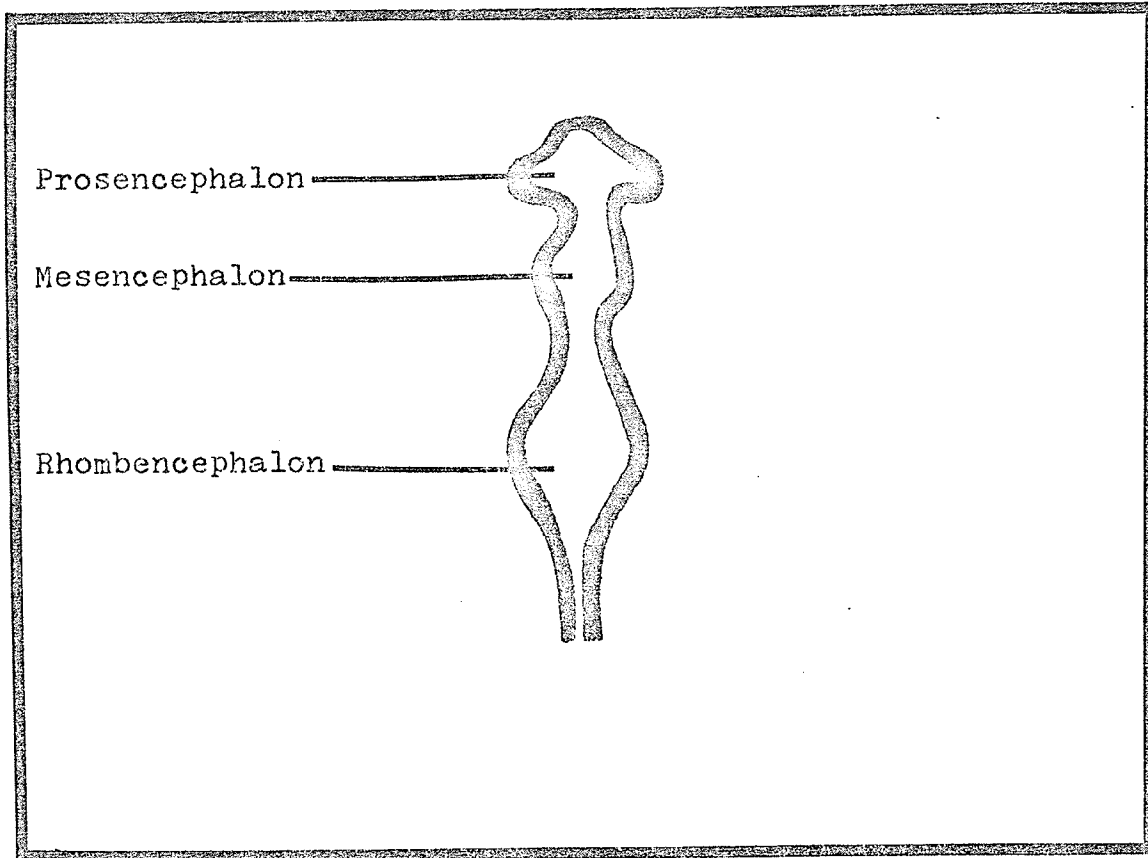
- VALVERDE, F. (1967). Apical dendritic spines of the visual cortex and light deprivation in the mouse. *Ex. Brain Res.* 3: 337-352.
- VAZQUEZ, A.J., G. KRIP and C. PINSKY (1969). Evidence for a muscarinic inhibitory mechanism in the cerebral cortex. *Ex. Neurol.* 23: 318-331.
- VINCENT, W.S. (1963). Cited by De Robertis. *Int. Rev. Cytol.* 4: p. 269.
- VOGT, C. and O. VOGT (1919). Allgemeine Ergebnisse unserer Hirnforschung. Vierte Mitteilung: Die physiologische Bedeutung der architektonischen Rindenreizungen. *J. Psychol. u. Neurol.* 25: 279-462.
- VOLKMANN, R. v. (1932). Cited by Hyden. *Z. wiss. Mikroskop.* 49: p. 457.
- WALDEYER, H.W.G. (1891). Uber Einige neuere Forschungen im Gebiete der Anatomie des Zentralnervensystems. *Dtsch. med. Wschr.* 17: 1213-1218.
- WALLER, A. (1852). Sur la reproduction des nerfs et sur la structure et les fonctions des ganglions spinaux. *Arch. f. Anat., Physiol. u. wissensch. Med.*
- WEED, L.H. (1922). The cerebrospinal fluid. *Physiol. Rev.* 2: 171-203.
- WEIGERT, C. (1885). Eine Verbesserung der Hamatoxylin-Blutlaugensalzmethode fur das Centralnervensystem. *Zschr. wissen. Mik.* 2: 399-401.
- WEISKRANTZ, L. (1958). Sensory deprivation and the cat's optic nervous system. *Nature (Lond.)* 181: 1047-1050.
- WEISS, P. and H. WONG (1936). Neurofibrils in Living Ganglion Cells of the Chick, Cultivated in vitro. *Anat. Rec.* 67: 105-117.
- WERNDLE, L. and G.W. TAYLOR (1943). Cited by Hyden. *J. Cell Physiol.* 21: p. 281.
- WILDER, B.G. (1873). The outer cerebral fissures of Mammalia and the limits of their homology. *Amer. Assoc. Proc.* XXII: 214-234.

- WILDER, B.G. (1879). Notes on the anatomy of the cat's brain. Meeting A.A.A.S.
- WILDER, B.G. (1880). The cerebral fissures of the domestic cat, Felis domestica. Science, 1: 49-51.
- WILDER, B.G. (1881). The Brain of the Cat, Felis Domestica. Proc. Amer. Phil. Soc. 19: 524-562.
- WILDER, B.G. (1901). Brain, An Anatomical Study. Reference Handbook of the Medical Sciences. 2: 136-217.
- WILLIAMS, H.S. (1875). The bones, ligaments and muscles of the domesticated cat. New York.
- WILSON, M.E. (1968). Cortico-cortical connexions of the cat visual areas. J. Anat. 102: 375-386.
- WILSON, M.E. and B.G. CRAGG (1967). Projections from the lateral geniculate nucleus in the cat and monkey. J. Anat. 101: 677-692.
- WINKLER, C. (1914). An Anatomical Guide to Experimental Researches on the Cat's Brain. Amsterdam: Versluys.
- WISCHNITZER, S. (1960). The ultrastructure of the nucleus and nucleocytoplasmic relations. Int. Rev. Cytol. 10: 137-162.
- WOOLSEY, C.N. (1961). Organization of cortical auditory system. In Sensory Communication. New York: Wiley.
- WUNSCHER, W. and R. KUSTNER (1967). A study of the quantitative distribution of lipofuscin and of vitamin E deficiency pigment in the nerve cells of rats of different age groups. Gerontologia (Basel). 13/3: 153-164.
- YAMADA, E. (1958). Some observations on the fine structure of centriole in the mitotic cell. Kurume Med. J. 5: 36-38.
- YOUNG, J.Z. (1957). The Life of Mammals. New York: Oxford.
- YOUNG, J.Z. (1964). A Model of the Brain. London: Oxford.

ZEGLIO, P. (1935). Cited by Hyden. Arch. Ital. Anat.
35: p. 371.

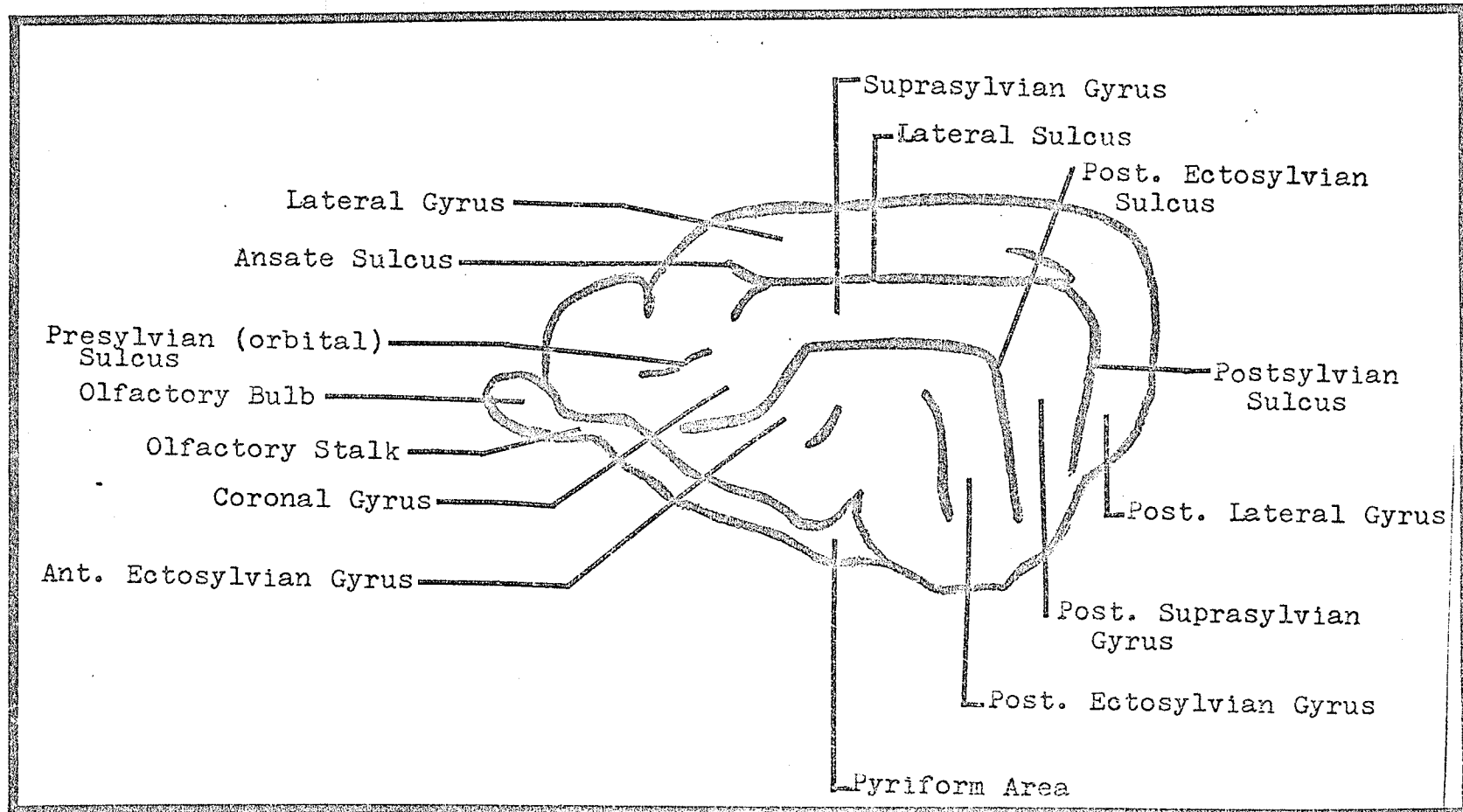
ZEIGER, K. (1955). In Handbuch der Allgemeinen
Pathologie. Vol. 2 p. 1. Berlin: Springer.

APPENDIX



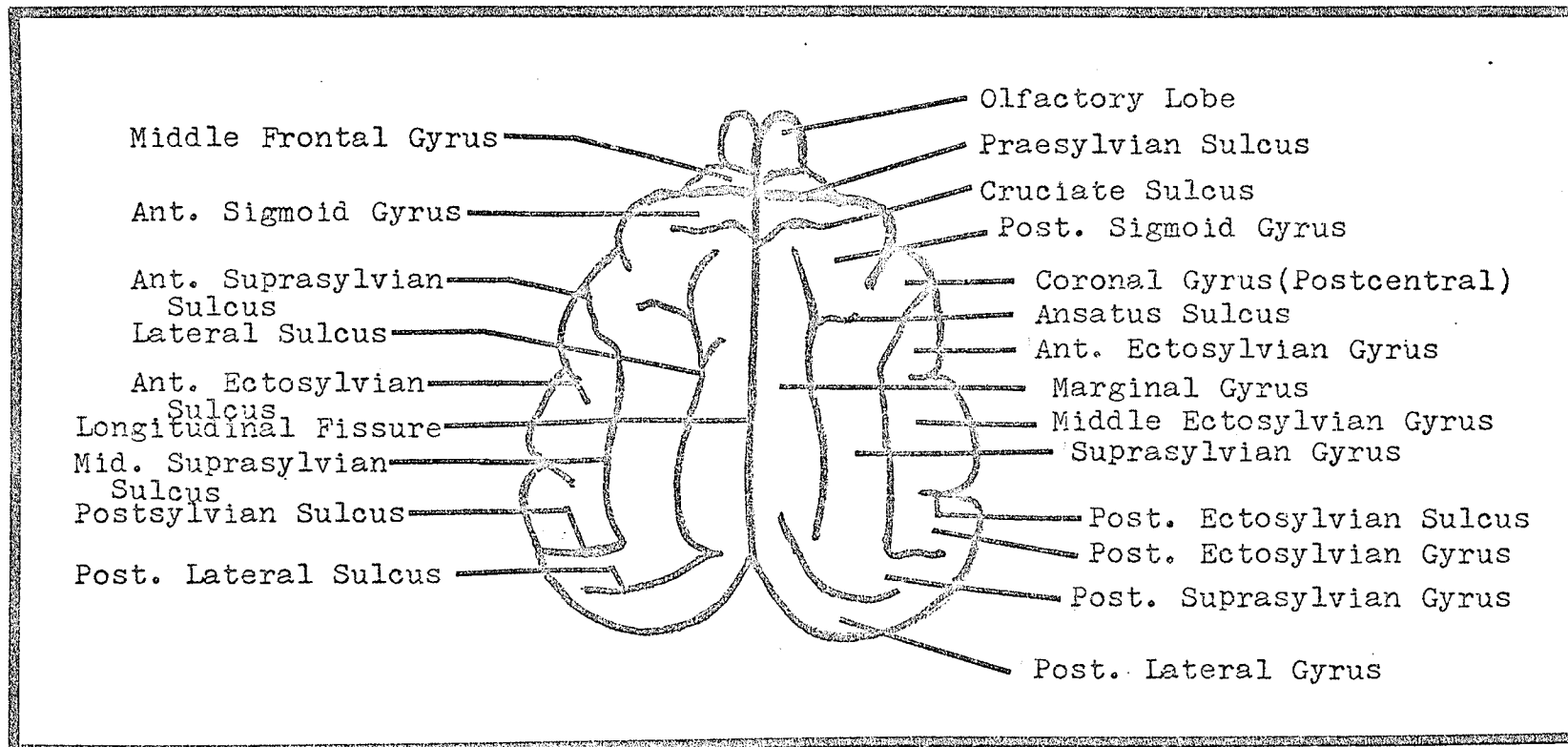
Appendix. Fig. 1. Longitudinal Section of Four Week Old Human Embryo.

Three brain vesicles of brain are thin-walled and epithelial in appearance.



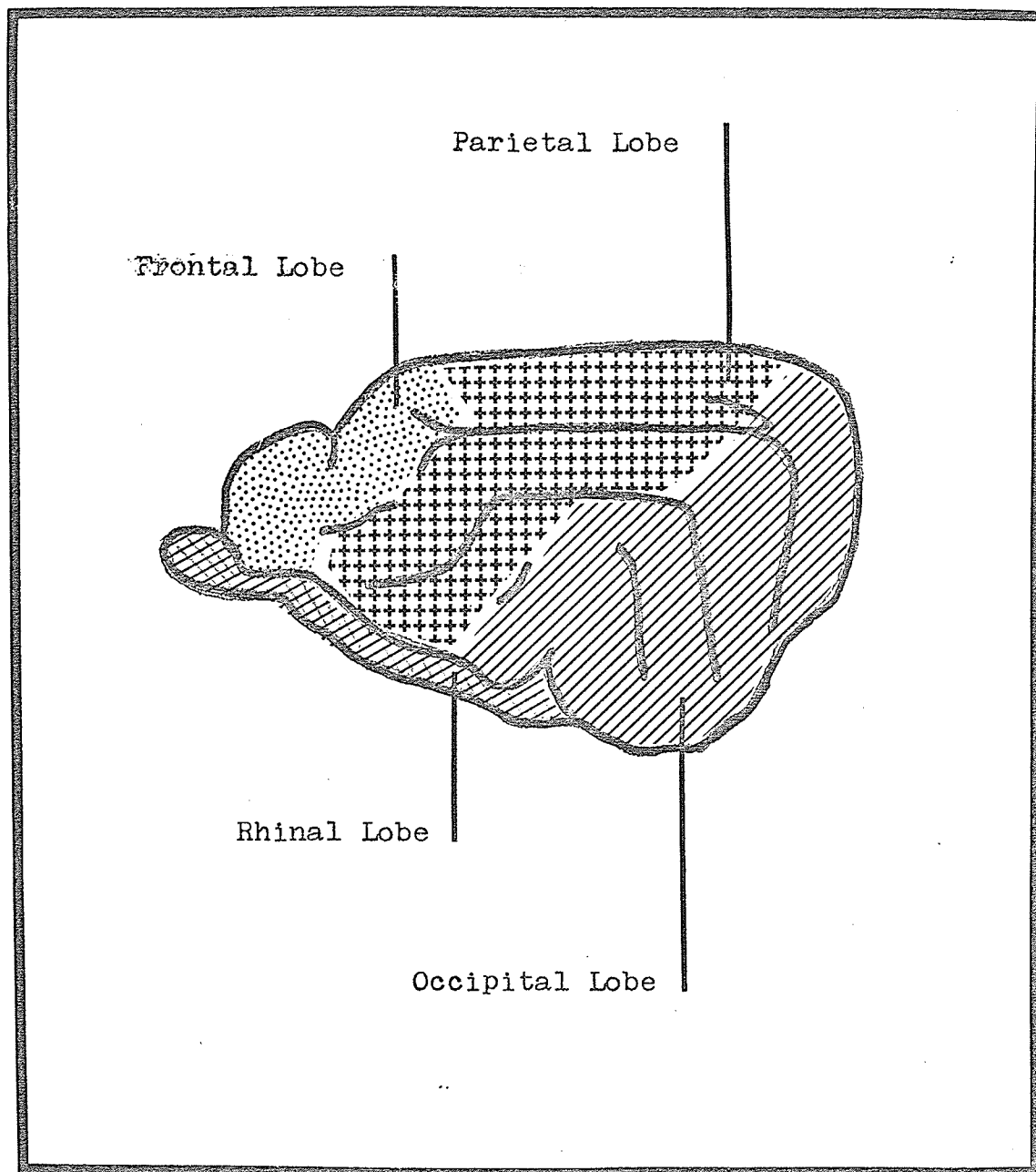
Appendix. Fig. 2. Lateral and Ventral Aspects of Cat's Cerebral Hemispheres

Terminology after Papez (1929) and Reighard and Jennings (1951).



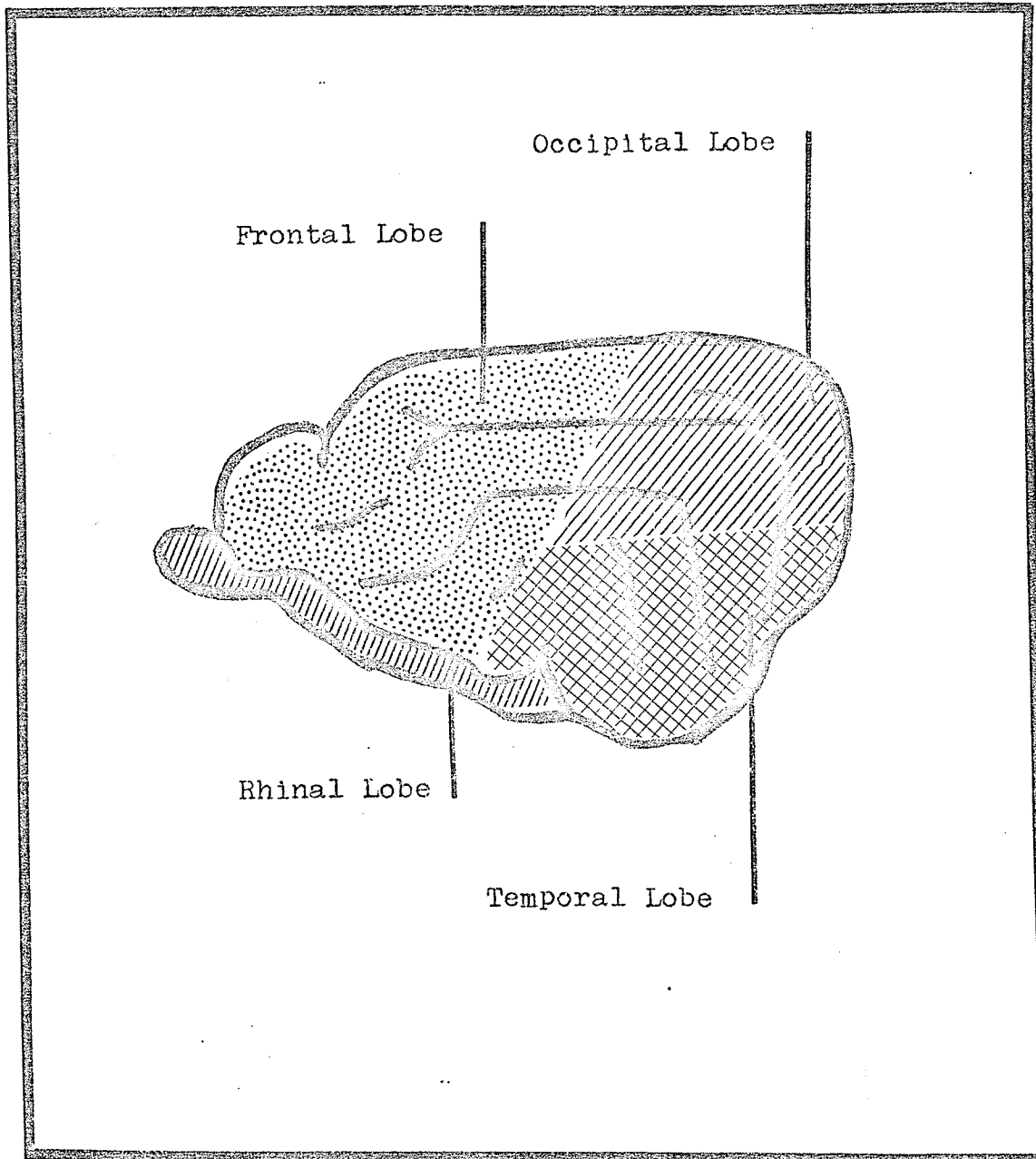
Appendix. Fig. 3. Dorsal Surface of Cat's Cerebral Hemispheres.

Terminology after Papez (1929) and Reighard and Jennings (1951).



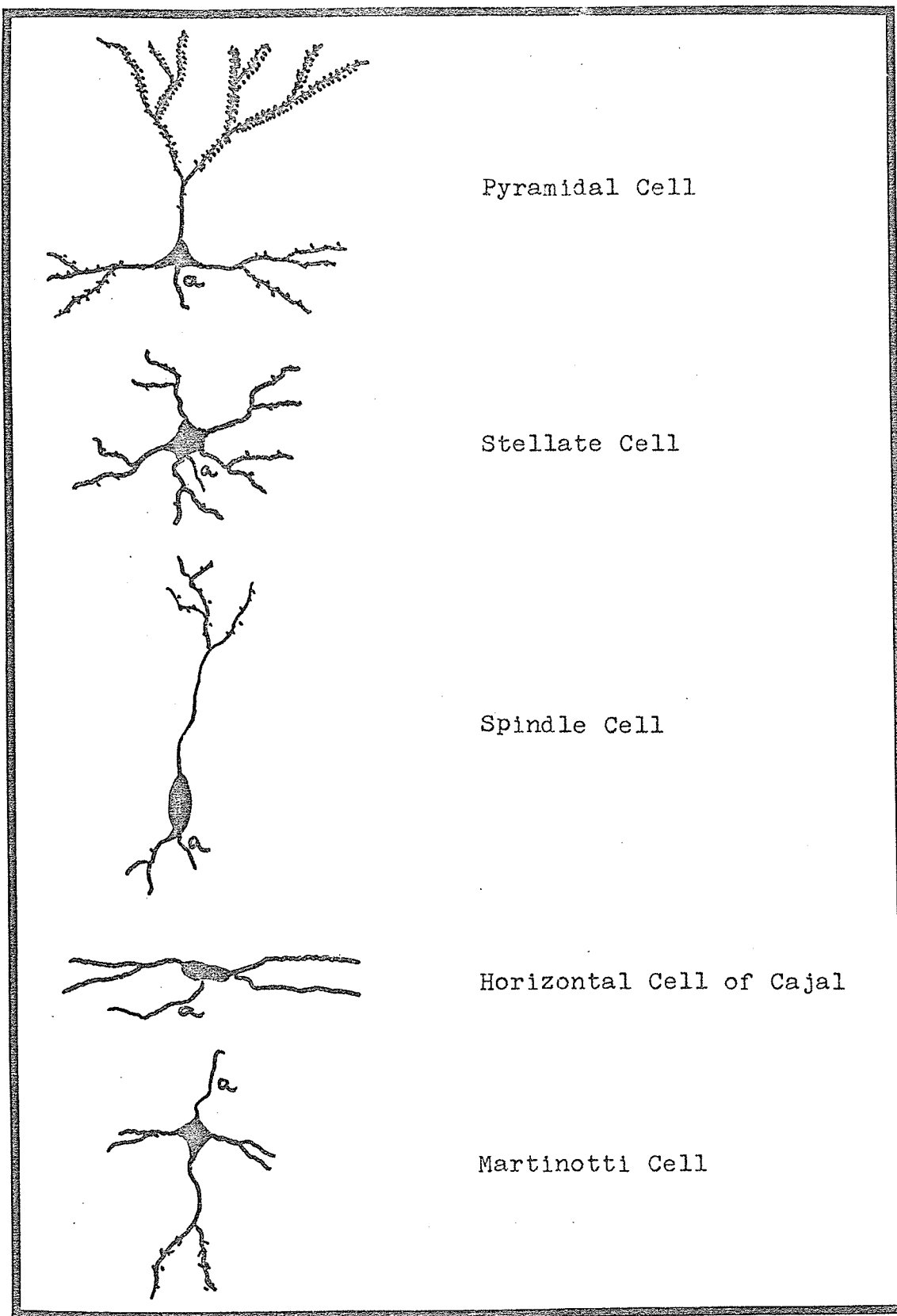
Appendix. Fig. 4. Lateral Aspect of Cat Cerebral Hemisphere

Lobe category according to Papez (1929).

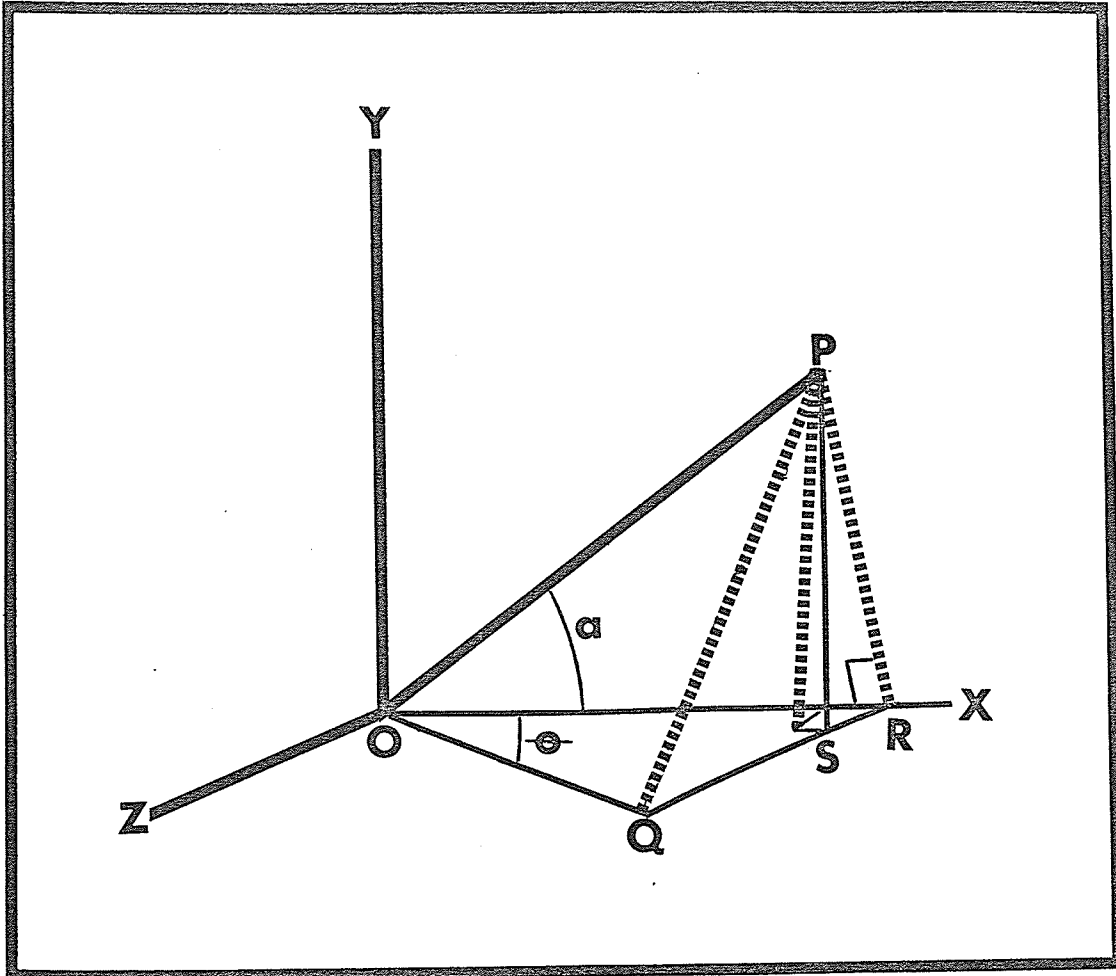


Appendix. Fig. 5. Lateral Aspect of Cat Cerebral Hemisphere

Lobe category according to Reighard and Jennings (1951).



Appendix. Fig. 6. Representative Drawings of Cerebral Cortical Neurons, Following the Golgi Preparation Technique



Appendix. Fig. 7. Trigonometric Correction Factor

Diagram provided by E.W. Mazerall.

Legend for Appendix Fig. 7

The lines OX, OY and OZ are orthogonal axes.

Dendrite branch point is at "O".

One dendrite section is taken as lying on the X-axis;
the other section is represented by the line OP.

$\angle^{le} a$ is the angle sought.

The line OR was measured as $5u$.

The line OQ is the projection of OP on the X-Z plane.

The line PS is the vertical height at $5u$ from the branch point, of the dendrite section above the X-Z plane, as measured with the vertical fine stage adjustment.

$\angle^{le} a$ is the angle observed in the goniometer.

The desired angle, "a", is given by the formula

$$a = \tan^{-1} \frac{\sqrt{(PS)^2 + (OR \tan \ominus)^2}}{OR}$$

Data were fed into FOCAL program for solution.

Formula and program provided by E.W. Mazerall.